

Copyright is owned by the Author of the thesis. Permission is given for a copy to be downloaded by an individual for the purpose of research and private study only. The thesis may not be reproduced elsewhere without the permission of the Author.

Synergistic triple combination antibiotic therapy for
Gram-negative bacterial infections

A thesis presented in partial fulfilment of the
requirements for the degree of

Doctor of Philosophy
in
Microbiology and Genetics

at Massey University, Manawatu,
New Zealand

Catrina Diane Olivera

2021

Abstract

The continuing emergence of multidrug-resistant bacteria and the slowing down of the discovery and development of novel antibiotics have made antimicrobial resistance an ominous threat to human health. As reflected in the World Health Organization's priority pathogens list, this problem is notably more severe in multidrug-resistant Gram-negative bacteria. This situation needs to be rectified through alternative approaches, such as the revival of 'old' antibiotics and the development of combination therapies.

This thesis focuses on the combination of the 'old' antibiotics, nitrofurans and vancomycin (VAN) with the secondary bile salt sodium deoxycholate (DOC). The synergistic interaction of these antibacterials was demonstrated in the *in vitro* growth inhibition and killing of Gram-negative bacteria, including the clinically relevant pathogens such as carbapenemase-producing *Escherichia coli*, *Klebsiella pneumoniae*, and *Acinetobacter baumannii*. The synergy increased the efficacy and reduced the doses of each of the components compared to monotherapy use, with the advantage of mitigating nitrofuran mutagenicity.

Using a transcriptomics approach, underlying mechanisms of the individual and combined action of nitrofurans, VAN, and DOC in *E. coli* were elucidated. The nitrofuran antibiotic, furazolidone (FZ), and DOC elicited highly similar gene perturbations indicative of iron starvation response, decreased respiration and metabolism, and translational stress. VAN, on the other hand, induced extracytoplasmic stress response in agreement with its known role in peptidoglycan synthesis inhibition. Through genetic and biochemical approaches, Fur (ferric uptake regulator) protein inactivation was confirmed

to be important in the synergy of FZ and DOC and to contribute to the synergy of the triple combination. Similarly, the SOS response to DNA damage was shown to be essential for the synergy between FZ and VAN and to also contribute to the synergy of the triple combination. Taken together, the findings of this thesis strongly suggest the presence of multiple interaction points, that leads to the triple synergy, and support the proposed mechanism of synergy where the combined effects lead to the amplification of damaging effects and suppression of resistance mechanisms.

Overall, this thesis shows the synergistic triple combination of nitrofurans, DOC, and VAN as a promising therapy for Gram-negative infections. Furthermore, this work significantly increases the understanding of drug interaction mechanisms that lead to synergy, which is hoped to help advance this combination further into the development pipeline. Transcriptomics analyses and the follow-up experiments provide key fundamental insights into the physiological impact that these three antimicrobials have on enterobacterium *E. coli* and highlight the advantage of combined targets in bacterial killing. These findings, in turn, will help design novel antibiotics, mono- or combined therapies, against multidrug-resistant bacteria.

Acknowledgements

The accomplishment of this thesis is the result of massive support and encouragement from many people, including my supervisors, lab colleagues, my family, and friends.

First and foremost, I would like to thank my primary supervisor, A/Prof. Jasna Rakonjac, for offering me this amazing opportunity. I appreciate your encouragement, guidance, and your professional and personal advice throughout my PhD journey. I would also like to thank my co-supervisors, Prof. Murray Cox, Dr Pat Edwards, and A/Prof. Gareth Rowlands for all their support and expertise.

I would like to express my sincere gratitude to the staff of the School of Fundamental Sciences, especially Ann, Cynthia, Debbie, Fiona, Paul, and Penny who keep everything running so smoothly and who are always happy to help with anything and everything.

I thank all the people that have contributed to this experience in one way or another, SFS staff and students, the PhD student community, and anyone else that I have met throughout this journey.

I am incredibly grateful to present and former members of the Rakonjac lab, especially, Rayen, Vuong, Steph, and Cathy, for making the lab a supportive and fun work environment. Your company made a great deal of difference in being able to cope with all the stress.

Lastly, I thank my family and Sam for all the love, support, and encouragement. Thank you for sharing this journey with me. This accomplishment would not be possible without you.

Table of Contents

Abstract	i
Acknowledgements	iii
Table of Contents	iv
List of Figures	vii
List of Tables	x
Abbreviations	xi
1 Introduction	1
1.1 Antimicrobial resistance	2
1.2 Antimicrobial resistance in Gram-negative bacteria.....	5
1.3 Strategies to combat antimicrobial resistance	8
1.3.1 Novel antibiotics and revival of 'old' antibiotics	8
1.3.2 Synergistic antibiotic combinations	9
1.4 Nitrofurans	14
1.5 Sodium deoxycholate	18
1.6 Vancomycin	21
1.7 Synergy between nitrofurans, DOC, and VAN.....	24
1.7.1 Nitrofurans and DOC	24
1.7.2 Nitrofurans and VAN	24
1.8 The aerobic electron transport chain of <i>E. coli</i>	25
1.9 <i>E. coli</i> stress responses to antibiotics	26
1.9.1 Oxidative stress response	26
1.9.2 SoxS-MarA-Rob regulon.....	30
1.9.3 SOS response.....	31
1.9.4 Iron starvation response.....	33
1.9.5 Extracytoplasmic stress response	36
1.10 Rationale and objectives of the study	39
2 Materials and methods	41
2.1 Antibiotics	42

2.2	Bacterial strains and growth conditions	42
2.3	Susceptibility testing	45
2.4	Checkerboard assay.....	45
2.5	Time-kill assay	46
2.6	MTT assay for cellular viability.....	47
2.7	IC50 (half-maximal (50%) inhibitory concentration) determination for transcriptome study	48
2.8	Total RNA extraction.....	48
2.9	RNA sequencing	49
2.10	RNA-seq data analysis	50
2.11	Metal concentration analysis by ICP-MS	51
2.12	Oxygen consumption	52
2.13	Mutagenicity assay.....	52
2.14	Ethidium bromide accumulation and efflux.....	53
3	<i>In vitro</i> characterisation of nitrofurans, vancomycin, and sodium deoxycholate synergy against Gram-negative pathogens.....	55
3.1	Introduction	56
3.2	Results	57
3.2.1	Susceptibility testing.....	57
3.2.2	Nitrofurans, VAN, and DOC synergy against Gram-negative pathogens.....	59
3.2.3	Indifferent interaction of FZ, DOC, and VAN against Gram-positive bacteria	65
3.2.4	Interactions of bile salts mixture with FZ and VAN against <i>E. coli</i>	67
3.2.5	Interactions of lipoglycopeptides with FZ and DOC against <i>E. coli</i>	67
3.2.6	<i>In vitro</i> cytotoxicity of FZ, VAN, and DOC combination is indifferent.....	68
3.3	Discussion	71
4	Characterising the mechanism of action and synergy of furazolidone, vancomycin, and sodium deoxycholate against <i>Escherichia coli</i> using transcriptomics	77
4.1	Introduction	78
4.2	<i>E. coli</i> K12 strain K1508.....	79
4.3	Experimental design.....	81
4.4	Pre- and post-sequencing quality control.....	84
4.5	Results	86
4.5.1	Transcriptional response to individual antibacterials	86
4.5.2	Transcriptional response to FZ, DOC, and VAN combination	90

4.5.3	Comparison of differentially expressed gene clusters in the presence of combination and single antibacterials at IC ₅₀	92
4.5.4	Extracytoplasmic stress response to VAN treatment	94
4.5.5	SOS response to FZ treatment.....	95
4.5.6	Iron starvation responses	96
4.5.7	FZ and DOC upregulation of protein synthesis.....	98
4.5.8	Downregulation of the electron transport chain and central carbon metabolism.	100
4.5.9	Oxidative stress	102
4.5.10	Antibiotic-induced resistance mechanisms	102
4.6	Discussion	104
5	Investigating pathways involved in the action and synergy of furazolidone, sodium deoxycholate, and vancomycin.....	115
5.1	Introduction	116
5.2	Results.....	118
5.2.1	Fur plays a role in the synergy of FZ and DOC	118
5.2.2	Intracellular metal homeostasis is affected by FZ and DOC.....	122
5.2.3	The electron transport chain	124
5.2.4	FZ and DOC decelerates <i>E. coli</i> aerobic ETC.....	126
5.2.5	Possible efflux inhibitory activity of FZ and DOC	128
5.2.6	FZ dose reduction in the combination decreases mutagenicity.....	132
5.2.7	SOS response is involved in the synergy between FZ and VAN.....	134
5.3	Discussion	136
6	General discussion	145
6.1	General discussion	146
6.2	Conclusion	151
6.3	Future directions	152
	References	155
	Appendices	183
Appendix A	Supplementary figures and tables	184
Appendix B	Supplementary files.....	191

List of Figures

Figure 1. The cell wall structure of bacteria	5
Figure 2. Drug synergy models based on effect-based approaches.....	10
Figure 3. Checkerboard assay and isobologram of drug interactions based on the Loewe additivity model	13
Figure 4. Chemical structures of nitrofurans	14
Figure 5. Type I (oxygen-insensitive) two-electron reduction of nitrofuran.....	16
Figure 6. Type II (oxygen-sensitive) one-electron reduction of nitrofuran.....	17
Figure 7. Bile salt biosynthesis and metabolism by intestinal bacteria	19
Figure 8. Vancomycin inhibition of peptidoglycan synthesis	22
Figure 9. The electron transport chain of <i>E. coli</i>	25
Figure 10. Thiol-disulfide switch transcriptional regulation by OxyR.....	27
Figure 11. Transcription activation of SoxS-MarA-Rob regulon.....	29
Figure 12. SOS response induction	32
Figure 13. Iron-dependent transcriptional regulation by Fur	34
Figure 14. <i>E. coli</i> extracytoplasmic stress response systems.....	37
Figure 15. Time-kill analysis of FZ, VAN, and DOC combinations in killing (A) <i>E. coli</i> ATCC 25922, (B) <i>S. dysenteriae</i> NZRM 1015, (C) <i>C. gillenii</i> PMR001, and (D) <i>A. baumannii</i> NZRM 3697.....	63
Figure 16. Time-kill analysis of FZ, VAN, and DOC combinations in killing carbapenemase-producing (A) <i>E. coli</i> NZRM 4364 and (B) <i>A. baumannii</i> NZRM 4408, and (C) multidrug-resistant ESBL-producing <i>K. pneumoniae</i> NZRM 4387.....	64
Figure 17. Concentration-response curves of FZ, VAN, and DOC on HEK293T.....	69
Figure 18. Integrity of the purified total RNA samples.....	84

Figure 19. Principal component analysis	85
Figure 20. Genome-wide expression changes in response to individual antibacterials	87
Figure 21. Gene ontology term enrichment analysis of FZ and DOC DEGs.....	89
Figure 22. Genome-wide expression changes in response to triple FZ+DOC+VAN combination	90
Figure 23. Overlap of DEGs between FZ+DOC+VAN IC50 combination and single antibacterials at the same concentrations used in the combination	91
Figure 24. Heatmap of DEG clusters and GO term enrichment.	93
Figure 25. Differential expression of genes involved in SOS response.....	95
Figure 26. Differential expression of genes involved in iron import and iron-sulfur cluster assembly.....	97
Figure 27. Upregulation of genes encoding protein synthesis machinery	99
Figure 28. Downregulation of the central carbon metabolism and electron transport chain	101
Figure 29. Differential expression of genes involved in oxidative stress and antibiotic-induced resistance mechanisms	103
Figure 30. Proposed interaction of FZ, DOC, and VAN that leads to synergy.....	107
Figure 31. FZ-DOC interactions in the absence of Fur.....	120
Figure 32. Intracellular metal levels after treatment with FZ, DOC, and VAN and the triple combination.....	123
Figure 33. Survival of electron transport chain deletion mutants at sub-MIC FZ	125
Figure 34. Oxygen consumption rate in antibacterial-containing cultures	127
Figure 35. Effect of FZ, DOC, and VAN ethidium bromide accumulation.....	129
Figure 36. Effect of FZ, DOC, and VAN on ethidium bromide efflux.....	131
Figure 37. Rifampicin resistance mutation frequency in <i>E. coli</i> K1508 treated with FZ, DOC, and VAN alone and in combination.....	133
Figure 38. Interactions between FZ and DOC or VAN in the SOS-response-deficient mutant <i>ΔrecA</i>	135

Appendix

Figure A- 1. Interaction of nitrofurans, VAN, and DOC in the growth inhibition of <i>E. coli</i> ATCC 25922	185
Figure A- 2. Interaction of FZ, VAN, and Ox gall bile salts in the growth inhibition of <i>E. coli</i> ATCC 25922.....	186
Figure A- 3. Interaction of lipoglycopeptides A) dalbavancin or B) oritavancin with FZ, and DOC in the growth inhibition of <i>E. coli</i> ATCC 25922	187
Figure A- 4. Interaction of FZ, VAN, and DOC in the growth inhibition of <i>E. coli</i> K1508 in A) 2xYT and B) cation-adjusted Mueller-Hinton media.....	188
Figure A- 5. Interaction of FZ, VAN, and DOC in the growth inhibition of <i>E. coli</i> K1508 A) Δfur and B) $\Delta recA$ mutants.....	189

List of Tables

Table 1. Bacterial strains used in the study	43
Table 2. Minimum inhibitory concentrations.....	58
Table 3. Minimum inhibitory concentrations and fractional inhibitory concentration indices for the most synergistic two-drug and three-drug combinations of FZ, VAN, and DOC against Gram-negative strains identified in a checkerboard assay.....	60
Table 4. Minimum inhibitory concentrations and fractional inhibitory concentration indices for the most synergistic two-drug and three-drug combinations of FZ, VAN, and DOC against Gram-positive pathogens identified in a checkerboard assay.....	66
Table 5. Concentrations ($\mu\text{g}/\text{mL}$) that resulted in 20%, 50%, or 90% inhibition in HEK293T and the calculated FICI.	70
Table 6. Drug concentrations used in the transcriptomics study.....	83
Table 7. Significantly differentially expressed genes in response to VAN treatment	94
Table 8. Minimum inhibitory concentrations of <i>fur</i> mutants using broth microdilution	118
Table 9. Minimum inhibitory concentrations of electron transport chain mutants.....	124
Table 10. Fractional inhibitory concentration index for FZ-DOC interactions in electron transport chain mutants	126

Appendix

Table A- 1. Variants detected between <i>E. coli</i> MC4100 and K1508 genome	190
--	-----

Abbreviations

ATP	Adenosine triphosphate
CCCP	Carbonyl cyanide m-chlorophenylhydrazine
CDC	Centers for Disease Control and Prevention
CFU	Colony forming unit
CLSI	Clinical Laboratory Standards Institute
DMSO	Dimethyl sulfoxide
DNA	Deoxyribonucleic acid
ssDNA	Single-stranded DNA
DOC	Sodium deoxycholate
DEG	Differentially expressed gene
EDTA	Ethylenediaminetetraacetic acid
ESBL	Extended-spectrum β -lactamase
ETC	Electron transport chain
FDA	Food and Drug Administration
Fe-S	Iron-sulfur
FIC	Fractional inhibitory concentration
FICI	Factional inhibitory concentration index
Fur	Ferric uptake regulator protein
FRT	FLP recombinase recognition target
FZ	Furazolidone
GO	Gene ontology
IC ₅₀	Half-maximal (50%) inhibitory concentration
ICP-MS	Inductively coupled plasma mass spectrometry
log ₂ FC	log ₂ fold change
LPS	Lipopolysaccharide
MH	Mueller-Hinton
MIC	Minimum inhibitory concentration
MRSA	Methicillin-resistant <i>Staphylococcus aureus</i>
MTT	(3-[4,5-dimethylthiazol-2-yl]-2,5-diphenyltetrazolium bromide
NIT	Nitrofurantoin
NFZ	Nitrofurazone

OD600	Optical density at 600 nm
PBS	Phosphate buffered saline
PCA	Principal component analysis
PMF	Proton motive force
ppGpp	Guanosine 5', 3'-(bis)diphosphate
pppGpp	Guanosine 5'-triphosphate, 3'-diphosphate
RNA	Ribonucleic acid
mRNA	Messenger RNA
rRNA	Ribosomal RNA
sRNA	Small RNA
ROS	Reactive oxygen species
rpm	Rotations per minute
SDS	Sodium dodecyl sulfate
TCA	Tricarboxylic acid
VAN	Vancomycin
WHO	World Health Organization

1 Introduction

1.1 Antimicrobial resistance

Throughout most of human history, what we now know as bacterial infections were usually treated with herbal medicines, potions, or extracts. These were often not enough; therefore, even uncomplicated bacterial infections often led to death. Since the introduction of the first commercially available antibiotic in the 1930s, these drugs have significantly improved life and are now an integral part of modern medicine.

The discovery of penicillin in 1928 heralded the start of the golden age of antibiotics (Fleming, 1929). During this time, most of the antibiotics that we know today were developed and introduced to the market (Gould, 2016). However, with the decline of new antibiotics under development in recent years and the continuing emergence of antimicrobial-resistant bacteria, we are at risk of running out of antibiotics. The world is facing an antibiotic crisis, where bacterial infections are again a threat.

Antimicrobial resistance is a phenomenon where bacteria develop mechanisms to resist the effects of an antibiotic that was previously effective against them (Munita *et al.*, 2016; Peterson *et al.*, 2018). Bacteria can develop mutations or acquire resistance genes through horizontal gene transfer, through mechanisms such as antibiotics modification or degradation (Wright, 2005), alteration of antibiotic targets (Schaenzer *et al.*, 2020), increasing export through efflux pumps (Poole, 2007), and decreasing antibiotic entry by decreasing expression of porins (Fernández *et al.*, 2012). The first cases of antimicrobial resistance were observed shortly after the introduction of every new antibiotic. For example, penicillin was first used to treat *Staphylococcus aureus* bacteraemia in 1940, and a hospital reported its first case of penicillin-resistant *S. aureus* in 1942 (Rammelkamp *et al.*, 1942). Back in the 1940s to the 1960s, resistance development was not a concern as the discovery of new antibiotics kept pace with the emergence of

resistance. However, as we now know today, resistance occurs naturally over time and is inevitable; the misuse and overuse of antibiotics and its widespread use in food production has dramatically accelerated this process (Ayukekbong *et al.*, 2017; Ma *et al.*, 2021; Kirchhelle, 2018).

The World Health Organization (WHO) has identified the misuse and overuse of antibiotics in humans and animals as the main drivers of antimicrobial resistance. The Centers for Disease Control and Prevention (CDC) reported that of the 154 million antibiotic prescriptions in outpatient settings in the United States from 2010 through 2011, at least 30% were unnecessary (Fleming-Dutra *et al.*, 2016). The majority of these unnecessary antibiotic prescriptions were for upper respiratory tract infections caused by viruses. Additionally, prescription of wrong antibiotics, such as the use of excessively broad-spectrum instead of narrow-spectrum drugs and prescribing before tests confirm a bacterial infection, are the biggest contributors to this problem. Likewise, patients are also to blame, with the pressure they put on physicians to prescribe antibiotics and not finishing an antibiotic course (Cole, 2014; Fletcher-Lartey *et al.*, 2016; Strumiło *et al.*, 2016). In some developing countries, antibiotics are even readily accessible from pharmacies without a prescription, which makes it easy to self-medicate (Auta *et al.*, 2019; Ocan *et al.*, 2015).

Another area that contributes to antimicrobial resistance is the use of antibiotics in food-producing animals (Landers *et al.*, 2012). Antibiotics are used not just in treating diseases but also as prophylactics, feed additives, and growth promoters. Meat production accounts for an estimated 73% of the global use of antibiotics (Van Boeckel *et al.*, 2019). After years of widespread use in food-producing animals, guidelines and regulations are just now being introduced to combat antimicrobial resistance in this area. In 2017, the United States introduced new guidelines that made the use of antibiotics for non-

therapeutic purposes in food-producing animals illegal. As a result, antibiotic use in livestock has decreased by 33% (US Food & Drug Administration, 2017).

Similarly, efforts to combat antimicrobial resistance in the European Union saw more than 32% decrease in the overall sales of veterinary antimicrobials between 2011 and 2017 (European Medicines Agency, 2019). However, a survey found that only 42% of countries have limited the use of antibiotics critical for treating humans on animal production (World Health Organization *et al.*, 2018). Global trends predict that by 2030, the global consumption of all antimicrobials in food animals will increase by approximately 50% (Van Boeckel *et al.*, 2017).

Today, multidrug-resistant bacteria and superbugs that are resistant to last resort antibiotics are continuously emerging. Last resort antibiotics are usually reserved for infections where all other common antibiotic options have failed. For instance, carbapenem-resistant *Enterobacteriaceae* are on the "urgent threat list" by the CDC since this group of pathogens frequently exhibit resistance to most or all antibiotics (Centers for Disease Control and Prevention, 2019). Although these instances are still extreme cases, it is predicted to become common unless new antibiotic therapies are discovered. An independent review in 2014 estimated that, without appropriate actions, antimicrobial-resistant infections, which already cause 700,000 deaths each year, could grow to 10 million deaths coupled with a loss of 100 trillion USD of economic output by 2050 (O'Neill, 2014).

1.2 Antimicrobial resistance in Gram-negative bacteria

Multidrug-resistant Gram-negative pathogens are an urgent issue in tackling antimicrobial resistance. The threat from Gram-negative bacteria is more severe compared to that of Gram-positive bacteria due to an additional protective layer, called an outer membrane (Breijyeh *et al.*, 2020). This membrane acts as an additional barrier inhibiting the entry of both hydrophilic and hydrophobic toxic molecules (Figure 1).

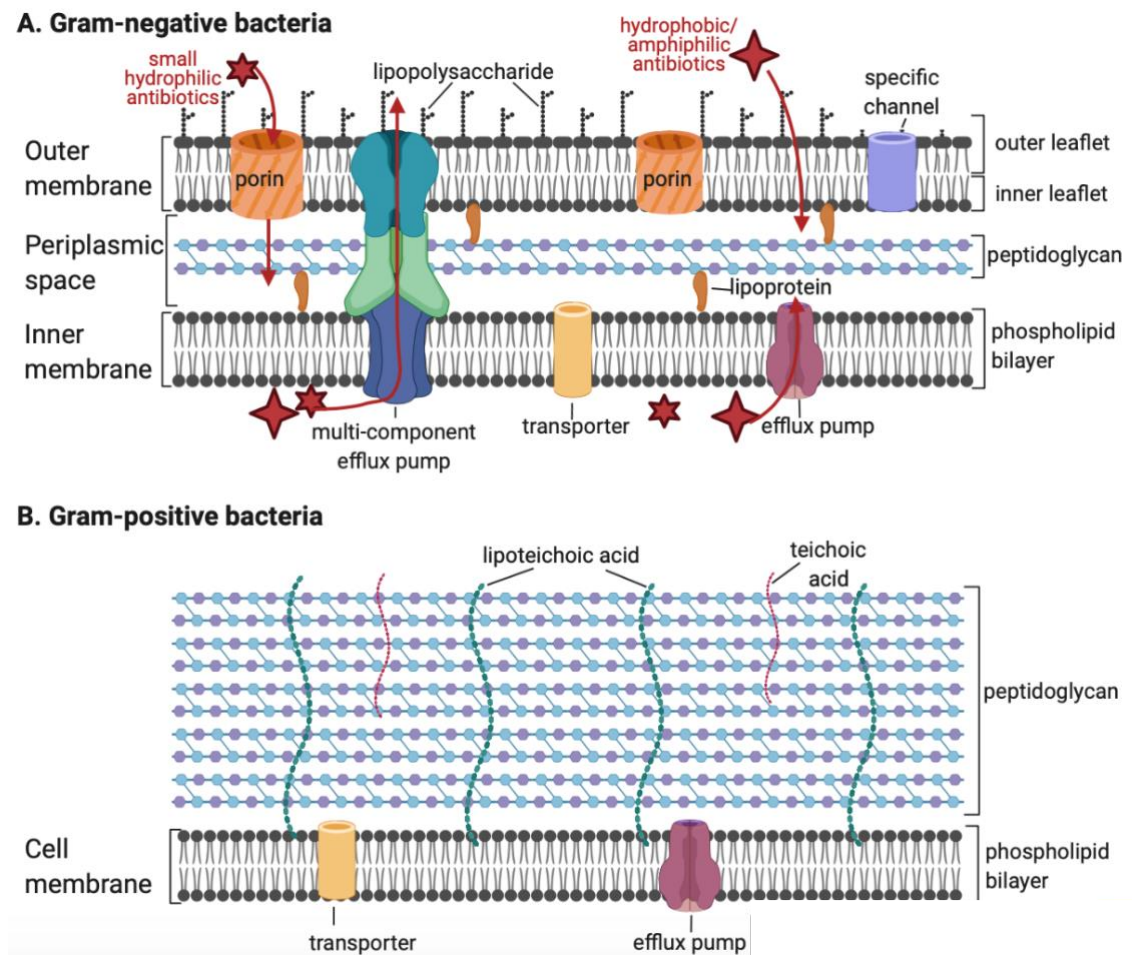


Figure 1. The cell wall structure of bacteria

A) The cell wall of Gram-negative bacteria is composed of an inner cell membrane and an outer membrane with a peptidoglycan layer in-between. **B)** The cell wall of Gram-positive bacteria does not have an outer membrane but has more layers of peptidoglycan compared to Gram-negative bacteria. Created with BioRender.com.

The outer membrane is an asymmetric lipid bilayer into which transmembrane proteins such as porins are embedded. This asymmetric lipid bilayer is composed of an outer leaflet primarily made up of lipopolysaccharides (LPS) and an inner leaflet composed of phospholipids (Nikaido, 2003). The composition of the outer membrane plays a significant role in its selective permeability. Firstly, anionic parts of the LPS allow neighbouring LPS molecule to form intermolecular ionic interactions *via* divalent cations (Nikaido, 2003; Nascimento *et al.*, 2014). These cross-bridging interactions result in a tight seal and a rigid structure that prevents the entry of molecules and slows down the passive diffusion of amphiphilic and hydrophobic molecules (Plésiat *et al.*, 1992). Second, the LPS contains saturated fatty acid chains which make the outer membrane much less fluid compared to a typical phospholipid bilayer and prevents entry of hydrophilic molecules. Instead, hydrophilic molecules must gain access to the cell through β -barrel protein channels called porins. These channels are grouped, based on selectivity, into specific and "general diffusion" porins and strictly limit the size of molecules that can enter the cell (~ 600 Da cut-off) (Vergalli *et al.*, 2020). For example, in *Escherichia coli*, the most abundant outer membrane proteins are the non-specific porins OmpC and OmpF, which act as an entryway for small hydrophilic molecules (Choi *et al.*, 2019a). Lastly, Gram-negative pathogens express a range of efflux pumps that recognise and transport noxious compounds, such as antibiotics and detergents, out of the cell (Venter *et al.*, 2015). These properties of the outer membrane are the reasons for Gram-negative bacteria's intrinsic resistance to a wide range of antibiotics, including the large hydrophilic antibiotic vancomycin (VAN) and bile salts.

Gram-negative bacteria are common causes of hospitalisations and community-acquired infections. ESKAPE pathogens which include four Gram-negative bacteria, *Klebsiella pneumoniae*, *Acinetobacter baumannii*, *Pseudomonas aeruginosa*, and *Enterobacter*

spp., cause most healthcare-associated infections and commonly exhibit multidrug resistance. They cause a broad range of diseases which include gastrointestinal illnesses, urinary tract infections (UTI), and bloodstream infections. In 2017, WHO released a list of priority pathogens, classified into critical, high, and medium priority, that urgently need research and development of new antibiotics (World Health Organization, 2017). The majority of these pathogens are Gram-negative bacteria including three pathogens deemed critical, carbapenem-resistant *A. baumannii*, *P. aeruginosa*, and *Enterobacteriaceae*. Carbapenem antibiotics are usually the last line of treatment for these multidrug-resistant bacteria, and in the case of carbapenem-resistance, the highly toxic polypeptide antibiotic colistin has been reserved as a last resort. However, the emergence of colistin resistance genes is now increasingly being reported globally, including countries like the US (McGann *et al.*, 2016) and China (Chen *et al.*, 2018; Liu *et al.*, 2016). This trend leads to the inability to treat infections, and further demonstrates the need for novel antibacterial strategies, especially for Gram-negative pathogens.

1.3 Strategies to combat antimicrobial resistance

1.3.1 Novel antibiotics and revival of 'old' antibiotics

A novel class of antibiotic is defined as having a unique core chemical structure, not a derivative of a previous class, and has not been previously used as an antibacterial. The golden age of antibiotics saw more than 20 novel classes of antibiotics introduced to the market (Coates *et al.*, 2011). Since then, most new antibiotics are analogues or variations of these classes, and so are also inhibited by existing resistance mechanisms. In the years 2000 to 2019, only five first-in-class new drugs were introduced to the market; none of which target Gram-negative bacteria (Butler *et al.*, 2017; The Pew Charitable Trusts, 2019). In the five years from 2014 to 2019, the US Food and Drug Administration (FDA) approved only 13 drugs that have antibacterial indications. Of these, none belong to a novel class of antibiotics, and none are indicated for WHO critical pathogens. The UK Prime Minister-commissioned report on antimicrobial resistance recommends 15 new antibiotics, including four that have a truly novel mechanism of action, every decade to keep up with the emergence of resistance and meet medical needs (O'Neill, 2015). However, as of December 2019, data by The Pew Charitable Trusts lists only 41 antibiotics under development, and if this is to follow historical trends, only 14% will be successful (World Health Organization, 2019a).

As multidrug resistance continues to emerge, it is apparent that finding novel antibiotics is getting harder and that the current clinical pipeline is insufficient to tackle the problem, especially for WHO priority pathogens and Gram-negative bacteria (World Health Organization, 2019a). This issue is made worse by most pharmaceutical companies abandoning the field due to low success rates and unprofitable antibiotic market, with many reduced to bankruptcy even after successfully marketing a new antibiotic (Mullard,

2019). To fill the gap, scientists are turning to alternatives such as the revival of 'old' antibiotics.

'Old' antibiotics are agents that were developed decades ago and were currently abandoned or less favoured due to a variety of reasons, such as toxicity and discovery of better alternatives. For example, the 'old' antibiotics, fosfomycin and nitrofurantoin (NIT) are again being used to treat uncomplicated UTI due to low prevalence of resistance compared to fluoroquinolones and cephalosporins, which suffer from widespread resistance (Kranz *et al.*, 2017; Cassir *et al.*, 2014).

1.3.2 Synergistic antibiotic combinations

Drug synergy is defined as drug combinations having enhanced effects than the simple additive effects expected from each drug individually. The increased efficacy imparted by the synergy allows the reduction of the effective doses of each drug, which can result in the mitigation of off-target toxicities (Tallarida, 2011).

There are different approaches currently used to assess drug combination synergy. These approaches include effect-based strategies, which compare the effects of a drug combination directly to their individual effects, and dose-effect based strategies, which compare doses of the drug individually and in the combination that give an equivalent effect (Foucquier *et al.*, 2015). Examples of effect-based strategies are response additivity, highest single agent, and the Bliss Independence model.

In the response additivity model (Figure 2A), a combination of drugs A and B is considered synergistic when the combined effect is greater than the sum of the individual effects of A and B. In the highest single-agent approach (Figure 2B), the effect of the combination is compared to the individual drug that caused the greatest effect. The

combination is synergistic if its effect is higher than the highest single agent, and antagonistic otherwise. Lastly, Bliss Independence assumes that drugs that act independently follow the law of probability (Bliss, 1939). Therefore, in a combination, the effects of individual drug components are independent yet competing events. The expected combination effect can be calculated by the equation $(E_A + E_B) - (E_A \times E_B)$, where E_A and E_B are the effects of drug A and B expressed as a probability (0-1). For example, drug A causes 50% inhibition and drug B causes 20% inhibition on their own. If the two drugs are additive, then their combined effect will be $(0.5 + 0.2) - (0.5 \times 0.2) = 0.6$. Based on this model (Figure 2C), a combination is synergistic if the actual combination effect is higher, and antagonistic otherwise.

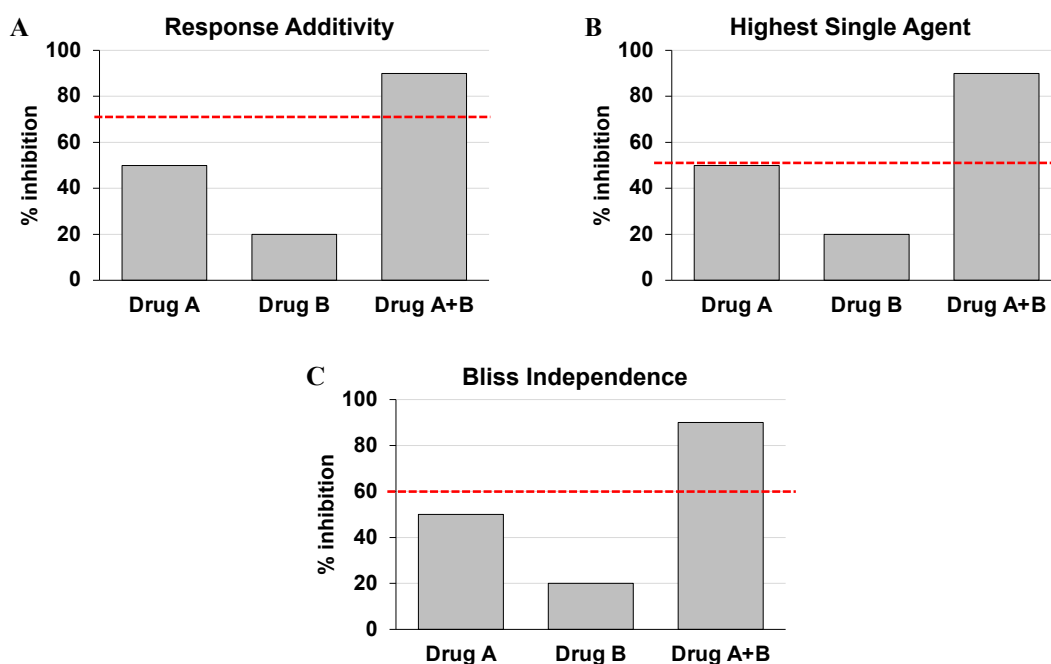


Figure 2. Drug synergy models based on effect-based approaches

A) Response additivity - the combination is synergistic when the effect of the combination is higher than the sum of its individual effects. B) Highest single agent - the combination is synergistic when the combined effect is higher than the single agent that caused the biggest effect. C) Bliss independence - the combination is synergistic if its effect is higher than the expected additive effect calculated by the equation $(E_A + E_B) - (E_A \times E_B)$. Red dashed line indicates the additive effect of A+B combination.

Another approach to analysing drug interactions is the dose-effect approach, such as the Loewe additivity theory. Loewe additivity assumes that a drug does not interact with itself (Loewe, 1953). Therefore, assuming drugs A and B are the same and do not interact, the combined effect of $0.5 \times$ minimum inhibitory concentration (MIC) of drug A and $0.5 \times$ MIC of drug B is equivalent to the effect of $1 \times$ MIC of either drug A or drug B (Yeh *et al.*, 2009). A standard metric used to define drug interactions is the fractional inhibitory concentration index (FICI), which uses Loewe additivity as the basis of non-interaction. FICI is calculated as follows:

$$\text{FICI} = \text{FIC A} + \text{FIC B} + \text{FIC C}$$

$$\text{FICI} = \frac{\text{MIC}_{\text{A(com)}}}{\text{MIC}_{\text{A(alone)}}} + \frac{\text{MIC}_{\text{B(com)}}}{\text{MIC}_{\text{B(alone)}}} + \frac{\text{MIC}_{\text{C(com)}}}{\text{MIC}_{\text{C(alone)}}}$$

where $\text{MIC}_{\text{A(com)}}$ is the minimum inhibitory concentration (MIC) of drug A when used in combination and $\text{MIC}_{\text{A(alone)}}$ is the MIC of drug A when used alone.

Using this approach, $\text{FICI} = 1$ means no interaction (based on Loewe additivity), $\text{FICI} < 1$ means synergy, and $\text{FICI} > 1$ means antagonism. However, to avoid misinterpreting FICI data that are only slightly above or below the theoretical cutoff of 1, a more conservative interpretation is commonly used in drug combination studies. Synergism is usually defined as $\text{FICI} \leq 0.5$, indifference as $0.5 < \text{FICI} \leq 4$, and antagonism as $\text{FICI} > 4$ (Odds, 2003).

FICI determination for drug combinations is commonly determined using a checkerboard inhibition assay. For a two-drug combination, a checkerboard assay is typically

performed in a multiwell plate with two-fold dilution gradients of the two drugs, as shown in Figure 3A. As for a three-drug combination, a three-dimensional checkerboard assay is performed, which uses multiple multiwell plates to have three drug gradients, as shown in Figure 3C. A graphical illustration, called an isobologram, can complement the FICI calculations, where each data point along the line represent the concentrations that give the chosen effect (Tallarida, 2011). A combination is considered synergistic when the data points are below the additivity line (for a two-drug combination) or additivity plane (for a three-drug combination), and antagonistic otherwise (Figure 3B and Figure 3D) (Huang *et al.*, 2019).

The use of synergistic antibiotic combinations is a promising alternative to combat antimicrobial resistance. An example is the broad-spectrum antibiotic combination trimetoprim-sulfamethoxazole. Trimetoprim and sulfamethoxazole, also known as cotrimoxazole, target sequential steps in the tetrahydrofolate biosynthesis pathway and potentiates each other's effects leading to synergy (Minato *et al.*, 2018). Advantages of using such combinations include enhanced efficacy, improved clearance of pathogens, deceleration of resistance development, and reduction of toxicities compared to use of each drug individually (Bollenbach, 2015; Yeh *et al.*, 2009). Using new antibiotics in synergistic combinations can prolong their life as the enhanced therapeutic effect can slow down resistance development (Moellering, 1983). Repurposing of currently available antibiotics into combinations is also a less costly and faster way of bringing new therapies into clinical use if they are already approved for human use and can speed up the development process (Chong *et al.*, 2007). For these reasons, reviving 'old' or currently available antibiotics through their use as synergistic combinations is a promising source of new antimicrobial therapies.

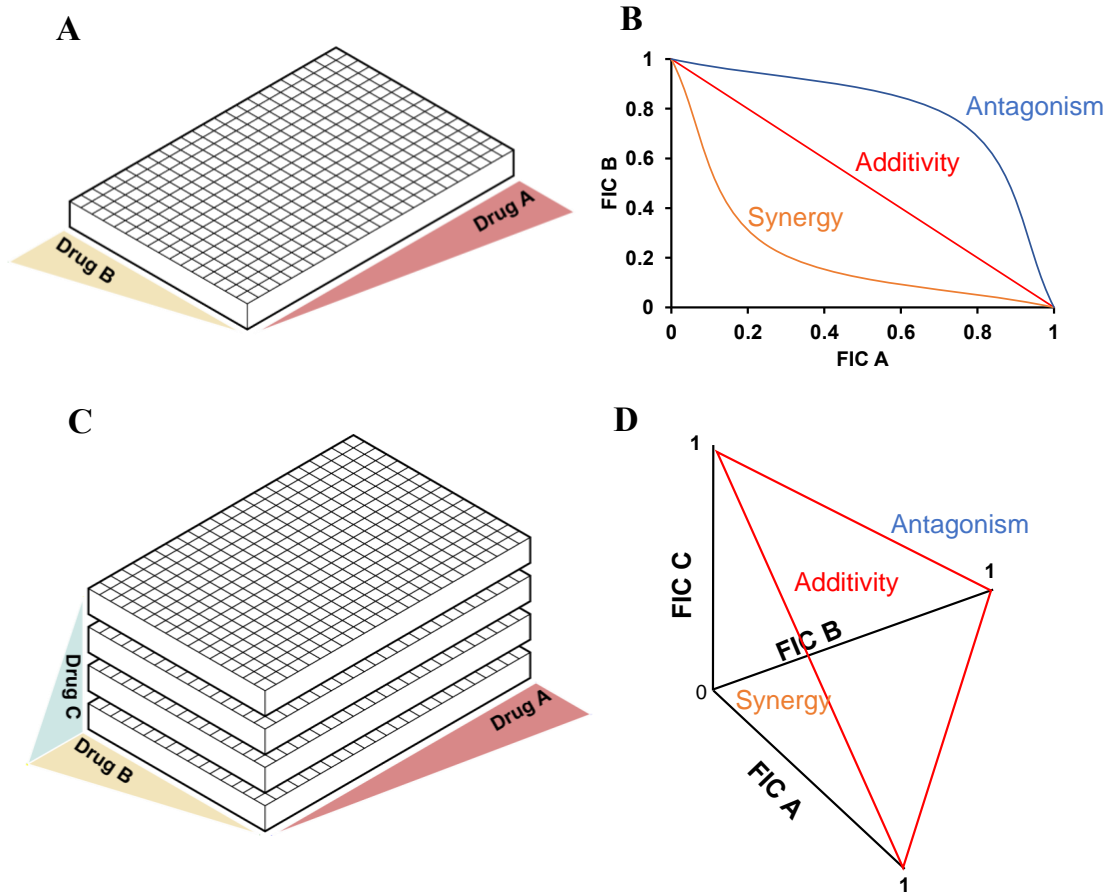


Figure 3. Checkerboard assay and isobologram of drug interactions based on the Loewe additivity model

A, B) Two-drug combinations; C, D) Three-drug combinations. Each data point of the isobologram represents the concentrations presented as FIC that give a chosen quantitative effect (e.g. 90% inhibition). The combination is synergistic if the data points are below the additivity line or plane connecting FIC 1 on all the axes.

1.4 Nitrofurans

Nitrofurans are a group of synthetic compounds with a nitrofuran moiety, a nitro group attached at the furan C5 position (Figure 4). This 'old' class of broad-spectrum antibiotics were clinically introduced in the 1940s to 1950s. They possess antibacterial and some antiprotozoal properties, and are currently used as human and veterinary drugs (Vass *et al.*, 2008). Furazolidone (FZ) is used to treat enteritis and diarrhoea caused by bacterial and protozoal infections, nitrofurantoin (NIT) is used to treat UTI, and nitrofurazone (NFZ) is used as a topical agent for burns and wounds. In addition to these commercially available nitrofurans, CM4 is a nitrofuran that was identified in a small molecule drug screen to possess antibacterial properties (Spagnuolo, J., Jobsis, C. & Rakonjac, J., unpublished).

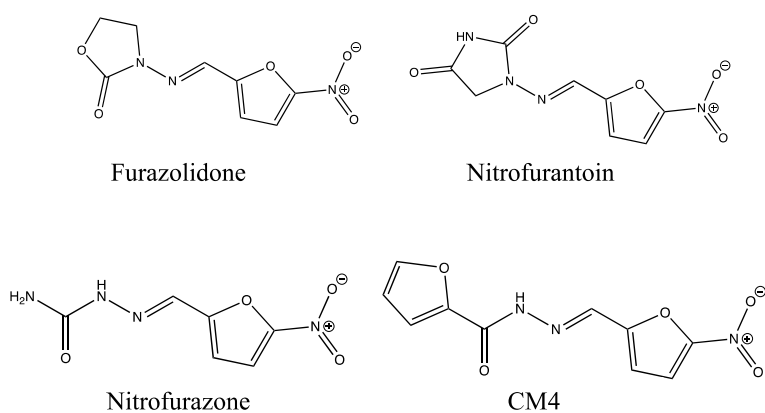


Figure 4. Chemical structures of nitrofurans

The nitrofuran class of antibiotics have a nitro group attached at the furan C5 position.

The use of nitrofurans had been controversial. Before their prohibition for use in food-producing animals, nitrofurans were widely used as a feed additive and veterinary antibiotic. However, findings of nitrofuran residues in food were concerning as they are stable and do not degrade upon standard food preparations (Cooper *et al.*, 2007). Also,

nitrofurans are mutagenic, and it is considered that consumption of nitrofurantoin-contaminated food presents a health risk since the drug residues can accumulate in tissues over time (McCracken *et al.*, 2007; Barbosa *et al.*, 2011). Studies on mice provided evidence of nitrofurantoin intake-related carcinogenicity and toxicity, with symptoms such as increased incidence of tumours and seizures (Kari *et al.*, 1989). For these reasons, the use of nitrofurans in food-producing animals, except for some topical uses, was banned by the FDA in 1991. In 2002, however, the FDA tightened the rules and prohibited the use of all nitrofurans in food-producing animals since topical applications also led to residues in edible tissues. Currently, many countries, including the European Union, Australia, and Japan, prohibit the use of nitrofurans in food production (Vass *et al.*, 2008). The exact mechanism of nitrofurans' mutagenicity in mammalian cells is not fully understood. It is proposed that the metabolism of nitrofurans leads to unstable active metabolites that could interact with DNA (McCalla *et al.*, 1975). The same hypothesis has been proposed as the mechanism of nitrofurantoin cytotoxicity in bacteria. Upon activation by bacterial enzymes, active metabolites derived from nitrofurans were hypothesised to form adducts with DNA (Wentzell *et al.*, 1980), cause frameshift mutations (Obaseiki-Ebor *et al.*, 1986), and interact with proteins and ribosomal RNA (rRNA) (McOsker *et al.*, 1994; Yu *et al.*, 1976). NFZ, for example, was shown to directly and reversibly inhibit DNA synthesis (Ona *et al.*, 2009) and NIT was reported to cause complete inhibition of protein synthesis (McOsker *et al.*, 1994). However, the active metabolites that are responsible for these activities remain unknown.

Despite their controversial history, the nitrofurans are still used today in human infections, in part due to their low prevalence of resistance. For example, NIT was approved by the FDA in 1953 for the treatment of UTI. Despite decades of use, resistance remains relatively rare. In a study conducted in six European countries, out of 775 *E. coli*

isolates collected from female patients with uncomplicated UTI, only 1.2% were resistant to NIT (Ny *et al.*, 2019). More importantly, NIT remains effective for some UTIs caused by multidrug-resistant *Enterobacteriaceae*, such as extended-spectrum β -lactamase (ESBL)-producing strains (Raja, 2019). Similarly, for FZ, which is used as a component of combination therapy for *Helicobacter pylori* infections, epidemiological data shows low prevalence of resistance in *Helicobacter* isolates (Zamani *et al.*, 2017; Kwon *et al.*, 2001; Choi *et al.*, 2019b).

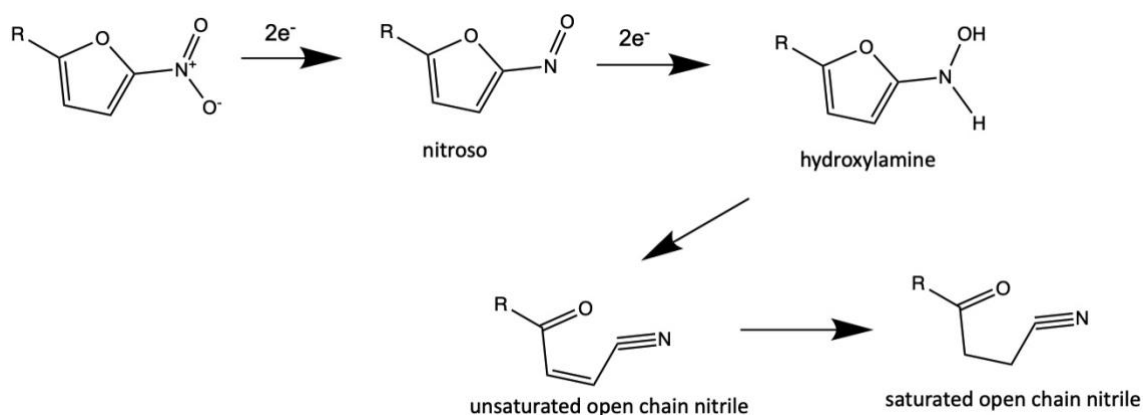


Figure 5. Type I (oxygen-insensitive) two-electron reduction of nitrofurane

Type I nitroreductase performs two-electron step-wise reduction to nitroso then a hydroxylamine derivative.

Just like many nitroheterocyclic compounds, nitrofurans are prodrugs and must undergo activation by specific enzymes. In *E. coli*, the nitroreductases NfsA and NfsB are known to be the primary activation catalysts (Whiteway *et al.*, 1998). Because of this, it is not surprising that the main resistance mechanisms are mutations in *nfsA* and *nfsB* genes (Sandegren *et al.*, 2008; Shanmugam *et al.*, 2016; Whiteway *et al.*, 1998; Mottaghizadeh *et al.*, 2019). These enzymes are type I oxygen-insensitive nitroreductases that are proposed to catalyse the two-electron reduction of nitrofurans (Figure 5). It has been shown that the main product of the aerobic reduction of NIT and NFZ by purified NfsB

is a hydroxylamine derivative (Race *et al.*, 2005). The reaction proceeds *via* two consecutive two-electron reductions; the second reduction step happens at a much faster rate, which explains why the nitroso intermediate was not observed. In another study, NFZ reduction by oxygen-insensitive nitroreductases only detected an open-chain nitrile, which was hypothesised to form through rearrangement of the hydroxylamine derivative followed by ring-opening (Figure 5) (Peterson *et al.*, 1979).

Similarly, nifurtimox, an antiprotozoal nitrofurans drug used to treat Chagas disease and trypanosomiasis, is also activated by trypanosomal type I oxygen-insensitive nitroreductase. This reaction gives a cytotoxic unsaturated open-chain nitrile as the major product and a stable saturated open-chain nitrile as a minor product (Bot *et al.*, 2013; Hall *et al.*, 2011).

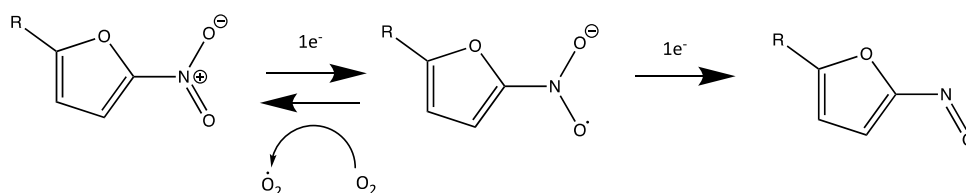


Figure 6. Type II (oxygen-sensitive) one-electron reduction of nitrofurans

Type II nitroreductase performs one-electron reduction to a nitro anion radical, which under aerobic conditions, undergoes futile cycling and regenerates back to nitrofurans.

Another type of nitroreductase in *E. coli* is type II oxygen-sensitive nitroreductase, which performs one-electron reduction (Figure 6). Besides NfsA and NfsB, other enzymes probably play a role in activating nitrofurans in *E. coli* since a double knockout of *nfsA* and *nfsB* genes does not confer full resistance to nitrofurans. In 1979, the presence of oxygen-sensitive nitroreductase was reported in *E. coli*, but the enzyme responsible was not identified. This reduction involves a nitro anion free radical, which in the presence of

oxygen, oxidises back to a nitrofurane with the concomitant generation of superoxide (Peterson *et al.*, 1979). Recent studies by Le *et al.* (2019) involving *nfsA nfsB* double-knockout *E. coli* mutants selected for increased FZ resistance indicated that a loss of function mutation of the gene *ahpF* leads to increased resistance to FZ. Subsequent biochemical studies then demonstrated AhpF to be another nitrofurane-activating enzyme with characteristic properties of type II oxygen-sensitive nitroreductase.

1.5 Sodium deoxycholate

Bile salts are essential components in lipid digestion, intestinal homeostasis, and antimicrobial protection (Begley *et al.*, 2005; Urdaneta *et al.*, 2017). They are produced in the liver, stored in the gall bladder, secreted into the small intestines, and recycled *via* the enterohepatic circulation.

Figure 7 shows a summary of bile salt synthesis and metabolism. Firstly, the primary bile salts, cholate and chenodeoxycholate, are produced in the liver from cholesterol. These primary bile salts can exist in a conjugated form with glycine or taurine in the liver and gall bladder. After food ingestion, the primary bile salts and the conjugated bile salts are released into the intestines. Intestinal bacteria then transform these bile salts into secondary bile salts by dehydroxylation and deconjugation. Bile salts are facial amphiphilic, such that they contain both hydrophilic and hydrophobic faces, and can act as an emulsifier and a solubiliser. They are essential in facilitating cholesterol catabolism and promoting digestion and absorption of lipids and lipid-soluble nutrients. Bile salts are efficiently reabsorbed from the intestinal lumen and recycled back to the liver, and the cycle is repeated. In this process, ~95% of the total bile salt pool is recirculated *via* the enterohepatic system, while the rest is excreted in the faeces (Chiang, 2013).

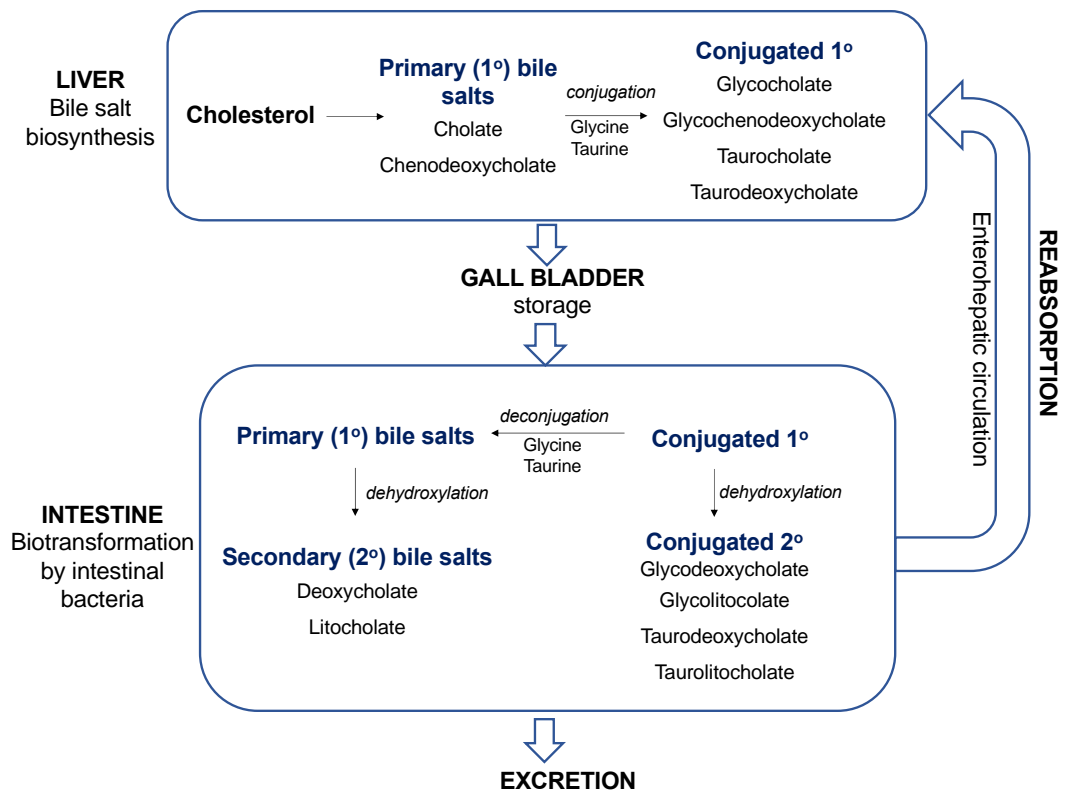


Figure 7. Bile salt biosynthesis and metabolism by intestinal bacteria

Primary bile salts are synthesised from cholesterol and conjugated with taurine and glycine in the liver. In the intestines, bacteria transform primary bile salts to secondary bile salts. Majority of bile salts are reabsorbed and recycled through the enterohepatic circulation.

Besides their roles in absorption and digestion, bile salts also function as signalling molecules that regulate various cellular and molecular processes (Hylemon *et al.*, 2009; Beuers, 1997), such as endocrine signalling (Houten *et al.*, 2006), and glucose metabolism (Nguyen *et al.*, 2008). Human bile salts also play an essential role in maintaining gut microbiota and protection against enteric pathogens. Abnormal bile salt patterns, such as reduced bile salt secretion in animals and humans with cirrhosis, usually lead to bacterial overgrowth (Fan *et al.*, 2009; Rosenberg *et al.*, 1967; Lorenzo-Zuniga *et al.*, 2003; Gunnarsdottir *et al.*, 2003).

The mechanism of bile salts' antimicrobial activity is not fully understood. They are active against *S. aureus* (Sannasiddappa *et al.*, 2017) and *H. pylori* (Itoh *et al.*, 1999), with

sodium deoxycholate (DOC) being the most potent bile salt. A study also showed that more hydrophobic bile salts, such as DOC, are more potent inhibitors of *E. coli* and *Enterococcus faecalis* growth than hydrophilic bile salts (Sung *et al.*, 1993).

Being amphiphilic, DOC has detergent properties, which was hypothesised to be responsible for its membrane-damaging effects (Begley *et al.*, 2005), including disruption of membrane integrity, cell leakage, and proton motive force (PMF) dissipation (Sannasiddappa *et al.*, 2017; Kurdi *et al.*, 2006). Besides these effects, it was also proposed that the bile salts DOC and sodium cholate can cause protein aggregation (Cremers *et al.*, 2014), and induce reactive oxygen species (ROS) production and DNA strand breaks (Negretti *et al.*, 2017; Merritt *et al.*, 2009).

Gram-negative bacteria use several mechanisms to increase tolerance and resistance to DOC. Primarily, this intrinsic resistance is attributed to the presence of multiple efflux pumps that restrict intracellular DOC accumulation (Gunn, 2000; Lin *et al.*, 2003; Venter *et al.*, 2015; Thanassi *et al.*, 1997). Bacteria also tolerate bile salts through other mechanisms such as activation of DNA repair, oxidative stress response, and RpoS general stress response pathways (Hernández *et al.*, 2012; Prieto *et al.*, 2006; Urdaneta *et al.*, 2019).

DOC is commonly used as a biological detergent, as a component of microbiological culture media, and recently as FDA-approved injectable drug to dissolve submental fat (Liu *et al.*, 2019). In the context of drug development, DOC can be used as a modifier of drugs as it can enhance solubility and absorption of both hydrophilic and hydrophobic drugs *via* chemical conjugation, and formation of micelles and bile salt-stabilised lipid bilayer vesicles, called bilosomes (Pavlović *et al.*, 2018; Sun *et al.*, 2010; Stojančević *et al.*, 2013; Bowe *et al.*, 1997). For example, bile salts, including DOC, can integrate into

lipid bilayers and alter membrane permeability by forming aqueous pores/channels, in which hydrophilic molecules can pass (Gordon *et al.*, 1985).

DOC, on its own, is not a very promising antibacterial agent against Gram-negative bacteria due to their intrinsic resistance to this bile salt. However, its natural presence in the gut could be advantageous for treating gastrointestinal illnesses. Another approach will be to use DOC in a combination that has a synergistic effect, where DOC's efficacy against Gram-negative bacteria can be enhanced.

1.6 Vancomycin

Vancomycin (VAN) is a glycopeptide antibiotic used to treat most Gram-positive infections. It is active against methicillin-resistant *S. aureus* (MRSA), *Clostridioides difficile*, and *Enterococcus spp.* VAN is a natural product initially isolated from the soil bacterium *Amycolatopsis orientalis* and was first introduced to the market in 1954. Shortly after its introduction, it was overshadowed by other antibiotics, particularly methicillin and first-generation cephalosporins that are more efficacious and less toxic (Levine, 2006). Widespread use of VAN began in the 1980s as an oral treatment for enterocolitis caused by *C. difficile* (Fekety *et al.*, 1993). It is currently included in the WHO list of essential medicines for adults and children as a second-choice treatment for *C. difficile* (World Health Organization, 2019b).

VAN kills Gram-positive bacteria by inhibiting cell wall biosynthesis (Hammes *et al.*, 1974). During peptidoglycan synthesis, precursor Lipid II is synthesised inside the cell. Lipid II is a disaccharide pentapeptide unit composed of N-acetylglucosamine (GlcNAc) and N-acetylmuramic acid (MurNAc), and a pentapeptide containing a terminal D-Ala-D-Ala chain. Lipid II precursors are translocated across the membrane to the sites of cell wall synthesis, where they are incorporated into the growing peptidoglycan through

transglycosylation and transpeptidation (Figure 8). During transglycosylation, a Lipid II unit is inserted into the growing peptidoglycan chain by the formation of glycosidic bonds. This process is followed by transpeptidation, where immature peptidoglycans crosslink *via* the formation of a peptide bond between two Lipid II pentapeptides.

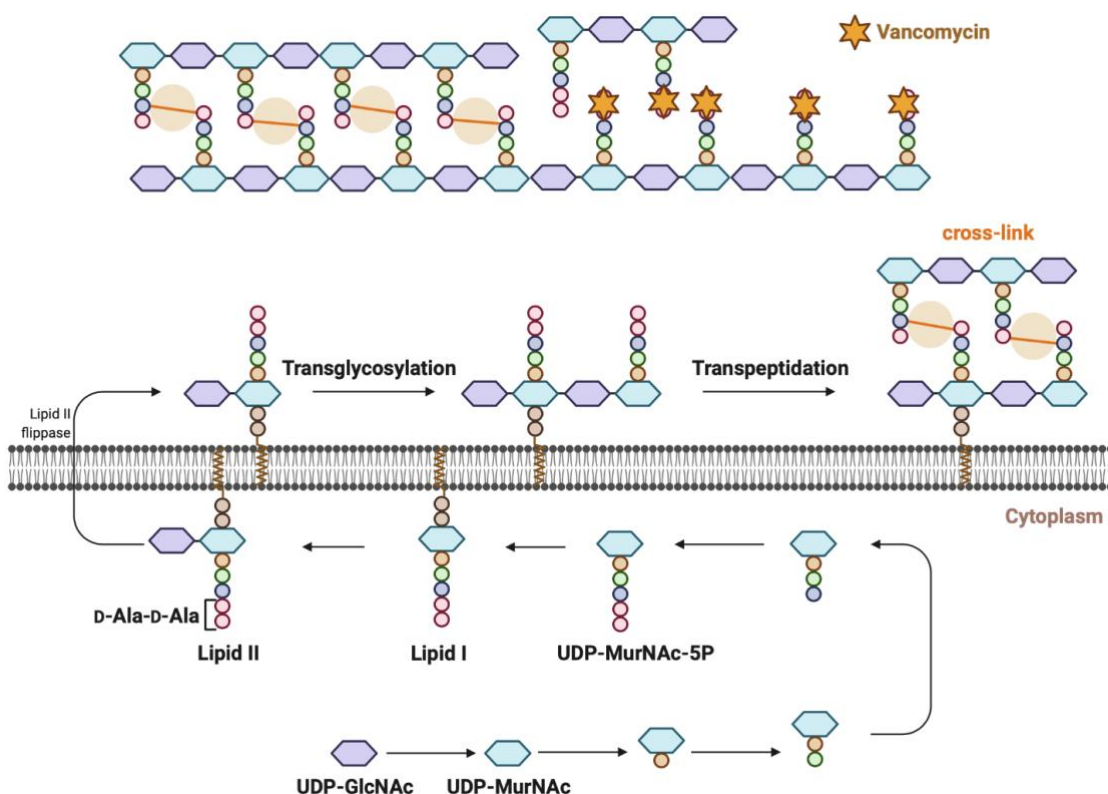


Figure 8. Vancomycin inhibition of peptidoglycan synthesis

VAN binding to D-Ala-D-Ala prevents the crosslinking that occurs during the transpeptidation step of peptidoglycan synthesis. Created with BioRender.com based on Figure 1 and review by Typas *et al.* (2012).

Outside the cell, VAN binds to the terminal D-Ala-D-Ala (Figure 8), thereby blocking the crosslinking between peptidoglycan intermediates that happens during transpeptidation (Liu *et al.*, 1994; Nieto *et al.*, 1971; Barna *et al.*, 1984). Additionally, the increased steric hindrance around the peptidoglycan precursors indirectly inhibits transglycosylation. The result is a weakened cell wall, which leads to cytolysis and cell death. Gram-negative

bacteria are naturally resistant to the effects of VAN due to the large size of the drug (~1450 Da), which renders it excluded from porins, and due to impenetrability of the outer membrane to hydrophilic molecules, unable to reach its target.

VAN forms a hydrogen-bonded complex with terminal D-Ala-D-Ala. Gram-positive bacteria such as *Enterococcus* develop resistance to VAN by altering D-Ala-D-Ala, for instance, to D-Ala-D-Lac or D-Ala-D-Ser, which result in a loss of a hydrogen bond with VAN or steric-hindrance-mediated loss of affinity, respectively (Bugg *et al.*, 1991; Lebreton *et al.*, 2011; Meziane-Cherif *et al.*, 2012).

One of the significant adverse effects of VAN is nephrotoxicity. The exact mechanism of this toxicity is not fully understood. However, it was proposed that increased ROS and oxidative stress are the main culprits (Öktem *et al.*, 2005). There are various risk factors associated with VAN-induced nephrotoxicity (Filippone *et al.*, 2017). Some examples are high doses, prolonged treatment, history of renal health problems, and concurrent use of interacting agents or other nephrotoxic agents (Rybak *et al.*, 1990). In addition, due to its poor oral bioavailability, VAN must be administered intravenously. Because of the adverse effects and complications with its intravenous administration (Roszell *et al.*, 2010), VAN is only used as a last line treatment, or for infections where β -lactams cannot be used such as in case of allergies or β -lactam resistance (Solensky, 2014; Solensky *et al.*, 2000).

Currently, there are five clinically used glycopeptide antibiotics. VAN was first in its class, followed by the natural product teicoplanin, and the semisynthetic drugs telavancin, oritavancin, and dalbavancin. Glycopeptides other than VAN all contain lipophilic substituents and therefore, have been termed lipoglycopeptides (Zhanel *et al.*, 2010). Having lipophilic side-chains and other modifications render these drugs with better antimicrobial properties and safety profiles compared to VAN (Crotty *et al.*, 2016).

1.7 Synergy between nitrofurans, DOC, and VAN

1.7.1 Nitrofurans and DOC

Studies in the Rakonjac laboratory have found synergy between some nitrofurans and DOC. Synergy has been observed on *Citrobacter gillenii*, *E. coli* O157: H7, and *Salmonella* sv. Typhimurium LT2 (Jobsis, C. & Rakonjac, J., unpublished). Specifically, the synergy between FZ and DOC has been demonstrated and characterised in enterobacteria (Le *et al.*, 2020). The mechanism of this synergy has not been fully elucidated; however, FZ-mediated inhibition of efflux pumps was reported to play a role. It was proposed that inhibition of TolC-associated efflux pumps allows DOC to accumulate inside the cells and exert its effect together with FZ.

1.7.2 Nitrofurans and VAN

Gram-negative bacteria are inherently resistant to VAN. However, in combination with nitrofurans, VAN can exert its effect by interacting synergistically. Synergy has been observed between NIT and VAN (Zhou *et al.*, 2015) and FZ and VAN (Weerasinghe, 2017) against *E. coli*. This synergy suggests that small amounts of VAN can enter Gram-negative bacteria, which on its own have a negligible effect, but together with nitrofuran can impart a synergistic inhibitory effect (Zhou *et al.*, 2015). The mechanism of this synergy is currently unknown.

1.8 The aerobic electron transport chain of *E. coli*

The aerobic electron transport chain (ETC) of *E. coli* couples successive transport of electrons from donors to acceptors with the electrogenic translocation of protons from the cytoplasm to the periplasmic space (Figure 9). The resulting electrochemical proton gradient and electrical potential across the inner membrane is called the proton motive force (PMF) (Mitchell, 1961), which can be utilised by energy-requiring processes, such as ATP synthesis and antibiotic efflux.

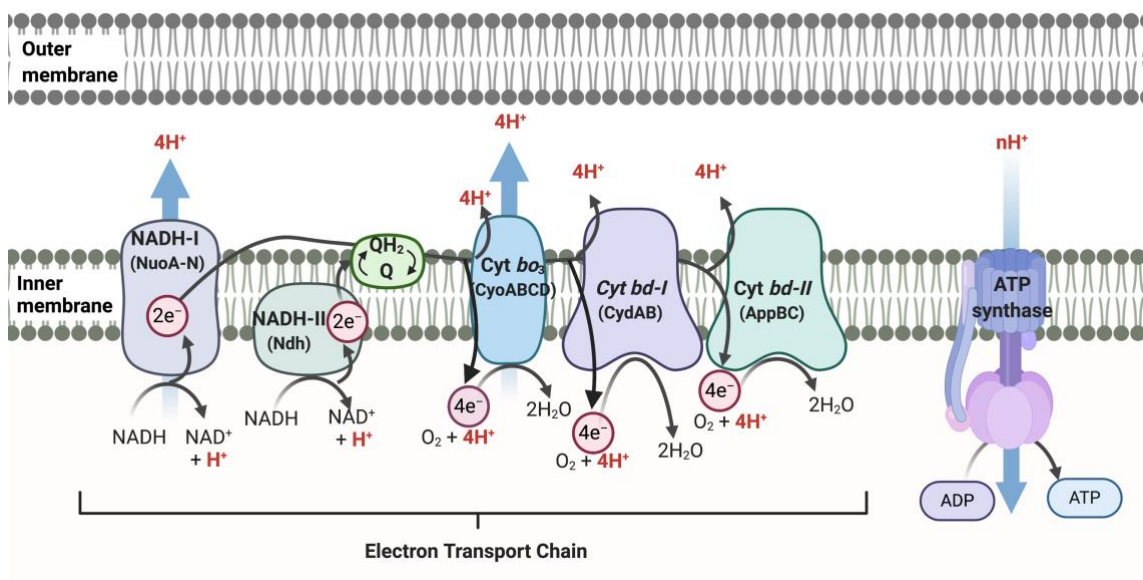


Figure 9. The electron transport chain of *E. coli*

The electron transport chain consists of membrane-bound proteins that pairs electron transport with the electrogenic translocation of proton to the periplasm. The resulting proton gradient and electrical potential across the membrane is called the proton motive force which drives ATP synthesis and other processes. Created with BioRender.com based on review by Unden *et al.* (1997).

The *E. coli* ETC consists of enzymes and complexes localised in the inner membrane: dehydrogenases and oxidoreductases that are linked by quinones, as shown in Figure 9. The two primary dehydrogenases Nuo (NADH dehydrogenase I), and Ndh (NADH

dehydrogenase II) oxidise the electron donor NADH by reducing membrane-associated quinones to quinols. The terminal quinol oxidases, cytochromes *bo₃* (Cyo), *bd-I* (Cyd), and *bd-II* (App), then re-oxidise the quinol by reducing oxygen to water. These dehydrogenases and oxidoreductases have overlapping functions, and their expressions are adjusted in response to environmental conditions, such as oxygen availability (Poole *et al.*, 2000). For example, the presence of oxygen induces the expression of quinol oxidases and represses terminal oxidoreductases of anaerobic ETCs. Cytochrome *bd-I*, which has a high affinity for oxygen, is highly expressed in microaerobic conditions, whereas cytochrome *bo₃*, which has a lower affinity, is synthesised maximally in oxygen-rich conditions (Cotter *et al.*, 1990; Tseng *et al.*, 1996).

Among these dehydrogenases and oxidoreductases, Nuo and cytochrome *bo₃* are proton pumping, while Ndh is non-proton pumping and does not generate PMF. In contrast, the non-proton pumping cytochrome *bd-I* and *bd-II* can generate PMF by transmembrane charge separation, where oxidation of quinol and reduction of oxygen happens on opposite sides of the membrane (Puustinen *et al.*, 1991; Miller *et al.*, 1985).

1.9 *E. coli* stress responses to antibiotics

1.9.1 Oxidative stress response

E. coli frequently encounter ROS endogenously as a consequence of aerobic metabolism. ROS such as superoxide (O_2^-) and hydrogen peroxide (H_2O_2) are inevitable byproducts of the reaction of oxygen with univalent electron donors, including flavins, quinones, and metal centres involved in the ETC (Messner *et al.*, 1999; González-Flecha *et al.*, 1995). These ROS can damage DNA, iron-sulfur (Fe-S) clusters, and protein residues, and can lead to cell death (Flint *et al.*, 1993; Jang *et al.*, 2007; Imlay, 2003; Imlay *et al.*, 1988). *E. coli*, therefore, have evolved to have oxidative stress sensing and response mechanisms

to increase their survival under aerobic conditions. Basal levels of superoxide dismutases and catalases detoxify low amounts of superoxide ($2\text{O}_2^- + 2\text{H}^+ \rightarrow \text{H}_2\text{O}_2 + \text{O}_2$) and hydrogen peroxide ($2\text{H}_2\text{O}_2 \rightarrow 2\text{H}_2\text{O} + \text{O}_2$) produced by normal metabolic processes. However, in the presence of exogenous ROS and agents that increase ROS production such as redox-cycling drugs, the basal scavenging enzymes are insufficient, and the transcription factors OxyR and SoxRS must tightly regulate the oxidative stress response (Farr *et al.*, 1991).

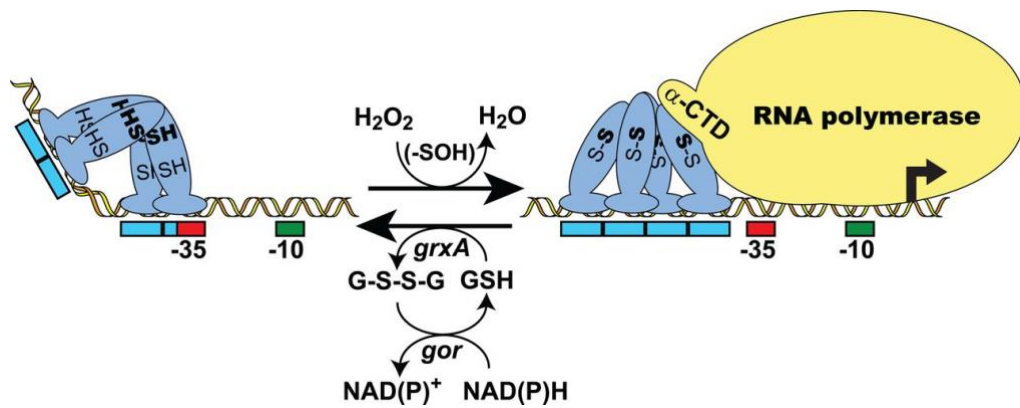


Figure 10. Thiol-disulfide switch transcriptional regulation by OxyR

In the presence of H_2O_2 , the "sensing" cysteine residue of OxyR is oxidised and forms a disulfide bond with a neighbouring cysteine. The conformational change results in DNA binding and interaction with RNA polymerase that allows induction of the target gene. Oxidised OxyR is reduced by the *grxA/gor* system, with the reduced OxyR able to function as a repressor. Reused with permission from American Society for Microbiology Journals: American Society for Microbiology, Journal of Bacteriology. Peroxide-Sensing Transcriptional Regulators in Bacteria (Figure 1), (Dubbs *et al.*, 2012), copyright 2012.

OxyR is the primary regulator for H_2O_2 response (Storz *et al.*, 1992). In the presence of H_2O_2 , OxyR's "sensing" cysteine residue is oxidised to a sulfenic acid that rapidly forms a disulfide bond with another cysteine (Figure 10). This disulfide bond could also arise in a pro-oxidising shift in thiol-disulfide redox status inside the cell (Aslund *et al.*, 1999). In both cases, the thiol-disulfide switch of OxyR results in a conformational change in

the tetrameric OxyR that alters DNA binding and interaction with RNA polymerase (Choi *et al.*, 2001; Zheng *et al.*, 1998; Lee *et al.*, 2004). OxyR can function as a transcriptional repressor or activator in its reduced and oxidised states. Oxidised OxyR, as an activator, contacts four adjacent major grooves on the DNA, while reduced OxyR, as a repressor, contacts two major grooves (Toledano *et al.*, 1994).

OxyR regulates the transcription of approximately 40 genes with functions that are essential for H₂O₂ detoxification, maintaining the thiol-disulfide redox status, and DNA protection from oxidative damage (Seo *et al.*, 2015). Some of these genes are *ahpCF* (alkyl hydroperoxide oxidoreductase), *katG* (hydroperoxidase I), *dps* (non-specific DNA-binding protein), *trxABC* (thioredoxins), *grxAB* (glutaredoxins) and *sufABCDSE* (Fe-S cluster assembly system).

SoxRS is another major regulator of the oxidative stress response, specifically towards superoxide (Greenberg *et al.*, 1990; Li *et al.*, 1994). SoxR and SoxS constitute a two-stage regulatory system, where the activation of SoxR induces the transcription of *soxS*, which in turn regulates the transcription of genes involved in superoxide stress response (Figure 11A) (Li *et al.*, 1994). SoxR is a homodimeric transcription factor which is activated *via* the oxidation of its [2Fe-2S] clusters (Gaudu *et al.*, 1997; Ding *et al.*, 1996). The mechanism of activation of SoxR is not fully understood. Whether superoxide itself oxidises and activates SoxR is debated since redox-cycling drugs can induce SoxR-regulated genes even in the absence of superoxide during anaerobic conditions (Privalle *et al.*, 1988; Gu *et al.*, 2011). However, redox-cycling drugs alone cannot fully account for SoxR activation, since SoxRS regulon members can be activated in superoxide dismutase mutants in the absence of redox-cycling drugs (Liochev *et al.*, 1999). The SoxRS regulon includes *sodA*, encoding superoxide dismutase for superoxide

detoxification, *acrAB*, encoding a multidrug efflux pumps, and *yggX* for protection of Fe-S proteins against oxidative damage (Pomposiello *et al.*, 2003).

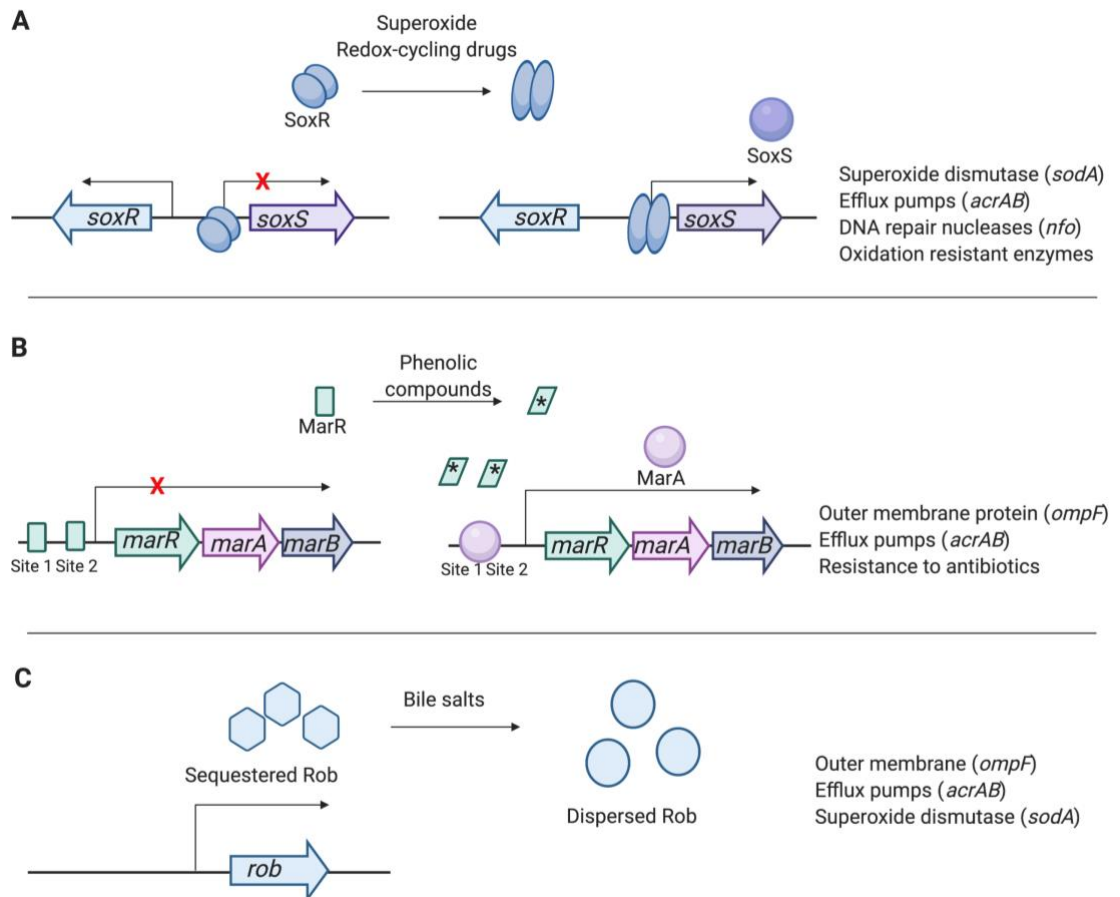


Figure 11. Transcription activation of SoxS-MarA-Rob regulon

A) Two-stage regulation of SoxRS regulon. SoxR activation induces transcription of *soxS*. SoxS in turn, induces transcription of its regulon members. **B)** MarR binds to two sites in the promoter region and inhibits transcription of its operon. Under inducing conditions, such as the presence of phenolic compounds, MarR is deactivated, and the promoter region is freed, allowing *mar* operon transcription. **C)** The DNA binding protein Rob is constitutively expressed in *E. coli* and present in a non-binding sequestered form under normal conditions. Presence of an inducing signal, such as bile salts, activates Rob, which can then bind DNA and influence transcription of its regulon members. Created with BioRender.com. Adapted from Figure 1 by Duval *et al.* (2013) under CC BY-SA 4.0.

1.9.2 SoxS-MarA-Rob regulon

SoxS, MarA, and Rob are global regulators responsible for adaptive mechanisms for different stress stimuli, such as antibiotics, oxidative, and chemical stresses (Duval *et al.*, 2013). They are homologous transcription factors of the AraC family of proteins that have overlapping regulons. As discussed before, SoxS is a regulator of genes involved in oxidative stress, and oxidised SoxR activates its transcription.

The *mar* (multiple antibiotic resistance) operon consists of *marRAB*. The transcriptional regulation by MarA is shown in Figure 11B. MarR represses the transcription of its operon by binding to two specific sites, sites I and II, within the operator/promoter regions in *marO* (Martin *et al.*, 1995). In the presence of certain compounds such as phenolic chemicals (Cohen *et al.*, 1993), MarR is deactivated, allowing MarA to activate the transcription by binding to a 20-bp region (*marbox*) in the promoter of the operon (Martin *et al.*, 1996).

Unlike MarA and SoxS, which are synthesised in the presence of stimuli, Rob is a DNA-binding protein that is constitutively expressed in the cell (Skarstad *et al.*, 1993). Rob is regulated post-translationally through a "sequestration-dispersal" mechanism shown in Figure 11C (Griffith *et al.*, 2009). In the absence of a stimulus, Rob is unable to bind the promoter of its regulated genes. This inactive form was proposed to be due to the C-terminal domain-mediated sequestration of Rob that blocks the N-terminal domain required for Rob-DNA binding (Kwon *et al.*, 2000). In the presence of an inducer, Rob becomes dispersed which exposes the N-terminal domain and allowing DNA binding. Unconjugated bile salts, decanoate (Rosenberg *et al.*, 2003), and dipyridyl (Rosner *et al.*, 2002) are some of the compounds that can induce Rob activation.

Although different mechanisms regulate SoxS, MarA, and Rob, they are also known to regulate each other's transcription. SoxS, MarA, and Rob can activate the *mar* operon

(Miller *et al.*, 1994; Chubiz *et al.*, 2012), and MarA and SoxS can repress Rob (McMurry *et al.*, 2010; Michán *et al.*, 2002). Activation of the SoxS-MarA-Rob regulon influences the transcription of genes involved in multiple resistance mechanisms, which include preventing the accumulation of antibiotics by increasing expression of efflux pumps (*acrAB*) and decreasing outer membrane permeability by decreasing expression of porins (*ompF*) (Chubiz *et al.*, 2011; Duval *et al.*, 2013).

1.9.3 SOS response

DNA damage in *E. coli* activates the SOS response pathways that are regulated by the action of LexA repressor. Under normal conditions, LexA binds to a 16-bp sequence, called the SOS box, usually located near or inside the RNA polymerase binding site in the promoter region of its target genes (Zhang *et al.*, 2010). The binding of LexA to the SOS box, therefore, represses the transcription of its regulon members (Figure 12) (Erill *et al.*, 2003).

The primary inducing signal for SOS response is the accumulation of single-stranded DNA (ssDNA) (Salles *et al.*, 1984). Sensing of this signal is provided by protein RecA, which binds ssDNA and forms a nucleoprotein filament that promotes the autoproteolytic cleavage of LexA (Menetski *et al.*, 1985; Craig *et al.*, 1981; Little, 1984). This event lowers the levels of LexA and derepresses the transcription of genes involved in the SOS response. Besides regulating *recA* and its own transcription, LexA also regulates more than 50 genes involved in DNA repair, DNA damage tolerance, and induction of delayed cell division (Fernández de Henestrosa *et al.*, 2000; Lewis *et al.*, 1994; Walker, 1984).

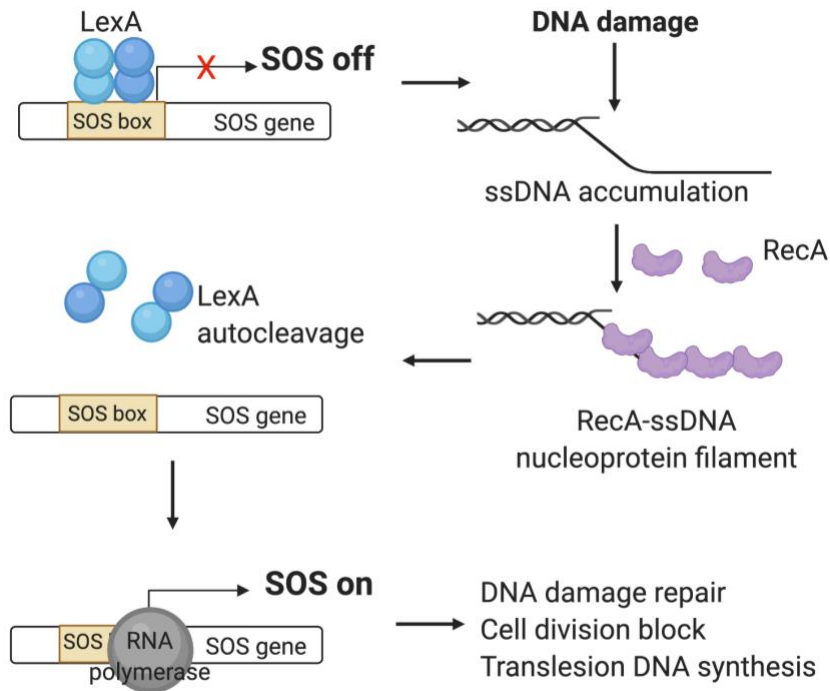


Figure 12. SOS response induction

LexA is the transcriptional repressor of SOS genes. When ssDNA accumulates due to DNA damage, RecA binds ssDNA and forms a nucleoprotein filament that stimulates LexA self-cleavage, which consequently derepresses transcription of SOS genes. Created with BioRender.com based on Figure 1 and review by Maslowska *et al.* (2019).

The SOS response allows for high fidelity DNA repair to take place first before low fidelity DNA tolerance pathways that have mutagenic potential. The first sets of genes to be induced are the nucleotide excision and homologous recombination genes (*uvrABCD*, *recA*, *ruvAB*) to repair the lesions (Moolenaar *et al.*, 2000). However, for lesions that are not easily repaired, activation of the mutagenic DNA damage tolerance pathways, such as translesion synthesis performed by the polymerases PolIII (*polB*), polIV (*dinB*), and PolV (*umuCD*), are essential to bypass the DNA damage and advance the replication fork. During SOS induction, *sulA* gene is also induced, which causes DNA damage checkpoint by inhibiting cell division and allow time for DNA repair (Trusca *et al.*, 1998).

1.9.4 Iron starvation response

Iron is an essential element in many biological processes, including cellular respiration, and energy metabolism. It is also a component of heme and Fe-S clusters, which are indispensable cofactors of enzymes with fundamental functions in these processes. However, despite the vital roles of iron in cells, it can also be toxic due to its ability to catalyse ROS production under aerobic conditions (Touati, 2000). Therefore, to achieve iron homeostasis, *E. coli* must balance the uptake of iron from its environment and manage the levels of cellular iron. In *E. coli*, the transcription factor Fur is the principal regulator of iron homeostasis (Troxell *et al.*, 2013).

Fur (Ferric Uptake Regulator) is a DNA-binding protein which uses ferrous ion (Fe^{2+}) as a corepressor and functions as a transcriptional repressor of genes in its regulon (Figure 13A). At high Fe^{2+} concentrations, Fur and Fe^{2+} form a homodimer that binds to 19-bp DNA sequences (Fur boxes) usually located in the promoter of its regulated genes, thus repressing their transcription (Bagg *et al.*, 1987; Baichoo *et al.*, 2002). In contrast, at low Fe^{2+} concentrations, the Fur- Fe^{2+} complex does not form, clearing the promoter region of the regulated genes, and allowing their transcription (Figure 13A). In addition to its role as a repressor, Fur's role as a direct and indirect activator has also been demonstrated in *E. coli* and other bacteria (Nandal *et al.*, 2010; Troxell *et al.*, 2013).

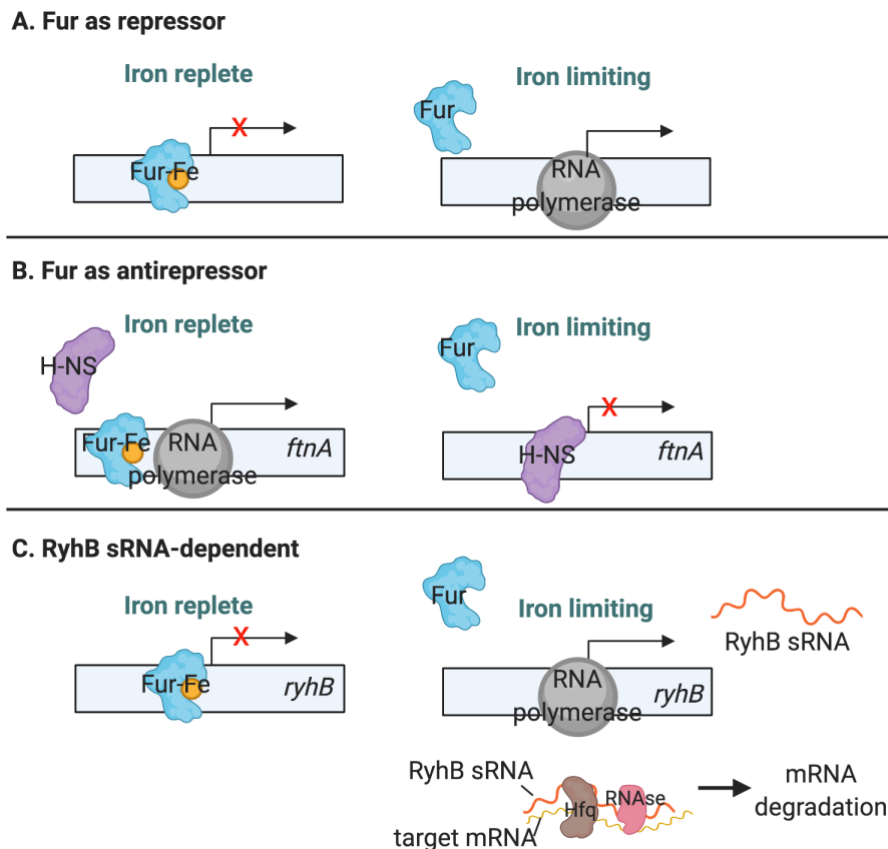


Figure 13. Iron-dependent transcriptional regulation by Fur

A) Fur regulates the transcription of its regulon by acting as a repressor with iron as its corepressor. In iron replete conditions, Fur-Fe binds to the furbox in the promoter region and prevents the transcription of the gene, while in iron limiting condition, Fur is inactive and does not bind the furbox. **B)** Fur can also act as an anti-repressor by preventing binding of another repressor. An example is the iron storage gene *ftnA*, which is repressed by H-NS. Binding of Fur-Fe to the promoter region of *ftnA* prevents repression by H-NS. **C)** RyhB sRNA, whose transcription is regulated by Fur, mediates post-transcriptional regulation of iron-utilising genes. During iron limiting conditions, *ryhB* transcription is induced. RyhB sRNA then pairs with its target mRNA and thereby prevents translation and facilitates degradation. Created with BioRender.com. Adapted from Figure 2 by Troxell *et al.* (2013) under CC BY 3.0.

During iron starvation, Fur-regulated genes are derepressed to activate pathways for iron import. Fe^{2+} are directly imported, while the insoluble ferric ion (Fe^{3+}) are imported as ferri-siderophore complexes. Another response to iron starvation is the down-regulation of genes relating to iron storage and non-essential iron-containing proteins (Seo *et al.*, 2014; McHugh *et al.*, 2003). *ftnA*, an iron storage gene, is downregulated during iron

limiting conditions with Fur acting as an anti-repressor by displacing the *ftnA* repressor, H-NS (Figure 13B) (Nandal *et al.*, 2010). Similarly, Fur can indirectly regulate the expression of iron-utilising proteins through small RNA (sRNA) RyhB (Figure 13C). RyhB, which is expressed under iron limiting conditions, pairs with its target mRNA with the help of chaperone Hfq, resulting in transcription termination of the growing mRNA or block of the translation (Massé *et al.*, 2002). In addition, RyhB recruits RNase E, which then degrades the target mRNA (Massé *et al.*, 2003). All of these mechanisms result in reduced RyhB target mRNA and gene product. The RyhB-dependent mechanism was found to regulate at least 56 genes in *E. coli* including *fumA* (fumarate hydratase), *sodB* (Fe-containing superoxide dismutase), *sdh* (succinate dehydrogenase), *isc* (Fe-S cluster synthesis), *nuo* (NADH dehydrogenase), *frd* (fumarate reductase), and *acnA* (aconitase A) (Desnoyers *et al.*, 2009; Massé *et al.*, 2002; Massé *et al.*, 2005).

Iron homeostasis pathways and oxidative stress response are interconnected. Iron starvation could be a product of a highly oxidative environment, and an oxidative environment could be a result of the iron starvation response (Cornelis *et al.*, 2011). Increased iron assimilation as a result of iron homeostasis perturbations could lead to increased iron levels that can enhance the Fenton reaction ($\text{Fe}^{2+} + \text{H}_2\text{O}_2 \rightarrow \text{Fe}^{3+} + \text{HO}\cdot + \text{OH}^-$) and lead to the production of ROS, such as the highly DNA-damaging hydroxyl radical (Imlay *et al.*, 1988). Similarly, increased ROS can result in iron limitation by oxidising Fe^{2+} to Fe^{3+} again *via* the Fenton reaction (Nunoshiba *et al.*, 1999). Therefore, the oxidative response and iron starvation response pathways are highly connected as evidenced by Fur regulation of the oxidative stress response genes *soxRS* (superoxide response) and *sodA* (Mn-containing superoxide dismutase) (Niederhoffer *et al.*, 1990).

1.9.5 Extracytoplasmic stress response

Comprising of the inner membrane, periplasmic space, and the outer membrane, the *E. coli* envelope is the interface between the intracellular and extracellular environment. It functions as a barrier against noxious chemicals and is also the site of essential processes such as respiration, nutrient transport, efflux, and adhesion (Silhavy *et al.*, 2010). Being the first barrier to the external environment, it is usually the first target of external stresses and must be able to tolerate changing conditions. *E. coli* have at least five extracytoplasmic stress response pathways that quickly sense a disruption in envelope homeostasis and repair any associated damage: Cpx, Bae, Rcs, Psp, and σ^E (Mitchell *et al.*, 2019). These response pathways have independent and overlapping induction signals and regulon members.

Cpx and Bae are classical two-component regulatory systems that rely on an inner membrane sensor (CpxA and BaeS) and a response regulator (CpxR and BaeR) (Raivio *et al.*, 1997; Raffa *et al.*, 2002). In the presence of a specific signal, the sensor histidine kinase autophosphorylates and transfers a phosphoryl group to the receiver domain of the response regulator (Figure 14AB). The response regulator becomes active and can bind DNA and regulate the expression of its regulon. One of the best-characterised roles of the Cpx response is in sensing and responding to stress due to misfolded envelope proteins, with at least 50 regulon members, some encoding chaperones and proteases involved in protein folding and degradation (Pogliano *et al.*, 1997; Price *et al.*, 2009). Other signals known to activate the Cpx response include alkaline pH (Danese *et al.*, 1998), adhesion (Otto *et al.*, 2002), and high osmolarity (Jubelin *et al.*, 2005). Bae, on the other hand, only have eight confirmed genes in its regulon: its operon (*baeSR*), multidrug efflux pumps (*mdtABC*, *mdtD*, and *acrD*), and a periplasmic protein (*spy*) (Raffa *et al.*, 2002; Baranova *et al.*, 2002; Leblanc *et al.*, 2011).

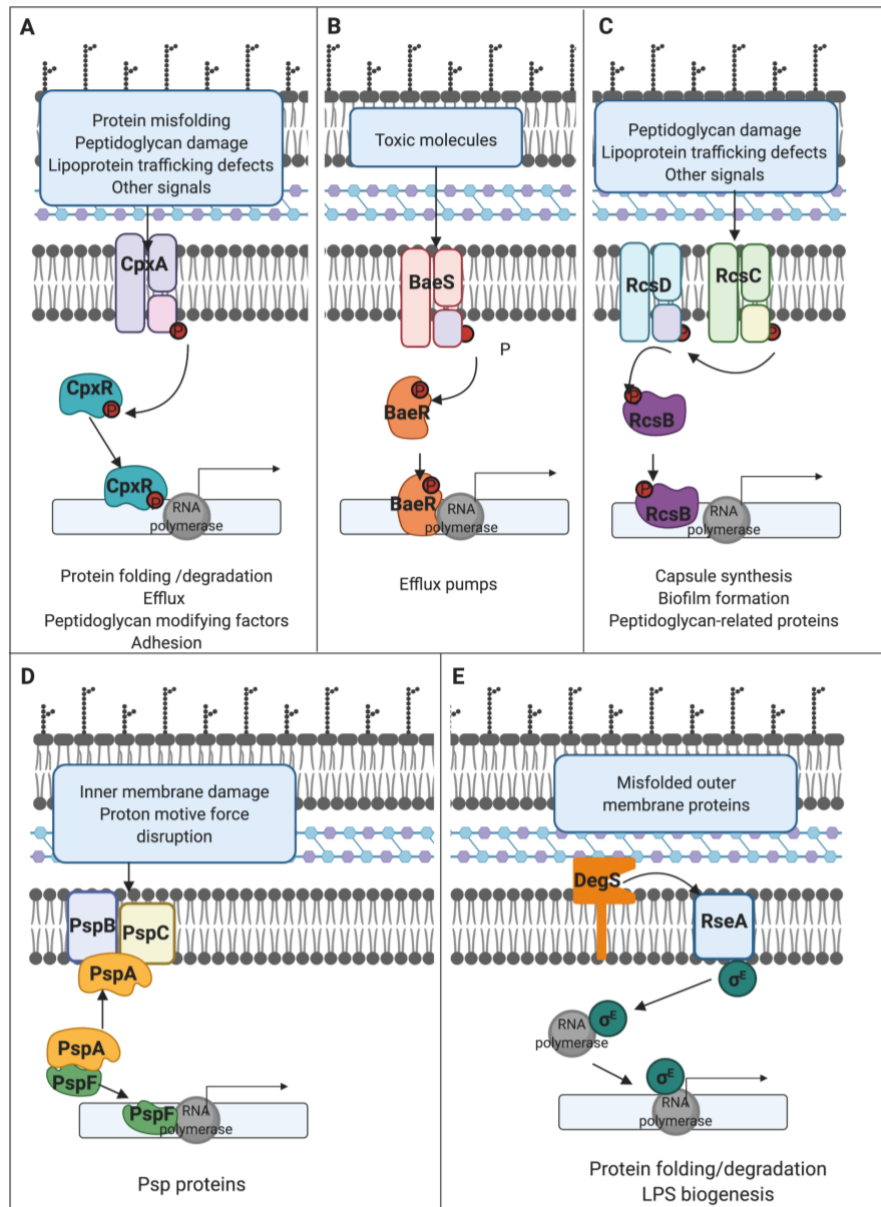


Figure 14. *E. coli* extracytoplasmic stress response systems

A, B) CpxRA and BaeRS two-component system- Inducing signals lead to the autophosphorylation of sensor CpxA or BaeS. Transfer of the phosphoryl group to the regulator CpxR or BaeR results in its activation, which allows it to bind DNA and regulate transcription of its target genes. **C)** Rcs phosphorelay system- Under inducing conditions, sensor protein RcsC autophosphorylates, then phosphorylates RcsD. RcsD, in turn, phosphorylates RcsB, leading to its activation and induction of its target genes. **D)** Psp phage shock protein system- Under inducing conditions, PspB and PspC interact with PspA, which releases PspF. PspF can then interact with RNA polymerase to induce transcription of its operon **E)** Alternative sigma factor σ^E -dependent pathway- Misfolded outer membrane proteins bind and activate protease DegS. DegS, then cleaves RseA, freeing σ^E , which can then interact with RNA polymerase to regulate expression of its target genes. Created with BioRender.com. Adapted by permission from Springer Nature: Springer Nature, Nature Reviews Microbiology. Envelope stress responses: balancing damage repair and toxicity (Figure 1), (Mitchell *et al.*, 2019), copyright 2019.

The Rcs phosphorelay system is also a two-component system, albeit more complex, with an intermediary protein RcsD between the sensor histidine kinase RcsC and the response regulator RcsB (Figure 14C) (Majdalani *et al.*, 2005). Initially determined as a regulator of colanic acid capsule synthesis (Gottesman *et al.*, 1985), the Rcs system is also activated by cell envelope stresses including exposure to β -lactam antibiotics (Laubacher *et al.*, 2008), damage to periplasmic peptidoglycan (Callewaert *et al.*, 2009), modification of peptidoglycan (Evans *et al.*, 2013), and defects in lipoprotein sorting (Tao *et al.*, 2012).

The last two systems are Psp and σ^E . Psp (phage shock response) is primarily induced by stresses that damage the inner membrane and disrupt the PMF (Jovanovic *et al.*, 2006). Under inducing conditions, inner membrane proteins PspB and PspC bind PspA to free PspF, which is normally bound by PspA (Figure 14D) (Flores-Kim *et al.*, 2016). PspF can then induce the σ^{54} -dependent transcription of the *psp* operon (Wigneshweraraj *et al.*, 2008). The Psp proteins function in repairing damage to the inner membrane and maintaining the PMF (Kobayashi *et al.*, 2007; Jovanovic *et al.*, 2006). Lastly, σ^E (sigma E) is an alternative sigma factor-dependent pathway that responds to misfolding of outer membrane proteins and stresses that ultimately lead to disruptions in outer membrane protein assembly, such as defects in LPS biosynthesis (Mecsas *et al.*, 1993; Lima *et al.*, 2013; Klein *et al.*, 2016). Inner membrane protein RseA normally sequesters σ^E (Campbell *et al.*, 2003). However, under inducing conditions such as the presence of unfolded outer membrane proteins, the protease DegS is activated and degrades RseA. σ^E is then able to interact with RNA polymerase and regulate gene expression (Figure 14D) (Ades *et al.*, 1999).

1.10 Rationale and objectives of the study

Antimicrobial resistance that renders existing antimicrobial therapies ineffective poses a significant threat to public health with an enormous social and economic burden globally. The issue is notably more severe concerning the Gram-negative bacterial pathogens than their Gram-positive counterparts since the former group is inherently resistant to many antimicrobial agents due to a highly impermeable outer membrane and a range of powerful efflux pumps (Breijyeh *et al.*, 2020). This problem is reflected in the WHO's list of priority pathogens that urgently need research and development of new antibiotics (World Health Organization, 2017). As multidrug resistance continues to emerge and spread globally, and with the current clinical development pipeline insufficient to keep pace (World Health Organization, 2019a), this problem needs to be rectified through alternative strategies, such as the revival of 'old' drugs by employing them in novel synergistic antibacterial combinations.

Previous studies in the Rakonjac lab focused on secretin channels have found secretin gate mutants that are 'leaky' to DOC and large antibiotics including Van (Spagnuolo *et al.*, 2010; Khanum, 2015). In a small molecule screen to find secretin gate-opening molecules that could sensitise *E. coli* to DOC or large antibiotics, synergy with nitrofurans was instead accidentally found. Studies have then shifted on pairwise synergies between the 'old' antibiotic nitrofurans and DOC or VAN applied to Gram-negative pathogens as an alternative strategy to tackle antimicrobial resistance. However, high concentrations of DOC and VAN in the two-drug combinations, even after the dose reduction imparted by the synergy, preclude the use of these combinations as viable treatment options for Gram-negative bacterial infections. To further improve the combination, it was hypothesised that the combination of the three antibacterials, nitrofurans, DOC, and VAN, if synergistic, will further enhance the efficacy and lower the individual doses,

which can mitigate adverse effects. Therefore, the focus of this research was to establish the combination of nitrofurans, DOC, and VAN as a potential therapy for Gram-negative bacterial infections.

The aims of this study were 1) to determine whether nitrofurans, DOC, and VAN are synergistic in Gram-negative pathogens by characterising the *in vitro* interaction in terms of growth inhibition and bacterial killing. To develop this combination into a potential therapy, understanding the mechanism of synergy is essential. The gap in the knowledge of the individual drugs' mechanisms of action in Gram-negative bacteria, however, impedes the understanding of the mechanistic bases of their synergistic interaction. Henceforth, the study also sought 2) to first determine the individual mechanisms of action of the antibacterials, followed by the 3) mechanism of synergy, by investigating the genome-wide transcriptional responses of the model Gram-negative bacterium *E. coli* to each of the antibacterials individually and in combination. Biochemical, physiological, and genetic approaches were subsequently combined to identify the roles of some key pathways hypothesised to be involved in the action and synergy of FZ, DOC, and VAN, based on the transcriptome analyses.

2 Materials and methods

2.1 Antibiotics

FZ, NIT, NFZ, and VAN were purchased from Goldbio (St. Louis, MO, USA). DOC was a kind gift from New Zealand Pharmaceuticals (Palmerston North, NZ). Dalbavancin and oritavancin were purchased from MuseChem (Fairfield, NJ, USA). Ox gall bile salts powder (Cat No. B3883) was purchased from SigmaAldrich (St. Louis, MO, USA).

2.2 Bacterial strains and growth conditions

All bacterial strains used in this study are described in Table 1. All strains were grown in trypticase soy broth at 37 °C with shaking at 200 rpm (rotations per minute), except for *E. coli* K12 laboratory strains which were grown in 2xYT medium. For *Staphylococcus*, *Streptococcus*, and *Pasteurella* strains, the growth medium was further supplemented with 5% sheep blood. For the preparation of exponential phase cells, fresh overnight culture was 100-fold diluted and incubated to reach the optical density at 600 nm (OD600) of 0.1–0.3. Unless otherwise stated, the cation-adjusted Mueller-Hinton (MH) II broth (Becton-Dickinson, USA) was used in the susceptibility testing, checkerboard, and time-kill assays. Since nitrofurans were prepared in dimethyl sulfoxide (DMSO), DMSO concentrations in the following assays were fixed to 1% or 0.1%, as stated.

The introduction of the *kan^R* gene deletion mutations into the *E. coli* K12 strain K1508 from the corresponding Keio collection *E. coli* K12 knock-out strains (Baba *et al.*, 2006) was performed using phage P1 transduction, as previously described (Thomason *et al.*, 2007). To eliminate potential polar effects on downstream genes in the operon, the FLP recombinase recognition target (FRT)-flanked *kan^R* cassette was removed using FLP-mediated recombination using plasmid pCP20 (FLP⁺, λ ci857⁺, λ p_R Rep^{ts}, Amp^R, Cm^R) (Cherepanov, 1995).

Table 1. Bacterial strains used in the study

Strains	Genotype/Description	Source
<i>E. coli</i> ATCC 25922	Antibiotic susceptibility reference/quality control strain	ATCC® 25922; NCTC 12241; NZRM 916
<i>E. coli</i> ERL034336	O157, human isolate	Dr Anne Midwinter, School of Veterinary Science, Massey University, Palmerston North, New Zealand
<i>E. coli</i> UPEC P191	Isolate from a feline urinary tract infection	New Zealand Veterinary Pathology (NZVP) diagnostic labs, Palmerston North, New Zealand
<i>E. coli</i> NZRM 4402	Plasmid-mediated AmpC β -lactamase-producing (<i>CMY-2</i>)	NZRM 4402
<i>E. coli</i> NZRM 4364	Carbapenemase (<i>IMP-4</i>) producing. Human isolate from hospital outbreak (Melbourne, Australia)	NZRM 4364
<i>E. coli</i> NZRM 4457	NDM-1 metallo- β -lactamase-producing, nitrofurantoin-resistant	ARL09/232 (Williamson <i>et al.</i> , 2012); NZRM 4457 (Olivera <i>et al.</i> , 2020)
<i>E. coli</i> NZRM 4524	Verotoxin-producing <i>E. coli</i> (VTEC). Serotype O45:H Rough	NZRM 4524
<i>Citrobacter gillenii</i> PMR001	Isolate from a municipal sewage processing (water purification) plant, Palmerston North, New Zealand	(Le <i>et al.</i> , 2020)
<i>Klebsiella pneumoniae</i> PMR001	Isolate from a municipal sewage processing (water purification) plant, Palmerston North, New Zealand	(Le <i>et al.</i> , 2020)
<i>Klebsiella pneumoniae</i> NZRM 4387	Beta-lactamase-producing. <i>SHV-11</i> , <i>TEM-1</i> , <i>CTX-M-15</i>	NZRM 4387
<i>Klebsiella pneumoniae</i> NZRM 4412	Carbapenemase-producing	ATCC® BAA-1705; NZRM 4412
<i>Klebsiella pneumoniae</i> NZRM 4498	OXA-181 carbapenemase-producing	NZRM 4498
<i>Salmonella enterica</i> sv. Typhimurium LT2	Type strain	ATCC® 43971
<i>Salmonella enterica</i> NZRM 4533	Human isolate (NZ)	NZRM 4533
<i>Shigella dysenteriae</i> NZRM 1015	Type strain	ATCC® 13313; NCTC 4837; NZRM 1015
<i>Acinetobacter lwoffii</i> NZRM 1218	Knee wound isolate (NZ)	NZRM 1218

<i>Acinetobacter baumannii</i> NZRM 3697	Human isolate from outbreak (Christchurch, NZ)	NZRM 3697
<i>Acinetobacter baumannii</i> NZRM 4408	OXA-27 carbapenemase-producing	NCTC 13304; NZRM 4408
<i>Pasteurella dagmatis</i> NZRM 959	Isolate from a feline oral cavity	NZRM 959
<i>Staphylococcus aureus</i> NZRM 3478	Methicillin-resistant. Human wound isolate (Auckland, NZ)	NZRM 3478
<i>Staphylococcus aureus</i> NZRM 4315	Human wound isolate. Erythromycin (<i>ermA</i>) resistant	ATCC® BAA-977; NZRM 4315
<i>Staphylococcus aureus</i> NZRM 4548	WR/AK1 strain. Panton-Valentine-leukocidin (PVL)-positive methicillin-resistant. Human isolate (NZ)	NZRM 4548
<i>Staphylococcus aureus</i> NZRM 4549	AK3 methicillin-resistant. Human isolate (NZ)	NZRM 4549
<i>Streptococcus pneumoniae</i> NZRM 2764	Antibiotic susceptibility reference/quality control strain	CDC 78-008107; NZRM 2764
<i>Streptococcus pyogenes</i> NZRM 4366	Exotoxin positive control	GAS 91/367; NZRM 4366
<i>E. coli</i> K12 laboratory strains	Genotype/Description	Source
BW25113	<i>rrnB3 ΔlacZ4787 hsdR514 Δ(araBAD)567 Δ(rhaBAD)568 rph-1</i>	Keio collection (Baba <i>et al.</i> , 2006) <i>kan^R</i> removed
K2578	BW25113 <i>ΔappB</i>	
K2579	BW25113 <i>ΔcyoB</i>	
K2580	BW25113 <i>ΔcydB</i>	
K2581	BW25113 <i>Δfur</i>	
K2582	BW25113 <i>Δndh</i>	
K2583	BW25113 <i>ΔnuoM</i>	
K1508	MC4100 [<i>F⁻ araD⁻ Δlac U169 relA1 spoT1 thiA rpsL (Str^R) ΔlamB106</i>]	(Spagnuolo <i>et al.</i> , 2010)
K2588	K1508 <i>ΔappB</i>	This study
K2589	K1508 <i>ΔcyoB</i>	
K2590	K1508 <i>Δfur</i>	
K2591	K1508 <i>Δndh</i>	
K2592	K2508 <i>ΔnuoM</i>	
K2600	K1508 <i>ΔcydB</i>	
K2605	K1508 <i>ΔrecA</i>	

NZRM, The New Zealand Reference Culture Collection: Medical Section

2.3 Susceptibility testing

The broth microdilution assay for antimicrobial susceptibility was performed according to the Clinical and Laboratory Standards Institute (CLSI) guidelines (Clinical and Laboratory Standards Institute, 2015) in a 384-well plate format. Each well contained 5×10^5 colony forming units (CFU)/mL in exponentially-growing phase, 1% DMSO, and the test antibacterial in a total volume of 50 μ L. Each treatment was performed in triplicate. The plate was incubated at 37 °C for 18 h for enterobacteria and *Staphylococcus*, and 24 h for *Acinetobacter* and *Streptococcus* as recommended by the CLSI guidelines (Clinical and Laboratory Standards Institute, 2015). The OD600 was measured to assess growth inhibition. The MIC is defined as the concentration that inhibits at least 90 % of growth at the endpoint (Campbell, 2011).

The CLSI guidelines were also followed for determining MIC using the agar dilution method. Briefly, 2xYT agar plates containing two-fold dilutions of test antibacterials were prepared. Onto these agar plates, 10 μ L of exponentially-growing bacterial inoculum (1×10^6 CFU/mL) were spotted in triplicate, such that each spot contains 10^4 CFU. The plates were incubated at 37 °C for 18 h before scoring, and the MIC was determined as the lowest concentration of antimicrobial agent that completely inhibits growth, disregarding a single colony or a faint haze caused by the inoculum.

2.4 Checkerboard assay

The synergy between the test antibacterials was examined using growth inhibition three-dimensional checkerboard microdilution assay in 384-well plates according to the CLSI guidelines (Clinical and Laboratory Standards Institute, 2015). Two-fold dilutions with a concentration range of $2 \times \text{MIC}$ to $0.06 \times \text{MIC}$ of the antibacterials and exponential-phase bacteria were prepared in BBL™ cation-adjusted MH II broth (Becton-Dickinson,

Sparks, MD, USA). Each well contained 5×10^5 CFU/mL, 1% DMSO, and the antibacterials in a total volume of 50 μ L. Each plate was incubated at 37 °C for the required time according to CLSI guidelines, and the OD600 was measured to quantify growth (Campbell, 2011). Each combination of concentrations was performed in triplicate and the mean growth inhibition was used to determine MIC values, which correspond to concentrations of combinations that result in at least 90% of growth inhibition. Fractional inhibitory concentration index (FICI) was calculated using the equation (Stein *et al.*, 2015):

$$FICI = \frac{MIC_{\text{nitrofurantoin}(\text{com})}}{MIC_{\text{nitrofurantoin}(\text{alone})}} + \frac{MIC_{\text{DOC}(\text{com})}}{MIC_{\text{DOC}(\text{alone})}} + \frac{MIC_{\text{VAN}(\text{com})}}{MIC_{\text{VAN}(\text{alone})}}$$

where $MIC_{\text{nitrofurantoin}(\text{com})}$, $MIC_{\text{DOC}(\text{com})}$, and $MIC_{\text{VAN}(\text{com})}$ is the MIC of nitrofurantoin, DOC, and VAN when used in combination and $MIC_{\text{nitrofurantoin}(\text{alone})}$, $MIC_{\text{DOC}(\text{alone})}$, and $MIC_{\text{VAN}(\text{alone})}$ is the MIC when used alone. Using the lowest FICI, the interactions were interpreted as synergistic if $FICI \leq 0.5$; indifferent if $0.5 < FICI \leq 4.0$ and antagonistic if $FICI > 4.0$ (Odds, 2003).

2.5 Time-kill assay

Exponentially-growing bacterial cultures were prepared at 5×10^5 CFU/mL and treated with individual antibacterial agents (FZ, DOC, VAN) or combinations thereof at specified concentrations in a final volume of 10 mL. The cultures treated with 1% DMSO were included as vehicle controls. Each treatment was performed in triplicate. The bacterial cultures were incubated at 37 °C with shaking at 200 rpm. At time points 0, 2, 4, 6, 8, and 24 h, 500 μ L was sampled from each culture and centrifuged at $10,000 \times g$ for 1 min. The pellet was then resuspended in 100 μ L of the maximum recovery diluent (0.1% peptone, 0.85% sodium chloride (NaCl), and 10-fold serial dilutions were drop-plated (10 μ L) on

2xYT agar. Plates were incubated at 37 °C overnight before counting colonies. The limit of detection is 60 CFU/mL or 1.78 log₁₀ CFU/mL. The synergy of the combination was defined as $\geq 2\log_{10}$ decrease in the cell count (CFU/mL) compared to the most potent single drug at 24 h.

2.6 MTT assay for cellular viability

Human embryonic kidney 293T (HEK293T) cells were grown in Gibco® Dulbecco's Modified Eagle Medium (Thermo Fisher Scientific, USA) supplemented with 10% fetal bovine serum (Moregate Biotech, New Zealand) at 37 °C in a 5% CO₂ atmosphere. HEK293T cells were first seeded into a 384-well plate at 1000 cells per well and incubated for 24 h. Two-fold serial dilutions of the test antibacterial(s) were then added into the cell culture, followed by 48 h incubation. Each treatment was prepared in triplicate, and the cultures without test antibacterials were included as negative controls. After incubation, MTT (3-[4,5-dimethylthiazol-2-yl]-2,5-diphenyltetrazolium bromide, Thermo Fisher Scientific, USA) was added at a final concentration of 0.5 mg/mL, and the plate was incubated at 37 °C for 2 h. The purple formazan crystals resulting from the MTT reduction were solubilised using SDS-HCl solution (10% w/v sodium dodecyl sulfate (SDS), 10 mM hydrochloric acid). After overnight incubation at 37 °C, the absorbance of the samples at 570 nm was recorded. Percentage inhibition were calculated, and a dose-response curve was fitted using the drc (v3.0-1) R package (Ritz *et al.*, 2016). From the fitted curves, 20%, 50%, and 90% inhibitory concentrations (IC₂₀, IC₅₀, IC₉₀), were then determined. The interaction of the antimicrobial agents was assessed using the FICI equation above, substituting inhibitory concentration (IC₂₀, IC₅₀, IC₉₀) values for MIC.

2.7 IC₅₀ (half-maximal (50%) inhibitory concentration) determination for transcriptome study

The IC₅₀ determination was performed in 384 well plates using exponentially-growing *E. coli* K1508 and two-fold drug dilutions prepared in 2xYT medium. Each well contained a starting inoculum of approximately 1×10^6 CFU/mL, 1% DMSO, and test antibacterial(s), in a final volume of 50 μ L. Negative control (vehicle only-1% DMSO) and media-only control (blank) were included. The plate was incubated at 37 °C for 24 h, and OD600 was read using Multiskan™ GO Microplate Spectrophotometer. The % inhibition was calculated using the following equation:

$$\% \text{ inhibition} = \left(1 - \frac{\text{Sample}_{\text{OD600}} - \text{Blank}_{\text{OD600}}}{\text{Negative Control}_{\text{OD600}} - \text{Blank}_{\text{OD600}}}\right) \times 100$$

The r package drc v. 3.0-1 (Ritz *et al.*, 2016) was used to plot the concentration-response (% inhibition) curves fitted with the four-parameter log-logistic model to determine the IC₅₀.

2.8 Total RNA extraction

Exponentially-growing cultures of the *E. coli* strain K1508 at 5×10^7 CFU/mL were treated with antibacterial(s) in a final volume of 25 mL. The DMSO concentration for all treatments were fixed at 0.1%. After incubation at 37 °C with shaking at 200 rpm for 1 h, the cultures were then harvested by centrifugation at 5000 \times g for 10 min, and the resulting pellet was subjected to phenol (pH 4.45)-chloroform RNA extraction, as follows:

The pellet was resuspended in 1 mL of resuspension buffer (20 mM sodium acetate (NaOAc) pH 5.5, 1 mM ethylenediaminetetraacetic acid (EDTA), 1% SDS) and

transferred to a 1.5 mL microtube containing an equal volume of phenol: chloroform (1:1) and 0.2 g of 425-600 μm acid-washed beads (Sigma-Aldrich). The samples were vortexed at top speed for 90 sec to lyse the cells. The phases were then separated by centrifugation (5 min, 3000 $\times g$, 4 $^{\circ}\text{C}$), and the aqueous phase was transferred to a 1.5 mL microtube containing an equal volume of phenol: chloroform (1:1). The aqueous phase was separated again and was washed a final time by chloroform extraction. The RNA was then precipitated by adding to the aqueous phase 1/10 volume of 3 M NaOAc pH 7.0 and 2.5 volumes of ethanol. The tube was mixed by inversion and allowed to precipitate at -80 $^{\circ}\text{C}$ overnight. The precipitated RNA was collected by centrifugation (30 min, 13000 $\times g$, 4 $^{\circ}\text{C}$), and the pellet was dissolved in diethylpyrocarbonate (DEPC)-treated water. The extracted RNA samples were subjected to DNase digest using RNase-free DNase I (Roche Applied Science) according to the manufacturer's instructions. The RNA was recovered using the phenol-chloroform-based method as described above (2 \times phenol: chloroform, 1 \times chloroform extractions, and ethanol precipitation), followed by being dissolved and stored in Tris-EDTA buffer pH 8.

RNA quantification and quality analysis were performed using Qubit RNA BR Assay (Life Technologies, Thermo Fisher Inc.) and LabChip GX nucleic acid analyzer (Caliper Life Sciences, PerkinElmer), respectively.

2.9 RNA sequencing

The RNA samples were sent to Novogene Co., Ltd. (Beijing, China) for library preparation and sequencing. Using 3 μg total RNA per sample, rRNA was first depleted from the total RNA using the Ribo-ZeroTM magnetic kit (Illumina) following the manufacturer's protocol. A total of 50 ng of the rRNA-depleted RNA per sample were used to construct cDNA libraries using NEBNext[®] UltraTM Directional Library Prep Kit

for Illumina® (New England Biolabs, USA). The resulting complementary DNA (cDNA) libraries were quality checked using Agilent 2100 Bioanalyzer, then quantified using quantitative PCR (qPCR). The libraries were subsequently subjected to 150-bp paired-end sequencing on the Illumina HiSeq 2500 platform, producing approximately 20 million paired-end reads for each library.

2.10 RNA-seq data analysis

The raw sequencing data were filtered by Novogene using their in-house Perl scripts, which included removing adapters, removing reads containing N > 10%, and removing reads containing low-quality base (Qscore \leq 5) which is over 50% of the total base.

Prior to analysing the data, the quality of the reads was checked using FastQC v0.11.7-5 (Andrews, 2010). The RNA sequencing reads (Appendix B, Supplementary files 6-13) were mapped against the *E. coli* K1508 genome (Appendix B, Supplementary file 1) using HISAT2 v2.1.0 (Kim *et al.*, 2015). The resulting mapping files in SAM format were sorted and converted to BAM format using SAMtools v1.7 (Li *et al.*, 2009). The number of reads that mapped to a gene was then counted using featureCounts v1.6.0 (Liao *et al.*, 2013).

To explore variability between and within treatment groups, a principal component analysis was performed using the plotPCA function of DESeq2 (v1.26.0) R package (Love *et al.*, 2014) on the regularised log-transformed normalised counts for all the genes of all the samples. The PCA was then visualised graphically using ggplot2 v3.3.0 (Wickham, 2016).

Differential expression analysis was performed using DESeq2 (Appendix B, Supplementary file 3). For genes with low counts or high variability, log₂ fold change (log₂FC) estimates will be higher and are not representative of gene expressions. To have

a better representation of gene rankings by effect size, log₂FC were shrunk using the apegglm shrinkage estimator v1.8.0 (Zhu *et al.*, 2018). Differentially expressed genes (DEG) were defined as genes with an adjusted p-value [multiple test adjustment using the Benjamini-Hochberg method (Benjamini *et al.*, 1995)] of less than 0.01, and shrunken fold changes greater than 1.5 ($|\log_2\text{FC}| > 0.58$).

Gene Ontology (GO) term analysis was performed on the DEGs using PANTHER 15.0 (Protein ANalysis THrough Evolutionary Relationships) (Mi *et al.*, 2018). The statistical overrepresentation test was performed using the Fisher's Exact test with Benjamini-Hochberg false discovery rate (FDR) multiple test correction. The significantly overrepresented GO terms were selected using an FDR cutoff of 0.05.

K means clustering was performed on regularised-log transformed normalised counts. *A priori*, a model-based optimal K number was determined according to Bayesian Information Criterion using the Mclust function of the mclust (v5.4.6) R package (Scrucca *et al.*, 2016). The K means clustering was visualised as a heatmap generated using the pheatmap (v1.01.12) R package (Kolde, 2019).

2.11 Metal concentration analysis by ICP-MS

Antibiotic-treated *E. coli* cultures in a total volume of 80 mL were prepared the same way as the RNA samples described above. After antibiotic treatment, samples were collected and prepared for inductively coupled plasma mass spectrometry (ICP-MS), as previously described (Williams *et al.*, 2019). Briefly, cells were harvested by centrifugation (5000 ×g, 10 min), then washed twice with 25 mL phosphate buffered saline (PBS) containing 0.5 mM EDTA, then twice with PBS. All samples were adjusted to a cell number of 2×10^9 CFU based on their OD₆₀₀ values. Washed cell pellets were then digested with 500 µL of 70% (wt/vol) nitric acid ($\geq 99.999\%$ trace metals basis) at 80 °C overnight. Each

sample was diluted 1:20 in Milli-Q H₂O (18.2 MΩ), giving a final acid matrix of 3.5%. The samples were then sent to The University of Waikato Mass Spectrometry Facility for analysis of metal content by ICP-MS on an Agilent 8900 system.

2.12 Oxygen consumption

E. coli K1508 was cultured in 2xYT and cells at OD₆₀₀ of 0.3 were treated with FZ, VAN, and DOC, alone and in combination at 37 °C for 1 h. Cells were then diluted in air-saturated 2xYT to OD₆₀₀ of 0.2, and dissolved oxygen was measured in a closed chamber with constant stirring using a Clark-type oxygen electrode (Rank Brothers Ltd.) linked to a chart recorder (Vernier LabQuest Mini). The electrode was calibrated using air-saturated 2xYT medium (~220 nmol/mL) and sodium dithionite (0 nmol/mL).

2.13 Mutagenicity assay

Exponentially-growing *E. coli* K1508 at 1×10^7 CFU/mL were treated with FZ, VAN, and DOC, alone and in combination in a final volume of 10 mL in 2xYT medium. The cultures were incubated at 37 °C with shaking at 200 rpm for 24 h. The cultures were then centrifuged at 5000 ×g for 10 min and resuspended in maximum recovery diluent (0.1% peptone, 0.85% NaCl). Serial dilutions were made and plated in triplicate onto 2xYT agar containing 100 µg/mL rifampicin to select for rifampicin-resistant colonies, and on non-selective 2xYT agar to count the total number of colonies. The plates were scored after 24 h incubation at 37 °C. The mutation frequency was calculated by dividing the number of rifampicin-positive colonies by the total number of colonies from 9-11 biological replicates.

2.14 Ethidium bromide accumulation and efflux

The ethidium bromide accumulation assay was performed as previously described (Viveiros *et al.*, 2008). Briefly, *E. coli* K1508 cultured in 2xYT was centrifuged at 5000 \times g for 10 min and resuspended in MOPS media (Neidhardt *et al.*, 1974) supplemented with 0.4% glucose and 0.1% casamino acids (MOPS-G-CA). Cells at OD600 of 0.3 were then dispensed in triplicate into a black 96-well plate containing FZ, VAN, and DOC alone and in combination, and 0.125 μ g/mL ethidium bromide. Fluorescence (544/590 nm) was monitored at 37 °C every 2 min for 1 h using the FluoStar Galaxy fluorescence microplate reader (BMG Labtech). Carbonyl cyanide m-chlorophenylhydrazine (CCCP) at 5 μ g/mL was used as a positive control.

For the efflux assay, *E. coli* K1508 cells were first loaded with ethidium bromide by incubating with 5 μ g/mL ethidium bromide and 5 μ g/mL CCCP at 37 °C with shaking at 200 rpm for 1 h. The bacteria were then centrifuged (5000 \times g, 10 min), washed with PBS, and resuspended in MOPS-G-CA. Cells were dispensed in triplicate into a 96-well plate containing FZ, DOC, and VAN alone and in combination, and the fluorescence monitored as described above.

**3 *In vitro* characterisation of nitrofurans,
vancomycin, and sodium deoxycholate
synergy against Gram-negative pathogens**

3.1 Introduction

Studies in our laboratory have identified pairwise synergies between nitrofurans and DOC or VAN against *E. coli* in a small-molecule screen. The synergy enhanced the efficacy and lowered inhibitory concentrations of the individual components. The combinations, therefore, have the potential of expanding the use of normally Gram-positive-only antibacterials, VAN and DOC, to Gram-negative bacteria. To further improve the combination in terms of efficacy and dose reduction to mitigate adverse effects, the three-way interaction of nitrofurans, VAN, and DOC was investigated. Since all these antibacterials are currently approved for clinical use in human indications, repurposing them will have the advantage of already having established toxicity studies which can accelerate the development timeline for this therapy.

This chapter demonstrates the *in vitro* synergy between nitrofurans, VAN, and DOC in the growth inhibition and killing of a range of clinical Gram-negative pathogenic isolates, including multidrug-resistant and carbapenemase-producing bacteria for which new therapies are urgently needed (World Health Organization, 2017). To explore the possibility of using the combination in treating WHO priority Gram-positive pathogens (e.g. MRSA), the interaction of these three antimicrobials was also evaluated in Gram-positive bacteria. Additionally, it was investigated whether the same synergistic effect can be achieved with other glycopeptides instead of VAN or a combination of bile salts instead of DOC. Lastly, the *in vitro* interaction of the antibacterials against mammalian cells was investigated.

3.2 Results

3.2.1 Susceptibility testing

The interaction of nitrofurans, VAN, and DOC was assessed on a range of lab strains and clinical isolates selected from the New Zealand Reference Culture Collection (NZRM) held by the Institute of Environmental Science and Research (ESR, New Zealand). A range of clinically relevant multidrug resistant strains, specifically those that are listed as priority pathogens by WHO (World Health Organization, 2017), were tested. These included enterobacteria and *Acinetobacter baumannii* harbouring carbapenem genes (*A. baumannii* NZRM 4408, *E. coli* NZRM 4364, *K. pneumoniae* NZRM 4412 and NZRM 4498) and β -lactam resistance genes (*E. coli* NZRM 4402 and NZRM 4457, *K. pneumoniae* NZRM 4387), and MRSA (NZRM 3478, NZRM 4548, NZRM 4549). The susceptibility of the strains were first determined according to the CLSI guidelines and the MIC for nitrofurans, DOC, and VAN are summarised in Table 2.

Table 2. Minimum inhibitory concentrations

Strain	MIC (µg/mL)					
	FZ	DOC	VAN	NIT	NFZ	CM4
Gram-negative						
<i>E. coli</i> ATCC 25922	1.25	80000	500	16	8	16
<i>E. coli</i> NZRM K1508	1.25	>80000	250	16	8	4
<i>E. coli</i> ERL034336	1.25	80000	250	16	8	32
<i>E. coli</i> UPEC P191	1.25	80000	250	16	8	16
<i>E. coli</i> NZRM 4364	0.25	>80000	125	NT	NT	NT
<i>E. coli</i> NZRM 4402	0.625	40000	500	NT	NT	NT
<i>E. coli</i> NZRM 4457	>128	80000	250	128	64	>128
<i>E. coli</i> NZRM 4524	1.25	80000	500	NT	NT	NT
<i>C. gillenii</i> PMR001	5	80000	500	16	16	32
<i>K. pneumoniae</i> PMR001	1.25	80000	1000	64	32	>64
<i>K. pneumoniae</i> NZRM 4387	2.5	80000	2000	NT	NT	NT
<i>K. pneumoniae</i> NZRM 4412	32	80000	2000	>128	128	>128
<i>K. pneumoniae</i> NZRM 4498	16	>80000	2000	>128	64	>128
<i>S. enterica</i> sv. Typhimurium LT2	2.5	40000	500	16	8	16
<i>S. enterica</i> NZRM 4533	2	80000	1000	32	8	8
<i>S. dysenteriae</i> NZRM 1015	4	>80000	250	8	8	4
<i>A. lwoffii</i> NZRM 1218	16	40000	62.5	NT	NT	NT
<i>A. baumannii</i> NZRM 3697	32	80000	125	NT	NT	NT
<i>A. baumannii</i> NZRM 4408	>128	80000	250	>128	32	>128
<i>P. dagmatis</i> NZRM 959	2	1250	31.25	4	4	16
Gram-positive						
<i>S. aureus</i> NZRM 3478	4	312.50	2	NT	NT	NT
<i>S. aureus</i> NZRM 4315	2	625	1	NT	NT	NT
<i>S. aureus</i> NZRM 4548	2	625	1	NT	NT	NT
<i>S. aureus</i> NZRM 4549	2	625	1	NT	NT	NT
<i>S. pyogenes</i> NZRM 4366	16	156.25	0.78	NT	NT	NT
<i>S. pneumoniae</i> NZRM 2764	2	625	0.78	NT	NT	NT

MIC, minimum inhibitory concentration; FZ, furazolidone; DOC, sodium deoxycholate; VAN, vancomycin; NIT, nitrofurantoin; NFZ, nitrofurazone; NT, not tested.

3.2.2 Nitrofurans, VAN, and DOC synergy against Gram-negative pathogens

Growth-inhibition checkerboard assays were performed to evaluate the synergy between nitrofurans, VAN, and DOC against a range of Gram-negative bacteria. As a proof of concept that the nitrofurans, as an antibiotic class, is synergistic with VAN and DOC, the antibacterial effect of the combinations of these two agents with either of the four nitrofurans (FZ, NIT, NFZ, and CM4) was evaluated in a checkerboard assay against the reference strain *E. coli* ATCC 25922. All four nitrofurans were found to be synergistic with DOC and VAN, with FICIs ranging from 0.11 to 0.15 (Appendix A, Figure A- 1).

Among the nitrofurans included in this study, FZ is the most potent against the strains tested (Table 2). Therefore, FZ was chosen as a representative of the nitrofurans in the expanded strain profiling by checkerboard and time-kill assays. The FICIs for the two-drug and three-drug combinations of FZ, VAN, and DOC are listed in Table 3. For some of the strains, where the MIC could not be determined, the FICI was calculated using the highest tested concentration. In this case, the actual FICI would be lower than the calculated value, and for some strains, it may not be possible to classify an interaction when the calculated FICI is bordering between synergistic and indifferent, such as in *E. coli* NZRM 4457.

FZ, VAN, and DOC combination was synergistic against 15 strains, indifferent against four strains (*S. enterica* sv. Typhimurium LT2, *K. pneumoniae* PMR001, *K. pneumoniae* NZRM 4412, and *P. dagmatis* NZRM 959), and unable to be classified as synergistic or indifferent against one strain (*E. coli* NZRM 4457). Of importance is the synergy of the combination against some of the WHO critical priority pathogens, carbapenemase-producing *E. coli* NZRM 4364 and *A. baumannii* NZRM 4408, and ESBL-producing *K. pneumoniae* NZRM 4387 (Table 3).

Table 3. Minimum inhibitory concentrations and fractional inhibitory concentration indices for the most synergistic two-drug and three-drug combinations of FZ, VAN, and DOC against Gram-negative strains identified in a checkerboard assay

Strain	FZ+DOC		FICI	FZ+VAN		FICI	DOC+VAN		FICI	FZ+VAN+DOC			FICI
	Concentration ^a ($\mu\text{g/mL}$)			Concentration ^a ($\mu\text{g/mL}$)			Concentration ^a ($\mu\text{g/mL}$)			Concentration ^a ($\mu\text{g/mL}$)			
	FZ	DOC		FZ	VAN		DOC	VAN		FZ	VAN	DOC	
<i>E. coli</i> ATCC 25922	0.16 (8-fold) ^a	2500 (32-fold)	0.16	0.31 (4-fold)	250 (2-fold)	0.75	1250 (64-fold)	250 (2-fold)	0.52	0.08 (16-fold)	10 (50-fold)	2500 (32-fold)	0.11
<i>E. coli</i> K1508	0.31 (4-fold)	20000 (>4-fold)	<0.50*	0.63 (2-fold)	62.5 (4-fold)	0.75	625 (>128-fold)	250 (0-fold)	<1.01*	0.31 (4-fold)	31.25 (8-fold)	10000 (>8-fold)	<0.50
<i>E. coli</i> ERL034336	0.31 (4-fold)	1875 (42-fold)	0.27	0.31 (4-fold)	62.5 (4-fold)	0.50	937.5 (85-fold)	250 (0-fold)	1.01	0.16 (8-fold)	31.25 (8-fold)	3750 (21-fold)	0.30
<i>E. coli</i> UPEC P191	0.16 (8-fold)	5000 (16-fold)	0.19	0.63 (2-fold)	62.5 (4-fold)	0.75	2500 (32-fold)	62.5 (4-fold)	0.28	0.08 (16-fold)	10 (25-fold)	5000 (16-fold)	0.17
<i>E. coli</i> NZRM 4364	0.06 (4-fold)	5000 (>16-fold)	<0.31*	0.06 (4-fold)	25 (5-fold)	0.45	1250 (64-fold)	62.5 (2-fold)	<0.52*	0.01 (32-fold)	31.25 (4-fold)	5000 (>16-fold)	<0.35*
<i>E. coli</i> NZRM 4402	0.04 (16-fold)	5000 (8-fold)	0.19	0.16 (4-fold)	125 (2-fold)	0.75	5000 (8-fold)	25 (20-fold)	0.23	0.01 (64-fold)	25 (20-fold)	5000 (8-fold)	0.19
<i>E. coli</i> NZRM 4457	4 (>32-fold)	40000 (2-fold)	<0.53*	1 (128-fold)	250 (0-fold)	<1.01*	625 (128-fold)	250 (0-fold)	1.01	32 (2-fold)	10 (25-fold)	20000 (4-fold)	<0.54*
<i>E. coli</i> NZRM 4524	0.16 (8-fold)	2500 (16-fold)	0.19	0.31 (4-fold)	25 (10-fold)	0.35	1250 (32-fold)	125 (2-fold)	0.53	0.08 (16-fold)	10 (25-fold)	2500 (16-fold)	0.17
<i>C. gillenii</i> PMR001	0.63 (8-fold)	3750 (21-fold)	0.17	1.25 (4-fold)	125 (4-fold)	0.5	937.5 (85-fold)	250 (2-fold)	0.51	0.625 (8-fold)	62.5 (8-fold)	1875 (42-fold)	0.27

<i>K. pneumoniae</i> PMR001	1.25 (0-fold)	625 (128- fold)	1.01	0.625 (2-fold)	31.25 (32-fold)	0.53	625 (128- fold)	1000 (0-fold)	1.01	0.21 (4-fold)	250 (4-fold)	625 (128- fold)	0.51
<i>K. pneumoniae</i> NZRM 4387	0.625 (4-fold)	5000 (16-fold)	0.31	1.25 (2-fold)	250 (8-fold)	0.63	625 (128- fold)	2000 (0-fold)	1.01	0.31 (8-fold)	250 (8-fold)	2500 (32-fold)	0.28
<i>K. pneumoniae</i> NZRM 4412	16 (2-fold)	40000 (2-fold)	1	16 (2-fold)	1000 (2-fold)	1	2500 (32-fold)	1000 (2-fold)	0.53	1 (32-fold)	1000 (2-fold)	1250 (64-fold)	0.54
<i>K. pneumoniae</i> NZRM 4498	8 (2-fold)	1250 (>64- fold)	<0.52*	4 (4-fold)	250 (8-fold)	0.38	625 (>128- fold)	2000 (0-fold)	<1.01*	2 (8-fold)	250 (8-fold)	2500 (>64- fold)	< 0.26*
<i>S. enterica</i> sv. Typhimurium LT2	0.63 (4-fold)	2500 (16-fold)	0.31	1.25 (2-fold)	31.25 (16-fold)	0.56	625 (64-fold)	500 (0-fold)	1.02	0.63 (4-fold)	125 (4-fold)	1250 (32-fold)	0.53
<i>S. enterica</i> NZRM4533	0.5 (4-fold)	10000 (8-fold)	0.38	0.5 (4-fold)	250 (4-fold)	0.5	40000 (2-fold)	500 (2-fold)	1	0.25 (8-fold)	20 (50-fold)	10000 (8-fold)	0.27
<i>S. dysenteriae</i> NZRM 1015	0.63 (8-fold)	10000 (>8-fold)	< 0.25*	1.25 (4-fold)	62.5 (4-fold)	0.5	1250 (>64- fold)	125 (2-fold)	<0.52*	0.63 (8-fold)	31.25 (8-fold)	2500 (>32- fold)	< 0.28*
<i>A. lwoffii</i> NZRM 1218	2 (8-fold)	5000 (8-fold)	0.25	8 (2-fold)	20 (3-fold)	0.82	2500 (16-fold)	25 (2.5- fold)	0.46	1 (16-fold)	10 (6-fold)	2500 (16-fold)	0.29
<i>A. baumannii</i> NZRM 3697	8 (4-fold)	2500 (32-fold)	0.28	16 (2-fold)	31.25 (4-fold)	0.75	625 (64-fold)	125 (0-fold)	1.02	8 (4-fold)	5 (25-fold)	1250 (32-fold)	0.32
<i>A. baumannii</i> NZRM 4408	4 (>32- fold)	2500 (16-fold)	< 0.09*	8 (>16- fold)	125 (2-fold)	0.56	312.5 (128- fold)	250 (0-fold)	1.01	8 (>16- fold)	7.81 (32-fold)	1250 (32-fold)	< 0.13*
<i>P. dagmatis</i> NZRM 959	0.5 (4-fold)	625 (2-fold)	0.75	1 (2-fold)	7.81 (4-fold)	0.75	625 (2-fold)	3.91 (8-fold)	0.63	0.06 (32-fold)	3.91 (8-fold)	625 (2-fold)	0.66

*, MIC is higher than the highest tested concentration which was used to calculate the FICI, therefore actual FICI is lower than calculated value; Values in **bold** indicate synergy (FICI ≤ 0.5); a, fold dose reduction compared to MIC when used alone are shown in brackets; FZ, furazolidone; DOC, sodium deoxycholate; VAN, vancomycin; FICI, fractional inhibitory concentration index.

To further investigate the interaction between FZ, VAN, and DOC in terms of bacterial killing, time-kill assays were performed on some representative pathogens for which the triple combination showed growth inhibition synergy in the checkerboard assay. The strains were exposed to sub-inhibitory concentrations of FZ, VAN, and DOC or two-drug and three-drug combinations of these concentrations over a time course of 24 h. The time-kill analysis for *E. coli* ATCC 25922, *S. dysenteriae* NZRM 1015, *C. gillenbergii* PMR001, and *A. baumannii* NZRM 3697 are shown in Figure 15. Combination of subinhibitory concentrations of FZ, VAN, and DOC resulted in $> 2\log_{10}$ reduction in viable cell count after 24-h exposure in comparison with the most active single drug, demonstrating the synergy in the bacterial killing of the three-drug combination in these strains. In these four examples, the triple combination led to the extinction of the challenged bacterial population at the end of the assay (a.k.a. below the limit of detection), that was not achieved by single drugs or double combinations at the same concentrations.

Time-kill assay for the three multidrug-resistant pathogens, *E. coli* NZRM 4364, *A. baumannii* NZRM 4408, and *K. pneumoniae* NZRM 4387 was performed and shown in Figure 16. Interestingly, bactericidal synergy was still retained against these strains, though the effect was less profound than against the drug-sensitive strains (Figure 15)

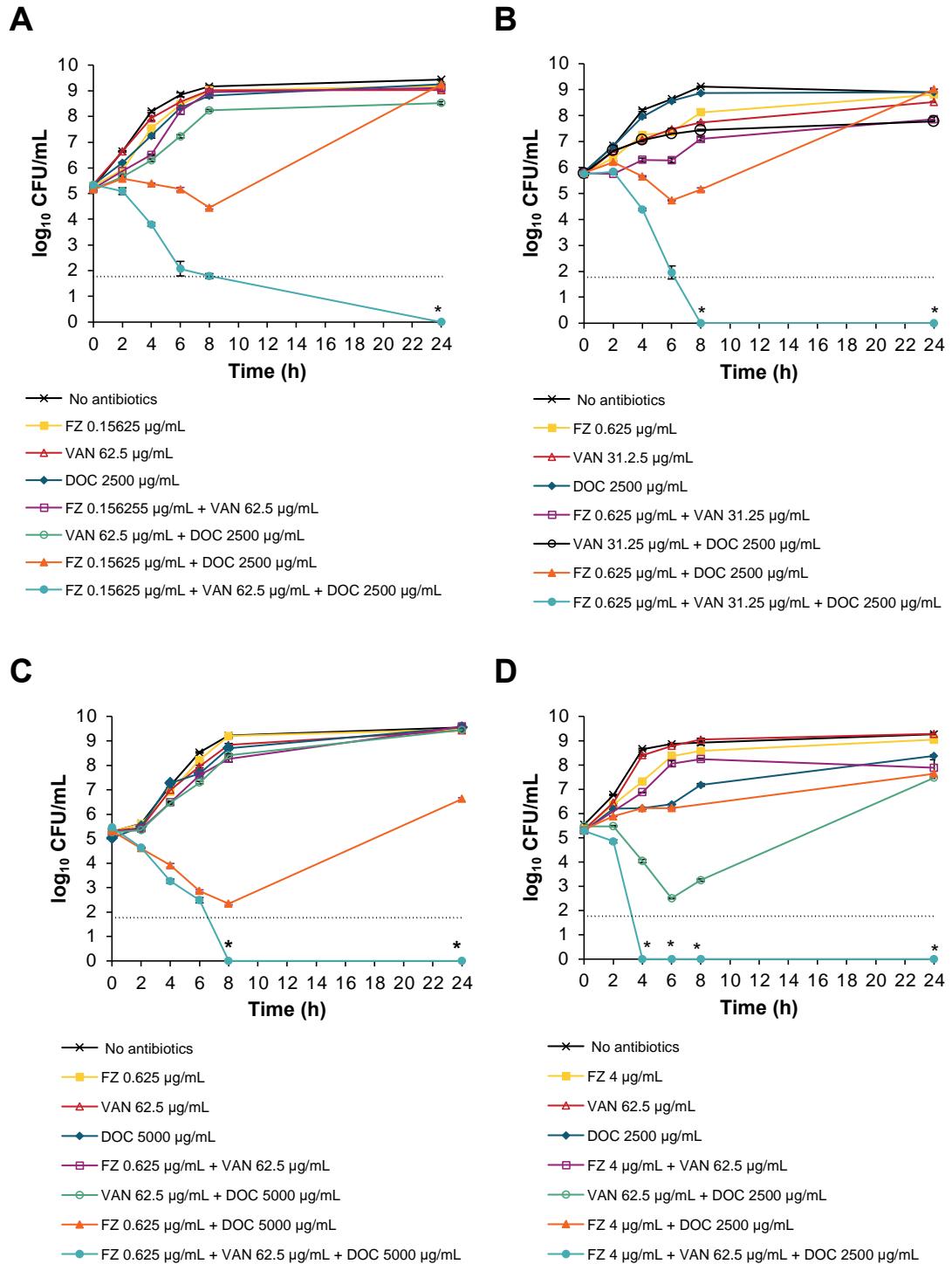


Figure 15. Time-kill analysis of FZ, VAN, and DOC combinations in killing (A) *E. coli* ATCC 25922, (B) *S. dysenteriae* NZRM 1015, (C) *C. gillenii* PMR001, and (D) *A. baumannii* NZRM 3697.

The data is presented as mean \pm standard error of the mean (SEM) of three independent measurements. The lower limit of detection was 60 CFU/mL; asterisk (*) indicates a data point that is below the limit of detection.

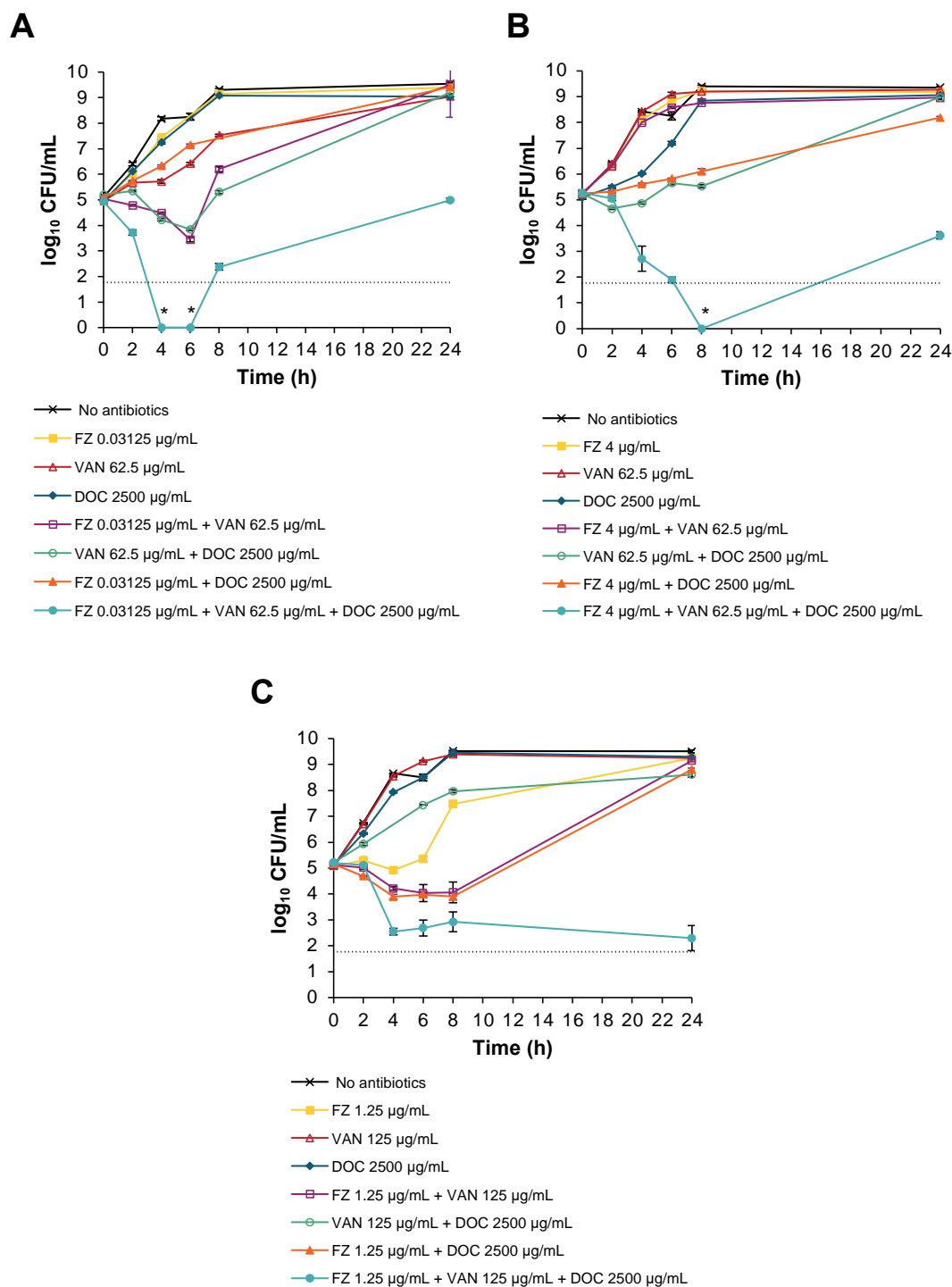


Figure 16. Time-kill analysis of FZ, VAN, and DOC combinations in killing carbapenemase-producing (A) *E. coli* NZRM 4364 and (B) *A. baumannii* NZRM 4408, and (C) multidrug-resistant ESBL-producing *K. pneumoniae* NZRM 4387.

The data is presented as mean \pm standard error of the mean (SEM) of three independent measurements. The lower limit of detection was 60 CFU/mL; asterisk (*) indicates a data point that is below the limit of detection.

3.2.3 Indifferent interaction of FZ, DOC, and VAN against Gram-positive bacteria

VAN is not the first choice for the treatment of Gram-positive infections due to its adverse effects (Bruniera *et al.*, 2015). Using VAN in a combination will allow lowering the effective dose of VAN, thus reducing or preventing its adverse effects. The interaction between FZ, VAN, and DOC against some important Gram-positive pathogens such as *Staphylococcus aureus*, *Streptococcus pneumoniae*, and *Streptococcus pyogenes* was investigated using checkerboard assay. In the six Gram-positive strains tested, all two-drug and three-drug combinations of FZ, VAN, and DOC were classified as indifferent, with FICIs ranging from 0.53 to 1.05 (Table 4). The MICs of at least two out of these three antibacterials, however, were lower than concentrations within Gram-negative-inhibitory triple combination.

Table 4. Minimum inhibitory concentrations and fractional inhibitory concentration indices for the most synergistic two-drug and three-drug combinations of FZ, VAN, and DOC against Gram-positive pathogens identified in a checkerboard assay

Strain	FZ+DOC		FICI	FZ+VAN		FICI	DOC+VAN		FICI	FZ+VAN+DOC			FICI
	Concentration ^a (µg/mL)			Concentration ^a (µg/mL)			Concentration ^a (µg/mL)			Concentration ^a (µg/mL)			
	FZ	DOC		FZ	VAN		DOC	VAN		FZ	VAN	DOC	
<i>S. aureus</i> NZRM 3478	2 (2-fold) ^a	156.25 (2-fold)	1	2 (2-fold)	1 (2-fold)	1	156.25 (2-fold)	1 (2-fold)	1	0.25 (16-fold)	1 (2-fold)	78.13 (4-fold)	0.81
<i>S. aureus</i> NZRM 4315	1 (2-fold)	312.5 (2-fold)	1	0.06 (32-fold)	1 (0-fold)	1.03	312.5 (2-fold)	0.5 (2-fold)	1	0.5 (4-fold)	0.5 (2-fold)	78.13 (8-fold)	0.88
<i>S. aureus</i> NZRM 4548	1 (2-fold)	312.5 (2-fold)	1	0.06 (32-fold)	1 (0-fold)	1.03	9.77 (64-fold)	1 (0-fold)	1.02	0.06 (32-fold)	1 (0-fold)	9.77 (64-fold)	1.05
<i>S. aureus</i> NZRM 4549	1 (2-fold)	312.5 (2-fold)	1	0.06 (32-fold)	1 (0-fold)	1.03	312.5 (2-fold)	0.5 (2-fold)	1	0.06 (32-fold)	0.5 (2-fold)	312.5 (2-fold)	1.03
<i>S. pyogenes</i> NZRM 4366	8 (2-fold)	19.53 (4-fold)	0.63	8 (2-fold)	0.10 (8-fold)	0.63	4.88 (32-fold)	0.39 (2-fold)	0.53	0.5 (32-fold)	0.39 (2-fold)	4.88 (32-fold)	0.56
<i>S. pneumonia</i> NZRM 2764	1 (2-fold)	19.53 (8-fold)	0.53	1 (2-fold)	0.20 (4-fold)	0.75	312.5 (2-fold)	0.39 (2-fold)	1	1 (2-fold)	0.05 (16-fold)	9.77 (64-fold)	0.58

a, fold dose reduction compared to MIC when used alone are shown in brackets; FZ, furazolidone; DOC, sodium deoxycholate; VAN, vancomycin; FICI, fractional inhibitory concentration index.

3.2.4 Interactions of bile salts mixture with FZ and VAN against *E. coli*

To explore whether a natural bile combination present in the human gut can aid treatment of gastrointestinal illness caused by enterobacteria in combination with FZ and VAN, the interaction of these two antibacterials with a bile salts mixture that is similar in composition to that in the human gut was investigated. Ox gall powder from Sigma-Aldrich (Cat No. B3883) was reported to have bile salt ratios closest to human bile (Hu *et al.*, 2018) and was therefore used in this study. The content of DOC in the ox gall powder, according to Hu *et al.* (2018) is 0.09% (wt/wt) or 2.09 mmol/kg.

The MIC of the ox gall powder for the *E. coli* strain ATCC 25922 was found to be 200 mg/mL, a much higher value than that of DOC (80 mg/mL). Checkerboard assay was performed to investigate interactions between FZ, VAN, and ox gall bile salts (Appendix A, Figure A- 2). In the two-way combinations of the ox gall bile salts with FZ or VAN, the FICI were both 1.02, indicating indifferent interaction in the double combinations. Three-way combination of ox gall bile salts, VAN, and FZ led to a modest decrease in the FICI (0.63), yet this value corresponds to an indifferent interaction.

3.2.5 Interactions of lipoglycopeptides with FZ and DOC against *E. coli*

Dalbavancin and oritavancin are two modified versions of VAN that have been reported to possess higher efficacy against Gram-positive bacteria and better safety profile than VAN (Crotty *et al.*, 2016). Given that they share the same mechanism of action with VAN, it was hypothesised that dalbavancin and oritavancin were also synergistic with FZ

and DOC in inhibiting Gram-negative pathogens. The highest achievable concentration of dalbavancin and oritavancin, due to limited solubility in media, is 200 µg/mL. This concentration was too low to inhibit the growth of *E. coli* ATCC 25922. The combination of 200 µg/mL dalbavancin or oritavancin with FZ (0.04 µg/mL) and DOC (625 µg/mL), resulted in the lowest FICI of <1.04, indicating indifferent interactions (Appendix A, Figure A- 3).

3.2.6 *In vitro* cytotoxicity of FZ, VAN, and DOC combination is indifferent

One advantage of repurposing drugs FZ, VAN, and DOC as a combination is that they are approved for clinical use in some form of human indication. This means that safety and toxicity studies have already been determined in a clinical setting. In this section, the cytotoxicity of the antibiotics and their combinations against HEK293T cell line was assessed. The purpose of this was not to investigate the toxicity of each of the drugs but rather to investigate the interaction of the drugs in terms of toxicity.

The HEK293T cell line was treated with FZ, VAN and DOC alone and in combination for 48 h before performing a colourimetric MTT assay to measure cellular viability. The individual drug concentration-response curves for HEK293T cell line after 48 h of treatment are shown in Figure 17. The R package *drc* (Ritz *et al.*, 2016) was used to fit a four-parameter log curve to identify the inhibitory concentration at different effects (20%, 50%, and 90% inhibition). Up to 5000 µg/mL of VAN was tested; however, this concentration did not achieve 90% HEK293T inhibition, hence the IC₉₀ could not be determined (Figure 17B). For the subsequent FICI calculations at 90% inhibition, the highest tested VAN concentration, 5000 µg/mL, was used as proxy to estimate the FICI.

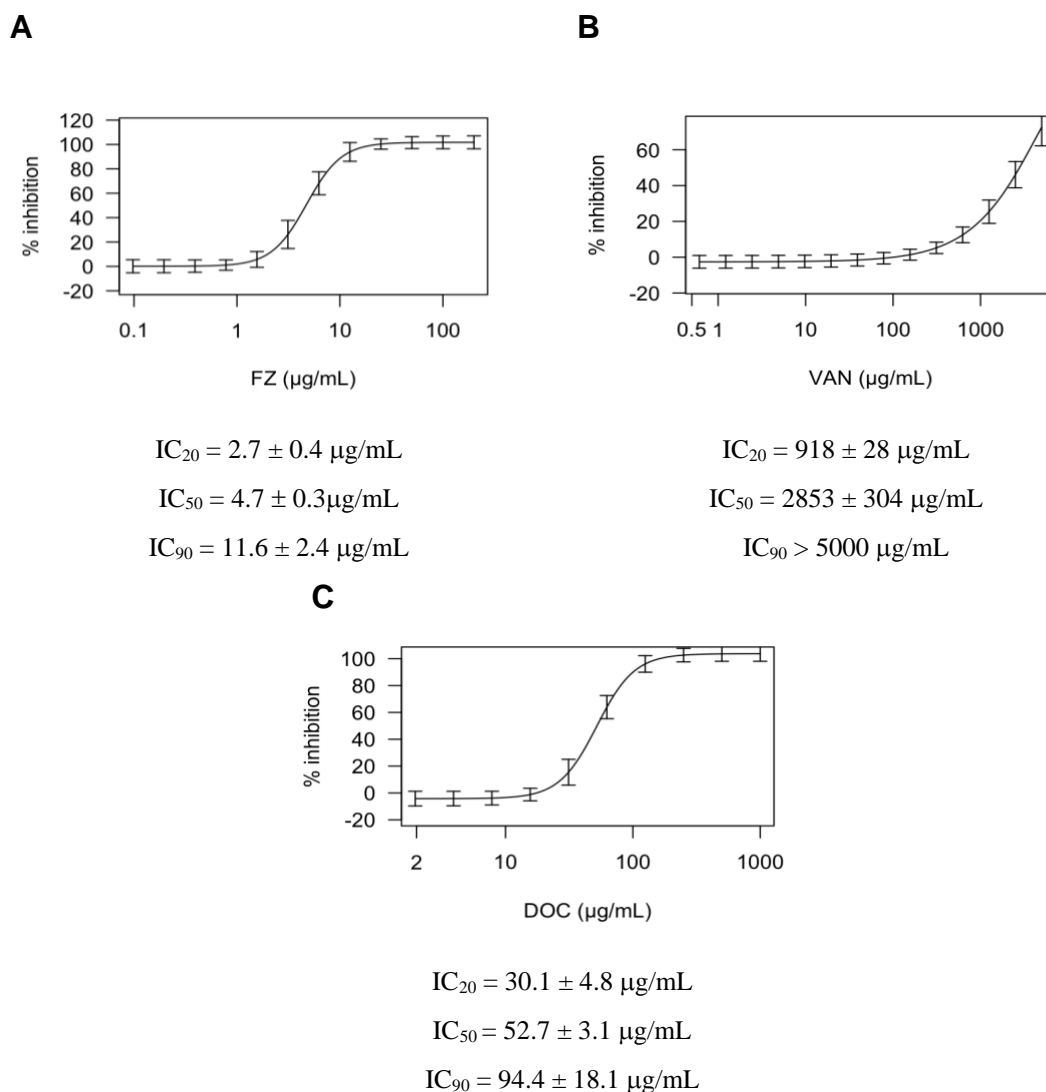


Figure 17. Concentration-response curves of FZ, VAN, and DOC on HEK293T

The inhibitory concentrations (20%, 50%, and 90%) showing mean ± standard error of three biological replicates were determined from the curves fitted using non-linear regression models.

Next, we investigated the interaction of FZ, VAN, and DOC in terms of cytotoxic effect. Cells were incubated with combinations of drugs at fixed ratios of the IC₅₀ of FZ, VAN, and DOC, and the number of viable cells after treatment was estimated using MTT assay. At low and high toxicity effects (20%-90%), the FICI's for the two-drug and three-drug combinations of FZ, VAN, and DOC ranged from 0.56 to 1.78, indicating indifferent interactions (Table 5).

Table 5. Concentrations ($\mu\text{g/mL}$) that resulted in 20%, 50%, or 90% inhibition in HEK293T and the calculated FICI.

		FZ	VAN	DOC	FICI
20% inhibition	FZ	2.70			
	VAN		918		
	DOC			30.10	
	FZ+DOC	0.75		8.43	0.56
	FZ+VAN	1.36	827		1.4
	VAN+DOC		371	6.85	0.63
	FZ+VAN+DOC	0.52	314	5.80	0.78
50% inhibition	FZ	4.70			
	VAN		2853		
	DOC			52.70	
	FZ+DOC	2.35		26.35	1
	FZ+VAN	4.18	2539		1.78
	VAN+DOC		1170	21.61	0.82
	FZ+VAN+DOC	1.55	941	17.39	0.99
90% inhibition	FZ	11.60			
	VAN		>5000		
	DOC			94.40	
	FZ+DOC	4.47		50.07	0.92
	FZ+VAN	5.88	3566		<1.22
	VAN+DOC		2568	47.43	1.02
	FZ+VAN+DOC	2.82	1712	31.62	<0.92

FZ, furazolidone; VAN, vancomycin; DOC, sodium deoxycholate; FICI, fractional inhibitory concentration index

3.3 Discussion

Novel effective therapies are urgently needed for Gram-negative bacteria, in particular, carbapenemase-producing *A. baumannii* and *Enterobacteriaceae* that top the list of WHO priority pathogens for which development of novel therapies is urgent. With the conventional approach of small molecule antibiotic development unable to keep pace with the continuing emergence and spread of multidrug resistance, alternative strategies are necessary to expand the therapeutic space. Synergistic combinations of currently available antibiotics show promise due to their enhanced activity with the advantage of improved clearance of pathogens, slowed-down resistance development, and decreased toxicity (Bollenbach, 2015).

VAN and DOC, on their own, are not effective against Gram-negative bacteria, as evidenced by their high MICs. Due to the relative impermeability of the outer membrane, large antibiotics such as VAN are not able to reach their targets in Gram-negative bacteria (Hammes *et al.*, 1974; Nieto *et al.*, 1971). These bacteria have also evolved to be highly resistant to bile salts, including DOC (Gunn, 2000; Raphael *et al.*, 2005; Paul *et al.*, 2014). As shown in this study, a Gram-negative-active agent, nitrofuran, somehow undermines tolerance of these bacteria to VAN and DOC, thereby allowing the use of these antimicrobials to be expanded beyond Gram-positive bacteria.

Because of the synergistic interaction, effective doses of individual drugs in the combinations have been significantly reduced. For example, in the reference strain *E. coli* ATCC 25922, the concentrations in the most synergistic triple combination are 16-fold, 32-fold and 50-fold lower for FZ, DOC, and VAN, respectively, compared to monotherapy. This reduction is especially significant for drugs that have adverse effects, such as VAN and nitrofurans. The massive decline in the use of these drugs after their

introduction to the market is due to their toxicity. Adverse reactions of VAN, including nephrotoxicity and ototoxicity (Filippone *et al.*, 2017; Forouzesh *et al.*, 2009), are partly the reasons why this antibiotic is considered a last resort treatment for Gram-positive infections. Similarly, nitrofuran use has been controversial due to its mutagenicity (Vass *et al.*, 2008). Harnessing of the synergy and using these antibiotics in a combination at low concentrations will allow the revival of these ‘old’ drugs due to the reduction or elimination of adverse effects.

Since lipoglycopeptide antibiotics dalbavancin and oritavancin have better safety profiles than VAN, their use can be expanded beyond Gram-positive bacteria by employing them in the triple combination instead of VAN (Section 3.2.5). The combination of these lipoglycopeptides with FZ and DOC was tested, and it was found that at the highest soluble concentration in liquid media, dalbavancin and oritavancin are not inhibitory to *E. coli*. The FICI’s of these lipoglycopeptides could not be calculated because insolubility precluded determination of their MIC for *E. coli*. Using maximal soluble concentrations as proxies, checkerboard analyses showed at least indifferent interaction with FZ and DOC; synergistic interaction, however, cannot be excluded.

Bile salts are present in the intestines. FZ is used to treat bacterial diarrhoea, and VAN is already available as an oral tablet to treat *C. difficile* diarrhoea and *S. aureus* enterocolitis. The combination, therefore, has a potential application in treating gastrointestinal illnesses. Because of its size and hydrophilicity, VAN is poorly absorbed in the gastrointestinal tract (Rao *et al.*, 2011). This property is an advantage when treating localised gastrointestinal infections. VAN can be administered as a low dose of 500 mg/day (125 mg qid) or as a high dose of >2000 mg/day (250mg or 500mg qid). A study has found that faecal concentrations of VAN, although affected by many factors, are generally proportional to the administered dosage. For 250 mg qid, faecal levels were

generally above 2000 mg/L, and for 500 qid, faecal concentrations are >4000 mg/L (Gonzales *et al.*, 2010). In all cases, the poor absorption of VAN, as evidenced by high faecal concentrations, proves that the *in vitro* combination concentration against Gram-negative bacteria that were identified in this study can be achieved *in vivo* by oral administration of VAN. The combination can, therefore, extend the use of VAN in gastrointestinal infections caused by Gram-negative bacteria.

Bile salts are present along the gastrointestinal tract. To take advantage of the bile salts' antibacterial activities in treating gastrointestinal infections, the combination of FZ, VAN, and a human-gut-like *in vitro* bile mixture (ox gall) was tested against *E. coli*, and it was found that this combination interacts indifferently (Section 3.2.4). These findings infer that components other than DOC (e.g. other bile salts) of ox gall powder have antibacterial properties, which act only additively with FZ and/or VAN, and that the DOC content of ox gall powder is not sufficient to result in synergy. An important consideration, however, is that bile salts are deconjugated and dehydroxylated along the gastrointestinal tract after they are released from the gall bladder (Urdaneta *et al.*, 2017). For that reason, ox gall powder may not be a suitable human bile model due to underrepresentation of DOC in comparison to the human intestines, where bile salt transformations lead to a higher DOC concentration. Notwithstanding this caveat, it can be concluded from the ox gall experiment that for treating gastrointestinal infections, DOC would need to be supplemented together with FZ and VAN to achieve the synergistic effect of the triple therapy.

Another potential application of the combination is in topical applications, such as ointments and wound dressings. DOC is known to have hydrogel-forming capabilities, with many studies reporting the synthesis of different DOC-containing hydrogels with different properties (Valenta *et al.*, 1999; McNeel *et al.*, 2015; Guo *et al.*, 2018). This

feature can be used to develop the combination as a hydrogel type ointment with DOC acting as the carrier system and as an antimicrobial. The FDA recently approved Kybella® (deoxycholic acid active ingredient) as a cosmetic injection for the reduction of submental fat. The maximum recommended single dose of Kybella® is 100 mg using 10 mg/mL injections. Since the 10 mg/mL injections are considered safe, the most synergistic combination concentration of DOC (e.g. 2500 µg/mL in *E. coli* reference strain ATCC 25922) required to inhibit Gram-negative pathogens *in vitro*, can also be considered safe for topical use. The topical administration of VAN has also been explored in the past. VAN powder has been used topically to lower the rate of surgical site infections (Mallela *et al.*, 2017). Additionally, its use in dressings has been tested in chronic wounds caused by Gram-positive infections such as MRSA and has been shown to reduce the bacterial load and achieve healing (Albaugh *et al.*, 2013; Saif *et al.*, 2019). The FZ, VAN, and DOC combination can be developed as a topical treatment for infections caused by both Gram-positive and Gram-negative pathogens.

In addition to testing the combination in Gram-negative pathogens, we also investigated the drug interaction in Gram-positive bacteria that cause skin and soft tissue infections such as *S. aureus* and *S. pyogenes* (Section 3.2.3). Although the three molecules are not synergistic against Gram-positive pathogens, the individual MICs of DOC and VAN are very low in comparison to those for Gram-negatives (Table 4). The combination therapy effective against Gram-negatives will therefore contain at least two molecules at concentrations above the Gram-positive MIC and will therefore inhibit these latter organisms. The combination therapy could, therefore, be considered an alternative therapeutic option for the WHO priority pathogens such as MRSA. Besides these Gram-positive bacteria, some Gram-negative pathogens, such as enterobacteria, can also cause skin and soft tissue infections, albeit at lower rates compared to Gram-positive pathogens

(Moet *et al.*, 2007). This study, showing indifference in Gram-positive bacteria and synergy against Gram-negative bacteria, provides evidence for the potential of the combination as a broad-spectrum treatment for Gram-negative and Gram-positive skin and wound infections.

Lastly, the interaction of FZ, VAN, and DOC against HEK293T cell line was investigated. A crucial part of drug development is the characterisation of drug safety. To assess the balance between safety and efficacy, a therapeutic index, which is the ratio of toxic dose and effective dose, can be calculated. The FZ, VAN, and DOC combination has a synergistic efficacy (Section 3.2.1, Table 3) against Gram-negative pathogens and indifferent cytotoxicity (Section 3.2.6, Table 5). Therefore, using these *in vitro* findings, it is expected that the therapeutic index will increase when the drugs are used in combination compared to monotherapy. Although *in vitro* toxicity experiments can be a good alternative during early drug development, *in vitro* results does not always translate *in vivo* (McKim, 2010). For example, DOC's IC_{50} against HEK293T cell line in this study is around 50 $\mu\text{g/mL}$, which is consistent with other *in vitro* cytotoxic effect studies of DOC and deoxycholic acid on cell lines (Wang *et al.*, 2011; Gupta *et al.*, 2009). In contrast, Kybella® whose active ingredient is deoxycholic acid is approved by the Food and Drug Administration for a maximum dose of 10 mg in 10 mg/mL subcutaneous injections, which is 200 \times the IC_{50} in the cell line model. Therefore, in this regard, the effect of the combination will still need to be assessed using *in vivo* animal models.

As part of developing the combination as a clinical treatment, it is crucial to study the mechanism of synergy. Understanding how the drugs interact will explain why the combination is not synergistic in some Gram-negative strains. The mechanism of synergy between FZ and DOC was proposed to be mediated by inhibition of efflux pumps by FZ, which allows DOC to accumulate inside the cell (Le *et al.*, 2020). In this study, we have

shown the lack of synergy between FZ, VAN, and DOC in Gram-positive bacteria, which further demonstrates that the presence of an outer membrane as a barrier to DOC and VAN is part of the mechanism of synergy in Gram-negative bacteria.

In summary, this chapter presented the synergistic combination of FZ, VAN, and DOC against Gram-negative pathogens. The synergistic interaction allows the use of antimicrobials, such as VAN and DOC, that would otherwise be ineffective against Gram-negative pathogens. Also, potential applications of the combinations were discussed such as treatment for gastrointestinal infections caused by enterobacteria, with the advantage of preventing antibiotic-associated *C. difficile* diarrhoea, and as a broad-spectrum topical treatment for skin and wound infections. Further work needs to be done, which includes testing the combination *in vivo* and understanding the mechanism of synergy.

4 Characterising the mechanism of action and synergy of furazolidone, vancomycin, and sodium deoxycholate against *Escherichia coli* using transcriptomics

4.1 Introduction

The previous chapter presented the synergistic interaction of nitrofurans, DOC, and VAN as a basis for combination therapy against susceptible Gram-negative pathogens. Their synergy *in vitro* has been characterised; however, the mechanism of synergy or how these antibacterials interact with each other to elicit a synergistic effect is currently unknown. To add to the problem, the exact mechanism of action of the two individual components, nitrofurans and DOC, are not fully understood. Nitrofurans and DOC have been reported to have variable effects on Gram-negative bacteria, depending on concentration. These include DNA damage (Ona *et al.*, 2009; Merritt *et al.*, 2009), protein aggregation (Cremers *et al.*, 2014), and membrane damage (Begley *et al.*, 2005). It is unclear, however, whether these effects are results of the direct attack on their targets (*i.e.* DNA, protein, membrane) or downstream effects upon interaction with their unknown target(s). In contrast, VAN's mechanism of action and target in Gram-positive bacteria are well-characterised, but its effects against Gram-negative bacteria are currently unknown. Several studies have challenged the existing notion that VAN, being a large hydrophilic molecule, cannot diffuse across the outer membrane nor be transported through porins of Gram-negative bacteria. Zhou *et al.* (2015) have proposed that small amounts of VAN can enter *E. coli*, which makes it possible for VAN to be synergistic with NIT (Zhou *et al.*, 2015). Additionally, *E. coli tolC* and *acrAB* null mutants were reported to be more resistant to VAN, suggesting the possibility that VAN can penetrate the outer membrane through the AcrAB-TolC efflux pump complex (Krishnamoorthy *et al.*, 2013; Weeks *et al.*, 2010).

In this study, a transcriptomics approach was employed to understand the mechanisms of action and synergy of the nitrofuran FZ, DOC, and VAN against a well-characterised

model Gram-negative bacterium, *E. coli* K12. This chapter presents the transcriptional responses of *E. coli* to these three antibacterials alone and in combination, and discusses the possible mechanistic bases of their synergy.

4.2 *E. coli* K12 strain K1508

E. coli K12 strain K1508 used in this study was derived from strain MC4100, but with a *lamB* (maltose outer membrane channel) deletion (Misra *et al.*, 1988). Strain MC4100 is a commonly used K12 lineage in many genetic experiments, with a fully sequenced and annotated genome (Laehnemann *et al.*, 2014). Based on similarities in genotypes and close genealogy, MC4100 genome could be used as the reference for this transcriptomics study, with only the *lamB* deletion to take into account. However, the MC4100 strain was constructed more than 40 years ago (Casadaban, 1976), and variations in stocks of K12 strains between different laboratories are common. Henceforth, *E. coli* K1508 genome was analysed by sequencing in order to generate the sequence reference for the transcriptome study. Sequencing was carried out using 250-bp paired-end sequencing on the Illumina MiSeq platform, and variations between the MC4100 genome and K1508 were detected using Pilon v1.23 (Walker *et al.*, 2014). The MC4100 genome sequence and annotation (NCBI GenBank Accession: [HG738867](#)) were then modified based on the detected variants (Appendix A, Table A- 1), and the resulting genome and annotation (Appendix B, Supplementary file 1 and 2) were used as the reference for the study.

E. coli K1508, like MC4100, harbours *relA1* and *spoT1* mutations. These two genes encode enzymes that regulate the levels of the alarmones guanosine 5', 3'-(bis)diphosphate (ppGpp) and guanosine 5'-triphosphate, 3'-diphosphate (pppGpp) involved in regulating the stringent response (Condon *et al.*, 1995). RelA is a (p)ppGpp synthase, and SpoT is a bifunctional ppGpp synthase/hydrolase. The *relA1* allele contains

an IS2 insertion in the *relA* gene that disrupts RelA (p)ppGpp-synthase activity (Metzger *et al.*, 1989). As a consequence, *E. coli* strains containing this *relA1* mutation display lower basal levels of (p)ppGpp than wild-type and do not accumulate (p)ppGpp in response to amino acid starvation (Lagosky *et al.*, 1980). The *spoT1* allele, on the other hand, contains missense mutations in the portion of the open reading frame (ORF) encoding the synthase domain and an in-frame insertion of six nucleotides, resulting in extra two amino acids in the hydrolase domain of the SpoT protein (Spira *et al.*, 2008). This SpoT variant (*spoT1*), therefore has a disrupted SpoT (p)ppGpp-hydrolase activity and strains containing this *spoT1* allele display elevated basal levels of (p)ppGpp compared to wildtype (Laffler *et al.*, 1974). Together, however, these two alleles compensate for each other's effect on (p)ppGpp levels, which was proposed to be the reason for strains evolving to have both alleles in their genome. Even with the counteracting effects of *relA1* and *spoT1* on (p)ppGpp levels, the more predominant effect is a higher basal level of (p)ppGpp compared to wildtype. Given that (p)ppGpp stimulates expression of the *rpoS* gene (Gentry *et al.*, 1993; Kvint *et al.*, 2000), the strains containing these two mutations contain higher levels of RpoS (Spira *et al.*, 2008), the transcriptional regulator for general stress response, that is upregulated at the entry into the stationary phase of growth. Strains containing *relA1* and *spoT1* alleles, including K1508, are therefore considered to be a 'relaxed' strain (*i.e.* does not respond to amino acid starvation by initiating a stringent response) with increased stress resistance due to increased RpoS levels.

Preliminary work to screen for the synergy between FZ, DOC, and VAN was performed using the rich growth medium 2xYT (instead of the standard MH broth). Stronger synergy has been identified in *E. coli* strain K1508 in 2xYT, with FICI of 0.13, instead of an FICI

of 0.5 in MH broth (Appendix A, Figure A- 4). For these reasons, this medium was chosen for the following transcriptomics study.

4.3 Experimental design

To determine drug concentrations to be used in the transcriptomics study, a concentration-response (% inhibition) curve was plotted to identify the IC₅₀ of the antibacterials on *E. coli* K1508. For the combination, the concentrations that gave the lowest FICI (most synergistic combination) in a checkerboard assay using 2xYT medium were first determined, then fixed-ratio dilutions of these concentrations were used to plot a concentration-response curve.

A sublethal concentration (IC₅₀) and a short incubation time were chosen to prevent the transcriptome profile being overwhelmed by stochastic expression of cell death genes. Cell death can lead to transcriptomic changes unrelated to the drug perturbations, and thereby confound the mechanism of action studies. The short incubation time also ascertains that the amino acid source in the medium is not exhausted, to avoid amino acid starvation, which strain K1508 cannot properly respond to. In addition, since gene expression is profoundly affected by growth (Klumpp *et al.*, 2009), a time point when the treated samples were in exponential phase and were growing at a similar rate as the control was chosen for the transcriptome analysis in order to prevent differentially expressed genes arising from the difference in the growth phase of treated and untreated (control) samples. It was experimentally determined that these conditions are fulfilled one hour after drug addition (data not shown).

The study has three main objectives: to investigate the (i) mechanism of action of FZ, DOC, and VAN individually, (ii) mechanism of the synergy of the combination of FZ, DOC, and VAN, and (iii) differences in effect on *E. coli* physiology when a drug is

applied individually *vs* in combination. The design consisted of eight treatments with four biological replicates each, totalling 32 samples. The treatments were control (vehicle only; 0.1% DMSO), IC₅₀ concentrations of FZ, DOC, and VAN individually, the triple combination of FZ, DOC, and VAN that gave 50% inhibition, and the single drug controls for the combination (i.e. same concentrations used in the combination). The concentrations used and names of the analysed samples are summarised in Table 6.

Analyses corresponding to the three objectives stated above were as follows: (i) Gene expression profiles of cultures exposed to single antibacterials (FZ, DOC, VAN) were first compared against the no-antibacterials control, and gene ontology (GO) term enrichment analysis was performed on the differentially expressed genes (DEGs; adj $p < 0.01$, FC > 1.5) to identify perturbed pathways; (ii) The DEGs of the triple combination treatment (FZ+DOC+VAN) were analysed for enriched GO terms and compared with the results of the controls containing individual antibacterials at concentrations applied in combination (FZ 3d, DOC 3d, VAN 3d); (iii) Lastly, gene expression profiles for each of the individual antibacterials and the triple combination at IC₅₀ (FZ, DOC, VAN, FZ+DOC+VAN) were compared to determine DEGs and pathways that are differentially expressed in the single antibacterials compared to the combination but have the same overall effect on bacterial growth.

Table 6. Drug concentrations used in the transcriptomics study

		Sample name	Treatment	Concentration ($\mu\text{g/mL}$)		
				FZ	DOC	VAN
Aim iii	Aim i	Control	0.1% DMSO	0	0	0
		FZ	FZ IC50	1.9	0	0
		DOC	DOC IC50	0	5000	0
		VAN	VAN IC50	0	0	190
	Aim ii	FZ+DOC+VAN	FZ+DOC+VAN IC50	0.117	1875	7.5
		FZ 3d	FZ 3-drug control	0.117	0	0
		DOC 3d	DOC 3-drug control	0	1875	0
		VAN 3d	VAN 3-drug control	0	0	7.5

FZ, furazolidone; DOC, sodium deoxycholate; VAN, vancomycin; IC50, 50% inhibitory concentration.

4.4 Pre- and post-sequencing quality control

The purified total RNA samples were analysed by electrophoresis to determine RNA quality before sequencing. There were two major bands expected for 23s and 16s rRNA at 2.9 kb and 1.5 kb, respectively, and fast-migrating bands (< 200 nt) corresponding to 5s rRNA and tRNA. The samples showed no signs of genomic DNA or protein contamination, normally visible as bands running above the 23s rRNA band. All the samples (Figure 18) appeared to be intact and had RNA integrity number higher than 9, according to LabChip® GX nucleic acid analyser (PerkinElmer).

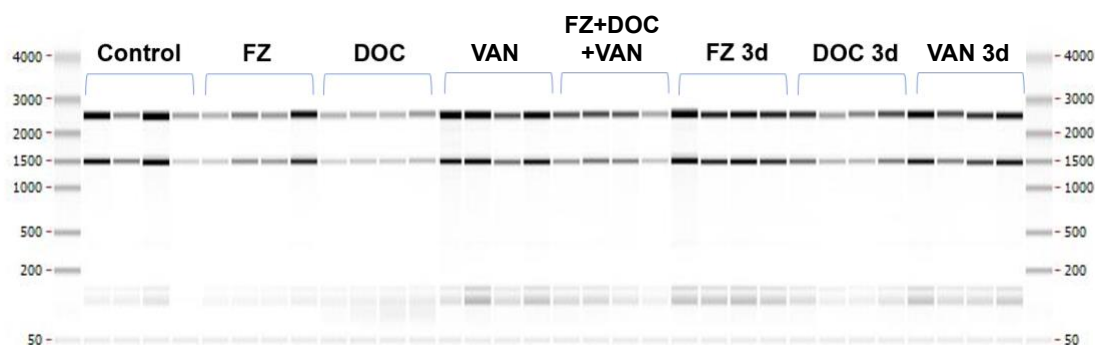


Figure 18. Integrity of the purified total RNA samples

The qualities of the total RNA samples were analysed by gel electrophoresis in the LabChip GX nucleic acid analyser. All samples had an RNA integrity number higher than 9. Bands from top to bottom indicate 23s rRNA, 16s rRNA, 5s rRNA, and tRNA.

A principal component analysis (PCA) was performed to assess the overall similarity between the samples. PCA is a technique for dimensionality reduction or summarisation of the patterns of variation in the data. Before performing the PCA, a regularised log-transformation was applied to the normalised counts to reduce the effects of few highly expressed genes and stabilise the variance across the mean. As shown in Figure 19, the

within-group replicates clustered together, showing low variation between replicates. In terms of between-group variability, FZ, DOC, and FZ+DOC+VAN showed clear separation from the other groups, while VAN, FZ 3d, DOC 3d, and VAN 3d overlapped with the control.

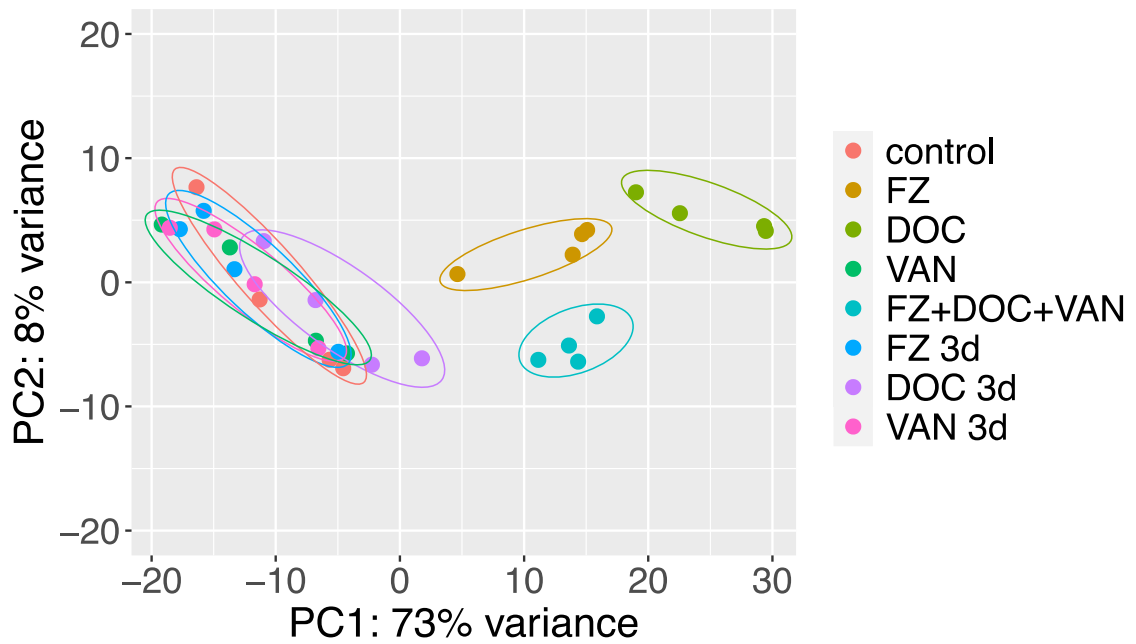


Figure 19. Principal component analysis

PCA plot showing variation and clustering within and between treatment groups. The axes show two principal components that explain the greatest proportion (73% and 8%) of variation in regularised log-transformed normalised counts for all genes.

4.5 Results

4.5.1 Transcriptional response to individual antibacterials

FZ, DOC, and VAN applied individually at IC₅₀ resulted in 1212, 1968, and 17 DEGs relative to the control, respectively (list of all DEGs is available in Appendix B, Supplementary file 4). Figure 20 shows these genome-wide expression changes of *E. coli* exposed to FZ, DOC, or VAN visualised as volcano plots to identify specific genes with large expression level differences and statistical significance. These plots show differences in RNA counts between antibacterial-containing cultures and no-antibacterial control as shrunken log₂ fold changes (log₂FCs) against the adjusted (adj) *p* values (see Chapter 2, Section 2.10); the red dots indicate DEGs. VAN treatment resulted in only 17 DEGs. This small number of DEGs explains the overlap with the control in the PCA (Figure 19), that is based on expression levels of the vast majority of genes that are very similar in these two treatments.

For FZ-treated samples, *fhuF* (ferric iron reductase), *sodA* (superoxide dismutase), and *dinI* (DNA damage inducible protein I) were among the most upregulated, while *glp* regulon genes (involved in glycerol and glycerol-3-phosphate catabolism) and *nanC* (encoding an outer membrane channel protein) were among the most down-regulated. For DOC-treated samples, the most upregulated gene is *grxA* (glutaredoxin) and among the most upregulated are the translation-related genes *leuV*, *aspV*, *valW*, *proM*, *serT*, and *glyY*.

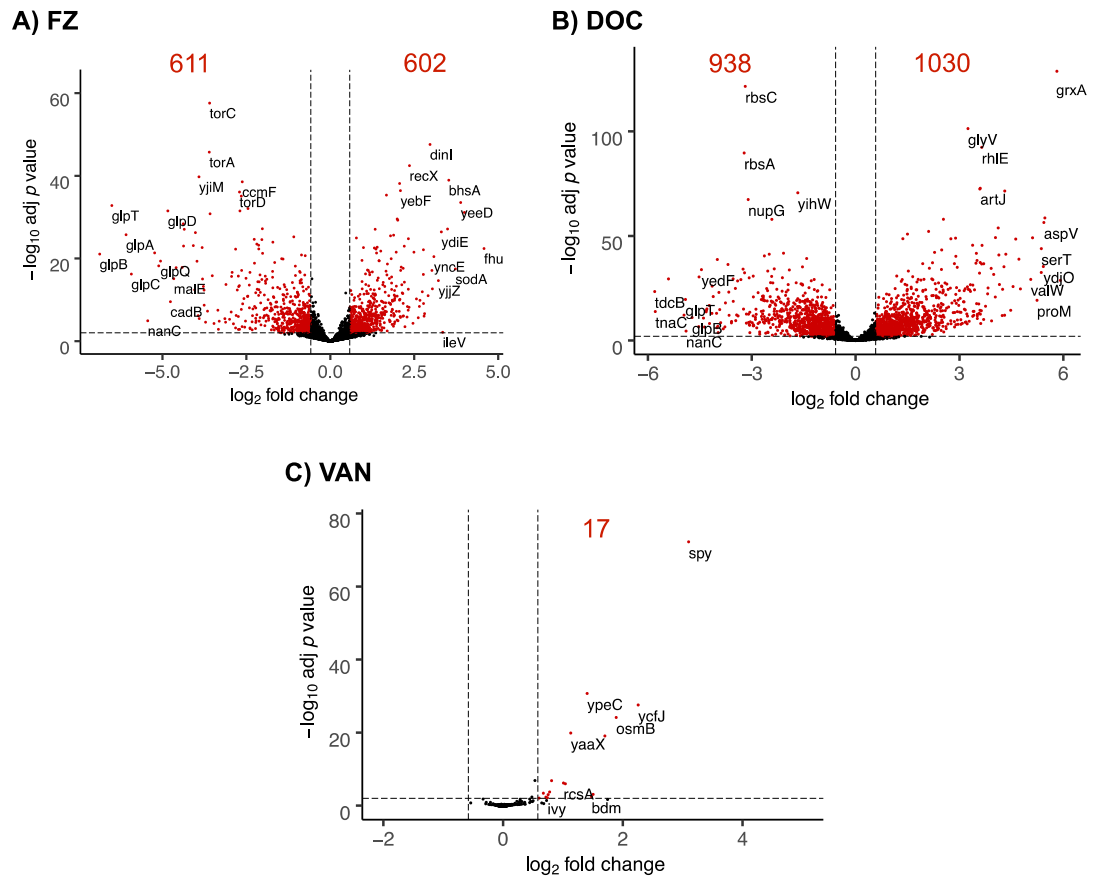


Figure 20. Genome-wide expression changes in response to individual antibacterials (A) FZ, (B) DOC, or (C) VAN at the respective IC₅₀ concentrations (compared to control). The scatter plots display the shrunken log₂FCs and the adjusted *p* values. Red dots represent significantly differentially expressed genes (adjusted *p* < 0.01, |log₂FC| > 0.58) relative to control, with numerical annotations to indicate the number of differentially expressed genes. The ten most upregulated, downregulated, and statistically significant genes are labelled in each plot.

The sets of differentially up- ($\log_2FC > 0.58$) and downregulated genes ($\log_2FC < 0.58$) for FZ and DOC treatments were also separately analysed for significantly enriched GO term annotations (Appendix B, Supplementary file 5). In FZ-treated samples, the second most enriched GO term for upregulated genes is SOS response, the canonical response to severe DNA damage. GO terms associated with ribosome assembly, iron uptake, and translation are significantly enriched in both FZ and DOC upregulated genes (Figure 21A). On the other hand, cellular respiration, carbohydrate transport, and tricarboxylic acid (TCA) cycle are enriched in the downregulated genes (Figure 21B).

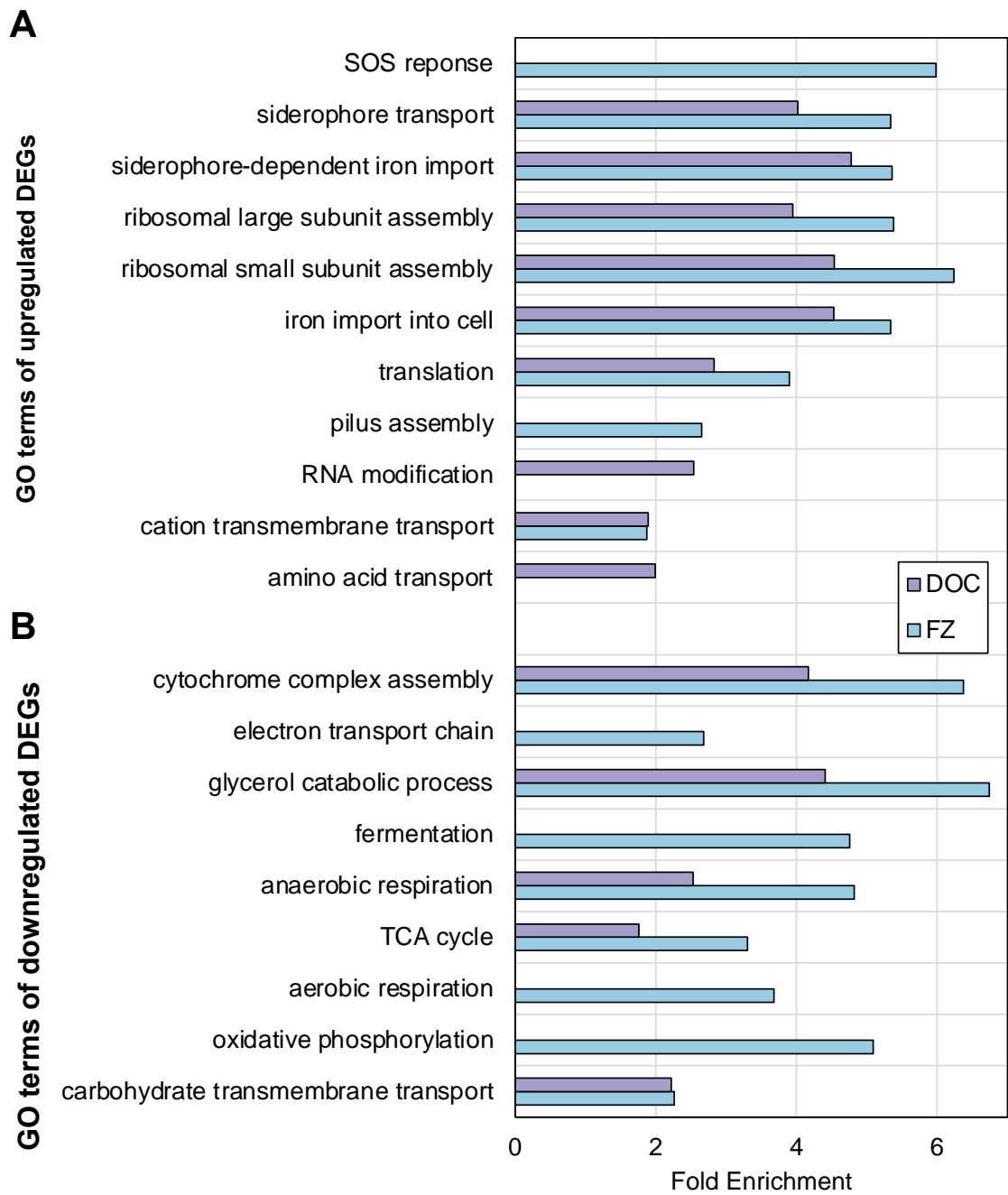


Figure 21. Gene ontology term enrichment analysis of FZ and DOC DEGs

Significantly overrepresented (FDR < 0.05) biological process GO terms in FZ and DOC (A) upregulated and (B) downregulated DEGs (adj p < 0.01, $|\log_2FC| > 0.58$) using PANTHER GO overrepresentation test.

4.5.2 Transcriptional response to FZ, DOC, and VAN combination

FZ+DOC+VAN combination resulted in 1384 DEGs, while FZ 3d, DOC 3d, and VAN 3d alone at the same concentration resulted in 3, 119, and 1 DEGs, respectively (list of all DEGs is available in Appendix B, Supplementary file 4). Figure 22 shows the volcano plots for FZ+DOC+VAN and its 3-drug controls. The low numbers of DEGs in FZ 3d, VAN 3d, and DOC 3d alone explains their overlap with the control samples, as shown in the PCA (Figure 19).

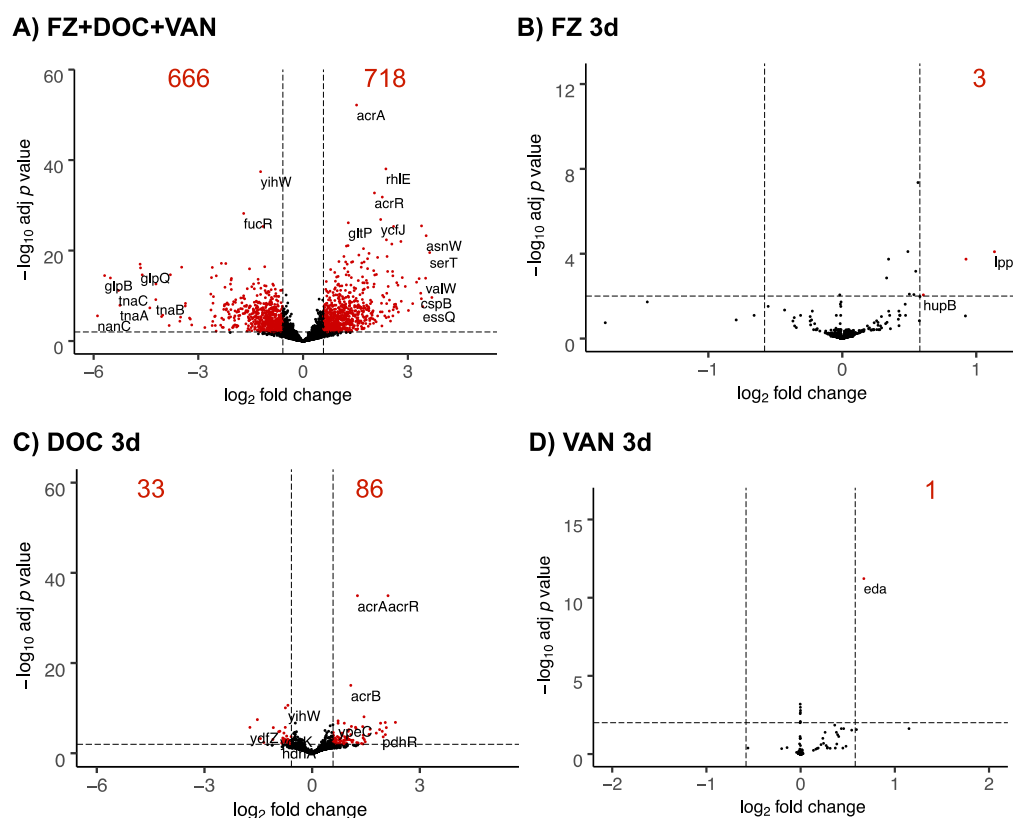


Figure 22. Genome-wide expression changes in response to triple FZ+DOC+VAN combination

The scatter plots display the shrunken log₂FCs and the adjusted *p* values (Benjamini-Hochberg). Red dots represent significantly differentially expressed genes (adj *p* < 0.01, |log₂FC| > 0.58) relative to control, with numerical annotations to indicate the number of differentially expressed genes. The ten most upregulated, downregulated, and statistically significant genes are labelled in each plot.

As presented in the volcano plots (Figure 22), the synergy of the combination was evidenced by the number of DEGs in the combination being more than the sum of DEGs when each antibacterial was applied alone at the same absolute concentrations (FZ 3d, DOC 3d, or VAN 3d). Physiologically, the synergy is reflected by the growth-inhibitory effect of FZ+DOC+VAN combination and the lack thereof in FZ 3d, DOC 3d or VAN 3d cultures. The most upregulated genes in the cultures containing FZ+DOC+VAN combination were *serT* (serine tRNA) and *valW* (valine tRNA), whereas the most downregulated were *nanC* and genes belonging to the *glp* regulon. The only DEGs for FZ 3d were *lpp* (major outer membrane lipoprotein), *dinQ* (uncharacterised protein whose expression is DNA damage-inducible), and *hupB* (DNA-binding protein), while the only DEG for VAN 3d was *eda*, a gene encoding a multifunctional aldolase enzyme. Lastly, the majority (~80%) of DOC 3d DEGs fall within those seen for the combination (Figure 23), with *acrAB* (efflux pump) among the most upregulated genes.

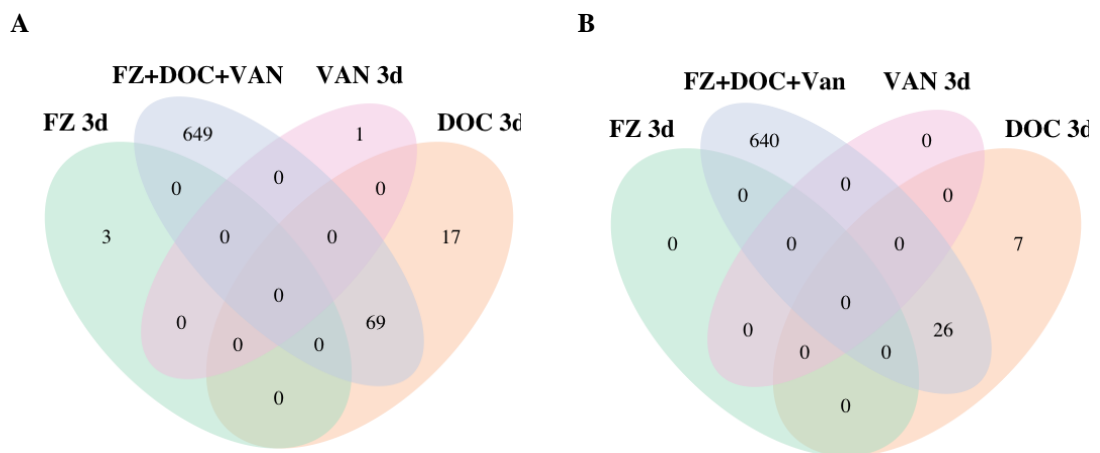


Figure 23. Overlap of DEGs between FZ+DOC+VAN IC50 combination and single antibacterials at the same concentrations used in the combination

Venn diagrams show the numbers of (A) upregulated and (B) downregulated DEGs in response to FZ+DOC+VAN treatment and the 3-drug controls.

4.5.3 Comparison of differentially expressed gene clusters in the presence of combination and single antibacterials at IC₅₀

To analyse in more detail the physiological processes affected by combination and single antibacterials at IC₅₀, all DEGs were subjected to K means clustering analyses using the identified optimal K number (K=7), and the resulting clusters were subjected to GO term enrichment analysis. The heatmap and GO terms enriched in each cluster are shown in Figure 24.

As shown in the heatmap, the combination resulted in the same pattern of regulation of gene clusters as cultures containing only FZ or DOC. For example, the FZ+DOC+VAN combination upregulated genes involved in ribosome assembly, translation (Cluster 2), and amino acid transport (Cluster 4), and downregulated genes encoding enzymes of TCA cycle (Cluster 7) and those encoding proteins involved in carbohydrate transport (Cluster 3), similar to cultures containing only FZ or DOC.

An important difference between the FZ and triple combination is that the former upregulated SOS response genes (Cluster 5) indicative of DNA damage and the latter failed to induce these responses, reflecting a significantly decreased DNA damage in the presence of triple combination. It is noticeable, however, that the changes in expression of some of the gene clusters (e.g. Cluster 3, 4, and 6) are not as pronounced in the presence of the triple combination compared to the single-antibacterials cultures.

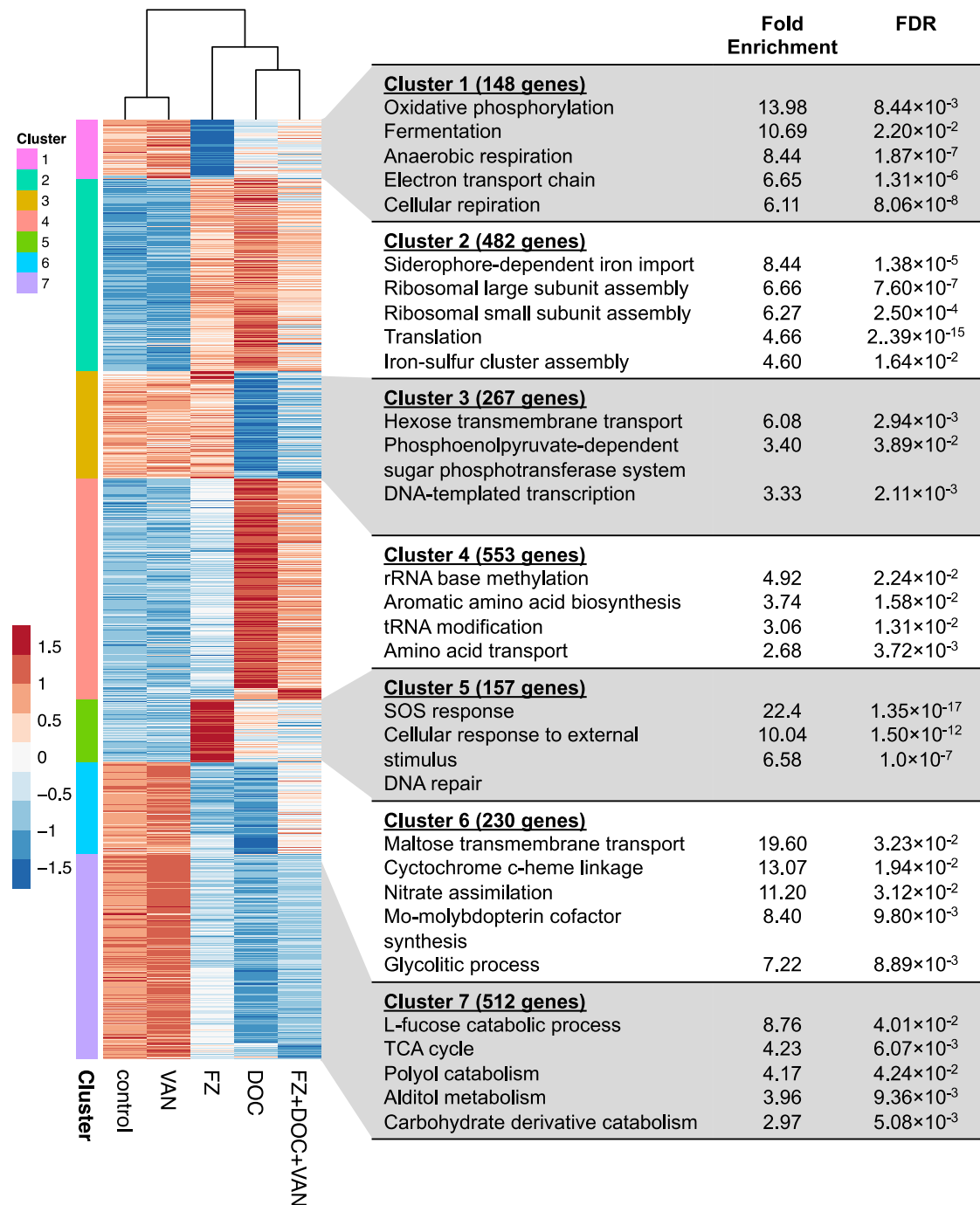


Figure 24. Heatmap of DEG clusters and GO term enrichment.

K means clustering was performed on the regularised log-transformed normalised counts of all the DEGs in FZ, DOC, VAN, and FZ+DOC+VAN. The model-based optimal number of K (K=7) was determined *a priori*. The colours in the map represent row-scaled expression levels: blue indicates the lowest expression, white indicates intermediate expression, and red indicates the highest expression. Each cluster was subjected to PANTHER biological process GO term overrepresentation test and the tops 5 enriched GO terms are shown along with their false discovery rates (FDR).

4.5.4 Extracytoplasmic stress response to VAN treatment

GO term enrichment analysis of all the 17 DEGs detected in the cultures exposed to VAN at IC₅₀ (Table 7) resulted in no overrepresented GO terms. Perturbed pathways were therefore identified based on the transcriptional master regulators of all the DEGs. Most of the DEGs were found to belong to one or more stress response regulons, most frequently Rcs (11 genes), followed by σ^S (3), Cpx (2), and Lrp (2), with only one gene each belonging to Bae and σ^{32} . Of the induced pathways, three (Rcs, Cpx and Bae) respond to envelope stresses. Upregulation of these pathways is in agreement with the VAN target in Gram-positive bacteria, peptidoglycan synthesis (Hammes *et al.*, 1974), known to induce cell envelope stress (Jordan *et al.*, 2008).

Table 7. Significantly differentially expressed genes in response to VAN treatment

Gene	Gene product/Function	log2FC	Regulon
<i>spy</i>	Periplasmic chaperone Spy	3.10	Cpx, Bae, Rcs
<i>ycfJ</i>	Uncharacterised periplasmic protein YcfJ	2.26	Rcs
<i>osmB</i>	Osmotically-inducible lipoprotein B	1.89	Rcs, σ^S
<i>yaiY</i>	Inner membrane protein YaiY	1.70	Lrp
<i>glyX</i>	Glycine tRNA	1.50	ND ^a
<i>bdm</i>	Biofilm dependent modulation protein	1.48	Rcs
<i>ypeC</i>	Uncharacterised protein YpeC	1.40	Rcs
<i>yaaX</i>	Uncharacterised protein YaaX	1.13	Lrp
<i>ygaC</i>	Uncharacterised protein YgaC	1.04	Rcs, Fur
<i>rcsA</i>	Regulator of capsular synthesis	1.01	Rcs
<i>ypfG</i>	Uncharacterised protein YpfG	0.81	ND ^a
<i>hslJ</i>	Heat shock protein HslJ	0.78	σ^{32}
<i>ymgD</i>	Uncharacterised protein YmgD	0.75	Rcs
<i>ivy</i>	Inhibitor of vertebrate lysozyme	0.74	Rcs, σ^S
<i>cpxP</i>	Periplasmic protein CpxP	0.72	Cpx, σ^S
<i>ydhA</i>	Putative lipoprotein	0.67	Rcs
<i>ymgG</i>	Uncharacterised protein	0.60	Rcs

^aND, regulators not determined

4.5.5 SOS response to FZ treatment

FZ upregulated the SOS response and DNA repair genes as shown in Figure 25. These genes are part of the LexA regulon which responds to DNA damage (Fernández de Henestrosa *et al.*, 2000; Lewis *et al.*, 1994; Walker, 1984). Some of these genes encode proteins that function in nucleotide excision repair (*uvr*, *ruv*), homologous recombination (*rec*), translesion synthesis (*umuC*, *umuD*, *dinB*, *polB*), and delayed cell division (*sulA*); the upregulation of which are indicative of the induction of the SOS response of *E. coli*.

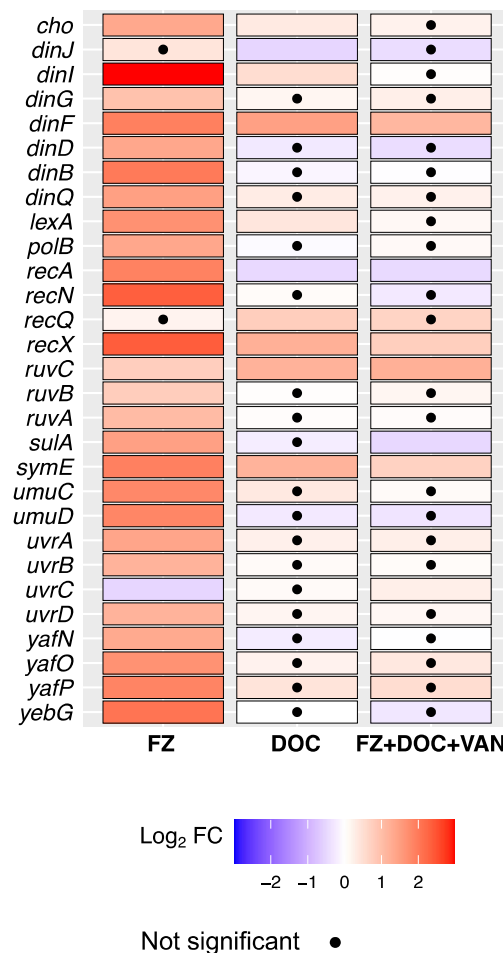


Figure 25. Differential expression of genes involved in SOS response

The heatmaps show the log₂FC of the DEGs in cultures containing a single antibacterial (FZ or DOC), and the triple combination (FZ+DOC+VAN). Significant genes have adjusted $p < 0.01$.

4.5.6 Iron starvation responses

FZ and DOC induced the iron starvation response. Upregulated genes were enriched in Fe²⁺ uptake and siderophore-dependent Fe³⁺ uptake, such as *feo* for Fe²⁺ uptake, *ent* for enterobactin synthesis and export, *exbB*, *exbD*, *tonB*, *fhu*, *fep*, and *fec* for ferri-siderophore complex uptake (Figure 26A). Fe-S cluster biogenesis genes, *isc* and *suf* (Figure 26B) were also upregulated, indicating an increased need for Fe-S cluster biogenesis and repair.

Another response to iron starvation is down-regulation of genes relating to iron storage and non-essential iron-containing proteins. FZ and DOC downregulated the iron storage genes *ftnA* and *bfr*. Additionally, *ryhB* expression was upregulated, and RyhB sRNA-mediated inhibition of iron-utilising proteins could explain the down-regulation of *sodB* (Fe-containing superoxide dismutase), and the respiratory genes *nuo*, *frd*, *sdh*, *hyb*, and *cyd* (Desnoyers *et al.*, 2009; Massé *et al.*, 2002; Massé *et al.*, 2005).

Upregulation of iron uptake genes, Fe-S cluster biogenesis genes, oxidative stress genes, and downregulation of genes encoding non-essential iron-containing proteins and iron storage, all point to the Fur inactivation induced by FZ and DOC. Interestingly, this effect is less pronounced in FZ+DOC+VAN, with most of the iron import DEGs of FZ- and DOC-containing cultures not statistically significant in the combination, albeit also upregulated (Figure 26).

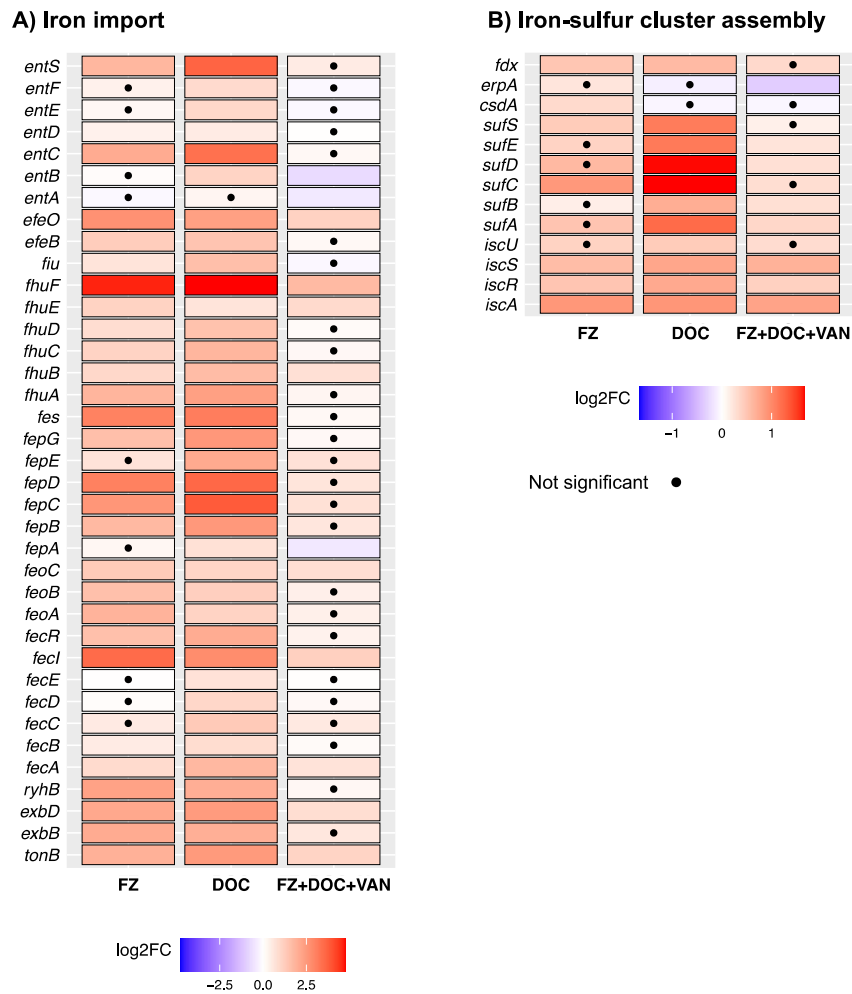


Figure 26. Differential expression of genes involved in iron import and iron-sulfur cluster assembly

The heatmaps show the log₂FC of the DEGs in cultures containing a single antibacterial (FZ or DOC), and the triple combination (FZ+DOC+VAN). Significant genes have adjusted $p < 0.01$.

4.5.7 FZ and DOC upregulation of protein synthesis

FZ, DOC, and the triple combination FZ+DOC+VAN upregulated a shared set of genes enriched for those encoding ribosome proteins and enzymes involved in protein synthesis (Figure 27). The *rps* and *rpl* genes encoding ribosomal small and large subunit proteins and translation-related genes were upregulated. The ribosomal/translational machinery requires both an abundance of amino acids and ATP. It is, therefore expected that increased cellular ATP is needed to increase ribosomal gene transcription, and subsequent increase in ribosomes for translation (Schneider *et al.*, 2002; Gaal *et al.*, 1997). For these reasons, it is not surprising that RNA polymerase (*rpoABC*), and amino acid transport genes were also upregulated, in agreement with the abundance of amino acids needed by the upregulated production of translational machinery.

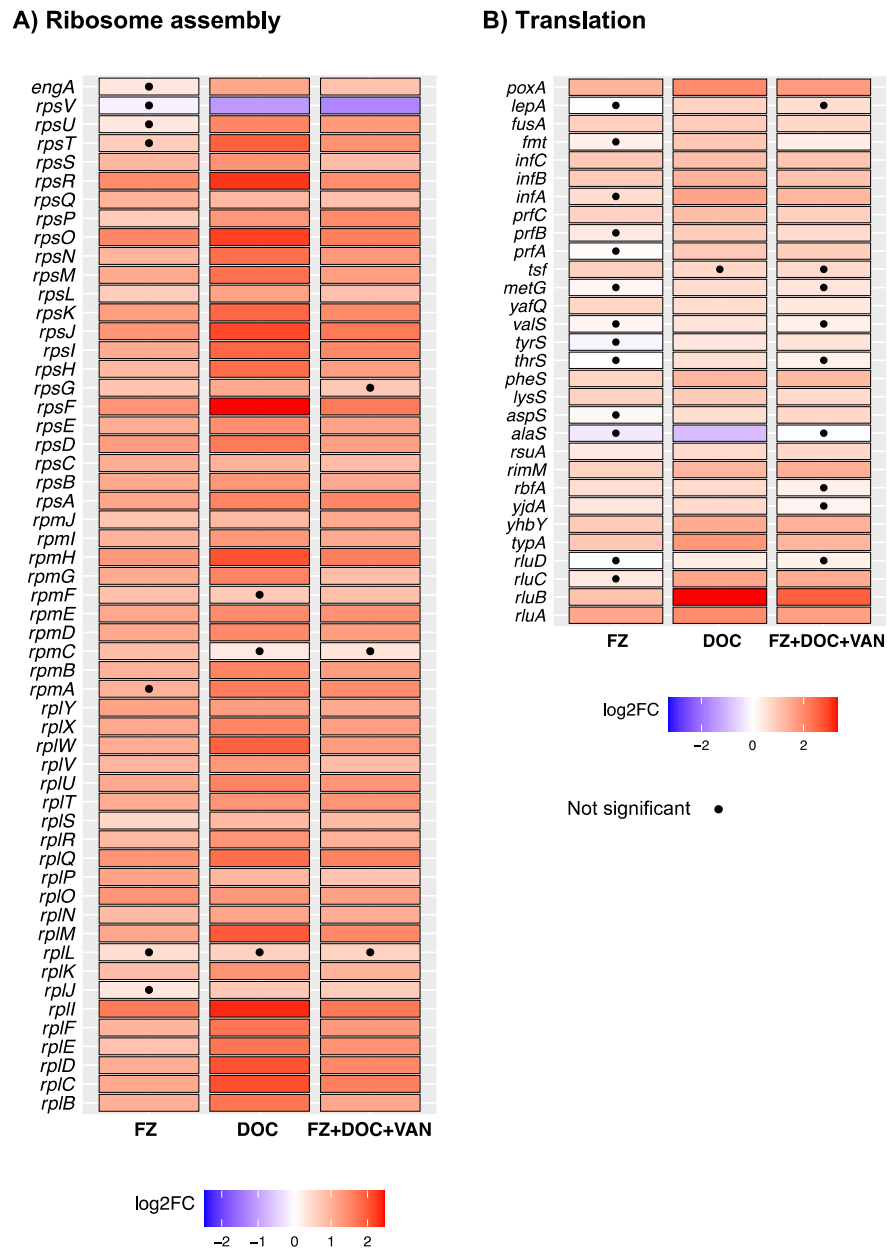


Figure 27. Upregulation of genes encoding protein synthesis machinery

The heatmaps show the log₂FC of the DEGs in cultures containing a single antibacterial (FZ or DOC), and the triple combination (FZ+DOC+VAN). Significant genes have adj $p < 0.01$.

4.5.8 Downregulation of the electron transport chain and central carbon metabolism

FZ and DOC both downregulated genes involved in the central carbon metabolic pathways such as glycolysis, pentose phosphate pathway, and TCA cycle, as shown in Figure 28. Additionally, these two antibacterials, when applied individually, also resulted in the downregulation of genes encoding dehydrogenase and oxidoreductase genes of the ETC/respiratory chains (Figure 28). Some of the genes encoding NADH dehydrogenase I (*nuoABCDEFGHIJKLMN*), glycerol-3-phosphate dehydrogenase (*glpABC*), formate dehydrogenase (*fdnGHI*), hydrogenase I (*hyaABC*), and hydrogenase II (*hybABC*) were downregulated. Similarly, quinol oxidase *bd*-I (*cydAB*), periplasmic nitrate reductase (*napFDAGHBC*), nitrate reductase (*nrfABCDEFGF*), nitrate reductase A (*narGHJI*), DMSO reductase (*dmsABC*), TMAO reductase (*torACD*), fumarate reductase (*frdABCD*), and quinol oxidase *bd*-II (*appBC*) were downregulated. Most of these genes encode proteins from the DMSO reductase family of molybdoenzymes: Nitrate, TMAO, DMSO reductases, and formate dehydrogenase. Downregulations of these molybdoenzyme genes could then explain the lowered expression of genes involved in molybdate uptake (*modABC*) and molybdopterin cofactor synthesis (*moa, mob, moc, mog*), which suggest a decreased need for molybdenum. Interestingly, the triple combination (FZ+DOC+VAN) caused changes of the same direction as FZ and DOC alone, however, these were less pronounced (mostly not statistically significant).

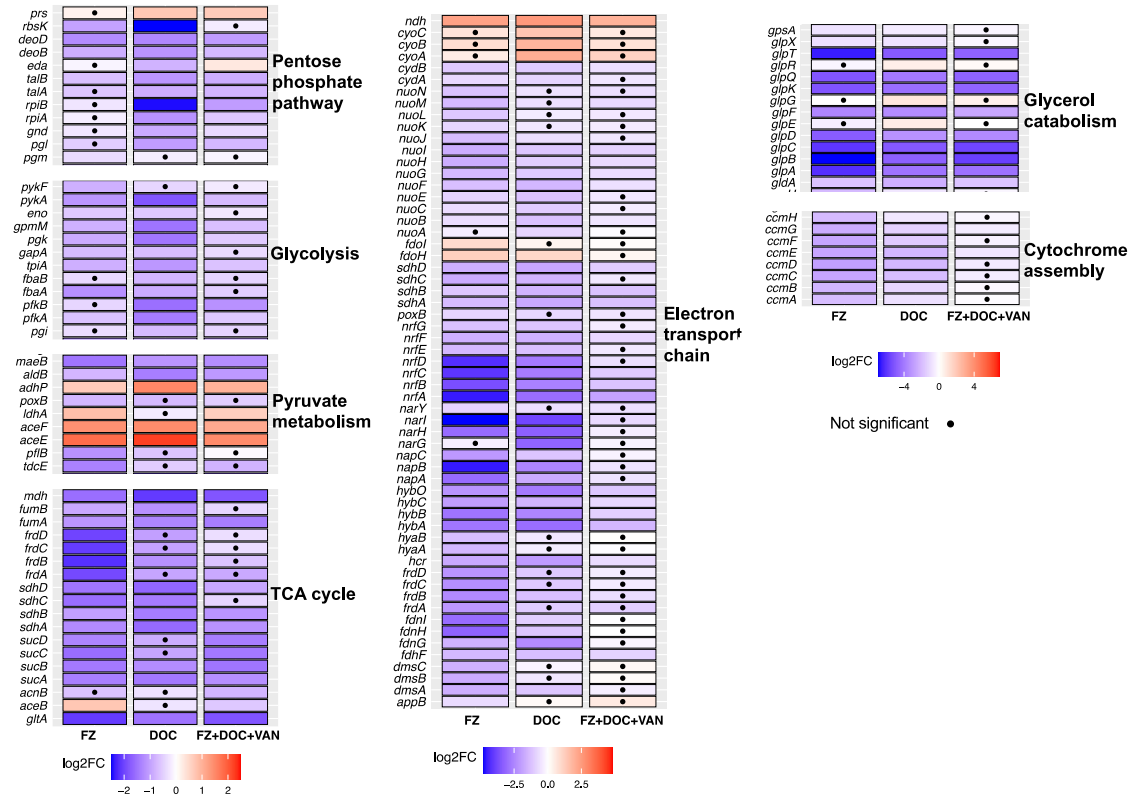


Figure 28. Downregulation of the central carbon metabolism and electron transport chain

The heatmaps show the log₂FC of the DEGs in containing a single antibacterial (FZ or DOC), and the triple combination (FZ+DOC+VAN). Significant genes have adjusted $p < 0.01$.

4.5.9 Oxidative stress

FZ and DOC treatment resulted in changes in the expression of genes of the OxyR and SoxRS regulons, indicative of oxidative stress (Figure 29). SoxS-regulated *sodA*, which is involved in eliminating superoxide, was upregulated in both FZ and DOC. In the FZ-treated samples, the usual OxyR-regulated genes that protect the cell from H₂O₂ toxicity such as *ahpCF* were not differentially expressed. In addition, the expression of *katG*, a catalase that eliminates H₂O₂ via degradation to water and oxygen, and *dps*, a protector of DNA to the effects of oxidative stress (Choi *et al.*, 2000), were downregulated. Unlike FZ, DOC upregulated OxyR-regulated genes *ahpC*, *ahpF*, *katG*, *dps*, *grxA* and *trxC* indicative of H₂O₂ stress.

4.5.10 Antibiotic-induced resistance mechanisms

FZ and DOC, besides inducing stress related to their antibacterial effect, also induce transcriptional responses that favour increased resistance by increasing the capacity for expulsion of antibacterials out of the cells. Multiple antibiotic resistance (*mar*) genes *marA* and *marB*, of which the former is a master regulator of large number of genes involved in increased antibiotic resistance, were overexpressed in all three cultures. Among the efflux pumps, *acrA* and *acrB* were upregulated in the presence of DOC, by more than two-fold (Figure 29). AcrAB, along with TolC, makes up a key multidrug efflux pump and an essential mechanism for resistance to multiple antibiotics (Okusu *et al.*, 1996; Nikaido *et al.*, 2008). Besides upregulation of the efflux pumps, *E. coli* also responds to antibiotic stress by altering the expression of outer membrane porins, such as OmpF and OmpC. FZ downregulated both *ompC* (~1.6-fold) and *ompF* (~3.3-fold), while DOC downregulated *ompF* by more than 2-fold.

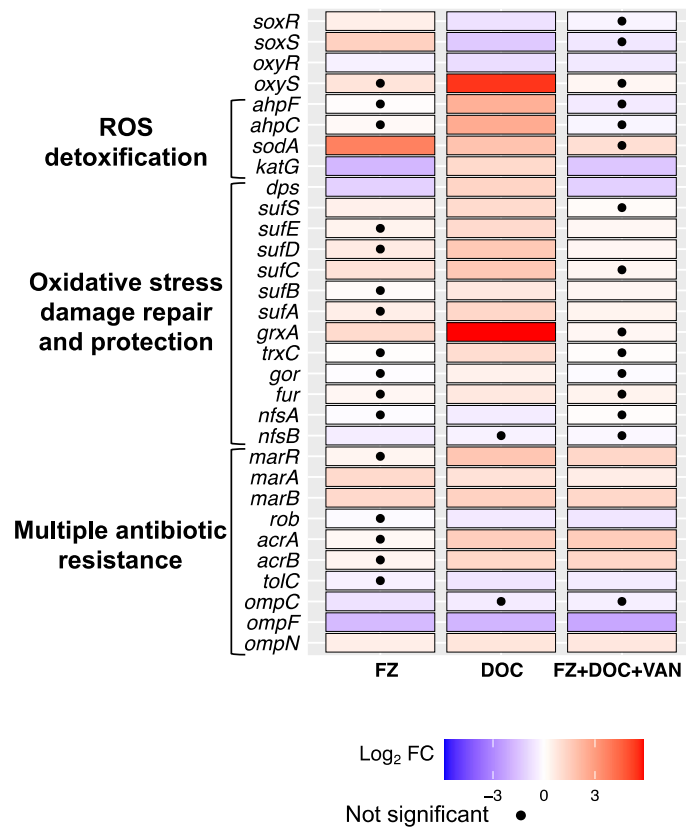


Figure 29. Differential expression of genes involved in oxidative stress and antibiotic-induced resistance mechanisms

The heatmaps show the log₂FC of the DEGs in cultures containing a single antibacterial (FZ or DOC), and the triple combination (FZ+DOC+VAN). Significant genes have adj *p* < 0.01.

4.6 Discussion

The synergistic combination of nitrofurans, DOC, and VAN was shown in Chapter 3 to be a promising approach to tackle antimicrobial resistance. However, the underlying mechanism for their synergy was unknown. Although the interactions between drugs cannot always be inferred or predicted from the individual components' mechanisms of action (Ankomah *et al.*, 2013), knowledge of these individual modes of action can help with understanding the mechanistic basis of synergy.

In Gram-positive bacteria, VAN binds to its target D-Ala-D-Ala of Lipid II and inhibits the peptidoglycan synthesis (Liu *et al.*, 1994; Hammes *et al.*, 1974). Gene expression analyses of *E. coli* treated with the peptidoglycan synthesis inhibitors, such as β -lactam antibiotics (Laubacher *et al.*, 2008) and colicin M (Kamenšek *et al.*, 2013), showed upregulation of the Rcs-regulated genes, including the set of DEGs in Table 7. Furthermore, the transcriptomic response of an *E. coli* strain with a compromised outer membrane to VAN also showed differential expression of Rcs pathway genes (O'Rourke *et al.*, 2020). In another study, growth of *E. coli* at low temperatures was found to increase susceptibility to VAN. This increased susceptibility can be suppressed by heterologous expression of *Enterococcus* VAN resistance cluster (*vanHBX*), suggesting a mechanism of action through inhibition of peptidoglycan synthesis, same as in Gram-positive bacteria (Stokes *et al.*, 2016). Results from this study, along with the abovementioned published findings, support the notion that VAN can enter *E. coli*, and exert the same peptidoglycan synthesis inhibition that induces envelope stress and activates the Rcs pathway.

Based on all the findings presented in this study, FZ and DOC seem to have highly correlated target pathways that result in almost the same transcriptional perturbations in the same biological processes. Computational approaches to explore drug combination

network interactions suggest that drugs that target functionally related pathways or have directly connected targets are more likely to lead to a synergistic effect. (Wang *et al.*, 2012; Zou *et al.*, 2012; Chen *et al.*, 2016). FZ+DOC+VAN affected the same pathways as did FZ and DOC when applied alone; production of ribosome components and translation were induced, while the central carbon metabolism and carbohydrate transport/uptake were downregulated. FZ and DOC monotherapy also affected iron uptake and respiratory chain/ETC genes, but the combination's effects on these pathways were less pronounced. Of importance is the lack of SOS induction in the combination, which indicates the absence of major DNA damage. This could be attributed to the significantly reduced dose of FZ in the combination or another mechanism that suppresses FZ-induced DNA damage. Since increased frequency of mutation results in higher frequency of resistance, and DNA damage in eukaryotic (host) cells is known to lead to oncogenesis (Hiraku *et al.*, 2004; Olive *et al.*, 1977), this finding highlights the advantage of using the combination over FZ or another nitrofurantoin alone, in terms of mitigating mutagenicity in bacterial cells or DNA damage to the eukaryotic cells.

Based on the transcriptomics data presented in this chapter, target pathways that are either affected or induced in response to FZ, DOC, and VAN in *E. coli* can be traced, and their interactions leading to synergy can be proposed (Figure 30). FZ and DOC both resulted in the upregulation of genes encoding iron uptake systems and downregulation of those encoding iron storage and iron-utilising proteins (Section 4.5.6). These results are indicative of iron limiting conditions or inactivation of the transcriptional regulator Fur caused by the presence of FZ or DOC. The induction of iron uptake mechanisms in response to DOC is consistent with a microarray study by Hamner *et al.* (2013), where bile salt treatment of enteropathogenic *E. coli in vitro* resulted in increased expression of iron acquisition genes. The authors have proposed that bile acted as a signal for the iron-

restricted host intestinal environment. It still remains to be elucidated, however, whether bile salt physiologically causes iron imbalance *in vitro*, to which *E. coli* responds appropriately, or if it is instead (or in addition) a signal activating the iron uptake response, notwithstanding the iron starvation. Similarly, these findings are consistent with a microarray study by Fu *et al.* (2007) of FZ-treated *Shigella flexneri*, which showed an upregulation of iron uptake genes. Currently, the mechanism by which FZ disturbs the iron homeostasis remains unknown.

The iron-sparing mechanisms that are induced by Fur inactivation or iron limitation also result in the downregulation of iron-containing proteins such as respiratory enzymes (Massé *et al.*, 2005). Both FZ and DOC downregulated genes encoding ETC proteins including NADH dehydrogenase I (encoded by multiple *nuo* genes) and cytochrome *bd-I* (encoded by multiple *cyd* genes) (Figure 28). NADH dehydrogenase I (containing FeS centres) and cytochrome *bd-I* ubiquinol oxidase (containing FeS centres and cytochromes) are two primary proton-translocating complexes of the ETC, and therefore, generators of PMF. Downregulation of the *nuo* and *cyd* genes by both FZ and DOC could lead to the dissipation of PMF which powers multiple multidrug efflux pumps. Another cause for reduction of the number of proton-transferring complexes could be the failure to assemble Fe-S clusters (centres) within NADH dehydrogenase I, ultimately caused by potential inactivation of Fur. Low Fur leads to the switch from the Isc to Suf machinery for Fe-S cluster biogenesis (Mettert *et al.*, 2014; Lee *et al.*, 2008). The Suf system was reported to be insufficient for maturation of multi-Fe-S-complex-containing Nuo protein, the key component of NADH dehydrogenase I, whose further depletion in this way likely leads to diminished PMF (Ezraty *et al.*, 2013). Given that PMF is directly or indirectly required for the function of efflux pumps, low PMF is conducive for the accumulation of DOC and FZ inside the cells by preventing their efflux. These findings support a previous

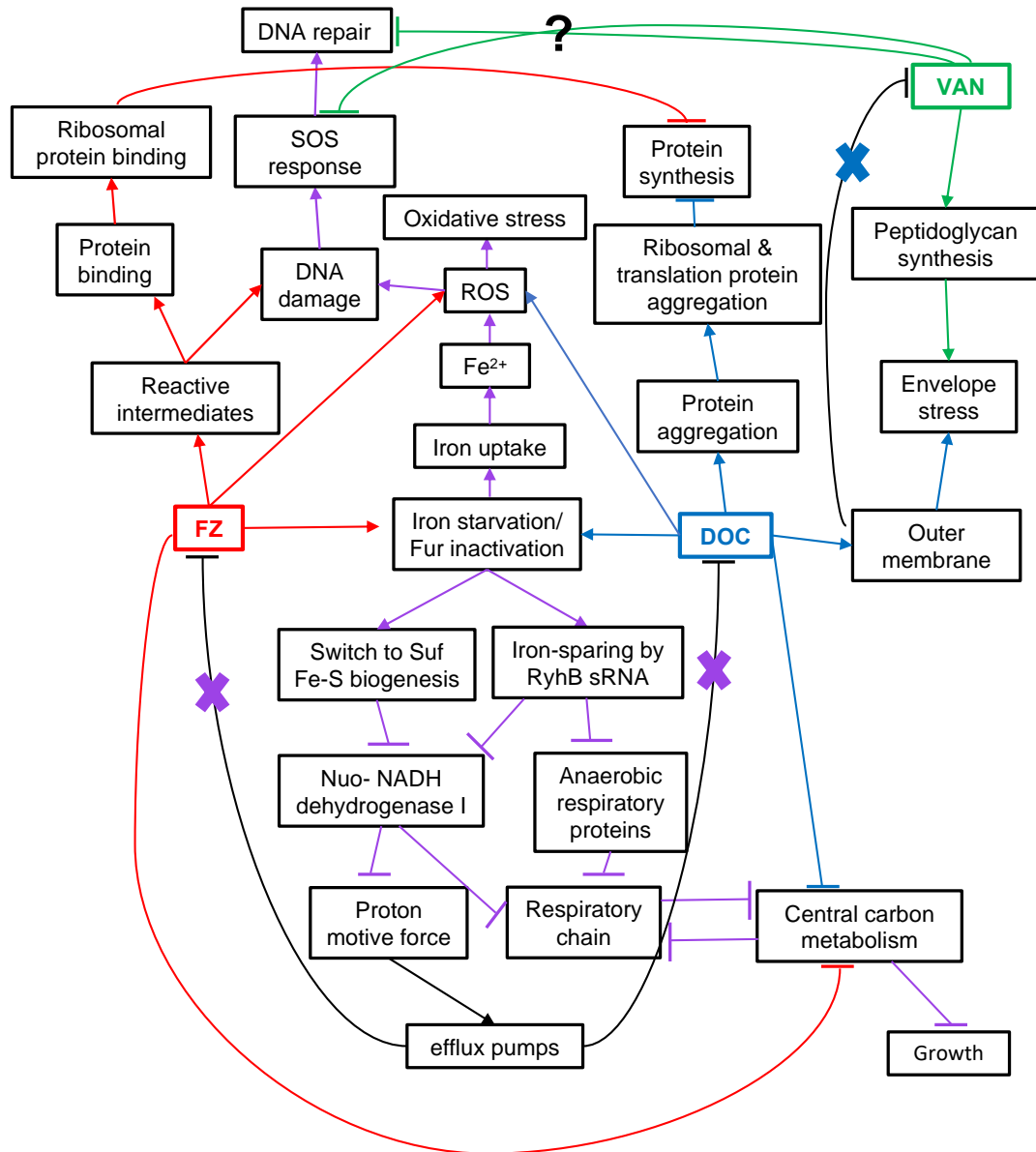


Figure 30. Proposed interaction of FZ, DOC, and VAN that leads to synergy

FZ and DOC upregulated iron uptake and downregulated iron-utilising respiratory chain, indicative of Fur inactivation. Downregulation of genes involved in the electron transport chain likely leads to the diminishing of the proton motive force that powers efflux pumps, which in turn, could lead to the inhibition of efflux and accumulation of FZ and DOC inside the cells. Moreover, transcriptomic data by O'Rourke et al. (2020) showed that VAN downregulates SOS response genes. This effect would contribute to synergy, as the failure to repair major lesions caused by DNA-damaging effects of FZ and DOC would indeed result in bacterial death. Lastly, FZ and DOC downregulated the central carbon metabolism, an effect commonly observed in bacteriostatic antibiotics. Red, blue, and green indicate effects specific to FZ, DOC and VAN, respectively, whereas purple indicates effects that are common to FZ and DOC. Black lines indicate known *E. coli* resistance mechanisms to the antibacterials.

study in which the deletion of *tolC* resulted in the loss of synergistic interaction between FZ and DOC, suggesting the importance of efflux in the synergistic interaction (Le *et al.*, 2020).

Another effect observed in both FZ- and DOC-containing cultures is oxidative stress (Section 4.5.9). If these drugs disrupt Fur protein leading to its loss of function/inactivation, the labile Fe²⁺ iron pool will be in excess, and Fe²⁺ can catalyse the Fenton reaction and produce ROS that causes oxidative stress and DNA damage leading to the SOS response (Imlay *et al.*, 1988). In this study, FZ treatment only showed induction of superoxide response genes, while DOC showed induction of both superoxide and hydrogen peroxide stress responses (Figure 29). An important fact to consider is that the lack of change in the expression of *ahpCF* and the downregulation of *dps* and *katG* in FZ-treated *E. coli* does not necessarily mean that there is no H₂O₂ stress. The observed downregulation of *katG* and *dps* could be a downstream result of another FZ effect such as iron starvation. For example, KatG is a protein that uses heme as a cofactor, and under iron starvation, heme synthesis and utilisation could be limited. Additionally, since OxyR activation is known to be H₂O₂ concentration-dependent (González-Flecha *et al.*, 1997; Seaver *et al.*, 2001), it is possible that the H₂O₂ concentration at the sample collection timepoint is still below the concentration needed to activate OxyR. Another possibility is that FZ only results in the production of low levels of H₂O₂ that is quickly detoxified by basal H₂O₂ scavenging enzymes, hence there is no need to activate the OxyR regulon. In *Shigella flexneri*, however, FZ was shown to upregulate the expression of *ahpC* and *ahpF*, which indicates the presence of H₂O₂ stress (Fu *et al.*, 2007).

In terms of DNA damage, as predicted, FZ treatment led to the induction of the SOS response (Section 4.5.5), consistent with the DNA-damaging effects of nitrofurans that have been reported extensively. FZ and NIT were shown to cause filamentation in

Salmonella due to inhibition of cell division that occurs during SOS response (Chadfield *et al.*, 2004). The DNA damage has been speculated to be caused by the reactive byproducts and intermediates of nitrofurantoin reduction. For example, superoxide, produced during Type II nitroreduction (Chapter 1, Figure 6), can readily transform to DNA-damaging hydroxyl radical (Imlay *et al.*, 1988), and hydroxylamine derivatives, produced during Type I nitroreduction (Chapter 1, Figure 5), are reported to cause DNA damage and mutagenicity (Stolarski *et al.*, 1987; Sakano *et al.*, 2004; Yamamoto *et al.*, 1993). α,β -unsaturated nitriles can also be formed (Hall *et al.*, 2011), and these derivatives have the same Michael acceptor property as α,β -unsaturated carbonyls, which are known inducers of DNA damage and mutagenesis (Janzowski *et al.*, 2003; Eder *et al.*, 1993; Eder *et al.*, 1990).

DOC, on the other hand, only resulted in significant differential expression of a few genes involved in DNA repair (Section 4.5.5, Figure 25): Only four genes, *recX*, *ruvC*, *recQ*, and *dinF* were upregulated by more than 1.5-fold ($\log_2FC > 0.58$), while *lexA*, *cho* (*uvrC* homologue), and *dinI* were statistically significant ($\text{adj } p < 0.01$), but were only differentially expressed by less than 1.5-fold. ROS generation and DNA damage have been reported to be induced by bile salts in bacteria such as *Campylobacter* (Negretti *et al.*, 2017) and *Salmonella* (Walawalkar *et al.*, 2016). Using reporter genes, DOC was also found to induce *dinD*, a gene associated with DNA damage, in *E. coli* (Bernstein *et al.*, 1999). It is, therefore, not surprising that *Salmonella* and *Campylobacter* DNA repair mutants (e.g. *recBCD*, *addAB*) are more sensitive to DOC in comparison to the wildtype parents (Prieto *et al.*, 2006; Gourley *et al.*, 2017). The absence of the upregulation of most genes involved in SOS response and DNA repair during the first 60 min of exposure to DOC, may be due to premature sampling, if the effect of DOC is secondary and requires

longer incubation time. Alternatively, the concentration of DOC may have been too low to induce the required level of DNA damage for an SOS response.

FZ and DOC both downregulated the central carbon metabolic pathways (Section 4.5.8, Figure 28). This effect could be a result of the drop in the proton-pumping ETC complexes. Due to less energy demand and lower NADH use, the central carbon metabolism could be downregulated through metabolite feedback mechanisms. This effect is commonly observed in bacteriostatic antimicrobials, which inhibit growth by reducing cellular metabolism. FZ and DOC at inhibitory concentrations are bactericidal. The concentrations used in this study are subinhibitory, and since the exact modes of action of these two antibacterials are not fully understood, bacteriostatic action at these concentrations cannot be ruled out. A microarray study of bacteriostatic translation inhibitors kasugamycin and puromycin in *E. coli* showed downregulation of genes of the glycolytic, pentose phosphate pathway, and TCA cycle (Sabina *et al.*, 2003). Also, chlortetracycline, which is another bacteriostatic translation inhibitor, showed downregulation of similar metabolic proteins in an *E. coli* proteome study (Lin *et al.*, 2014).

FZ and DOC also resulted in the upregulation of genes encoding ribosomal proteins and other components of translation machinery (Section 4.5.7). Since samples were collected at a time point when the growth rate of treated samples is similar, if not lower, than that of the untreated samples, the upregulation of ribosomal and translation genes in the treated samples cannot be attributed to increased growth rate. A similar effect has been reported by Mathieu *et al.* (2016) in *E. coli* treated with sublethal concentrations of antibiotics (ampicillin, norfloxacin, and gentamicin). These antibiotics have different mechanisms of action; however at sublethal concentrations ($\frac{1}{2} \times \text{MIC}$), they elicited the

same increase in ribosomal and translational capacity and increased energy production, all while growth rates were identical to the untreated samples. The authors have proposed that, at sublethal concentrations, the antibiotics trigger a response in *E. coli* whereby it maintains growth, along with cell repair and maintenance as long as sufficient nutrients are present (Mathieu *et al.*, 2016). This hypothesis could explain the increased expression of ribosome and translation genes at sublethal FZ and DOC concentrations used here. Similar to the abovementioned report, at the time point of sample collection, the antibacterial-containing cultures had an almost identical growth rate as no-antibacterial controls, showing that the cells were keeping up with rapid growth all while dealing with stress and damage induced by the antibiotics.

This effect is also commonly observed in cultures with protein synthesis inhibitors and acts as a counteracting mechanism to the reduced translational activity, enabling the cells to keep the pace of protein synthesis at low levels of translation inhibition (O'Rourke *et al.*, 2020; Sabina *et al.*, 2003; Lin *et al.*, 2014; Dennis, 1976). Reactive intermediates of nitrofurans have been reported to bind ribosomal protein subunits and rRNA non-specifically; this interaction was proposed to cause translation inhibition (McOsker *et al.*, 1994; Yu *et al.*, 1976). DOC, on the other hand, was demonstrated to be able to aggregate proteins (89 total); 23 of which were ribosomal and other translation machinery proteins (Cremers *et al.*, 2014). FZ and DOC have also been reported to result in the production of ROS, which are major sources of damage to macromolecules, primarily nucleic acids (Liu *et al.*, 2012). ROS have been shown to damage rRNA and inhibit the ribosome during protein synthesis (Willi *et al.*, 2018). Additionally, Zhong *et al.* (2015) reported a reduction of tRNA levels during oxidative stress that resulted in the deceleration of translation. In conclusion, direct FZ and DOC effects on ribosomal and translation proteins *via* aggregation, together with effect on rRNA *via* ROS, result in translational

stress, to which *E. coli* responds by increasing the expression of translation and rRNA synthesis genes, as observed in FZ and DOC treatment.

The synergy between FZ and DOC is apparent in their correlated transcriptional responses. One way in which synergy can arise is if one drug inhibits the resistance mechanism(s) of the other, such as in the case of β -lactams and β -lactamase inhibitors (Kobayashi *et al.*, 1989). Cultures containing DOC alone and the FZ+DOC+VAN combination both upregulated the expression of efflux pump component genes, *acrA* and *acrB* (Figure 29). Although in this study upregulation of *acrA* and *acrB* by FZ was not statistically significant, upregulation of these genes by FZ has been reported previously (Fu *et al.*, 2007). Upregulation of efflux pumps will prevent the accumulation of these antibacterials inside the cells. In this instance, synergy could arise through the combined effect of FZ and DOC in diminishing the PMF, in turn, de-energising the efflux pumps and preventing drug efflux. This mechanism allows the accumulation of drugs inside the cell and exertion of their effects on their targets.

This study only uncovered 17 genes that are affected significantly by VAN. Therefore, it is difficult to draw conclusions on the possible sources of synergy from VAN effects. DOC is known to disrupt the outer membrane (Begley *et al.*, 2005) and even integrate into membranes and form aqueous channels in which hydrophilic molecules can pass (Gordon *et al.*, 1985). It is possible that membrane disruption by DOC allows more VAN to enter and exert its effect. Using the transcriptomics data by O'Rourke *et al.* (2020), who investigated the transcriptional response of an *E. coli* strain with a compromised outer membrane to various antibiotics including VAN, another pathway affected by VAN was revealed. Biological process GO term enrichment of significantly downregulated genes (FDR < 0.01, log₂FC < 0) using PANTHER showed SOS response to be overrepresented. The SOS response genes downregulated by VAN in the O'Rourke *et al.*

dataset are *umuC*, *umuD*, *uvrB*, *uvrC*, *uvrD*, *recN*, *dinB*, *dinG*, *polB*, *cho*, and *sulA*.

Downregulation of these genes could then explain the synergy between NIT and VAN reported by Zhou *et al.* (2015), who hypothesised that VAN must increase DNA-damaging effects when combined with DNA-damaging agents (NIT or trimethoprim), thereby eliciting a synergistic effect. If VAN exerts the same inhibition of SOS/DNA repair in wildtype *E. coli*, this effect would contribute to the triple synergy through amplification of the FZ and DOC DNA-damaging effects.

In summary, this chapter searched for the possible mechanistic bases of the synergy between FZ, DOC, and VAN using a transcriptomics approach. The transcriptional responses shed light on the modes of action of FZ and DOC, whose primary targets are most likely multiple. In the absence of a single target, it was impossible to precisely determine which are the target effects and which are the downstream responses for these two antibacterials. Nonetheless, by analysing the highly correlated perturbed pathways of FZ and DOC, in combination with VAN effects, it was possible, based on identified changes in gene expression, to formulate hypotheses on the mechanisms involved in the suppression of resistance and amplification of damaging effects. Some of these will be investigated in the following chapter.

5 Investigating pathways involved in the action and synergy of furazolidone, sodium deoxycholate, and vancomycin

5.1 Introduction

Chapter 4 presented the transcriptomic response of *E. coli* to single antibacterials (FZ, DOC, or VAN) and their triple combination. Results showed the lack of SOS response induction in the combination despite strong induction in cultures containing FZ alone, highlighting the advantage of synergistic interactions in mitigating adverse effects. The transcriptional responses also indicated a role of the Fur regulon in the FZ and DOC action, which could be contributing to the synergy of the combination. FZ and DOC caused gene expression changes consistent with the inactivation of Fur, mimicking a reversal of Fur's transcriptional repression of iron uptake genes that occurs during iron limitation. This activity is expected to have downstream effects on iron-rich proteins, such as TCA cycle and transmembrane redox enzyme complexes of the ETC (Massé *et al.*, 2005), and could therefore explain the downregulation of some ETC genes after FZ and DOC treatment.

The ETC produces PMF that drives ATP synthesis (Maloney *et al.*, 1974) and is utilised by energy-requiring processes such as solute transport (Paulsen *et al.*, 1996; Mitchell, 1976). The PMF consists of two components: the electric potential ($\Delta\Psi$) arising from the charge separation across the membrane, and the transmembrane proton gradient (ΔpH). Disruption of the PMF could occur through inhibition of specific membrane-associated ETC proteins, which could lead to membrane depolarisation (Hards *et al.*, 2015). Also, some membrane-damaging agents, which are usually lipophilic, can disrupt multiple targets through interaction with the membrane, resulting in the loss of membrane integrity, inhibition of membrane proteins, and dissipation of the PMF (Feng *et al.*, 2015; Sikkema *et al.*, 1995; Straus *et al.*, 2006). Downregulation of ETC genes (Chapter 4), combined with the reported membrane-damaging effects of VAN and DOC, could lead

to the disruption of the PMF, and subsequently the inhibition of the PMF-dependent efflux pumps (Paulsen *et al.*, 1996), which play a significant role in antibiotic resistance.

Another affected pathway that could be contributing to the synergy is the DNA damage-DNA repair pathway. Intermediates or byproducts of nitrofurantoin activation are DNA-damaging and induce the SOS response (Ona *et al.*, 2009; Mitošć *et al.*, 2019). Although no DNA damage response was found in DOC-treated *E. coli* in this study, DOC and other bile salts have been reported to cause DNA damage and induce the SOS response in *E. coli* and other bacteria (Prieto *et al.*, 2006; Merritt *et al.*, 2009), at concentrations and under growth conditions that are different from those used in Chapter 4. Moreover, as shown in Chapter 4 and reported previously, both of these agents result in the production of ROS that cause oxidative DNA damage (Prieto *et al.*, 2006; Negretti *et al.*, 2017). VAN, on the other hand, has been shown not to induce SOS response in *S. aureus* (Plata *et al.*, 2013). However, it is generally accepted that bactericidal antibiotics, such as VAN, ultimately generate ROS that can damage DNA and lead to cell death (Kohanski *et al.*, 2007). O'Rourke *et al.* (2020) transcriptomics dataset showed that VAN treatment of outer membrane-compromised *E. coli* downregulated genes involved in the SOS response. This effect, if proven, could explain the synergy between nitrofurantoin and VAN, reported in this study and by Zhou *et al.* (2015).

This chapter aims to validate the findings of the transcriptomic analysis and explore potential pathways involved in synergy. Firstly, the role of the Fur protein and the ETC enzymes in the action and synergy of FZ, DOC, and VAN, along with possible downstream effects on efflux, were investigated through the use of gene deletion mutants and biochemical approaches. Next, since the combination did not show induction of SOS response genes, the mutagenicity of the monotherapies and combination were determined

to confirm that the significantly decreased dose of FZ in the combination lowers mutation frequency in *E. coli*. Lastly, the role of the SOS response in the synergy was investigated.

5.2 Results

5.2.1 Fur plays a role in the synergy of FZ and DOC

The transcriptomic analyses showed gene expression changes consistent with the inactivation of Fur protein after FZ and DOC treatment. A *fur* deletion mutant was constructed in strain K1508 to investigate the involvement of Fur protein in the action of FZ and DOC. Since Fur is the transcriptional repressor of iron uptake genes, Δfur mutant accumulates iron inside the cells and can be used to investigate the effects of increased iron levels in antibiotic susceptibility. The MIC of FZ, DOC, and VAN were determined in *E. coli* K1508 (wildtype for *fur*) and derived Δfur mutant using broth microdilution method, and it was found that the deletion of *fur* increased susceptibility to FZ by 2-fold, while DOC and VAN MICs were unchanged (Table 8). These results were further confirmed in the Keio collection strain *E. coli* BW25113, whose *fur* deletion mutant also showed decreased MIC (2-fold) of FZ.

Table 8. Minimum inhibitory concentrations of *fur* mutants using broth microdilution

	MIC ($\mu\text{g/mL}$)		
	FZ	DOC	VAN
K1508	2.5	>80000	250
K1508 Δfur	1.25	>80000	250
BW25113	2	>80000	250
BW25113 Δfur	1	>80000	250

MIC, minimum inhibitory concentration; FZ, furazolidone; DOC, sodium deoxycholate; VAN, vancomycin

Interestingly, the effect of *fur* deletion on VAN susceptibility has already been assayed on agar, and this deletion was shown to increase susceptibility to VAN (Liu *et al.*, 2010). This contradiction to the present results could be attributed to the different methods used to determine susceptibility (in liquid *vs* on solid medium). Therefore, MIC determination was also performed using the agar dilution method (Clinical and Laboratory Standards Institute, 2015). High concentrations of DOC, however, precluded MIC determination using this method, since they result in self-induced gelation that interferes with solidification of agar. Similar to the broth method, *fur* deletion increased FZ susceptibility, but the difference was more pronounced (4-fold; K1508 MIC was 1 µg/mL and K1508 Δfur 0.25 µg/mL). Moreover, Δfur mutant showed a 2-fold increase in susceptibility to VAN (K1508 MIC was 250 µg/mL and K1508 Δfur is 125 µg/mL), in agreement with the Liu *et al.* (2010) study. Lastly, since DOC solubility level in media is preventing MIC determination, any effects of *fur* deletion on DOC susceptibility cannot be ruled out.

The transcriptional analysis of FZ- and DOC-treated *E. coli* resembled Fur inactivation (Chapter 4, Section 4.5.6). This Fur inactivation could be contributing to the effect of FZ and DOC on *E. coli* through the increase of Fe²⁺ that could lead to oxidative stress by potentiating the Fenton reaction (Imlay, 2003). In addition, it could also result in the downregulation of PMF-generating enzymes (Seo *et al.*, 2014), leading to the inhibition of PMF-dependent efflux. For these reasons, it was hypothesised that the combined action of FZ and DOC, which results in the inactivation of Fur, is a possible source of the synergy of FZ and DOC that was previously reported (Le *et al.*, 2020). Furthermore, since deletion of *fur* increased susceptibility to VAN on solid media, it is possible that the inactivation of Fur by FZ and DOC increases susceptibility to VAN effects, and contributes to the triple-drug combination synergy. If these scenarios were true,

disruption of Fur would make this combined activity on Fur inactivation redundant, thus increasing the interaction index (FICI) in the *fur* deletion mutant relative to that in the *fur*⁺ parent strain.

To validate this model, checkerboard assay was performed on K1508 and its Δfur mutant. Deletion of *fur* in K1508 caused a shift from the synergistic interaction between FZ and DOC in the wildtype (FICI < 0.09) to indifferent interaction (FICI < 0.63), as shown in Figure 31A. These results were also confirmed in the *E. coli* strain BW25113 (Figure 31B), which also showed a loss of synergistic interaction in the Δfur mutant.

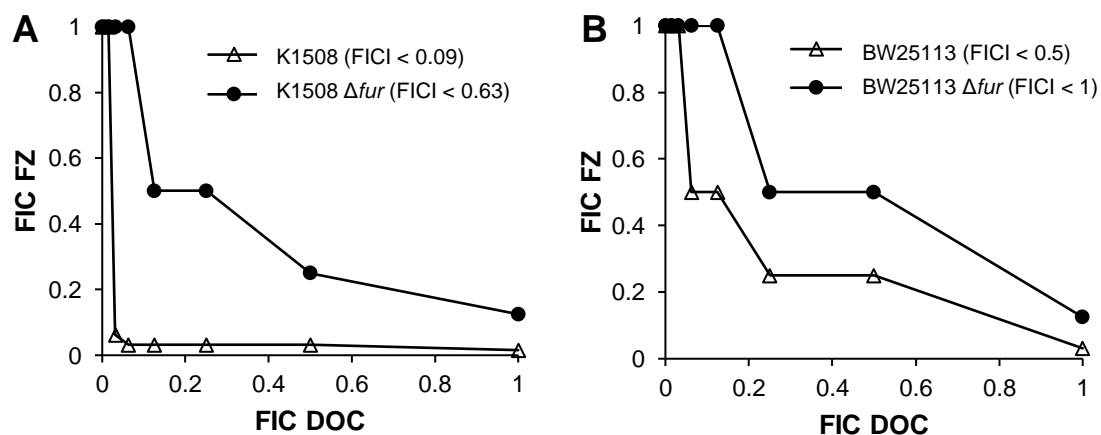


Figure 31. FZ-DOC interactions in the absence of Fur

The isobolograms of FZ and DOC interaction in growth inhibition of A) K1508 and B) BW25113 strains and derived Δfur mutants. Each data point corresponds to the fractional inhibitory concentrations (FICs; ratios of the MIC in combination vs. alone).

A triple combination checkerboard assay was performed for K1508 and derived Δfur mutant to investigate whether Fur also plays a role in the triple combination synergy. Only a slight increase in the FICI of FZ+DOC+VAN was measured in the Δfur mutant (FICI < 0.27) compared to the wildtype (FICI < 0.13), indicating only a slight decrease

in synergy (Appendix A, Figure A- 5A). Taken together, these findings support the hypothesis that Fur is an interacting point for the synergy between FZ and DOC. In terms of the triple combination synergy, however, the action on Fur is contributing to the synergy, but other major sources are likely, given that deletion of *fur* still results in a synergistic interaction, albeit less profound.

5.2.2 Intracellular metal homeostasis is affected by FZ and DOC

Since FZ and DOC resulted in dysregulation of iron homeostasis, the effect of the antibacterials and their combination (at the same concentrations used in the transcriptomics study in Chapter 4) on intracellular iron levels was investigated using ICP-MS analysis. Given that regulation of multiple metal homeostases in bacteria is interconnected (Chandrangsu *et al.*, 2017), the levels of other essential metals, including magnesium, zinc, nickel, manganese, and copper were also measured.

The intracellular levels were measured for the higher-abundance metals, magnesium, iron, and zinc (Figure 32A) and lower-abundance metals nickel, manganese, and copper (Figure 32B). FZ treatment resulted in a 1.8-fold decrease in iron ($p < 0.001$) and a 3-fold increase in manganese levels ($p < 0.001$). DOC, on the other hand, resulted in a more than 9-fold decrease in magnesium ($p < 0.001$), a 1.6-fold decrease in iron ($p < 0.05$), an almost 2-fold decrease in manganese ($p < 0.001$), and a 2.5-fold increase in copper levels ($p < 0.05$). Lastly, the triple combination's effect on the levels of these metals is the same as DOC, indicating DOC's effect to be the most predominant in the combination. The fold changes caused by the combination, however, are much more pronounced than those by DOC, such as the 18-fold decrease in magnesium ($p < 0.001$), a 1.9-fold decrease in iron ($p < 0.001$), an almost 5-fold decrease in manganese ($p < 0.001$), and a 6.5-fold increase in copper ($p < 0.001$).

There was no significant change in the total intracellular zinc and nickel levels in the presence of any of the single antibacterials or combination, as compared to the no-antibacterials control; while VAN treatment resulted in no significant change in the total intracellular levels of any of the metals that were analysed in this study. Taken together,

FZ and DOC, besides affecting iron homeostasis, also result in the dysregulation of other essential metals, including manganese, magnesium, and copper.

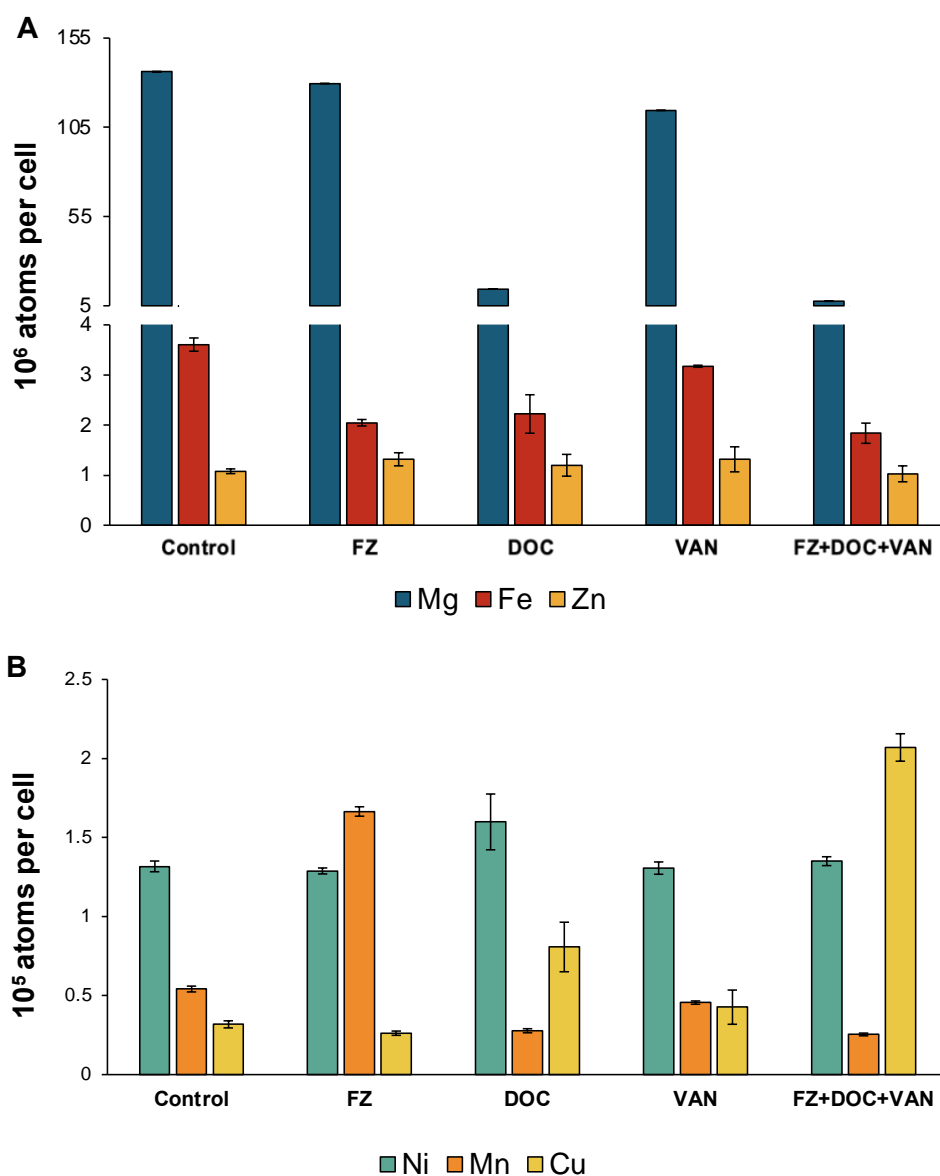


Figure 32. Intracellular metal levels after treatment with FZ, DOC, and VAN and the triple combination

Intracellular metal concentrations were measured using ICP-MS in K1508 cells exposed to IC₅₀ doses of FZ, DOC and VAN alone and FZ+DOC+VAN combination for 1 h. Data show the mean of 3 biological replicates) ± standard error of the mean. Statistical significance (Student's t-test of treatment vs control) is indicated by asterisks as follows: *, $p < 0.05$; ***, $p < 0.001$.

5.2.3 The electron transport chain

The transcriptomic analysis (Chapter 4) showed downregulation of some ETC genes. This could be a result of the Fur inactivation, which induces an iron-sparing mechanism mediated by the sRNA RyhB, and is known to regulate the ETC genes *cyd* (cytochrome *bd-I*) and *nuo* (NADH dehydrogenase I) (Massé *et al.*, 2005). In addition, downregulation of the central carbon metabolism can explain the downregulation of these genes through a feedback mechanism for less energy demand. It cannot be ruled out, however, that a separate pathway that leads to the downregulation of these genes are affected by FZ and DOC. Nevertheless, these findings prompted the investigation of the role of the ETC in the action of FZ, VAN, and DOC.

Table 9. Minimum inhibitory concentrations of electron transport chain mutants

	MIC (µg/mL) using broth microdilution			MIC (µg/mL) using agar dilution		
	FZ	DOC	VAN	FZ	DOC	VAN
K1508	2.5	>80000	250	1	ND	250
K1508 Δ<i>appB</i>	2.5	>80000	250	1	ND	250
K1508 Δ<i>cyoB</i>	2.5	>80000	250	1	ND	250
K1508 Δ<i>cydB</i>	2.5	>80000	250	1	ND	<31.25
K1508 Δ<i>ndh</i>	2.5	>80000	250	1	ND	500
K1508 Δ<i>nuoM</i>	2.5	>80000	250	1	ND	250

MIC, minimum inhibitory concentration; FZ, furazolidone; DOC, sodium deoxycholate; VAN, vancomycin; ND, not determined

To investigate the involvement of each of the major aerobic ETC enzymes, deletion mutants (Δ *appB* - cytochrome *bd-II*, Δ *cyoB* - cytochrome *bo3*, Δ *cydB* - cytochrome *bd-I*, Δ *ndh* -NADH dehydrogenase II, Δ *nuoM* - NADH dehydrogenase I) were constructed by P1 transduction. The MIC of FZ, DOC, and VAN in each of the mutants were determined

using broth microdilution and agar dilution methods, as shown in Table 9. Using broth microdilution, there was no change in the MIC of the knockouts compared to wildtype, while using agar dilution, increased susceptibility and resistance to VAN was observed in $\Delta cydB$ and Δndh mutants, respectively.

Although the MIC of FZ in the knockout mutants remained unchanged using the agar dilution method, a slightly increased survival of $\Delta cyoB$ and Δndh mutants can be observed on agar containing $\frac{1}{2} \times$ MIC concentration (0.5 $\mu\text{g/mL}$) of FZ (Figure 33). Interestingly, *cyoB* and *ndh* are the only ETC genes that were upregulated by FZ and DOC in the transcriptomics study, while the rest were downregulated (Chapter 4, Figure 28).

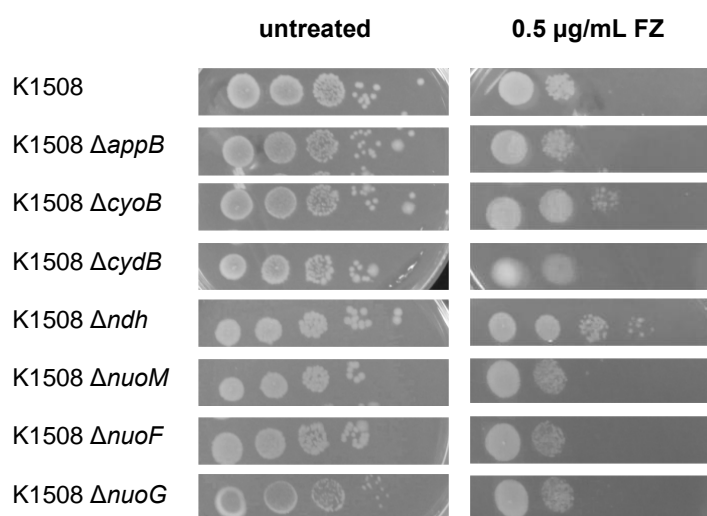


Figure 33. Survival of electron transport chain deletion mutants at sub-MIC FZ

Logarithmically growing *E. coli* K1508 wildtype, $\Delta appB$ (cytochrome bd-II), $\Delta cyoB$ (cytochrome bo3), $\Delta cydB$ (cytochrome bd-I), Δndh (NADH dehydrogenase II), and, $\Delta nuoM$ (NADH dehydrogenase I) were ten-fold serially diluted and spotted onto 2xYT plates containing 0.5 $\mu\text{g/mL}$ FZ ($\frac{1}{2} \times$ MIC), and incubated overnight at 37 °C overnight. The experiment was conducted three times, and a representative result is shown.

The possibility that the ETC genes play a role in the synergy of FZ and DOC was also investigated using checkerboard assays. There was no change in FZ and DOC FICI for $\Delta appB$ and $\Delta cyoB$ mutants compared to the wildtype parent strain K1508, while the FICIs for $\Delta cydB$, Δndh , and $\Delta nuoM$ increased slightly, but are still considered synergistic (Table 10). To confirm these results, checkerboard assay was also performed on deletion mutants of the Keio collection strain BW25113, and it was found that only *ndh* deletion resulted in a decrease in synergistic interaction between FZ and DOC (Table 10).

Table 10. Fractional inhibitory concentration index for FZ-DOC interactions in electron transport chain mutants

	FICI FZ-DOC		FICI FZ-DOC
K1508	<0.09	BW25113	<0.5
K1508 $\Delta appB$	<0.09	BW25113 $\Delta appB$	<0.5
K1508 $\Delta cyoB$	<0.09	BW25113 $\Delta cyoB$	<0.5
K1508 $\Delta cydB$	<0.16	BW25113 $\Delta cydB$	<0.5
K1508 Δndh	<0.28	BW25113 Δndh	<0.63
K1508 $\Delta nuoM$	<0.16	BW25113 $\Delta nuoM$	<0.5

FICI FZ-DOC, lowest fractional inhibitory concentration index from furazolidone and sodium deoxycholate interaction assessed using checkerboard assay.

5.2.4 FZ and DOC decelerates *E. coli* aerobic ETC

Downregulation of genes encoding ETC enzymes prompted the assessment of physiological changes at the level of cellular respiration, induced by FZ, DOC, or VAN (at the same concentrations as those used in Chapter 4). Oxygen is the major electron acceptor of the *E. coli* aerobic ETC (Ingledeew *et al.*, 1984). Therefore, to investigate the overall effect of the antibiotics on aerobic respiration, the rates of oxygen consumption were measured using a Clark-type oxygen electrode (Figure 34).

Exposure to FZ and DOC for 1 h significantly decreased the oxygen consumption rate, causing a 1.6-fold ($p < 0.001$) and 1.7-fold ($p < 0.001$) decrease, respectively, in comparison to the no-antibacterial control. VAN, on the other hand, only caused a slight decrease (~1.15-fold) compared to the untreated control, but this change was still considered statistically significant ($p < 0.05$). Similarly, the FZ+DOC+VAN combination decreased oxygen consumption by ~1.7-fold ($p < 0.001$). In the single-antibacterial cultures where concentrations of each antibacterial were lowered to the same absolute concentration as in the combination (FZ 3d, DOC 3d, or VAN 3d), only DOC 3d resulted in a significant decrease in oxygen consumption compared to the no-antibiotic control. These findings are in agreement with the downregulation of aerobic ETC genes by FZ, DOC, and the FZ+DOC+VAN combination observed in Chapter 4 (Section 4.5.8).

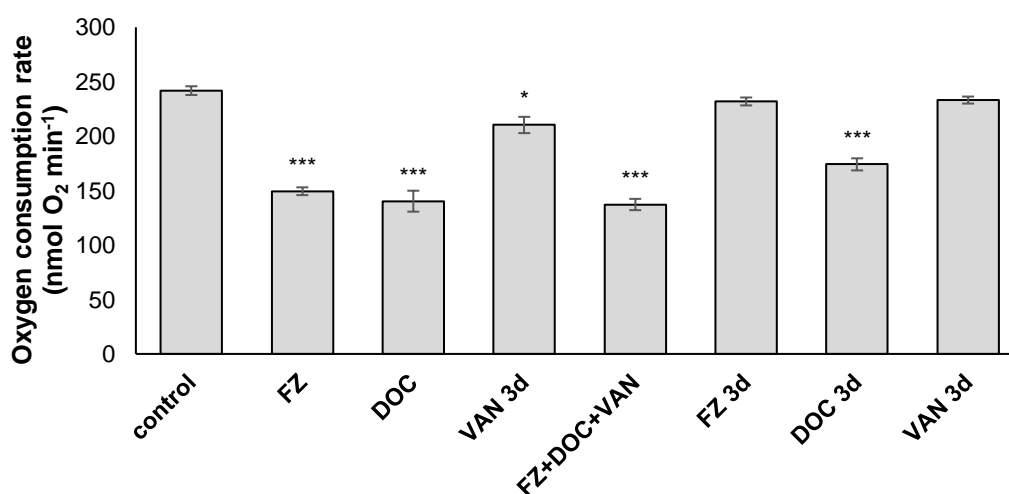


Figure 34. Oxygen consumption rate in antibacterial-containing cultures

Oxygen consumption by K1508 cultures was measured with a Clark-type closed-chamber oxygen electrode during exposure to FZ, DOC, and VAN alone and in combination. The cells were pre-treated with the drugs for 1 h, then oxygen consumption was measured for up to 5 min. Data show the mean of 3 replicates \pm standard error of the mean. Statistical significance (Student's t-test of treatment vs control) is indicated by asterisks as follows: *, $p < 0.05$; ***, $p < 0.001$.

5.2.5 Possible efflux inhibitory activity of FZ and DOC

Downregulation of ETC genes, supported by the lowered oxygen consumption rates, indicate diminished PMF and possibly lower ATP concentration due to diminished activity of ATP synthase. These changes may, in turn, affect the PMF-dependent efflux pumps. Given that, at a minimum, DOC resistance is majorly reliant on efflux pumps (Thanassi *et al.*, 1997), one possible synergy mechanism could be through decreased rate of expulsion. If FZ and VAN do result in the inhibition of efflux, this activity could be a source of the synergistic interaction.

To investigate whether FZ, DOC, VAN, or triple combination inhibit efflux pumps, ethidium bromide accumulation and efflux assays were performed. Ethidium bromide is a DNA-intercalating agent that fluoresces when bound to DNA (Olmsted *et al.*, 1977), and is also an efflux pump substrate. Therefore, drug effects on efflux can be investigated by monitoring accumulation or extrusion of ethidium bromide using fluorometry. In these assays, carbonyl cyanide 3-chlorophenylhydrazone (CCCP) was used as a positive control. CCCP is a protonophore that dissipates the proton gradient across the inner membrane, leading to a drop in PMF. By majorly compromising PMF, CCCP uncouples oxidative phosphorylation (ATP synthesis) from ETC, leading to a drop in oxidative phosphorylation and ATP production, as well as inhibition of efflux pumps (Heytler, 1963; Kasianowicz *et al.*, 1984).

Firstly, the highest ethidium bromide concentration (0.125 µg/mL) that does not result in accumulation in untreated cells was identified experimentally. Figure 35A shows the ethidium bromide accumulation during treatment with FZ, DOC, and VAN monotherapies and combination. As expected, CCCP increased the accumulation of ethidium bromide. Similarly, all cultures containing DOC (DOC, FZ+DOC+VAN, DOC

3d) and cultures containing VAN also increased ethidium bromide accumulation starting at 10 min and 20 min time points, respectively. Lastly, FZ did not result in any observable change in ethidium bromide fluorescence compared to the control.

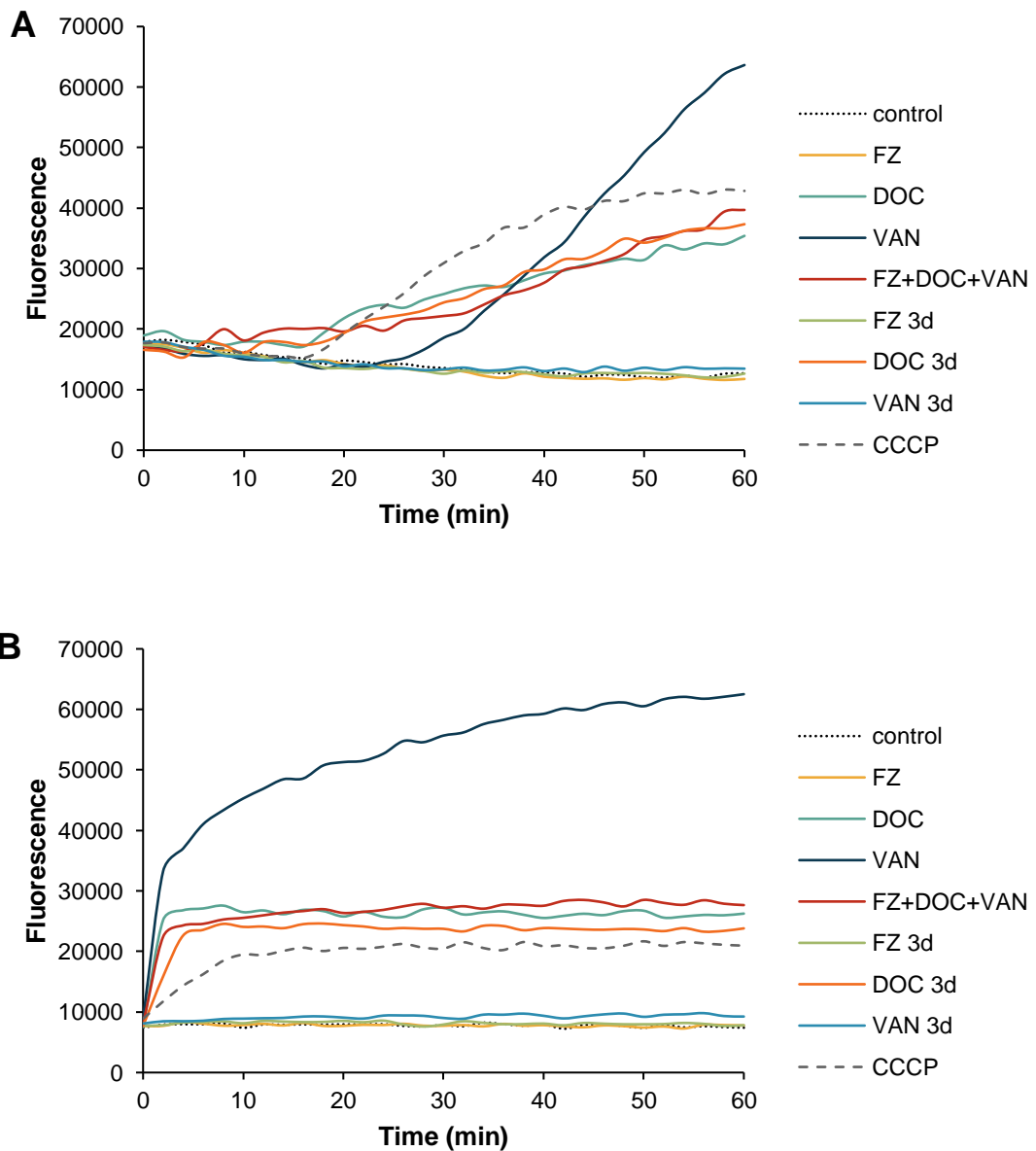


Figure 35. Effect of FZ, DOC, and VAN ethidium bromide accumulation

A) 0.125 $\mu\text{g/mL}$ ethidium bromide and antibiotics were added to *E. coli* K1508 and the fluorescence was monitored at 37 $^{\circ}\text{C}$ for 1 h. B) *E. coli* K1508 were first treated with the antibiotics for 1 hr then 0.125 $\mu\text{g/mL}$ ethidium bromide was added, and the fluorescence monitored.

To check whether a prolonged exposure to antibacterials (or CCCP) will have a more pronounced effect on efflux, especially for FZ, cultures were pre-treated with the drugs for 1 h before the addition of ethidium bromide. In Figure 35B, almost immediate accumulation of ethidium bromide fluorescence was observed in the presence of CCCP, VAN, and DOC, but still, no changes were observed in the presence of FZ.

To confirm the results obtained above on the accumulation of ethidium bromide, an efflux assay was also performed. Initially, cells were subjected to conditions that promote significant ethidium bromide accumulation over a period of 1 h: incubation with 5 $\mu\text{g/mL}$ ethidium bromide and 5 $\mu\text{g/mL}$ CCCP in 2xYT at 37 °C. After this ethidium bromide-loading step, the cells were washed, then resuspended in medium containing the test antibacterials with or without 0.4% glucose, which is commonly used to re-energise efflux pumps (Paixão *et al.*, 2009). As shown in Figure 36A, efflux takes place readily in the presence of glucose at 37 °C, an activity that is inhibited in the presence of CCCP and to a lesser extent in cultures containing DOC (DOC, FZ+DOC+VAN, and DOC 3d). In the absence of glucose, the same results were obtained, except a slight delay in the decrease of ethidium bromide fluorescence was observed in the presence of FZ (indicated by an arrow in Figure 36B).

Contrary to the accumulation assay, VAN did not slow down the extrusion of ethidium bromide. This finding most likely points to the increased membrane permeability caused by VAN, as the reason for increased ethidium bromide accumulation inside the cell, which is a dominant process in the accumulation assays (Figure 35), whereas the extrusion assay only measures efflux of ethidium bromide (Figure 36). Interestingly, in the presence of DOC treatments, the ethidium bromide fluorescence does not decrease to the same levels as the control and seem to be followed by re-accumulation. From these results, it can be inferred that DOC does inhibit efflux, which is evident by the delay in

the extrusion of ethidium bromide seen at the beginning of treatment, and that because of this efflux inhibition, ethidium bromide released in the media re-accumulates inside the cell.

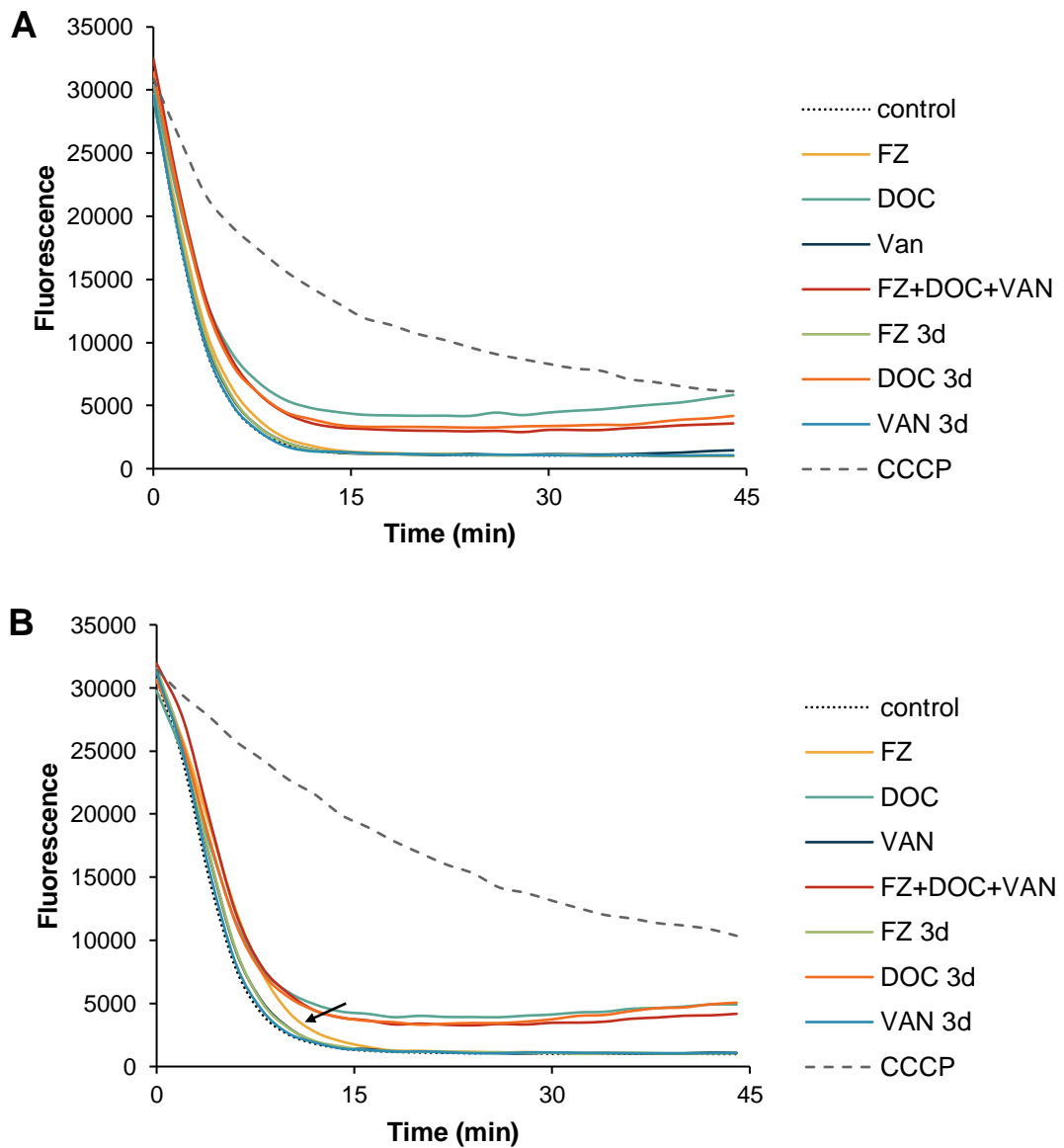


Figure 36. Effect of FZ, DOC, and VAN on ethidium bromide efflux

E. coli K1508 were pre-loaded with ethidium bromide, and the efflux was monitored by measuring fluorescence cultures containing FZ, DOC, and VAN alone or in combination, in the (A) presence and (B) absence of glucose (0.4%). Arrow indicates delayed ethidium bromide efflux in FZ-treated cells.

5.2.6 FZ dose reduction in the combination decreases mutagenicity

Since FZ has been reported to be a DNA-damaging agent (Olive *et al.*, 1977), it was not surprising that the transcriptomics analysis in this study showed FZ-induced upregulation of genes involved in the SOS response, the canonical response to DNA damage. The SOS response plays a role in increasing the survival of *E. coli* to nitrofurans by preventing irreversible DNA fragmentation (Bryant *et al.*, 1980). However, besides DNA repair, the SOS response also triggers error-prone mechanisms that result in increased mutation rate. This mutagenicity is one of the reasons the nitrofurans have fallen out of favour (Vass *et al.*, 2008). One of the aims of using nitrofuran in a synergistic combination is to take advantage of the reduced doses, which could possibly mitigate adverse effects. The transcriptional response to the combination did not show the same upregulation of SOS response genes as FZ alone, which indicates the absence of severe DNA damage.

To assess the levels of DNA damage the antibacterials alone and in combination (at the same concentrations used in Chapter 4) elicit in *E. coli*, the mutation frequencies were determined by counting the number of bacteria that gain the ability to grow on rifampicin plates. Rifampicin is an RNA polymerase inhibitor, and resistance to this antibiotic can arise through single base substitutions in the RNA polymerase gene *rpoB* (Wehrli, 1983). *E. coli* K1508 is rifampicin-susceptible and did not have mutations in *rpoB*, as indicated by the genome sequence. Under nonstress conditions (control), the spontaneous mutation frequency of *E. coli* K1508 is around 7 mutants per 10^8 cells (Figure 37). Expectedly, given FZ's DNA-damaging effects, this number significantly increased (the mean frequency more than doubled) upon FZ treatment. DOC, on the other hand, has also been reported to cause DNA damage; however, the DOC concentrations used in this study did not result in any significant change in rifampicin mutation frequency. The combination and the monotherapies at the concentration used in the combination (FZ 3d, DOC 3d, and

VAN 3d) also did not result in a statistically significant change in the mutation frequency compared to the control, which confirms that the reduced concentration of FZ in the combination does not induce severe DNA damage that triggers the SOS response resulting in mutagenicity.

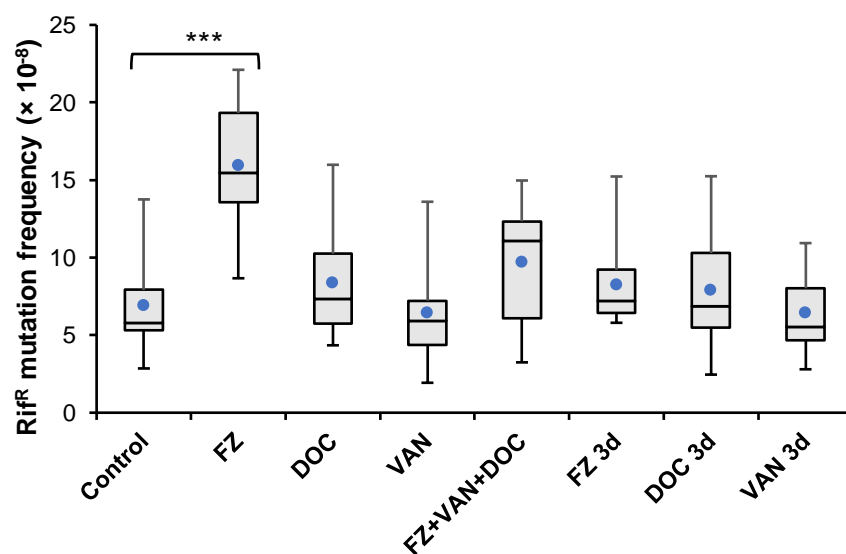


Figure 37. Rifampicin resistance mutation frequency in *E. coli* K1508 treated with FZ, DOC, and VAN alone and in combination.

The mutation frequency of *E. coli* K1508 cells in the presence of antibacterials determined by counting the colonies able to grow on rifampicin (100 $\mu\text{g}/\text{mL}$) plates after 24-h incubation. Box plots are derived from 9-11 biological replicates. Boxes show the interquartile range and the whiskers indicate the minimum and maximum values. The mean is indicated by a blue datapoint. Statistical significance (Mann-Whitney U test of treatment vs control) is indicated by asterisks, ***, $p < 0.001$.

5.2.7 SOS response is involved in the synergy between FZ and VAN

The SOS response is a resistance mechanism of bacteria against conditions causing DNA-damage, such as large lesions and fragmentation. Evidently, removal of the SOS response through mutations of *lexA*, the transcriptional repressor of the SOS response, and *recA*, the sensor and inducer of the SOS response, increases susceptibility of *E. coli* or *Salmonella* to genotoxic agents and UV radiation (Mount *et al.*, 1972; Mamber *et al.*, 1993).

Zhou *et al.* (2015) have demonstrated the synergistic effect of VAN with NIT and trimethoprim, and proposed that VAN must be increasing DNA-damaging effects, possibly through oxidative stress, that results in a synergistic interaction. Moreover, a closer look at the transcriptomic analysis dataset by O'Rourke *et al.* (2020) for VAN treatment of *E. coli* with a compromised outer membrane showed downregulation of 11 genes involved in the SOS response. If these findings were to be validated, this downregulation of the SOS response by VAN could amplify the DNA-damaging effect of nitrofurans and could explain their synergistic interaction.

To investigate the involvement of the SOS response in the synergy, a $\Delta recA$ mutant of *E. coli* K1508 was constructed by P1 transduction. *recA* deletion increased the susceptibility to FZ by 32-fold relative to the parent (MIC = 0.078 $\mu\text{g}/\text{mL}$) in a broth microdilution assay. Likewise, this deletion also decreased DOC MIC to 80000 $\mu\text{g}/\text{mL}$ from more than 80000 $\mu\text{g}/\text{mL}$ in the wildtype. VAN MIC, on the other hand, remained unchanged. A checkerboard assay was also performed on the $\Delta recA$ mutant to investigate the role of SOS response in the interaction of FZ, DOC, and VAN. As shown in Figure 38A, the FICI of FZ and DOC in the $\Delta recA$ mutant increased slightly, but the combination is still highly synergistic (FICI = 0.13). In terms of FZ and VAN interaction, deletion of *recA*

resulted in a shift to indifferent interaction ($FICI = 1$), instead of the synergy observed in the wildtype ($FICI < 0.5$) (Figure 38B).

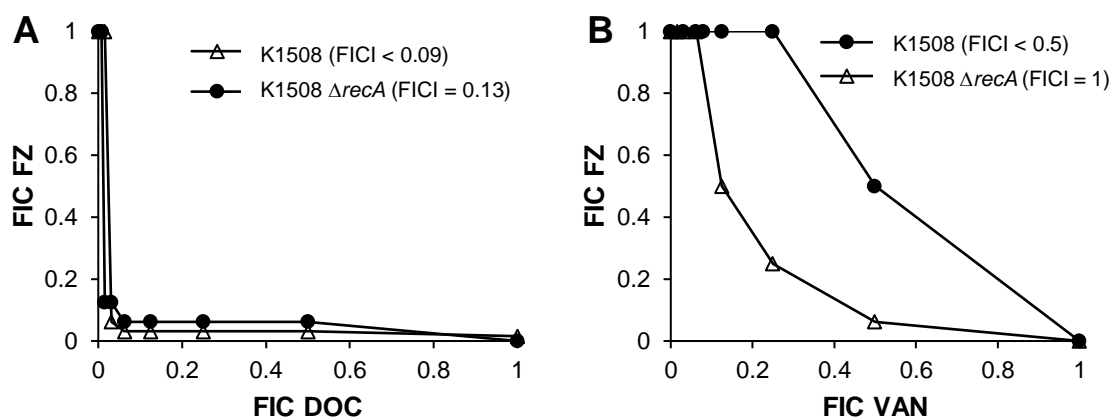


Figure 38. Interactions between FZ and DOC or VAN in the SOS-response-deficient mutant $\Delta recA$

The isobolograms derived from the checkerboard assays of A) FZ and DOC and B) FZ and VAN. Each data point corresponds to the fractional inhibitory concentrations (FICs; ratios of the MIC in combination vs. alone).

To investigate whether SOS response also plays a role in the triple combination synergy, a three-drug combination checkerboard assay was also performed on K1508 and K1508 $\Delta recA$ mutant. Results show an increase in the FICI of FZ+DOC+VAN in the $\Delta recA$ mutant ($FICI < 0.22$) compared to the wildtype ($FICI < 0.16$), indicating only a slight decrease in synergy (Appendix A, Figure A- 5B). Taken together, these findings support the hypothesis that the SOS response is an interacting point for the synergy between FZ and VAN. In terms of the triple combination synergy, however, the SOS response is contributing to the synergy, but, given that deletion of *recA* still results in a highly synergistic interaction, other factors contributing to synergy are present.

5.3 Discussion

In this chapter, some insights into the underlying mechanisms of synergy between FZ, DOC, and VAN against *E. coli* were investigated. Deletion of *fur* gene, encoding the master regulator of iron homeostasis, caused a considerable decrease in the synergy leading to an indifferent interaction between FZ and DOC. Similarly, deletion of *recA*, which disables the SOS response ability of *E. coli*, resulted in the loss of synergy between FZ and VAN. These two pathways also play a role in the triple combination synergy, since both deletion mutations caused a slight decrease in synergy. This small decrease in synergy due to the single-gene deletions are likely due to multiple pathways being involved in the synergistic triple interaction of FZ, DOC, and VAN. Multiple gene deletions will be required to observe a significant loss of synergy of the triple combination.

Fur is the transcriptional repressor of iron uptake genes and is essential for the maintenance of iron homeostasis (Troxell *et al.*, 2013). Our transcriptional analysis demonstrated that most of the previously identified Fur regulon members (Seo *et al.*, 2014) are upregulated in *E. coli* treated with FZ or DOC. In fact, the transcriptional response closely resembled that of an *E. coli fur* deletion mutant (Seo *et al.*, 2014). Three possible scenarios can be inferred from this finding: (i) FZ or DOC somehow deplete the extracellular iron, causing an iron-depleted environment; (ii) *E. coli* treated with FZ and DOC are exposed to stress conditions that trigger intracellular iron depletion that induce the upregulation of iron uptake mechanisms, and downregulation of iron storage and iron-utilising proteins, in order to replenish the perceived depleted intracellular iron pools and re-prioritise iron use to essential proteins; (iii) FZ or DOC may result in direct or indirect inactivation of Fur-Fe²⁺ protein complex. Inactivation of Fur would misleadingly send an

iron starvation signal to the cell, inducing a misplaced response that would cause iron overload.

From the ICP-MS analysis, FZ and DOC resulted in the 1.8- and 1.6-fold decrease in total intracellular iron levels, respectively (Figure 32A). *E. coli* grown in iron-depleted media has been demonstrated to result in a more significant lowering (14-fold decrease) of intracellular iron levels (Abdul-Tehrani *et al.*, 1999). A much less pronounced decrease observed here rules out iron depletion in the medium by FZ or DOC. The extent of decrease in iron concentrations shown in this study more closely resembled that of *E. coli fur* mutant in iron-replete conditions, which has been shown to decrease intracellular iron levels by 2.5-fold compared to wildtype (Abdul-Tehrani *et al.*, 1999). The lowered level of intracellular iron seems contradictory to the fact that *fur* mutants constitutively express iron import systems. This contradiction, however, could be resolved by invoking mechanisms that prevent iron overload, possibly through iron export (Pi *et al.*, 2017a). Alternatively, lowered iron content could reflect lower levels of iron storage proteins (Abdul-Tehrani *et al.*, 1999). If so, despite the overall decrease in total intracellular iron due to Fur inactivation or in *fur* mutants, the labile iron pool has been demonstrated to increase (Pi *et al.*, 2017b; Keyer *et al.*, 1996). This increase in free iron can explain the increased sensitivity of Δfur mutant to FZ and VAN, as these agents are reported to induce ROS production (Li *et al.*, 2015; Wang *et al.*, 2015), that can be worsened by the iron-catalysed Fenton reaction.

The mechanisms by which FZ or DOC inactivate Fur and induce an iron starvation-like response are currently unknown. It could be as simple as ROS, such as H₂O₂, produced in response to FZ or DOC directly inactivating Fur protein by oxidising Fe²⁺ to Fe³⁺ (Varghese *et al.*, 2007). Furthermore, ROS could be damaging the Fe-S clusters, providing an additional pathway for oxidising useable Fe²⁺ to unusable Fe³⁺ *via* the

Fenton reaction (Imlay, 2006). If so, iron import would be upregulated to supply iron to the Fe-S cluster machinery and the labile iron pool. Fur-Fe²⁺ complex has also been shown to be inactivated by nitric oxide (NO) (D'Autreaux *et al.*, 2002). Incidentally, nitroheterocyclic drug reduction has been proposed to result in a NO byproduct (Kumar *et al.*, 2014), though direct evidence for NO production during nitrofurantoin activation has not yet been demonstrated.

Since homeostasis regulatory mechanisms of various metals in bacteria are interrelated, and excess of some metals, like zinc and nickel, have been shown to perturb iron homeostasis (Xu *et al.*, 2019; Washington-Hughes *et al.*, 2019), any disruption to the levels of other essential metals was investigated through ICP-MS (Section 5.2.2). FZ increased manganese levels by 3-fold (Figure 32). This is in agreement with the reported induction of MntH manganese import systems during iron deficiency in the cells. It is thought that manganese can replace iron as a cofactor, allowing some enzymes to retain function even during iron deficiency (Kehres *et al.*, 2002). Besides low iron, H₂O₂ stress can also induce MntH manganese uptake system to replace the readily oxidisable Fe²⁺ cofactors with a less oxidisable manganese cation, and prevent oxidative protein damage (Anjem *et al.*, 2009). Surprisingly, even though DOC induced the OxyR regulon, indicating H₂O₂ stress, at the same time, it caused a decrease in total intracellular manganese levels. In addition, the triple-drug combination also resulted in a decrease in manganese levels, indicating opposite effects of FZ and DOC on this metal, in which DOC effects predominate.

Another metal that was significantly affected by the antibiotic treatments is copper. DOC increased the levels of intracellular copper by 2.5-fold, while the combination resulted in a 6.5-fold increase. This significant increase in copper levels could be a result of upregulation of copper-dependent proteins NADH dehydrogenase II (*ndh*) (Rapisarda *et*

al., 2002) and cytochrome *bo3* (*cyo*) (Chepuri *et al.*, 1990). FZ, DOC, and FZ+DOC+VAN upregulated these genes to similar levels compared to the control, and if this reflects the amount of protein in the cell, it would be expected that all three treatments should result in a similar increase of the intracellular copper. Observed differences in the intracellular copper levels between DOC-only and the triple-antibacterial combination cultures could be due to additional regulation at posttranscriptional level that could result in different amounts of these copper-dependent proteins. Interestingly, copper excess is known to cause Fe-S cluster degradation and even block Fe-S cluster assembly (Tan *et al.*, 2014; Macomber *et al.*, 2009). Furthermore, in *Bacillus subtilis* and in *E. coli*, copper excess-induced damage was demonstrated to stimulate an iron starvation response (Chillappagari *et al.*, 2010; Steunou *et al.*, 2020). From these findings, it appears that disturbance in copper homeostasis is another possible cause of Fur inactivation in *E. coli* treated with DOC.

Another metal that was affected by DOC is magnesium. DOC and FZ+DOC+VAN lowered total intracellular magnesium levels by 9-fold and 18-fold, respectively, indicating a synergistic effect in the magnesium homeostasis dysregulation. Mg^{2+} is the most abundant divalent cation in bacterial cells. While it plays essential roles in many processes, including stabilising macromolecules and as an enzyme cofactor, a substantial fraction of Mg^{2+} in *E. coli* cells are ribosome-bound and are involved in ribosome stabilisation (Goldberg, 1966). The observed low levels of magnesium in DOC is in contrast with the upregulation of genes involved in ribosomal proteins and translation reported in Chapter 4. It is possible, however, that what causes the translational stress, in which *E. coli* tries to counter by increasing ribosome assembly and translation, is the low Mg^{2+} levels caused by DOC treatment.

In *Salmonella*, insufficient cytosolic Mg^{2+} induces MgtA and MgtB transporters to import Mg^{2+} , and MgtC to lower ATP and inhibit rRNA transcription (Pontes *et al.*, 2016; Soncini *et al.*, 1996). Besides lowering the ATP, MgtC was also proposed to influence the intracellular levels of (p)ppGpp (Pontes *et al.*, 2016; Pontes *et al.*, 2015), the stringent response alarmone that binds RNA polymerase, and ultimately inhibits protein synthesis (Artsimovitch *et al.*, 2004; Sanchez-Vazquez *et al.*, 2019). Since all bacterial ribosomes are stabilised by Mg^{2+} and powered by ATP, this mechanism is thought to be highly conserved across species. Although *E. coli* lacks *mgtC*, this bacterium also inhibits rRNA transcription and exhibits lower levels of ATP during Mg^{2+} limitation, suggesting a mechanism similar to that of *Salmonella*, mediated by a yet unidentified protein (Pontes *et al.*, 2016). Since *E. coli* K1508 is a *relA1spoT1* mutant and cannot regulate (p)ppGpp levels, this could explain the increase in rRNA transcription even at insufficient intracellular Mg^{2+} concentrations. Consistent with this theory, *Salmonella relA spoT* double null mutant, which is unable to synthesise (p)ppGpp, was reported to have retained high ATP levels and exhibited increased *rrs* (16s rRNA) transcripts compared to wildtype under cytosolic Mg^{2+} limitation (Pontes *et al.*, 2016).

Checkerboard assays of the ETC mutants of *E. coli* K1508 and BW25113 showed a slight decrease in the synergy between FZ and DOC only for Δndh mutant, indicating that the action on Ndh is an interacting point of antibacterials' action that leads to synergy. The lack of change in FICI for other mutants cannot rule out the involvement of these ETC enzymes in the mechanism of action and synergy of FZ and DOC. This is because the respiratory enzymes have overlapping functions (Anraku *et al.*, 1987); thus, deletion in one of them could be easily compensated by another. In addition, if the hypothesis that the effect on the ETC is a more downstream effect of FZ and DOC, resulting from Fur inactivation, downregulation of metabolism, or some other mechanism, then deletion of

ETC genes will not have much effect on the synergy, as has been observed here. Interestingly, although FZ MIC remained unchanged for all of the ETC mutants, *ndh* and *cyoB* deletion increased the survival to sub-MIC FZ (Figure 33). *ndh* and *cyo* were the only genes upregulated by FZ treatment in *E. coli*, and the increase in resistance when these genes are deleted indicates that they are somehow involved in the FZ mechanism of action. A possibility is that these enzymes are involved in ROS production as is often the case with redox enzymes of the ETC. Deletion of these genes would, therefore, lower the burden of oxidative stress caused by FZ, thereby increasing the resistance.

Another pathway that was hypothesised to contribute to the synergy is the inhibition of efflux pumps. We have previously proposed a mechanism of synergy between FZ and DOC to be caused by FZ-mediated inhibition of TolC-associated efflux pumps that allows accumulation of DOC inside the cells (Le *et al.*, 2020). By measuring oxygen consumption, it has been confirmed that FZ and DOC result in an overall inhibitory effect on the ETC (Figure 34). Since TolC-dependent efflux pumps and many other efflux systems associated with antibiotic resistance are energised by the PMF (Paulsen *et al.*, 1996), it was posited that inhibition of the ETC, could lead to the dissipation of PMF and inhibition of efflux. Using ethidium bromide accumulation and efflux assays (Section 5.2.5), DOC has been shown to inhibit efflux, while VAN was shown to increase membrane permeability. FZ results, on the other hand, were inconclusive since no effect was observed in ethidium bromide accumulation, but a very small inhibitory effect was seen in ethidium bromide efflux assay. This can be rationalised as follows: since FZ was found to induce the expression of efflux pumps (Chapter 4, Section 4.5.10, Figure 29), the FZ-induced inhibition of the ETC that possibly results in diminished PMF cannot fully inhibit efflux; hence FZ efflux inhibition can only be observed in media without glucose that depend more on ETC activity as a source of energy. In this regard, a more

direct measurement of PMF should be performed, such as the measurement of the membrane potential ($\Delta\Psi$) component of the PMF (Benarroch *et al.*, 2020; Suzuki *et al.*, 2003).

Lastly, the role of the SOS response in the synergy was investigated. FZ has been reported to induce the SOS response, and this study has demonstrated FZ's ability to increase mutagenicity (Figure 37). Taking advantage of the synergy, doses of the components in the combination, including FZ, have been reduced, and this has now been confirmed to mitigate mutagenicity while preserving the MIC (Figure 37). The SOS response can be seen as a resistance mechanism against a variety of DNA-damaging agents (including FZ and DOC) that cause major lesions in the bacterial chromosome (Merritt *et al.*, 2009; Ona *et al.*, 2009). Since inhibition of resistance is a commonly accepted principle that gives way to synergy, it was investigated whether the SOS response is somehow involved in the synergy. Deletion of *recA* eliminated the synergy and resulted in an indifferent interaction between FZ and VAN, while only a slight decrease in synergy has been observed in FZ+DOC and FZ+DOC+VAN interactions (Section 5.2.7). The mechanism by which SOS response plays a role in the mechanism of synergy between FZ and VAN could involve inhibitory effect of VAN on SOS induction, as reflected by O'Rourke *et al.* (2020) transcriptome dataset.

In summary, this study offered some insights into the observed transcriptional response of *E. coli* to FZ, DOC, VAN, or triple combination of these antibacterials. Evidence for Fur regulon and SOS pathway as interacting points in the synergy of FZ and DOC, and FZ and VAN, respectively, was provided, along with demonstration of the inhibitory effect on the ETC that could be contributing to the synergy. In terms of the triple combination synergy, multiple other pathways could be involved, in addition to Fur and SOS, given that the single-gene deletions lead to a slight decrease in the triple

combination synergy. However, since it is highly likely that these drugs interact at multiple points in multiple different pathways, multiple gene deletions may be required to observe a more significant decrease in the triple combination synergy.

6 General discussion

6.1 General discussion

The continuous emergence of multidrug-resistant bacteria and the massive decline in the rate of novel antibiotic discovery in recent years have necessitated the exploration of alternative strategies to tackle antimicrobial resistance. Effective therapies are especially needed for Gram-negative pathogens, as reflected in the WHO priority pathogens list (World Health Organization, 2017). To develop a novel therapy, this study employed the alternative approach of reviving ‘old’ antibiotics and making some Gram-positive-only antibacterials effective against Gram-negative bacteria through a synergistic effect.

This thesis reports the *in vitro* synergistic interaction between nitrofurans, DOC, and VAN against a wide range of Gram-negative pathogens, including clinically relevant multidrug-resistant strains. The choice of this combination was prompted by previous discoveries of the pairwise synergies between nitrofurans and VAN or DOC (Le *et al.*, 2020; Weerasinghe, 2017; Zhou *et al.*, 2015). Although these two-drug combinations showed synergy in Gram-negative bacteria, the MICs of VAN and DOC are still high and precluded their use as a viable medical treatment option due to toxicity. So in an attempt to improve the combination, the interaction of the triple combination was investigated and was found to be synergistic, further decreasing the MICs of individual components.

Gram-negative bacteria, due to their outer membrane and a range of powerful efflux pumps, are intrinsically resistant to VAN and DOC (Prieto *et al.*, 2006; Breijyeh *et al.*, 2020; Thanassi *et al.*, 1997). This is evidenced by their high MICs in Gram-negatives compared to Gram-positives (Chapter 3, Table 2 and Table 4). However, due to synergistic interaction, the MICs of these agents decrease significantly in combination with the Gram-negative active-agent nitrofurans, allowing their use to be expanded beyond Gram-positive bacteria. This synergistic interaction is not just advantageous for enabling

the use of VAN and DOC; nitrofurantoin use has been unfavourable due to its mutagenicity (Vass *et al.*, 2008). The increase in efficacy of the combination will thereby lower the effective doses of each of the components, including nitrofurantoin, which can mitigate adverse effects. In Chapter 4 (Section 4.5.5), the combination was found not to induce the SOS response, indicating the lack of severe DNA damage that results in mutagenicity; and in Chapter 5 (Section 5.2.6), this mitigation of mutagenicity has been demonstrated in *E. coli*. This finding highlights the advantage of mitigating mutagenicity to decrease resistance frequency in bacterial cells and oncogenesis-causing DNA damage in eukaryotic cells.

Besides nitrofurantoin, VAN also has adverse effects, such as nephrotoxicity, that are partly the reason why it is not a first-choice treatment (Filippone *et al.*, 2017). Since the combination has synergistic effects against bacterial cells, it is possible that the toxic effects of the drugs in mammalian cells will also be synergistic and would be detrimental for the development of this combination. Preliminary investigation on the toxic effects using an *in vitro* mammalian cell line model found that the cytotoxic effect of the combination is indifferent (Chapter 3, Table 5). Considering only *in vitro* results showing that the efficacy is synergistic and that the toxicity is indifferent, the therapeutic index of the combination would be higher than if the drugs were used as monotherapies, and the use of the drugs would therefore be more advantageous if used as a combination. However, since this was an *in vitro* assay, its clinical relevance warrants further investigation (McKim, 2010).

Although the combination is not synergistic in Gram-positive bacteria, their interaction is at least additive (Chapter 3, Section 3.2.3), and the concentrations of the antibacterials in combination that inhibit Gram-negative bacteria are already effective against Gram-positives. For these reasons, the combination can be used as a broad-spectrum therapy,

and potential uses, such as gastrointestinal illness therapy and topical treatment for skin and wound infections, were discussed in Chapter 3.

The finding that nitrofurans, DOC, and VAN does not interact synergistically against Gram-positive bacteria alludes to the importance of the outer membrane in the synergistic interaction. This can be rationalised by the fact that the outer membrane and the presence of efflux pumps prevent the entry and accumulation of VAN and DOC, respectively, inside the cells; but when used together with nitrofurans, these resistance mechanisms are somehow inhibited allowing the agents to enter the cell and exert their effects. Indeed, this interpretation was proposed for the loss or decrease of synergy between FZ and DOC when *tolC* or *acrA* efflux pump components were deleted (Le *et al.*, 2020).

Using a transcriptomics approach (Chapter 4), the underlying mechanisms of action and synergy of the antibacterials were investigated. The apparent similarity in the transcriptional responses induced by FZ and DOC in *E. coli* is likely the source of their synergy. This is in line with studies that found a higher likelihood of synergy occurring in drug combinations that induce very similar or very opposite gene perturbations (Bansal *et al.*, 2014; Yang *et al.*, 2020). In particular, FZ and DOC induced gene expression consistent with Fur protein inactivation that usually occurs during the iron starvation response (Seo *et al.*, 2014). Through measurements of the total intracellular iron levels, it was ruled out that these drugs cause real iron starvation, for example, through iron chelation or sequestration (Jacobs *et al.*, 1970). FZ and DOC more likely cause an iron starvation-like response through oxidative stress damage or destabilisation/unfolding of iron-containing proteins, interaction with the Fur protein, and in the case of DOC, metal homeostasis dysregulation causing copper toxicity to Fe-S clusters. Despite the overall decrease of iron content in the cells, it is possible that the inactivation of Fur will lead to

an increase in the labile iron pool inside the cell that can increase oxidative damage and stress *via* the Fenton reaction (Keyer *et al.*, 1996).

The combined effect on Fur protein was confirmed to be a source of synergy between FZ and DOC, given that deletion of *fur* resulted in the shift to indifferent interaction. Fur also plays a role in the triple combination synergy, but other interacting points are obviously present besides the Fur pathway, since *fur* deletion only increased the triple combination FICI slightly, and the interaction is still synergistic (Chapter 5, Section 5.2.1).

FZ and DOC also showed gene perturbations usually observed in bacteriostatic translation inhibitors, such as downregulation of central carbon metabolism and upregulation of ribosomal proteins (Sabina *et al.*, 2003; Lin *et al.*, 2014; O'Rourke *et al.*, 2020). Protein synthesis inhibition by nitrofurans has been reported before and was proposed to be due to non-specific binding to ribosomal proteins (McOsker *et al.*, 1994; Yu *et al.*, 1976). However, translation inhibition by DOC has not been demonstrated before. Given that Mg^{2+} content of the cells is dramatically lowered by DOC (Chapter 5, Figure 32), a connection between magnesium homeostasis dysregulation by DOC and translational stress can be proposed: The decrease in total magnesium levels by DOC will decrease the number of functioning ribosomes and inhibit translation in *E. coli* due to activation of the stringent response. However, due to the absence of (p)ppGpp regulation in the *E. coli* K1508 strain used in this work (Chapter 4, Section 4.2), translation control based on Mg^{2+} levels is possibly absent, leading to the unchecked upregulation of ribosome assembly even during Mg^{2+} deficiency.

FZ and DOC upregulated efflux pump genes (*acrA*, *acrB*), downregulated porins (*ompC*, *ompF*) (Chapter 4, Section 4.5.10), and induced stress responses that increase the tolerance to these agents. In this context, it seems contradictory that the combination is synergistic and not antagonistic. A possible explanation is that some of these resistance

mechanisms are somehow being inhibited by the combined action of the drugs. A proposed pathway in which this might come about is through Fur inactivation or downregulation of the central carbon metabolism. Both of these activities will have an inhibitory effect on the ETC. Incidentally, most of the ETC genes were shown to be downregulated by FZ, DOC, and the combination (Chapter 4, Section 4.5.8). This inhibition of aerobic ETC has been confirmed in Chapter 5, where FZ and DOC were demonstrated to decrease oxygen consumption (Chapter 5, Figure 34). It was therefore posited that FZ and DOC could be causing a dissipation of the PMF, which could inhibit the PMF-dependent efflux, leading to synergy. Using ethidium bromide efflux and accumulation assay (Chapter 5, Section 5.2.5), apparent inhibition of efflux by DOC was demonstrated, along with the increased permeability caused by VAN. FZ, however, does not seem to affect the efflux.

The role of the ETC enzymes in the action and synergy of the antibacterials were also investigated using single-gene deletion mutants (Chapter 5, Section 5.2.3). However, a limitation of this assay is the redundancy of the ETC enzymes, which have overlapping functions (Anraku *et al.*, 1987), and so deletion of one can be compensated by another. Expectedly, none of the individual deletion mutants affected the MIC of FZ and DOC, and only some caused a slight decrease in synergy. The ETC likely only has a minor contribution to the individual action of these drugs, possibly as a source of oxidative stress. Alternatively, the contribution of the ETC enzymes is masked due to redundancy. Construction of multiple mutations will be required to resolve these two possibilities.

VAN treatment of *E. coli* did not induce a considerable change in the overall gene expression compared to the control (Chapter 4, Section 4.5.4). Even though only 17 genes were significantly differentially expressed, these genes gave insights into the initial effects of VAN, which contradicts the commonly accepted notion that Gram-negative

bacteria are relatively impermeable to VAN. Majority of the 17 DEGs are members of the extracytoplasmic stress responses, particularly the Rcs pathway, which has been demonstrated to be induced by peptidoglycan-targeting antibiotics (Laubacher *et al.*, 2008). Taken together, these findings indicate that VAN can somehow cross the outer membrane of *E. coli*, although only in very small amounts, and inhibit the peptidoglycan synthesis. Compromised peptidoglycan can, in turn, affect envelope integrity and permeability, and thereby cause the observed increased accumulation of ethidium bromide in VAN-containing cultures (Chapter 5, Section 5.2.5).

From the known mechanisms of action of VAN (peptidoglycan synthesis inhibitor) and nitrofurans (DNA damage), there does not seem to be an obvious connection as to why these drugs interact synergistically (Zhou *et al.*, 2015). One important mechanism of resistance to nitrofurans is the SOS response to DNA damage. Surprisingly, deletion of *recA*, making *E. coli* unable to mount an SOS response, resulted in the loss of synergy between FZ and VAN (Chapter 5, Figure 38B). Data presented here indicate the involvement of SOS response in the synergy between FZ and VAN, possibly through inhibition of SOS induction by VAN, which can decrease the resistance to the DNA-damaging effect of FZ. The *recA* deletion also increased the FICI for the triple combination, but again the interaction is still synergistic, supporting the concept of multiple interaction points that contribute to the synergy of the triple combination. In this regard, multiple gene deletions may be needed to observe a more significant loss of synergy of the triple combination.

6.2 Conclusion

This thesis presents the synergistic combination of nitrofurans, DOC, and VAN as a potential therapy for Gram-negative infections. The synergistic interaction has been

characterised *in vitro*, and the reduced effective doses were demonstrated to mitigate nitrofurans' adverse effects. Pathways perturbed by the antibacterials were identified, and from these findings, mechanisms for the action and synergy have been proposed. Nitrofurans, DOC, and VAN affected correlated pathways that likely result in the suppression of resistance mechanisms and amplification of toxic effects, leading to synergy. Lastly, evidence for the involvement of some of the pathways, particularly the iron starvation-like response and SOS response, in the synergy of the pairwise and three-drug combinations were provided, but further work is warranted to fully elucidate the mechanism of interaction. It is hoped that the work presented in this thesis, along with any future investigations, will lay the groundwork for the development and even improvement of this combination into a viable clinical therapy for tackling multidrug-resistant bacterial infections.

6.3 Future directions

Altogether, this thesis provided evidence for the *in vitro* synergy of FZ, DOC, and VAN against a wide range of Gram-negative pathogens and provided insights into the mechanism of interaction leading to synergy. Future work is warranted to confirm the clinical relevance of our findings and confirm the efficacy and safety of the combination through *in vivo* animal models. Additionally, more work is needed to fully elucidate the mechanisms underlying the synergy of the combination.

Firstly, the mechanism by which FZ and DOC inactivate Fur protein needs to be investigated. FZ- and DOC-mediated disruption of Fur interaction with the target promoters can be tested using electrophoretic gel mobility assay (EMSA) or DNase protection assays, as previously described (Berg *et al.*, 2020; D'Autreaux *et al.*, 2002). Briefly, this consists of incubating the drugs with Fur-Fe²⁺ protein complex and

oligonucleotides or plasmids containing a Furbox (Fur binding site), and looking at whether the drugs inhibit binding of Fur to the DNA. Since nitrofurans are prodrugs, the assay should also include nitrofurans activating enzyme (NfsA or NfsB) and enzyme cofactors. This assay can rule out direct inactivation of Fur protein, leaving only oxidative or copper stress-induced iron starvation-like response as culprits. Next, a more direct measurement of PMF can be employed, such as measurement of membrane potential (Benarroch *et al.*, 2020; Suzuki *et al.*, 2003), to confirm the proposed dissipation or decrease of PMF by FZ and DOC. Another area that requires further work is the proposed SOS response inhibition by VAN. Using reporter gene systems, SOS gene expression in *E. coli* treated with FZ, VAN, and their combination can be measured to investigate whether VAN inhibits SOS induction by FZ.

Lastly, resistance evolution is an area that is essential to advance the development of this triple combination. Evolution of antibiotic resistance to the triple combination can be compared to the single antibacterials, to gain insights as to whether the combination suppresses, increases, or does not affect the probability of resistance emergence. Identification of triple combination-resistance mutations can also help with the elucidation of the mechanism of action and interaction of FZ, DOC, and VAN.

References

- Abdul-Tehrani, H., Hudson, A. J., Chang, Y.-S., Timms, A. R., Hawkins, C., Williams, J. M., Harrison, P. M., Guest, J. R. & Andrews, S. C. 1999. Ferritin mutants of *Escherichia coli* are iron deficient and growth impaired, and *fur* mutants are iron deficient. *Journal of Bacteriology*, 181, 1415-1428. doi: 10.1128/jb.181.5.1415-1428.1999
- Ades, S. E., Connolly, L. E., Alba, B. M. & Gross, C. A. 1999. The *Escherichia coli* sigma(E)-dependent extracytoplasmic stress response is controlled by the regulated proteolysis of an anti-sigma factor. *Genes & Development*, 13, 2449-2461. doi: 10.1101/gad.13.18.2449
- Albaugh, K. W., Biely, S. A. & Cavorsi, J. P. 2013. The effect of a cellulose dressing and topical vancomycin on methicillin-resistant *Staphylococcus aureus* (MRSA) and Gram-positive organisms in chronic wounds: A case series. *Ostomy Wound Management*, 59, 34-43.
- Andrews, S. 2010. *FastQC: A quality control tool for high throughput sequence data* [Online]. Available: <http://www.bioinformatics.babraham.ac.uk/projects/fastqc> [Accessed January 2019].
- Anjem, A., Varghese, S. & Imlay, J. A. 2009. Manganese import is a key element of the OxyR response to hydrogen peroxide in *Escherichia coli*. *Molecular Microbiology*, 72, 844-58. doi: 10.1111/j.1365-2958.2009.06699.x
- Ankomah, P., Johnson, P. J. T. & Levin, B. R. 2013. The pharmaco –, population and evolutionary dynamics of multi-drug therapy: Experiments with *S. aureus* and *E. coli* and computer simulations. *PLoS Pathogens*, 9, e1003300. doi: 10.1371/journal.ppat.1003300
- Anraku, Y. & Gennis, R. B. 1987. The aerobic respiratory chain of *Escherichia coli*. *Trends in Biochemical Sciences*, 12, 262-266. doi: 10.1016/0968-0004(87)90131-9
- Artsimovitch, I., Patlan, V., Sekine, S., Vassylyeva, M. N., Hosaka, T., Ochi, K., Yokoyama, S. & Vassylyev, D. G. 2004. Structural basis for transcription regulation by alarmone ppGpp. *Cell*, 117, 299-310. doi: 10.1016/s0092-8674(04)00401-5
- Aslund, F., Zheng, M., Beckwith, J. & Storz, G. 1999. Regulation of the OxyR transcription factor by hydrogen peroxide and the cellular thiol-disulfide status. *Proceedings of the National Academy of Sciences of the United States of America*, 96, 6161-6165. doi: 10.1073/pnas.96.11.6161
- Auta, A., Hadi, M. A., Oga, E., Adewuyi, E. O., Abdu-Aguye, S. N., Adeloye, D., Strickland-Hodge, B. & Morgan, D. J. 2019. Global access to antibiotics without prescription in community pharmacies: A systematic review and meta-analysis. *Journal of Infection*, 78, 8-18. doi: 10.1016/j.jinf.2018.07.001
- Ayukekbong, J. A., Ntemgwa, M. & Atabe, A. N. 2017. The threat of antimicrobial resistance in developing countries: causes and control strategies. *Antimicrobial Resistance & Infection Control*, 6, 47. doi: 10.1186/s13756-017-0208-x

- Baba, T., Ara, T., Hasegawa, M., Takai, Y., Okumura, Y., Baba, M., Datsenko, K. A., Tomita, M., Wanner, B. L. & Mori, H. 2006. Construction of *Escherichia coli* K-12 in-frame, single-gene knockout mutants: the Keio collection. *Molecular Systems Biology*, 2, 2006.0008-2006.0008. doi: 10.1038/msb4100050
- Bagg, A. & Neilands, J. B. 1987. Ferric uptake regulation protein acts as a repressor, employing iron (II) as a cofactor to bind the operator of an iron transport operon in *Escherichia coli*. *Biochemistry*, 26, 5471-7. doi: 10.1021/bi00391a039
- Baichoo, N. & Helmann, J. D. 2002. Recognition of DNA by Fur: a reinterpretation of the Fur box consensus sequence. *Journal of Bacteriology*, 184, 5826-5832. doi: 10.1128/jb.184.21.5826-5832.2002
- Bansal, M., Yang, J., Karan, C., Menden, M. P., Costello, J. C., Tang, H., Xiao, G., Li, Y., Allen, J., Zhong, R., Chen, B., Kim, M., Wang, T., Heiser, L. M., Realubit, R., Mattioli, M., Alvarez, M. J., Shen, Y., Abbuehl, J.-P., Allen, J., Altman, R. B., Balcome, S., Bansal, M., Bell, A., Bender, A., Berger, B., Bernard, J., Bieberich, A. A., Borboudakis, G., Califano, A., Chan, C., Chen, B., Chen, T.-H., Choi, J., Coelho, L. P., Costello, J. C., Creighton, C. J., Dampier, W., Davisson, V. J., Deshpande, R., Diao, L., Di Camillo, B., Dundar, M., Ertel, A., Group, C., Gallahan, D., Goswami, C. P., Gottlieb, A., Gould, M. N., Goya, J., Grau, M., Gray, J. W., Heiser, L. M., Hejase, H. A., Hoffmann, M. F., Homicsko, K., Homilius, M., Hwang, W., Ijzerman, A. P., Kallioniemi, O., Karacali, B., Karan, C., Kaski, S., Kim, J., Kim, M., Krishnan, A., Lee, J., Lee, Y.-S., Lenselink, E. B., Lenz, P., Li, L., Li, J., Li, Y., Liang, H., Mattioli, M., Menden, M. P., Mpindi, J.-P., Myers, C. L., Newton, M. A., Overington, J. P., Parkkinen, J., Prill, R. J., Peng, J., Pestell, R., Qiu, P., Rajwa, B., Realubit, R., Sadanandam, A., Saez-Rodriguez, J., Sambo, F., Singer, D., Stolovitzky, G., Sridhar, A., Sun, W., Tang, H., Toffolo, G. M., Tozeren, A., Troyanskaya, O. G., Tsamardinos, I., van Vlijmen, H. W. T., *et al.* 2014. A community computational challenge to predict the activity of pairs of compounds. *Nature Biotechnology*, 32, 1213-1222. doi: 10.1038/nbt.3052
- Baranova, N. & Nikaido, H. 2002. The baeSR two-component regulatory system activates transcription of the *yegMNOB* (*mdtABCD*) transporter gene cluster in *Escherichia coli* and increases its resistance to novobiocin and deoxycholate. *Journal of Bacteriology*, 184, 4168-4176. doi: 10.1128/jb.184.15.4168-4176.2002
- Barbosa, J., Freitas, A., Moura, S., Mourão, J. L., Noronha da Silveira, M. I. & Ramos, F. 2011. Detection, accumulation, distribution, and depletion of furaltadone and nifursol residues in poultry muscle, liver, and gizzard. *Journal of Agricultural and Food Chemistry*, 59, 11927-11934. doi: 10.1021/jf2029384
- Barna, J. C. & Williams, D. H. 1984. The structure and mode of action of glycopeptide antibiotics of the vancomycin group. *Annual Review of Microbiology*, 38, 339-57. doi: 10.1146/annurev.mi.38.100184.002011
- Begley, M., Gahan, C. G. M. & Hill, C. 2005. The interaction between bacteria and bile. *FEMS Microbiology Reviews*, 29, 625-651. doi: 10.1016/j.femsre.2004.09.003
- Benarroch, J. M. & Asally, M. 2020. The microbiologist's guide to membrane potential dynamics. *Trends in Microbiology*, 28, 304-314. doi: 10.1016/j.tim.2019.12.008
- Benjamini, Y. & Hochberg, Y. 1995. Controlling the false discovery rate: A practical and powerful approach to multiple testing. *Journal of the Royal Statistical Society: Series B (Methodological)*, 57, 289-300. doi: 10.1111/j.2517-6161.1995.tb02031.x
- Berg, K., Pedersen, H. L. & Leiros, I. 2020. Biochemical characterization of ferric uptake regulator (Fur) from *Aliivibrio salmonicida*. Mapping the DNA sequence

- specificity through binding studies and structural modelling. *Biometals*, 33, 169-185. doi: 10.1007/s10534-020-00240-6
- Bernstein, C., Bernstein, H., Payne, C. M., Beard, S. E. & Schneider, J. 1999. Bile salt activation of stress response promoters in *Escherichia coli*. *Current Microbiology*, 39, 68-72. doi: 10.1007/s002849900420
- Beuers, U. 1997. Effects of bile acids on hepatocellular signaling and secretion. *The Yale Journal of Biology and Medicine*, 70, 341-346.
- Bliss, C. I. 1939. The toxicity of poisons applied jointly. *Annals of Applied Biology*, 26, 585-615. doi: 10.1111/j.1744-7348.1939.tb06990.x
- Bollenbach, T. 2015. Antimicrobial interactions: mechanisms and implications for drug discovery and resistance evolution. *Current Opinion in Microbiology*, 27, 1-9. doi: 10.1016/j.mib.2015.05.008
- Bot, C., Hall, B. S., Alvarez, G., Di Maio, R., Gonzalez, M., Cerecetto, H. & Wilkinson, S. R. 2013. Evaluating 5-nitrofurans as trypanocidal agents. *Antimicrobial Agents and Chemotherapy*, 57, 1638-47. doi: 10.1128/aac.02046-12
- Bowe, C. L., Mokhtarzadeh, L., Venkatesan, P., Babu, S., Axelrod, H. R., Sofia, M. J., Kakarla, R., Chan, T. Y., Kim, J. S., Lee, H. J., Amidon, G. L., Choe, S. Y., Walker, S. & Kahne, D. 1997. Design of compounds that increase the absorption of polar molecules. *Proceedings of the National Academy of Sciences of the United States of America*, 94, 12218-23. doi: 10.1073/pnas.94.22.12218
- Brejijeh, Z., Jubeh, B. & Karaman, R. 2020. Resistance of Gram-negative bacteria to current antibacterial agents and approaches to resolve it. *Molecules*, 25, 1340. doi: 10.3390/molecules25061340
- Bruniera, F., Ferreira, F., Saviolli, L., Bacci, M., Feder, D., Pedreira, M., Peterlini, M., Azzalis, L., Junqueira, V. & Fonseca, F. 2015. The use of vancomycin with its therapeutic and adverse effects: A review. *European Review for Medical and Pharmacological Sciences*, 19, 694-700.
- Bryant, D. W. & McCalla, D. R. 1980. Nitrofurantoin induced mutagenesis and error prone repair in *Escherichia coli*. *Chemico-Biological Interactions*, 31, 151-166. doi: 10.1016/0009-2797(80)90002-2
- Bugg, T. D., Wright, G. D., Dutka-Malen, S., Arthur, M., Courvalin, P. & Walsh, C. T. 1991. Molecular basis for vancomycin resistance in *Enterococcus faecium* BM4147: biosynthesis of a depsipeptide peptidoglycan precursor by vancomycin resistance proteins VanH and VanA. *Biochemistry*, 30, 10408-15. doi: 10.1021/bi00107a007
- Butler, M. S., Blaskovich, M. A. & Cooper, M. A. 2017. Antibiotics in the clinical pipeline at the end of 2015. *The Journal of Antibiotics*, 70, 3-24. doi: 10.1038/ja.2016.72
- Callewaert, L., Vanoirbeek, K. G. A., Lurquin, I., Michiels, C. W. & Aertsen, A. 2009. The Rcs two-component system regulates expression of lysozyme inhibitors and is induced by exposure to lysozyme. *Journal of Bacteriology*, 191, 1979-1981. doi: 10.1128/JB.01549-08
- Campbell, E. A., Tupy, J. L., Gruber, T. M., Wang, S., Sharp, M. M., Gross, C. A. & Darst, S. A. 2003. Crystal structure of *Escherichia coli* sigmaE with the cytoplasmic domain of its anti-sigma RseA. *Molecular Cell*, 11, 1067-78. doi: 10.1016/s1097-2765(03)00148-5
- Campbell, J. 2011. High-throughput assessment of bacterial growth inhibition by optical density measurements. *Current Protocols in Chemical Biology*, 3. doi: 10.1002/9780470559277.ch100115

- Casadaban, M. J. 1976. Transposition and fusion of the lac genes to selected promoters in *Escherichia coli* using bacteriophage lambda and Mu. *Journal of Molecular Biology*, 104, 541-55. doi: 10.1016/0022-2836(76)90119-4
- Cassir, N., Rolain, J.-M. & Brouqui, P. 2014. A new strategy to fight antimicrobial resistance: the revival of old antibiotics. *Frontiers in Microbiology*, 5. doi: 10.3389/fmicb.2014.00551
- Centers for Disease Control and Prevention. 2019. Antibiotic resistance threats in the United States. Atlanta, GA: U.S. Department of Health and Human Services. Available: <https://www.cdc.gov/drugresistance/biggest-threats.html>.
- Chadfield, M. S. & Hinton, M. H. 2004. *In vitro* activity of nitrofurantoin derivatives on growth and morphology of *Salmonella enterica* serotype Enteritidis. *Journal of Applied Microbiology*, 96, 1002-1012. doi: 10.1111/j.1365-2672.2004.02225.x
- Chandrangsu, P., Rensing, C. & Helmann, J. D. 2017. Metal homeostasis and resistance in bacteria. *Nature Reviews Microbiology*, 15, 338-350. doi: 10.1038/nrmicro.2017.15
- Chen, D., Zhang, H., Lu, P., Liu, X. & Cao, H. 2016. Synergy evaluation by a pathway-pathway interaction network: a new way to predict drug combination. *Molecular BioSystems*, 12, 614-623. doi: 10.1039/C5MB00599J
- Chen, L., Zhang, J., Wang, J., Butaye, P., Kelly, P., Li, M., Yang, F., Gong, J., Yassin, A. K., Guo, W., Li, J., Song, C. & Wang, C. 2018. Newly identified colistin resistance genes, *mcr-4* and *mcr-5*, from upper and lower alimentary tract of pigs and poultry in China. *PLoS One*, 13, e0193957. doi: 10.1371/journal.pone.0193957
- Chepuri, V., Lemieux, L., Au, D. C. T. & Gennis, R. 1990. The sequence of the *cyo* operon indicates substantial structural similarities between the cytochrome *o* ubiquinol oxidase of *Escherichia coli* and the aa3-type family of cytochrome *c* oxidases. *The Journal of Biological Chemistry*, 265, 11185-92.
- Cherepanov, P. P. W., W. 1995. Gene disruption in *Escherichia coli*: TcR and KmR cassettes with the option of Flp-catalyzed excision of the antibiotic-resistance determinant. *Gene*, 158, 9-14. doi: 10.1016/0378-1119(95)00193-A
- Chiang, J. Y. L. 2013. Bile acid metabolism and signaling. *Comprehensive Physiology*, 3, 1191-1212. doi: 10.1002/cphy.c120023
- Chillapagari, S., Seubert, A., Trip, H., Kuipers, O. P., Marahiel, M. A. & Miethke, M. 2010. Copper stress affects iron homeostasis by destabilizing iron-sulfur cluster formation in *Bacillus subtilis*. *Journal of Bacteriology*, 192, 2512-2524. doi: 10.1128/jb.00058-10
- Choi, H.-J., Kim, S.-J., Mukhopadhyay, P., Cho, S., Woo, J.-R., Storz, G. & Ryu, S.-E. 2001. Structural basis of the redox switch in the OxyR transcription factor. *Cell*, 105, 103-113. doi: 10.1016/S0092-8674(01)00300-2
- Choi, S. H., Baumber, D. J. & Kaspar, C. W. 2000. Contribution of *dps* to acid stress tolerance and oxidative stress tolerance in *Escherichia coli* O157:H7. *Applied and Environmental Microbiology*, 66, 3911-3916. doi: 10.1128/aem.66.9.3911-3916.2000
- Choi, U. & Lee, C.-R. 2019a. Distinct roles of outer membrane porins in antibiotic resistance and membrane integrity in *Escherichia coli*. *Frontiers in Microbiology*, 10. doi: 10.3389/fmicb.2019.00953
- Choi, Y., Jeong, S.-H., Chung, J.-W., Park, D., Kim, K.-O., Kwon, K., Kim, Y., So, S., Lee, j. h., Jeong, J.-Y. & Lee, S.-M. 2019b. Rifabutin and furazolidone could be the candidates of the rescue regimen for antibiotic-resistant *H. pylori* in Korea.

- Canadian Journal of Infectious Diseases and Medical Microbiology*, 2019, 1-7. doi: 10.1155/2019/9351801
- Chong, C. R. & Sullivan, D. J. 2007. New uses for old drugs. *Nature*, 448, 645-646. doi: 10.1038/448645a
- Chubiz, L. M., Glekas, G. D. & Rao, C. V. 2012. Transcriptional cross talk within the *mar-sox-rob* regulon in *Escherichia coli* is limited to the *rob* and *marRAB* Operons. *Journal of Bacteriology*, 194, 4867-4875. doi: 10.1128/jb.00680-12
- Chubiz, L. M. & Rao, C. V. 2011. Role of the *mar-sox-rob* regulon in regulating outer membrane porin expression. *Journal of Bacteriology*, 193, 2252-2260. doi: 10.1128/jb.01382-10
- Clinical and Laboratory Standards Institute 2015. Methods for dilution antimicrobial susceptibility tests for bacteria that grow aerobically 10th Ed. Wayne, PA: Clinical and Laboratory Standards Institute.
- Coates, A. R. M., Halls, G. & Hu, Y. 2011. Novel classes of antibiotics or more of the same? *British Journal of Pharmacology*, 163, 184-194. doi: 10.1111/j.1476-5381.2011.01250.x
- Cohen, S. P., Levy, S. B., Foulds, J. & Rosner, J. L. 1993. Salicylate induction of antibiotic resistance in *Escherichia coli*: activation of the *mar* operon and a *mar*-independent pathway. *Journal of Bacteriology*, 175, 7856-7862. doi: 10.1128/jb.175.24.7856-7862.1993
- Cole, A. 2014. GPs feel pressurised to prescribe unnecessary antibiotics, survey finds. *British Medical Journal*, 349, g5238. doi: 10.1136/bmj.g5238
- Condon, C., Squires, C. & Squires, C. L. 1995. Control of rRNA transcription in *Escherichia coli*. *Microbiological Reviews*, 59, 623-45. doi: 10.1128%2FM5BR.68.4.639-668.2004
- Cooper, K. M. & Kennedy, D. G. 2007. Stability studies of the metabolites of nitrofurantoin antibiotics during storage and cooking. *Food Additives and Contaminants*, 24, 935-42. doi: 10.1080/02652030701317301
- Cornelis, P., Wei, Q., Andrews, S. C. & Vinckx, T. 2011. Iron homeostasis and management of oxidative stress response in bacteria. *Metallomics*, 3, 540-549. doi: 10.1039/C1MT00022E
- Cotter, P. A., Chepuri, V., Gennis, R. B. & Gunsalus, R. P. 1990. Cytochrome o (*cyoABCDE*) and d (*cydAB*) oxidase gene expression in *Escherichia coli* is regulated by oxygen, pH, and the *fnr* gene product. *Journal of Bacteriology*, 172, 6333-6338. doi: 10.1128/jb.172.11.6333-6338.1990
- Craig, N. L. & Roberts, J. W. 1981. Function of nucleoside triphosphate and polynucleotide in *Escherichia coli* RecA protein-directed cleavage of phage lambda repressor. *The Journal of Biological Chemistry*, 256, 8039-44.
- Cremers, C. M., Knoefler, D., Vitvitsky, V., Banerjee, R. & Jakob, U. 2014. Bile salts act as effective protein-unfolding agents and instigators of disulfide stress *in vivo*. *Proceedings of the National Academy of Sciences of the United States of America*, 111, E1610-E1619. doi: 10.1073/pnas.1401941111
- Crotty, M. P., Krekel, T., Burnham, C.-A. D. & Ritchie, D. J. 2016. New Gram-positive agents: The next generation of oxazolidinones and lipoglycopeptides. *Journal of Clinical Microbiology*, 54, 2225-2232. doi: 10.1128/jcm.03395-15
- D'Autreaux, B., Touati, D., Bersch, B., Latour, J.-M. & Michaud-Soret, I. 2002. Direct inhibition by nitric oxide of the transcriptional ferric uptake regulation protein *via* nitrosylation of the iron. *Proceedings of the National Academy of Sciences of the United States of America*, 99, 16619-16624. doi: 10.1073/pnas.252591299

- Danese, P. N. & Silhavy, T. J. 1998. CpxP, a stress-combative member of the Cpx Regulon. *Journal of Bacteriology*, 180, 831-839. doi: 10.1128/jb.180.4.831-839.1998
- Dennis, P. P. 1976. Effects of chloramphenicol on the transcriptional activities of ribosomal RNA and ribosomal protein genes in *Escherichia coli*. *Journal of Molecular Biology*, 108, 535-546. doi: 10.1016/S0022-2836(76)80135-0
- Desnoyers, G., Morissette, A., Prévost, K. & Massé, E. 2009. Small RNA-induced differential degradation of the polycistronic mRNA *iscRSUA*. *The EMBO Journal*, 28, 1551-61. doi: 10.1038/emboj.2009.116
- Ding, H., Hidalgo, E. & Dimple, B. 1996. The redox state of the [2Fe-2S] clusters in SoxR protein regulates its activity as a transcription factor. *The Journal of Biological Chemistry*, 271, 33173-5. doi: 10.1074/jbc.271.52.33173
- Dubbs, J. M. & Mongkolsuk, S. 2012. Peroxide-sensing transcriptional regulators in bacteria. *Journal of Bacteriology*, 194, 5495-5503. doi: 10.1128/jb.00304-12
- Duval, V. & Lister, I. M. 2013. MarA, SoxS and Rob of *Escherichia coli* - Global regulators of multidrug resistance, virulence and stress response. *International Journal of Biotechnology for Wellness Industries*, 2, 101-124. doi: 10.6000/1927-3037.2013.02.03.2
- Eder, E., Hoffman, C., Bastian, H., Deininger, C. & Scheckenbach, S. 1990. Molecular mechanisms of DNA damage initiated by alpha, beta-unsaturated carbonyl compounds as criteria for genotoxicity and mutagenicity. *Environmental Health Perspectives*, 88, 99-106. doi: 10.1289/ehp.908899
- Eder, E., Scheckenbach, S., Deininger, C. & Huffman, C. 1993. The possible role of α,β -unsaturated carbonyl compounds in mutagenesis and carcinogenesis. *Toxicology Letters*, 67, 87-103. doi: 10.1016/0378-4274(93)90048-3
- Erill, I., Escribano, M., Campoy, S. & Barbé, J. 2003. *In silico* analysis reveals substantial variability in the gene contents of the gamma proteobacteria LexA-regulon. *Bioinformatics*, 19, 2225-2236. doi: 10.1093/bioinformatics/btg303
- European Medicines Agency. 2019. Sales of veterinary antimicrobial agents in 31 European countries in 2017: Trends from 2010 to 2017. Available: <https://www.ema.europa.eu/en/veterinary-regulatory/overview/antimicrobial-resistance/european-surveillance-veterinary-antimicrobial-consumption-esvac>.
- Evans, K. L., Kannan, S., Li, G., de Pedro, M. A. & Young, K. D. 2013. Eliminating a set of four penicillin binding proteins triggers the Rcs phosphorelay and Cpx stress responses in *Escherichia coli*. *Journal of Bacteriology*, 195, 4415-4424. doi: 10.1128/JB.00596-13
- Ezraty, B., Vergnes, A., Banzhaf, M., Duverger, Y., Huguenot, A., Brochado, A. R., Su, S. Y., Espinosa, L., Loiseau, L., Py, B., Typas, A. & Barras, F. 2013. Fe-S cluster biosynthesis controls uptake of aminoglycosides in a ROS-less death pathway. *Science*, 340, 1583-7. doi: 10.1126/science.1238328
- Fan, X. & Sellin, J. H. 2009. Review article: Small intestinal bacterial overgrowth, bile acid malabsorption and gluten intolerance as possible causes of chronic watery diarrhoea. *Alimentary Pharmacology & Therapeutics*, 29, 1069-77. doi: 10.1111/j.1365-2036.2009.03970.x
- Farr, S. B. & Kogoma, T. 1991. Oxidative stress responses in *Escherichia coli* and *Salmonella typhimurium*. *Microbiological Reviews*, 55, 561-585.
- Fekety, R. & Shah, A. B. 1993. Diagnosis and treatment of *Clostridium difficile* colitis. *JAMA*, 269, 71-5. doi: 10.1001/jama.1993.03500010081036
- Feng, X., Zhu, W., Schurig-Briccio, L. A., Lindert, S., Shoen, C., Hitchings, R., Li, J., Wang, Y., Baig, N., Zhou, T., Kim, B. K., Crick, D. C., Cynamon, M.,

- McCammon, J. A., Gennis, R. B. & Oldfield, E. 2015. Antiinfectives targeting enzymes and the proton motive force. *Proceedings of the National Academy of Sciences the United States of America*, 112, E7073-E7082. doi: 10.1073/pnas.1521988112
- Fernández de Henestrosa, A. R., Ogi, T., Aoyagi, S., Chafin, D., Hayes, J. J., Ohmori, H. & Woodgate, R. 2000. Identification of additional genes belonging to the LexA regulon in *Escherichia coli*. *Molecular Microbiology*, 35, 1560-1572. doi: 10.1046/j.1365-2958.2000.01826.x
- Fernández, L. & Hancock, R. E. W. 2012. Adaptive and mutational resistance: Role of porins and efflux pumps in drug resistance. *Clinical Microbiology Reviews*, 25, 661-681. doi: 10.1128/cmr.00043-12
- Filippone, E. J., Kraft, W. K. & Farber, J. L. 2017. The nephrotoxicity of vancomycin. *Clinical Pharmacology and Therapeutics*, 102, 459-469. doi: 10.1002/cpt.726
- Fleming, A. 1929. On the antibacterial action of cultures of a *Penicillium*, with special reference to their use in the isolation of *B. influenzae*. *British Journal of Experimental Pathology*, 10, 226-236.
- Fleming-Dutra, K. E., Hersh, A. L., Shapiro, D. J., Bartoces, M., Enns, E. A., File, T. M., Jr, Finkelstein, J. A., Gerber, J. S., Hyun, D. Y., Linder, J. A., Lynfield, R., Margolis, D. J., May, L. S., Merenstein, D., Metlay, J. P., Newland, J. G., Piccirillo, J. F., Roberts, R. M., Sanchez, G. V., Suda, K. J., Thomas, A., Woo, T. M., Zetts, R. M. & Hicks, L. A. 2016. Prevalence of Inappropriate antibiotic prescriptions among US ambulatory care visits, 2010-2011. *The Journal of the American Medical Association*, 315, 1864-1873. doi: 10.1001/jama.2016.4151
- Fletcher-Lartey, S., Yee, M., Gaarslev, C. & Khan, R. 2016. Why do general practitioners prescribe antibiotics for upper respiratory tract infections to meet patient expectations: a mixed methods study. *BMJ open*, 6, e012244-e012244. doi: 10.1136/bmjopen-2016-012244
- Flint, D. H., Tuminello, J. F. & Emptage, M. H. 1993. The inactivation of Fe-S cluster containing hydro-lyases by superoxide. *The Journal of Biological Chemistry*, 268, 22369-76.
- Flores-Kim, J. & Darwin, A. J. 2016. The phage shock protein response. *Annual Review of Microbiology*, 70, 83-101. doi: 10.1146/annurev-micro-102215-095359
- Forouzesh, A., Moise, P. A. & Sakoulas, G. 2009. Vancomycin ototoxicity: A reevaluation in an era of increasing doses. *Antimicrobial Agents and Chemotherapy*, 53, 483-486. doi: 10.1128/AAC.01088-08
- Fouquier, J. & Guedj, M. 2015. Analysis of drug combinations: Current methodological landscape. *Pharmacology Research & Perspectives*, 3. doi: 10.1002/prp2.149
- Fu, H., Leng, W., Wang, J., Zhang, W., Peng, J., Wang, L. & Jin, Q. 2007. Transcriptional profile induced by furazolidone treatment of *Shigella flexneri*. *Applied Microbiology and Biotechnology*, 77, 657-667. doi: 10.1007/s00253-007-1180-9
- Gaal, T., Bartlett, M. S., Ross, W., Turnbough, C. L. & Gourse, R. L. 1997. Transcription regulation by initiating NTP concentration: rRNA synthesis in bacteria. *Science*, 278, 2092-2097. doi: 10.1126/science.278.5346.2092
- Gaudu, P., Moon, N. & Weiss, B. 1997. Regulation of the *soxRS* oxidative stress regulon. Reversible oxidation of the Fe-S centers of SoxR *in vivo*. *The Journal of Biological Chemistry*, 272, 5082-6. doi: 10.1074/jbc.272.8.5082
- Gentry, D. R., Hernandez, V. J., Nguyen, L. H., Jensen, D. B. & Cashel, M. 1993. Synthesis of the stationary-phase sigma factor sigma s is positively regulated by ppGpp. *Journal of Bacteriology*, 175, 7982-7989. doi: 10.1128/jb.175.24.7982-7989.1993

- Goldberg, A. 1966. Magnesium binding by *Escherichia coli* ribosomes. *Journal of Molecular Biology*, 15, 663-673. doi: 10.1016/S0022-2836(66)80134-1
- Gonzales, M., Pepin, J., Frost, E. H., Carrier, J. C., Sirard, S., Fortier, L. & Valiquette, L. 2010. Faecal pharmacokinetics of orally administered vancomycin in patients with suspected *Clostridium difficile* infection. *BMC Infectious Diseases*, 10, 363. doi: 10.1186/1471-2334-10-363
- González-Flecha, B. & Demple, B. 1995. Metabolic sources of hydrogen peroxide in aerobically growing *Escherichia coli*. *The Journal of Biological Chemistry*, 270, 13681-7. doi: 10.1074/jbc.270.23.13681
- González-Flecha, B. & Demple, B. 1997. Homeostatic regulation of intracellular hydrogen peroxide concentration in aerobically growing *Escherichia coli*. *Journal of Bacteriology*, 179, 382-8. doi: 10.1128/jb.179.2.382-388.1997
- Gordon, G. S., Moses, A. C., Silver, R. D., Flier, J. S. & Carey, M. C. 1985. Nasal absorption of insulin: enhancement by hydrophobic bile salts. *Proceedings of the National Academy of Sciences of the United States of America*, 82, 7419-7423. doi: 10.1073/pnas.82.21.7419
- Gottesman, S., Trisler, P. & Torres-Cabassa, A. 1985. Regulation of capsular polysaccharide synthesis in *Escherichia coli* K-12: Characterization of three regulatory genes. *Journal of Bacteriology*, 162, 1111-1119. doi: 10.1128/jb.162.3.1111-1119.1985
- Gould, K. 2016. Antibiotics: from prehistory to the present day. *Journal of Antimicrobial Chemotherapy*, 71, 572-575. doi: 10.1093/jac/dkv484
- Gourley, C. R., Negretti, N. M. & Konkel, M. E. 2017. The food-borne pathogen *Campylobacter jejuni* depends on the AddAB DNA repair system to defend against bile in the intestinal environment. *Scientific Reports*, 7, 14777. doi: 10.1038/s41598-017-14646-9
- Greenberg, J. T., Monach, P., Chou, J. H., Josephy, P. D. & Demple, B. 1990. Positive control of a global antioxidant defense regulon activated by superoxide-generating agents in *Escherichia coli*. *Proceedings of the National Academy of Sciences of the United States of America*, 87, 6181-5. doi: 10.1073/pnas.87.16.6181
- Griffith, K. L., Fitzpatrick, M. M., Keen, E. F., 3rd & Wolf, R. E., Jr. 2009. Two functions of the C-terminal domain of *Escherichia coli* Rob: Mediating "sequestration-dispersal" as a novel off-on switch for regulating Rob's activity as a transcription activator and preventing degradation of Rob by Lon protease. *Journal of Molecular Biology*, 388, 415-430. doi: 10.1016/j.jmb.2009.03.023
- Gu, M. & Imlay, J. A. 2011. The SoxRS response of *Escherichia coli* is directly activated by redox-cycling drugs rather than by superoxide. *Molecular Microbiology*, 79, 1136-1150. doi: 10.1111/j.1365-2958.2010.07520.x
- Gunn, J. S. 2000. Mechanisms of bacterial resistance and response to bile. *Microbes and Infection*, 2, 907-13. doi: 10.1016/s1286-4579(00)00392-0
- Gunnarsdottir, S. A., Sadik, R., Shev, S., Simren, M., Sjøvall, H., Stotzer, P. O., Abrahamsson, H., Olsson, R. & Björnsson, E. S. 2003. Small intestinal motility disturbances and bacterial overgrowth in patients with liver cirrhosis and portal hypertension. *The American Journal of Gastroenterology*, 98, 1362-70. doi: 10.1111/j.1572-0241.2003.07475.x
- Guo, Y., Wang, R., Shang, Y. & Liu, H. 2018. Effects of polymers on the properties of hydrogels constructed using sodium deoxycholate and amino acid. *RSC Advances*, 8, 8699-8708. doi: 10.1039/C8RA00171E

- Gupta, A., Loboeki, C., Singh, S., Robertson, M., Akadiri, O. A., Malhotra, G. & Jackson, I. T. 2009. Actions and comparative efficacy of phosphatidylcholine formulation and isolated sodium deoxycholate for different cell types. *Aesthetic Plastic Surgery*, 33, 346-352. doi: 10.1007/s00266-008-9301-0
- Hall, B., Bot, C. & Wilkinson, S. 2011. Nifurtimox activation by trypanosomal type I nitroreductases generates cytotoxic nitrile metabolites. *Journal of Biological Chemistry*, 286, 13088-95. doi: 10.1074/jbc.M111.230847
- Hammes, W. P. & Neuhaus, F. C. 1974. On the mechanism of action of vancomycin: Inhibition of peptidoglycan synthesis in *Gaffkya homari*. *Antimicrobial Agents and Chemotherapy*, 6, 722-728. doi: 10.1128%2Faac.6.6.722
- Hamner, S., McInnerney, K., Williamson, K., Franklin, M. J. & Ford, T. E. 2013. Bile salts affect expression of *Escherichia coli* O157:H7 genes for virulence and iron acquisition, and promote growth under iron limiting conditions. *PLoS One*, 8, e74647. doi: 10.1371/journal.pone.0074647
- Hards, K., Robson, J. R., Berney, M., Shaw, L., Bald, D., Koul, A., Andries, K. & Cook, G. M. 2015. Bactericidal mode of action of bedaquiline. *Journal of Antimicrobial Chemotherapy*, 70, 2028-2037. doi: 10.1093/jac/dkv054
- Hernández, S. B., Cota, I., Ducret, A., Aussel, L. & Casadesús, J. 2012. Adaptation and preadaptation of *Salmonella enterica* to bile. *PLoS Genetics*, 8, e1002459. doi: 10.1371/journal.pgen.1002459
- Heytler, P. G. 1963. Uncoupling of oxidative phosphorylation by carbonyl cyanide phenylhydrazones. I. Some characteristics of m-Cl-CCP action on mitochondria and chloroplasts. *Biochemistry*, 2, 357-361. doi: 10.1021/bi00902a031
- Hiraku, Y., Sekine, A., Nabeshi, H., Midorikawa, K., Murata, M., Kumagai, Y. & Kawanishi, S. 2004. Mechanism of carcinogenesis induced by a veterinary antimicrobial drug, nitrofurazone, via oxidative DNA damage and cell proliferation. *Cancer Letters*, 215, 141-50. doi: 10.1016/j.canlet.2004.05.016
- Houten, S. M., Watanabe, M. & Auwerx, J. 2006. Endocrine functions of bile acids. *The EMBO Journal*, 25, 1419-1425. doi: 10.1038/sj.emboj.7601049
- Hu, P. L., Yuan, Y. H., Yue, T. L. & Guo, C. F. 2018. Bile acid patterns in commercially available oxgall powders used for the evaluation of the bile tolerance ability of potential probiotics. *PLoS One*, 13, e0192964-e0192964. doi: 10.1371/journal.pone.0192964
- Huang, R.-y., Pei, L., Liu, Q., Chen, S., Dou, H., Shu, G., Yuan, Z.-x., Lin, J., Peng, G., Zhang, W. & Fu, H. 2019. Isobologram analysis: A comprehensive review of methodology and current research. *Frontiers in Pharmacology*, 10. doi: 10.3389/fphar.2019.01222
- Hylemon, P. B., Zhou, H., Pandak, W. M., Ren, S., Gil, G. & Dent, P. 2009. Bile acids as regulatory molecules. *Journal of Lipid Research*, 50, 1509-20. doi: 10.1194/jlr.R900007-JLR200
- Imlay, J., Chin, S. & Linn, S. 1988. Toxic DNA damage by hydrogen peroxide through the Fenton reaction *in vivo* and *in vitro*. *Science*, 240, 640-642. doi: 10.1126/science.2834821
- Imlay, J. A. 2003. Pathways of oxidative damage. *Annual Review of Microbiology*, 57, 395-418. doi: 10.1146/annurev.micro.57.030502.090938
- Imlay, J. A. 2006. Iron-sulphur clusters and the problem with oxygen. *Molecular Microbiology*, 59, 1073-1082. doi: 10.1111/j.1365-2958.2006.05028.x
- Ingledeu, W. J. & Poole, R. K. 1984. The respiratory chains of *Escherichia coli*. *Microbiological Reviews*, 48, 222-271.

- Itoh, M., Wada, K., Tan, S., Kitano, Y., Kai, J. & Makino, I. 1999. Antibacterial action of bile acids against *Helicobacter pylori* and changes in its ultrastructural morphology: Effect of unconjugated dihydroxy bile acid. *Journal of Gastroenterology*, 34, 571-6. doi: 10.1007/s005350050374
- Jacobs, A. & Miles, P. M. 1970. The formation of iron complexes with bile and bile constituents. *Gut*, 11, 732-734. doi: 10.1136/gut.11.9.732
- Jang, S. & Imlay, J. A. 2007. Micromolar intracellular hydrogen peroxide disrupts metabolism by damaging iron-sulfur enzymes. *The Journal of Biological Chemistry*, 282, 929-37. doi: 10.1074/jbc.M607646200
- Janzowski, C., Glaab, V., Mueller, C., Straesser, U., Kamp, H. G. & Eisenbrand, G. 2003. Alpha,beta-unsaturated carbonyl compounds: Induction of oxidative DNA damage in mammalian cells. *Mutagenesis*, 18, 465-70. doi: 10.1093/mutage/geg018
- Jordan, S., Hutchings, M. I. & Mascher, T. 2008. Cell envelope stress response in Gram-positive bacteria. *FEMS Microbiology Reviews*, 32, 107-146. doi: 10.1111/j.1574-6976.2007.00091.x
- Jovanovic, G., Lloyd, L. J., Stumpf, M. P., Mayhew, A. J. & Buck, M. 2006. Induction and function of the phage shock protein extracytoplasmic stress response in *Escherichia coli*. *The Journal of Biological Chemistry*, 281, 21147-61. doi: 10.1074/jbc.M602323200
- Jubelin, G., Vianney, A., Beloin, C., Ghigo, J. M., Lazzaroni, J. C., Lejeune, P. & Dorel, C. 2005. CpxR/OmpR interplay regulates curli gene expression in response to osmolarity in *Escherichia coli*. *Journal of Bacteriology*, 187, 2038-49. doi: 10.1128/jb.187.6.2038-2049.2005
- Kamenšek, S. & Žgur-Bertok, D. 2013. Global transcriptional responses to the bacteriocin colicin M in *Escherichia coli*. *BMC Microbiology*, 13, 42. doi: 10.1186/1471-2180-13-42
- Kari, F. W., Huff, J. E., Leininger, J., Haseman, J. K. & Eustis, S. L. 1989. Toxicity and carcinogenicity of nitrofurazone in F344/N rats and B6C3F1 mice. *Food and Chemical Toxicology*, 27, 129-37. doi: 10.1016/0278-6915(89)90008-2
- Kasianowicz, J., Benz, R. & McLaughlin, S. 1984. The kinetic mechanism by which CCCP (carbonyl cyanidem-chlorophenylhydrazine) transports protons across membranes. *The Journal of Membrane Biology*, 82, 179-190. doi: 10.1007/BF01868942
- Kehres, D. G., Janakiraman, A., Slauch, J. M. & Maguire, M. E. 2002. Regulation of *Salmonella enterica* serovar Typhimurium *mntH* transcription by H₂O₂, Fe²⁺, and Mn²⁺. *Journal of Bacteriology*, 184, 3151-8. doi: 10.1128/jb.184.12.3151-3158.2002
- Keyer, K. & Imlay, J. A. 1996. Superoxide accelerates DNA damage by elevating free-iron levels. *Proceedings of the National Academy of Sciences of the United States of America*, 93, 13635-13640. doi: 10.1073/pnas.93.24.13635
- Khanum, S. 2015. Characterization of the secretins, large outer membrane channels of gram-negative bacteria. Doctor of Philosophy, PhD thesis, Massey University. <http://hdl.handle.net/10179/7732>
- Kim, D., Langmead, B. & Salzberg, S. L. 2015. HISAT: A fast spliced aligner with low memory requirements. *Nature Methods*, 12, 357-360. doi: 10.1038/nmeth.3317
- Kirchhelle, C. 2018. Pharming animals: a global history of antibiotics in food production (1935–2017). *Palgrave Communications*, 4, 96. doi: 10.1057/s41599-018-0152-2
- Klein, G., Stupak, A., Biernacka, D., Wojtkiewicz, P., Lindner, B. & Raina, S. 2016. Multiple transcriptional factors regulate transcription of the *rpoE* gene in

- Escherichia coli* under different growth conditions and when the lipopolysaccharide biosynthesis is defective. *The Journal of Biological Chemistry*, 291, 22999-23019. doi: 10.1074/jbc.M116.748954
- Klumpp, S., Zhang, Z. & Hwa, T. 2009. Growth rate-dependent global effects on gene expression in bacteria. *Cell*, 139, 1366-1375. doi: 10.1016/j.cell.2009.12.001
- Kobayashi, R., Suzuki, T. & Yoshida, M. 2007. *Escherichia coli* phage-shock protein A (PspA) binds to membrane phospholipids and repairs proton leakage of the damaged membranes. *Molecular Microbiology*, 66, 100-9. doi: 10.1111/j.1365-2958.2007.05893.x
- Kobayashi, S., Arai, S., Hayashi, S. & Sakaguchi, T. 1989. *In vitro* effects of beta-lactams combined with beta-lactamase inhibitors against methicillin-resistant *Staphylococcus aureus*. *Antimicrobial Agents and Chemotherapy*, 33, 331-335. doi: 10.1128/aac.33.3.331
- Kohanski, M. A., Dwyer, D. J., Hayete, B., Lawrence, C. A. & Collins, J. J. 2007. A common mechanism of cellular death induced by bactericidal antibiotics. *Cell*, 130, 797-810. doi: 10.1016/j.cell.2007.06.049
- Kolde, R. 2019. *heatmap: Pretty Heatmaps* [Online]. Available: <https://CRAN.R-project.org/package=heatmap> [Accessed March 2019].
- Kranz, J., Helbig, S., Mandraka, F., Schmidt, S. & Naber, K. G. 2017. The revival of old antibiotics for treatment of uncomplicated urinary tract infections in the era of antibiotic stewardship. *Current Opinion in Urology*, 27, 127-132. doi: 10.1097/mou.0000000000000365
- Krishnamoorthy, G., Tikhonova, E. B., Dhamdhare, G. & Zgurskaya, H. I. 2013. On the role of TolC in multidrug efflux: the function and assembly of AcrAB-TolC tolerate significant depletion of intracellular TolC protein. *Molecular Microbiology*, 87, 982-997. doi: 10.1111/mmi.12143
- Kumar, M., Adhikari, S. & Hurdle, J. G. 2014. Action of nitroheterocyclic drugs against *Clostridium difficile*. *International Journal of Antimicrobial Agents*, 44, 314-319. doi: 10.1016/j.ijantimicag.2014.05.021
- Kurdi, P., Kawanishi, K., Mizutani, K. & Yokota, A. 2006. Mechanism of growth inhibition by free bile acids in lactobacilli and bifidobacteria. *Journal of Bacteriology*, 188, 1979-86. doi: 10.1128/jb.188.5.1979-1986.2006
- Kvint, K., Farewell, A. & Nyström, T. 2000. RpoS-dependent promoters require guanosine tetraphosphate for induction even in the presence of high levels of sigma(s). *The Journal of Biological Chemistry*, 275, 14795-8. doi: 10.1074/jbc.C000128200
- Kwon, D. H., Lee, M., Kim, J. J., Kim, J. G., El-Zaatari, F. A. K., Osato, M. S. & Graham, D. Y. 2001. Furazolidone- and nitrofurantoin-resistant *Helicobacter pylori*: Prevalence and role of genes involved in metronidazole resistance. *Antimicrobial Agents and Chemotherapy*, 45, 306-308. doi: 10.1128/aac.45.1.306-308.2001
- Kwon, H. J., Bennik, M. H., Demple, B. & Ellenberger, T. 2000. Crystal structure of the *Escherichia coli* Rob transcription factor in complex with DNA. *Nature Structural Biology*, 7, 424-30. doi: 10.1038/75213
- Laehnemann, D., Peña-Miller, R., Rosenstiel, P., Beardmore, R., Jansen, G. & Schulenburg, H. 2014. Genomics of rapid adaptation to antibiotics: convergent evolution and scalable sequence amplification. *Genome Biology and Evolution*, 6, 1287-1301. doi: 10.1093/gbe/evu106
- Laffler, T. & Gallant, J. 1974. *spoT*, a new genetic locus involved in the stringent response in *E. coli*. *Cell*, 1, 27-30. doi: 10.1016/0092-8674(74)90151-2

- Lagosky, P. A. & Chang, F. N. 1980. Influence of amino acid starvation on guanosine 5'-diphosphate 3'-diphosphate basal-level synthesis in *Escherichia coli*. *Journal of Bacteriology*, 144, 499-508. doi: 10.1128/JB.144.2.499-508.1980
- Landers, T. F., Cohen, B., Wittum, T. E. & Larson, E. L. 2012. A review of antibiotic use in food animals: perspective, policy, and potential. *Public health reports (Washington, D.C. : 1974)*, 127, 4-22. doi: 10.1177/003335491212700103
- Laubacher, M. E. & Ades, S. E. 2008. The Rcs phosphorelay is a cell envelope stress response activated by peptidoglycan stress and contributes to intrinsic antibiotic resistance. *Journal of Bacteriology*, 190, 2065-2074. doi: 10.1128/JB.01740-07
- Le, V., Olivera, C., Spagnuolo, J., Davies, I. & Rakonjac, J. 2020. *In vitro* synergy between sodium deoxycholate and furazolidone against enterobacteria. *BMC Microbiology*, 20. doi: 10.1186/s12866-019-1668-3
- Le, V. V. H., Davies, I. G., Moon, C. D., Wheeler, D., Biggs, P. J. & Rakonjac, J. 2019. Novel 5-nitrofuranyl-activating reductase in *Escherichia coli*. *Antimicrobial Agents and Chemotherapy*, 63. doi: 10.1128/aac.00868-19
- Leblanc, S. K., Oates, C. W. & Raivio, T. L. 2011. Characterization of the induction and cellular role of the BaeSR two-component envelope stress response of *Escherichia coli*. *Journal of Bacteriology*, 193, 3367-75. doi: 10.1128/jb.01534-10
- Lebreton, F., Depardieu, F., Bourdon, N., Fines-Guyon, M., Berger, P., Camiade, S., Leclercq, R., Courvalin, P. & Cattoir, V. 2011. D-Ala-d-Ser VanN-type transferable vancomycin resistance in *Enterococcus faecium*. *Antimicrobial Agents and Chemotherapy*, 55, 4606-4612. doi: 10.1128/AAC.00714-11
- Lee, C., Lee, S. M., Mukhopadhyay, P., Kim, S. J., Lee, S. C., Ahn, W.-S., Yu, M.-H., Storz, G. & Ryu, S. E. 2004. Redox regulation of OxyR requires specific disulfide bond formation involving a rapid kinetic reaction path. *Nature Structural & Molecular Biology*, 11, 1179-1185. doi: 10.1038/nsmb856
- Lee, K.-C., Yeo, W.-S. & Roe, J.-H. 2008. Oxidant-responsive induction of the *suf* operon, encoding a Fe-S assembly system, through Fur and IscR in *Escherichia coli*. *Journal of Bacteriology*, 190, 8244-8247. doi: 10.1128/jb.01161-08
- Levine, D. P. 2006. Vancomycin: a history. *Clinical Infectious Diseases*, 42 Suppl 1, S5-12. doi: 10.1086/491709
- Lewis, L. K., Harlow, G. R., Gregg-Jolly, L. A. & Mount, D. W. 1994. Identification of high affinity binding sites for LexA which define new DNA damage-inducible genes in *Escherichia coli*. *Journal of Molecular Biology*, 241, 507-523. doi: 10.1006/jmbi.1994.1528
- Li, G.-q., Quan, F., Qu, T., Lu, J., Chen, S.-l., Cui, L.-y., Guo, D.-w. & Wang, Y.-c. 2015. Sublethal vancomycin-induced ROS mediating antibiotic resistance in *Staphylococcus aureus*. *Bioscience reports*, 35, e00279. doi: 10.1042/BSR20140167
- Li, H., Handsaker, B., Wysoker, A., Fennell, T., Ruan, J., Homer, N., Marth, G., Abecasis, G. & Durbin, R. 2009. The Sequence Alignment/Map format and SAMtools. *Bioinformatics*, 25, 2078-9. doi: 10.1093/bioinformatics/btp352
- Li, Z. & Dimple, B. 1994. SoxS, an activator of superoxide stress genes in *Escherichia coli*. Purification and interaction with DNA. *The Journal of Biological Chemistry*, 269, 18371-7.
- Liao, Y., Smyth, G. K. & Shi, W. 2013. featureCounts: an efficient general purpose program for assigning sequence reads to genomic features. *Bioinformatics*, 30, 923-930. doi: 10.1093/bioinformatics/btt656

- Lima, S., Guo, M. S., Chaba, R., Gross, C. A. & Sauer, R. T. 2013. Dual molecular signals mediate the bacterial response to outer-membrane stress. *Science*, 340, 837-41. doi: 10.1126/science.1235358
- Lin, J., Sahin, O., Michel, L. O. & Zhang, Q. 2003. Critical role of multidrug efflux pump CmeABC in bile resistance and *in vivo* colonization of *Campylobacter jejuni*. *Infection and Immunity*, 71, 4250-4259. doi: 10.1128/iai.71.8.4250-4259.2003
- Lin, X., Kang, L., Li, H. & Peng, X. 2014. Fluctuation of multiple metabolic pathways is required for *Escherichia coli* in response to chlortetracycline stress. *Molecular BioSystems*, 10, 901-908. doi: 10.1039/C3MB70522F
- Liochev, S. I., Benov, L., Touati, D. & Fridovich, I. 1999. Induction of the *soxRS* regulon of *Escherichia coli* by superoxide. *The Journal of Biological Chemistry*, 274, 9479-81. doi: 10.1074/jbc.274.14.9479
- Little, J. W. 1984. Autodigestion of *lexA* and phage lambda repressors. *Proceedings of the National Academy of Sciences of the United States of America*, 81, 1375-9. doi: 10.1073/pnas.81.5.1375
- Liu, A., Tran, L., Becket, E., Lee, K., Chinn, L., Park, E., Tran, K. & Miller, J. H. 2010. Antibiotic sensitivity profiles determined with an *Escherichia coli* gene knockout collection: Generating an antibiotic bar code. *Antimicrobial Agents and Chemotherapy*, 54, 1393-1403. doi: 10.1128/aac.00906-09
- Liu, J., Volk, K. J., Lee, M. S., Pucci, M. & Handwerker, S. 1994. Binding studies of vancomycin to the cytoplasmic peptidoglycan precursors by affinity capillary electrophoresis. *Analytical Chemistry*, 66, 2412-6. doi: 10.1021/ac00086a031
- Liu, M., Chesnut, C. & Lask, G. 2019. Overview of Kybella (deoxycholic acid injection) as a fat resorption product for submental fat. *Facial Plastic Surgery*, 35, 274-277. doi: 10.1055/s-0039-1688943
- Liu, M., Gong, X., Alluri, R. K., Wu, J., Sablo, T. & Li, Z. 2012. Characterization of RNA damage under oxidative stress in *Escherichia coli*. *Biological Chemistry*, 393, 123-32. doi: 10.1515/hsz-2011-0247
- Liu, Y. Y., Wang, Y., Walsh, T. R., Yi, L. X., Zhang, R., Spencer, J., Doi, Y., Tian, G., Dong, B., Huang, X., Yu, L. F., Gu, D., Ren, H., Chen, X., Lv, L., He, D., Zhou, H., Liang, Z., Liu, J. H. & Shen, J. 2016. Emergence of plasmid-mediated colistin resistance mechanism MCR-1 in animals and human beings in China: a microbiological and molecular biological study. *The Lancet Infectious Diseases*, 16, 161-8. doi: 10.1016/s1473-3099(15)00424-7
- Loewe, S. 1953. The problem of synergism and antagonism of combined drugs. *Arzneimittelforschung*, 3, 285-90.
- Lorenzo-Zuniga, V., Bartoli, R., Planas, R., Hofmann, A. F., Vinado, B., Hagey, L. R., Hernandez, J. M., Mane, J., Alvarez, M. A., Ausina, V. & Gassull, M. A. 2003. Oral bile acids reduce bacterial overgrowth, bacterial translocation, and endotoxemia in cirrhotic rats. *Hepatology*, 37, 551-7. doi: 10.1053/jhep.2003.50116
- Love, M. I., Huber, W. & Anders, S. 2014. Moderated estimation of fold change and dispersion for RNA-seq data with DESeq2. *Genome Biology*, 15, 550-550. doi: 10.1186/s13059-014-0550-8
- Ma, F., Xu, S., Tang, Z., Li, Z. & Zhang, L. 2021. Use of antimicrobials in food animals and impact of transmission of antimicrobial resistance on humans. *Biosafety and Health*, 3, 32-38. doi: 10.1016/j.bshealth.2020.09.004
- Macomber, L. & Imlay, J. A. 2009. The iron-sulfur clusters of dehydratases are primary intracellular targets of copper toxicity. *Proceedings of the National Academy of*

- Sciences of the United States of America*, 106, 8344-8349. doi: 10.1073/pnas.0812808106
- Majdalani, N. & Gottesman, S. 2005. The RcS phosphorelay: A complex signal transduction system. *Annual Review of Microbiology*, 59, 379-405. doi: 10.1146/annurev.micro.59.050405.101230
- Mallela, A. N., Abdullah, K. G., Brandon, C., Richardson, A. G. & Lucas, T. H. 2017. Topical vancomycin reduces surgical-site infections after craniotomy: A prospective, controlled study. *Neurosurgery*, 83, 761-767. doi: 10.1093/neuros/nyx559
- Maloney, P. C., Kashket, E. R. & Wilson, T. H. 1974. A protonmotive force drives ATP synthesis in bacteria. *Proceedings of the National Academy of Sciences of the United States of America*, 71, 3896-3900. doi: 10.1073/pnas.71.10.3896
- Mamber, S. W., Kolek, B., Brookshire, K. W., Bonner, D. P. & Fung-Tomc, J. 1993. Activity of quinolones in the Ames *Salmonella* TA102 mutagenicity test and other bacterial genotoxicity assays. *Antimicrobial Agents and Chemotherapy*, 37, 213-217. doi: 10.1128/aac.37.2.213
- Martin, R. G., Jair, K. W., Wolf, R. E., Jr. & Rosner, J. L. 1996. Autoactivation of the *marRAB* multiple antibiotic resistance operon by the MarA transcriptional activator in *Escherichia coli*. *Journal of Bacteriology*, 178, 2216-23. doi: 10.1128/jb.178.8.2216-2223.1996
- Martin, R. G. & Rosner, J. L. 1995. Binding of purified multiple antibiotic-resistance repressor protein (MarR) to *mar* operator sequences. *Proceedings of the National Academy of Sciences of the United States of America*, 92, 5456-60. doi: 10.1073/pnas.92.12.5456
- Masłowska, K. H., Makiela-Dzubska, K. & Fijalkowska, I. J. 2019. The SOS system: A complex and tightly regulated response to DNA damage. *Environmental and Molecular Mutagenesis*, 60, 368-384. doi: 10.1002/em.22267
- Massé, E., Escorcía, F. E. & Gottesman, S. 2003. Coupled degradation of a small regulatory RNA and its mRNA targets in *Escherichia coli*. *Genes & Development*, 17, 2374-2383. doi: 10.1101/gad.1127103
- Massé, E. & Gottesman, S. 2002. A small RNA regulates the expression of genes involved in iron metabolism in *Escherichia coli*. *Proceedings of the National Academy of Sciences*, 99, 4620-4625. doi: 10.1073/pnas.032066599
- Massé, E., Vanderpool, C. K. & Gottesman, S. 2005. Effect of RyhB small RNA on global iron use in *Escherichia coli*. *Journal of Bacteriology*, 187, 6962-6971. doi: 10.1128/JB.187.20.6962-6971.2005
- Mathieu, A., Fleurier, S., Frénoy, A., Dairou, J., Bredeche, M.-F., Sanchez-Vizueté, P., Song, X. & Matic, I. 2016. Discovery and function of a general core hormetic stress response in *E. coli* induced by sublethal concentrations of antibiotics. *Cell Reports*, 17, 46-57. doi: 10.1016/j.celrep.2016.09.001
- McCalla, D. R., Olive, P., Tu, Y. & Fan, M. L. 1975. Nitrofurazone-reducing enzymes in *E. coli* and their role in drug activation *in vivo*. *Canadian Journal of Microbiology*, 21, 1484-1491. doi: 10.1139/m75-220
- McCracken, R. J. & Kennedy, D. G. 2007. Detection, accumulation and distribution of nitrofur residues in egg yolk, albumen and shell. *Food Additives and Contaminants*, 24, 26-33. doi: 10.1080/02652030600967214
- McGann, P., Snesrud, E., Maybank, R., Corey, B., Ong, A. C., Clifford, R., Hinkle, M., Whitman, T., Lesho, E. & Schaecher, K. E. 2016. *Escherichia coli* harboring *mcr-1* and *blaCTX-M* on a novel IncF plasmid: First report of *mcr-1* in the United

- States. *Antimicrobial Agents and Chemotherapy*, 60, 4420-1. doi: 10.1128/aac.01103-16
- McHugh, J. P., Rodríguez-Quinoñes, F., Abdul-Tehrani, H., Svistunenko, D. A., Poole, R. K., Cooper, C. E. & Andrews, S. C. 2003. Global iron-dependent gene regulation in *Escherichia coli*: A new mechanism for iron homeostasis. *The Journal of Biological Chemistry*, 278, 29478-86. doi: 10.1074/jbc.M303381200
- McKim, J. M., Jr. 2010. Building a tiered approach to in vitro predictive toxicity screening: a focus on assays with in vivo relevance. *Combinatorial chemistry & high throughput screening*, 13, 188-206. doi: 10.2174/138620710790596736
- McMurry, L. M. & Levy, S. B. 2010. Evidence that regulatory protein MarA of *Escherichia coli* represses *rob* by steric Hindrance. *Journal of Bacteriology*, 192, 3977-3982. doi: 10.1128/jb.00103-10
- McNeel, K. E., Das, S., Siraj, N., Negulescu, I. I. & Warner, I. M. 2015. Sodium deoxycholate hydrogels: Effects of modifications on gelation, drug release, and nanotemplating. *The Journal of Physical Chemistry B*, 119, 8651-8659. doi: 10.1021/acs.jpcc.5b00411
- McOsker, C. C. & Fitzpatrick, P. M. 1994. Nitrofurantoin: mechanism of action and implications for resistance development in common uropathogens. *Journal of Antimicrobial Chemotherapy*, 33 Suppl A, 23-30. doi: 10.1093/jac/33.suppl_a.23
- Mecenas, J., Rouviere, P. E., Erickson, J. W., Donohue, T. J. & Gross, C. A. 1993. The activity of sigma E, an *Escherichia coli* heat-inducible sigma-factor, is modulated by expression of outer membrane proteins. *Genes & Development*, 7, 2618-28. doi: 10.1101/gad.7.12b.2618
- Menetski, J. P. & Kowalczykowski, S. C. 1985. Interaction of RecA protein with single-stranded DNA. Quantitative aspects of binding affinity modulation by nucleotide cofactors. *Journal of Molecular Biology*, 181, 281-95. doi: 10.1016/0022-2836(85)90092-0
- Merritt, M. E. & Donaldson, J. R. 2009. Effect of bile salts on the DNA and membrane integrity of enteric bacteria. *Journal of Medical Microbiology*, 58, 1533-1541. doi: 10.1099/jmm.0.014092-0
- Messner, K. R. & Imlay, J. A. 1999. The identification of primary sites of superoxide and hydrogen peroxide formation in the aerobic respiratory chain and sulfite reductase complex of *Escherichia coli*. *Journal of Biological Chemistry*, 274, 10119-10128. doi: 10.1074/jbc.274.15.10119
- Mettert, E. L. & Kiley, P. J. 2014. Coordinate regulation of the Suf and Isc Fe-S cluster biogenesis pathways by IscR is essential for viability of *Escherichia coli*. *Journal of Bacteriology*, 196, 4315-4323. doi: 10.1128/JB.01975-14
- Metzger, S., Schreiber, G., Aizenman, E., Cashel, M. & Glaser, G. 1989. Characterization of the *relA1* mutation and a comparison of *relA1* with new *relA* null alleles in *Escherichia coli*. *The Journal of Biological Chemistry*, 264, 21146-52.
- Meziane-Cherif, D., Saul, F. A., Haouz, A. & Courvalin, P. 2012. Structural and functional characterization of VanG D-Ala:D-Ser ligase associated with vancomycin resistance in *Enterococcus faecalis*. *The Journal of Biological Chemistry*, 287, 37583-37592. doi: 10.1074/jbc.M112.405522
- Mi, H., Muruganujan, A., Ebert, D., Huang, X. & Thomas, P. D. 2018. PANTHER version 14: more genomes, a new PANTHER GO-slim and improvements in enrichment analysis tools. *Nucleic Acids Research*, 47, D419-D426. doi: 10.1093/nar/gky1038

- Michán, C., Manchado, M. & Pueyo, C. 2002. SoxRS down-regulation of *rob* transcription. *Journal of Bacteriology*, 184, 4733-4738. doi: 10.1128/jb.184.17.4733-4738.2002
- Miller, M. J. & Gennis, R. B. 1985. The cytochrome d complex is a coupling site in the aerobic respiratory chain of *Escherichia coli*. *The Journal of Biological Chemistry*, 260, 14003-8.
- Miller, P. F., Gambino, L. F., Sulavik, M. C. & Gracheck, S. J. 1994. Genetic relationship between *soxRS* and *mar* loci in promoting multiple antibiotic resistance in *Escherichia coli*. *Antimicrobial Agents and Chemotherapy*, 38, 1773-9. doi: 10.1128/aac.38.8.1773
- Minato, Y., Dawadi, S., Kordus, S. L., Sivanandam, A., Aldrich, C. C. & Baughn, A. D. 2018. Mutual potentiation drives synergy between trimethoprim and sulfamethoxazole. *Nature Communications*, 9, 1003. doi: 10.1038/s41467-018-03447-x
- Misra, R. & Benson, S. A. 1988. Isolation and characterization of OmpC porin mutants with altered pore properties. *Journal of Bacteriology*, 170, 528-33. doi: 10.1128/jb.170.2.528-533.1988
- Mitchell, A. M. & Silhavy, T. J. 2019. Envelope stress responses: Balancing damage repair and toxicity. *Nature Reviews Microbiology*, 17, 417-428. doi: 10.1038/s41579-019-0199-0
- Mitchell, P. 1961. Coupling of phosphorylation to electron and hydrogen transfer by a chemi-osmotic type of mechanism. *Nature*, 191, 144-148. doi: 10.1038/191144a0
- Mitchell, P. 1976. Vectorial chemistry and the molecular mechanics of chemiosmotic coupling: Power transmission by proticity. *Biochemical Society Transactions*, 4, 399-430. doi: 10.1042/bst0040399
- Mitosch, K., Rieckh, G. & Bollenbach, T. 2019. Temporal order and precision of complex stress responses in individual bacteria. *Molecular Systems Biology*, 15, e8470. doi: 10.15252/msb.20188470
- Moellering, R. C. 1983. Rationale for use of antimicrobial combinations. *The American Journal of Medicine*, 75, 4-8. doi: 10.1016/0002-9343(83)90088-8
- Moet, G. J., Jones, R. N., Biedenbach, D. J., Stilwell, M. G. & Fritsche, T. R. 2007. Contemporary causes of skin and soft tissue infections in North America, Latin America, and Europe: Report from the SENTRY Antimicrobial Surveillance Program (1998–2004). *Diagnostic Microbiology and Infectious Disease*, 57, 7-13. doi: 10.1016/j.diagmicrobio.2006.05.009
- Moolenaar, G. F., Moorman, C. & Goosen, N. 2000. Role of the *Escherichia coli* nucleotide excision repair proteins in DNA replication. *Journal of Bacteriology*, 182, 5706-5714. doi: 10.1128/jb.182.20.5706-5714.2000
- Mottaghizadeh, F., Mohajjel shoja, H., Haيلي, M. & Darban-Sarokhalil, D. 2019. Molecular epidemiology and nitrofurantoin resistance determinants from nitrofurantoin non-susceptible *Escherichia coli* isolated from urinary tract infections. *Journal of Global Antimicrobial Resistance*. doi: 10.1016/j.jgar.2019.10.002
- Mount, D. W., Low, K. B. & Edmiston, S. J. 1972. Dominant mutations (*lex*) in *Escherichia coli* K-12 which affect radiation sensitivity and frequency of ultraviolet light-induced mutations. *Journal of Bacteriology*, 112, 886-893. doi: 10.1128/JB.112.2.886-893.1972
- Mullard, A. 2019. Achaogen bankruptcy highlights antibacterial development woes. *Nature Reviews Drug Discovery*, 18, 411. doi: 10.1038/d41573-019-00085-w

- Munita, J. M. & Arias, C. A. 2016. Mechanisms of antibiotic resistance. *Microbiology Spectrum*, 4, 10.1128/microbiolspec.VMBF-0016-2015. doi: 10.1128/microbiolspec.VMBF-0016-2015
- Nandal, A., Huggins, C. C., Woodhall, M. R., McHugh, J., Rodríguez-Quiñones, F., Quail, M. A., Guest, J. R. & Andrews, S. C. 2010. Induction of the ferritin gene (*ftnA*) of *Escherichia coli* by Fe²⁺-Fur is mediated by reversal of H-NS silencing and is RyhB independent. *Molecular Microbiology*, 75, 637-57. doi: 10.1111/j.1365-2958.2009.06977.x
- Nascimento, A., Pontes, F. J. S., Lins, R. D. & Soares, T. A. 2014. Hydration, ionic valence and cross-linking propensities of cations determine the stability of lipopolysaccharide (LPS) membranes. *Chemical Communications*, 50, 231-233. doi: 10.1039/C3CC46918B
- Negretti, N. M., Gourley, C. R., Clair, G., Adkins, J. N. & Konkel, M. E. 2017. The food-borne pathogen *Campylobacter jejuni* responds to the bile salt deoxycholate with countermeasures to reactive oxygen species. *Scientific Reports*, 7, 15455. doi: 10.1038/s41598-017-15379-5
- Neidhardt, F. C., Bloch, P. L. & Smith, D. F. 1974. Culture medium for enterobacteria. *Journal of Bacteriology*, 119, 736-47. doi: 10.1128/jb.119.3.736-747.1974
- Nguyen, A. & Bouscarel, B. 2008. Bile acids and signal transduction: role in glucose homeostasis. *Cell Signal*, 20, 2180-97. doi: 10.1016/j.cellsig.2008.06.014
- Niederhoffer, E. C., Naranjo, C. M., Bradley, K. L. & Fee, J. A. 1990. Control of *Escherichia coli* superoxide dismutase (*sodA* and *sodB*) genes by the ferric uptake regulation (*fur*) locus. *Journal of Bacteriology*, 172, 1930-8. doi: 10.1128/jb.172.4.1930-1938.1990
- Nieto, M. & Perkins, H. R. 1971. Modifications of the acyl-D-alanyl-D-alanine terminus affecting complex-formation with vancomycin. *The Biochemical Journal*, 123, 789-803. doi: 10.1042/bj1230789
- Nikaido, E., Yamaguchi, A. & Nishino, K. 2008. AcrAB multidrug efflux pump regulation in *Salmonella enterica* serovar Typhimurium by RamA in response to environmental signals. *The Journal of Biological Chemistry*, 283, 24245-53. doi: 10.1074/jbc.M804544200
- Nikaido, H. 2003. Molecular basis of bacterial outer membrane permeability revisited. *Microbiology and Molecular Biology Reviews*, 67, 593-656. doi: 10.1128/mmbr.67.4.593-656.2003
- Nunoshiba, T., Obata, F., Boss, A. C., Oikawa, S., Mori, T., Kawanishi, S. & Yamamoto, K. 1999. Role of iron and superoxide for generation of hydroxyl radical, oxidative DNA lesions, and mutagenesis in *Escherichia coli*. *The Journal of Biological Chemistry*, 274, 34832-7. doi: 10.1074/jbc.274.49.34832
- Ny, S., Edquist, P., Dumpis, U., Gröndahl-Yli-Hannuksela, K., Hermes, J., Kling, A.-M., Klingeberg, A., Kozlov, R., Källman, O., Lis, D. O., Pomorska-Wesołowska, M., Saule, M., Wisell, K. T., Vuopio, J. & Palagin, I. 2019. Antimicrobial resistance of *Escherichia coli* isolates from outpatient urinary tract infections in women in six European countries including Russia. *Journal of Global Antimicrobial Resistance*, 17, 25-34. doi: 10.1016/j.jgar.2018.11.004
- O'Neill, J. 2014. Antimicrobial Resistance: Tackling a crisis for the health and wealth of nations. Available: <https://amr-review.org/Publications.html>.
- O'Neill, J. 2015. Securing New Drugs for Future Generations: The pipeline of antibiotics. Available: <https://amr-review.org/Publications.html>.
- O'Rourke, A., Beyhan, S., Choi, Y., Morales, P., Chan, A. P., Espinoza, J. L., Dupont, C. L., Meyer, K. J., Spoering, A., Lewis, K., Nierman, W. C. & Nelson, K. E. 2020.

- Mechanism-of-action classification of antibiotics by global transcriptome profiling. *Antimicrobial Agents and Chemotherapy*, 64, e01207-19. doi: 10.1128/aac.01207-19
- Obaseiki-Ebor, E. E. & Akerele, J. O. 1986. Nitrofurantoin mutagenicity: induction of frameshift mutations. *Mutation Research Letters*, 175, 149-52. doi: 10.1016/0165-7992(86)90114-4
- Ocan, M., Obuku, E. A., Bwanga, F., Akena, D., Richard, S., Ogwal-Okeng, J. & Obua, C. 2015. Household antimicrobial self-medication: a systematic review and meta-analysis of the burden, risk factors and outcomes in developing countries. *BMC Public Health*, 15, 742-742. doi: 10.1186/s12889-015-2109-3
- Odds, F. C. 2003. Synergy, antagonism, and what the checkerboard puts between them. *Journal of Antimicrobial Chemotherapy*, 52, 1. doi: 10.1093/jac/dkg301
- Öktem, F., Arslan, M. K., Ozguner, F., Candir, Ö., Yilmaz, H. R., Ciris, M. & Uz, E. 2005. *In vivo* evidences suggesting the role of oxidative stress in pathogenesis of vancomycin-induced nephrotoxicity: Protection by erdosteine. *Toxicology*, 215, 227-233. doi: 10.1016/j.tox.2005.07.009
- Okusu, H., Ma, D. & Nikaido, H. 1996. AcrAB efflux pump plays a major role in the antibiotic resistance phenotype of *Escherichia coli* multiple-antibiotic-resistance (Mar) mutants. *Journal of Bacteriology*, 178, 306-308. doi: 10.1128/jb.178.1.306-308.1996
- Olive, P. L. & McCalla, D. R. 1977. Cytotoxicity and DNA damage to mammalian cells by nitrofurans. *Chemico-Biological Interactions*, 16, 223-33. doi: 10.1016/0009-2797(77)90131-4
- Olivera, C. & Rakonjac, J. 2020. Complete Genome Assembly of a Multidrug-Resistant New Delhi Metallo- β -Lactamase 1 (NDM-1)-Producing *Escherichia coli* Human Isolate from a New Zealand Hospital. *Microbiology Resource Announcements*, 9, e00780-20. doi: 10.1128/mra.00780-20
- Olmsted, J. & Kearns, D. R. 1977. Mechanism of ethidium bromide fluorescence enhancement on binding to nucleic acids. *Biochemistry*, 16, 3647-3654. doi: 10.1021/bi00635a022
- Ona, K. R., Courcelle, C. T. & Courcelle, J. 2009. Nucleotide excision repair is a predominant mechanism for processing nitrofurazone-induced DNA damage in *Escherichia coli*. *Journal of Bacteriology*, 191, 4959-65. doi: 10.1128/jb.00495-09
- Otto, K. & Silhavy, T. J. 2002. Surface sensing and adhesion of *Escherichia coli* controlled by the Cpx-signaling pathway. *Proceedings of the National Academy of Sciences of the United States of America*, 99, 2287-2292. doi: 10.1073/pnas.042521699
- Paixão, L., Rodrigues, L., Couto, I., Martins, M., Fernandes, P., de Carvalho, C. C. C. R., Monteiro, G. A., Sansonetty, F., Amaral, L. & Viveiros, M. 2009. Fluorometric determination of ethidium bromide efflux kinetics in *Escherichia coli*. *Journal of Biological Engineering*, 3, 18-18. doi: 10.1186/1754-1611-3-18
- Paul, S., Alegre, K. O., Holdsworth, S. R., Rice, M., Brown, J. A., McVeigh, P., Kelly, S. M. & Law, C. J. 2014. A single-component multidrug transporter of the major facilitator superfamily is part of a network that protects *Escherichia coli* from bile salt stress. *Molecular Microbiology*, 92, 872-84. doi: 10.1111/mmi.12597
- Paulsen, I. T., Brown, M. H. & Skurray, R. A. 1996. Proton-dependent multidrug efflux systems. *Microbiological Reviews*, 60, 575-608.

- Pavlović, N., Goločorbin-Kon, S., Danić, M., Stanimirov, B., Al-Salami, H., Stankov, K. & Mikov, M. 2018. Bile acids and their derivatives as potential modifiers of drug release and pharmacokinetic profiles. *Frontiers in Pharmacology*, 9. doi: 10.3389/fphar.2018.01283
- Peterson, E. & Kaur, P. 2018. Antibiotic resistance mechanisms in bacteria: Relationships between resistance determinants of antibiotic producers, environmental bacteria, and clinical pathogens. *Frontiers in Microbiology*, 9. doi: 10.3389/fmicb.2018.02928
- Peterson, F. J., Mason, R. P., Hovsepian, J. & Holtzman, J. L. 1979. Oxygen-sensitive and -insensitive nitroreduction by *Escherichia coli* and rat hepatic microsomes. *The Journal of Biological Chemistry*, 254, 4009-14.
- Pi, H. & Helmann, J. D. 2017a. Ferrous iron efflux systems in bacteria. *Metallomics*, 9, 840-851. doi: 10.1039/c7mt00112f
- Pi, H. & Helmann, J. D. 2017b. Sequential induction of Fur-regulated genes in response to iron limitation in *Bacillus subtilis*. *Proceedings of the National Academy of Sciences of the United States of America*, 114, 12785-12790. doi: 10.1073/pnas.1713008114
- Plata, K. B., Riosa, S., Singh, C. R., Rosato, R. R. & Rosato, A. E. 2013. Targeting of PBP1 by β -lactams determines recA/SOS response activation in heterogeneous MRSA clinical strains. *PLoS One*, 8, e61083. doi: 10.1371/journal.pone.0061083
- Plésiat, P. & Nikaido, H. 1992. Outer membranes of Gram-negative bacteria are permeable to steroid probes. *Molecular Microbiology*, 6, 1323-33. doi: 10.1111/j.1365-2958.1992.tb00853.x
- Pogliano, J., Lynch, A. S., Belin, D., Lin, E. C. & Beckwith, J. 1997. Regulation of *Escherichia coli* cell envelope proteins involved in protein folding and degradation by the Cpx two-component system. *Genes & Development*, 11, 1169-82. doi: 10.1101/gad.11.9.1169
- Pomposiello, P. J., Koutsolioutsou, A., Carrasco, D. & Demple, B. 2003. SoxRS-regulated expression and genetic analysis of the *yggX* gene of *Escherichia coli*. *Journal of Bacteriology*, 185, 6624-6632. doi: 10.1128/jb.185.22.6624-6632.2003
- Pontes, M. H., Sevostyanova, A. & Groisman, E. A. 2015. When too much ATP is bad for protein synthesis. *Journal of Molecular Biology*, 427, 2586-2594. doi: 10.1016/j.jmb.2015.06.021
- Pontes, M. H., Yeom, J. & Groisman, E. A. 2016. Reducing ribosome biosynthesis promotes translation during low Mg^{2+} stress. *Molecular Cell*, 64, 480-492. doi: 10.1016/j.molcel.2016.05.008
- Poole, K. 2007. Efflux pumps as antimicrobial resistance mechanisms. *Annals of Medicine*, 39, 162-76. doi: 10.1080/07853890701195262
- Poole, R. K. & Cook, G. M. 2000. Redundancy of aerobic respiratory chains in bacteria? Routes, reasons and regulation. *Advanced Microbial Physiology*, 43, 165-224. doi: 10.1016/s0065-2911(00)43005-5
- Price, N. L. & Raivio, T. L. 2009. Characterization of the Cpx regulon in *Escherichia coli* strain MC4100. *Journal of Bacteriology*, 191, 1798-1815. doi: 10.1128/jb.00798-08
- Prieto, A. I., Ramos-Morales, F. & Casadesús, J. 2006. Repair of DNA damage induced by bile salts in *Salmonella enterica*. *Genetics*, 174, 575-84. doi: 10.1534/genetics.106.060889

- Privalle, C. T. & Fridovich, I. 1988. Inductions of superoxide dismutases in *Escherichia coli* under anaerobic conditions. Accumulation of an inactive form of the manganese enzyme. *The Journal of Biological Chemistry*, 263, 4274-9.
- Puustinen, A., Finel, M., Haltia, T., Gennis, R. B. & Wikstrom, M. 1991. Properties of the two terminal oxidases of *Escherichia coli*. *Biochemistry*, 30, 3936-3942. doi: 10.1021/bi00230a019
- Race, P. R., Lovering, A. L., Green, R. M., Ossor, A., White, S. A., Searle, P. F., Wrighton, C. J. & Hyde, E. I. 2005. Structural and mechanistic studies of *Escherichia coli* nitroreductase with the antibiotic nitrofurazone. Reversed binding orientations in different redox states of the enzyme. *The Journal of Biological Chemistry*, 280, 13256-64. doi: 10.1074/jbc.M409652200
- Raffa, R. G. & Raivio, T. L. 2002. A third envelope stress signal transduction pathway in *Escherichia coli*. *Molecular Microbiology*, 45, 1599-1611. doi: 10.1046/j.1365-2958.2002.03112.x
- Raivio, T. L. & Silhavy, T. J. 1997. Transduction of envelope stress in *Escherichia coli* by the Cpx two-component system. *Journal of Bacteriology*, 179, 7724-7733. doi: 10.1128/jb.179.24.7724-7733.1997
- Raja, N. S. 2019. Oral treatment options for patients with urinary tract infections caused by extended spectrum beta-lactamase (ESBL) producing Enterobacteriaceae. *Journal of Infection and Public Health*, 12, 843-846. doi: 10.1016/j.jiph.2019.05.012
- Rammelkamp, C. H. & Maxon, T. 1942. Resistance of *Staphylococcus aureus* to the action of penicillin. *Experimental Biology and Medicine*, 51, 4.
- Rao, S., Kupfer, Y., Pagala, M., Chapnick, E. & Tessler, S. 2011. Systemic absorption of oral vancomycin in patients with *Clostridium difficile* infection. *Scandinavian Journal of Infectious Diseases*, 43, 386-8. doi: 10.3109/00365548.2010.544671
- Raphael, B. H., Pereira, S., Flom, G. A., Zhang, Q., Ketley, J. M. & Konkel, M. E. 2005. The *Campylobacter jejuni* response regulator, CbrR, modulates sodium deoxycholate resistance and chicken colonization. *Journal of Bacteriology*, 187, 3662-70. doi: 10.1128/jb.187.11.3662-3670.2005
- Rapisarda, V. A., Chehín, R. N., De Las Rivas, J., Rodríguez-Montelongo, L., Farías, R. N. & Massa, E. M. 2002. Evidence for Cu(I)-thiolate ligation and prediction of a putative copper-binding site in the *Escherichia coli* NADH dehydrogenase-2. *Archives of Biochemistry and Biophysics*, 405, 87-94. doi: 10.1016/s0003-9861(02)00277-1
- Ritz, C., Baty, F., Streibig, J. C. & Gerhard, D. 2016. Dose-response analysis using R. *PLoS One*, 10. doi: 10.1371/journal.pone.0146021
- Rosenberg, E. Y., Bertenthal, D., Nilles, M. L., Bertrand, K. P. & Nikaido, H. 2003. Bile salts and fatty acids induce the expression of *Escherichia coli* AcrAB multidrug efflux pump through their interaction with Rob regulatory protein. *Molecular Microbiology*, 48, 1609-1619. doi: 10.1046/j.1365-2958.2003.03531.x
- Rosenberg, I. H., Hardison, W. G. & Bull, D. M. 1967. Abnormal bile-salt patterns and intestinal bacterial overgrowth associated with malabsorption. *The New England Journal of Medicine*, 276, 1391-7. doi: 10.1056/nejm196706222762501
- Rosner, J. L., Dangi, B., Gronenborn, A. M. & Martin, R. G. 2002. Posttranscriptional activation of the transcriptional activator Rob by dipyriddy in *Escherichia coli*. *Journal of Bacteriology*, 184, 1407-16. doi: 10.1128/jb.184.5.1407-1416.2002
- Roszell, S. & Jones, C. 2010. Intravenous administration issues: a comparison of intravenous insertions and complications in vancomycin versus other antibiotics. *Journal of Infusion Nursing*, 33, 112-8. doi: 10.1097/NAN.0b013e3181cfcee4

- Rybak, M. J., Albrecht, L. M., Boike, S. C. & Chandrasekar, P. H. 1990. Nephrotoxicity of vancomycin, alone and with an aminoglycoside. *Journal of Antimicrobial Chemotherapy*, 25, 679-87. doi: 10.1093/jac/25.4.679
- Sabina, J., Dover, N., Templeton, L. J., Smulski, D. R., Söll, D. & LaRossa, R. A. 2003. Interfering with different steps of protein synthesis explored by transcriptional profiling of *Escherichia coli* K-12. *Journal of Bacteriology*, 185, 6158-6170. doi: 10.1128/jb.185.20.6158-6170.2003
- Saif, A. B., Jabbar, S., Akhtar, M. S., Mushtaq, A. & Tariq, M. 2019. Effects of topical vancomycin dressing on methicillin-resistant *Staphylococcus Aureus* (MRSA) positive diabetic foot ulcers. *Pakistan Journal of Medical Sciences*, 35, 1099-1103. doi: 10.12669/pjms.35.4.368
- Sakano, K., Oikawa, S., Hiraku, Y. & Kawanishi, S. 2004. Mechanism of metal-mediated DNA damage induced by a metabolite of carcinogenic acetamide. *Chemico-Biological Interactions*, 149, 52-9. doi: 10.1016/j.cbi.2004.06.005
- Salles, B. & Defais, M. 1984. Signal of induction of RecA protein in *E. coli*. *Mutation Research*, 131, 53-9. doi: 10.1016/0167-8817(84)90011-7
- Sanchez-Vazquez, P., Dewey, C. N., Kitten, N., Ross, W. & Gourse, R. L. 2019. Genome-wide effects on *Escherichia coli* transcription from ppGpp binding to its two sites on RNA polymerase. *Proceedings of the National Academy of Sciences*, 116, 8310-8319. doi: 10.1073/pnas.1819682116
- Sandegren, L., Lindqvist, A., Kahlmeter, G. & Andersson, D. I. 2008. Nitrofurantoin resistance mechanism and fitness cost in *Escherichia coli*. *Journal of Antimicrobial Chemotherapy*, 62, 495-503. doi: 10.1093/jac/dkn222
- Sannasiddappa, T. H., Lund, P. A. & Clarke, S. R. 2017. *In vitro* antibacterial activity of unconjugated and conjugated bile salts on *Staphylococcus aureus*. *Frontiers in Microbiology*, 8. doi: 10.3389/fmicb.2017.01581
- Schaenzer, A. J. & Wright, G. D. 2020. Antibiotic resistance by enzymatic modification of antibiotic targets. *Trends in Molecular Medicine*, 26, 768-782. doi: 10.1016/j.molmed.2020.05.001
- Schneider, D. A., Gaal, T. & Gourse, R. L. 2002. NTP-sensing by rRNA promoters in *Escherichia coli* is direct. *Proceedings of the National Academy of Sciences of the United States of America*, 99, 8602-7. doi: 10.1073/pnas.132285199
- Scrucca, L., Fop, M., Murphy, T. B. & Raftery, A. E. 2016. mclust 5: Clustering, classification and density estimation using Gaussian finite mixture models. *The R journal*, 8, 289-317.
- Seaver, L. C. & Imlay, J. A. 2001. Hydrogen peroxide fluxes and compartmentalization inside growing *Escherichia coli*. *Journal of Bacteriology*, 183, 7182-9. doi: 10.1128/jb.183.24.7182-7189.2001
- Seo, S. W., Kim, D., Latif, H., O'Brien, E. J., Szubin, R. & Palsson, B. O. 2014. Deciphering Fur transcriptional regulatory network highlights its complex role beyond iron metabolism in *Escherichia coli*. *Nature Communications*, 5, 4910-4910. doi: 10.1038/ncomms5910
- Seo, S. W., Kim, D., Szubin, R. & Palsson, B. O. 2015. Genome-wide reconstruction of OxyR and SoxRS transcriptional regulatory networks under oxidative stress in *Escherichia coli* K-12 MG1655. *Cell Reports*, 12, 1289-99. doi: 10.1016/j.celrep.2015.07.043
- Shanmugam, D., Esak, S. B. & Narayanaswamy, A. 2016. Molecular characterisation of *nfsA* gene in nitrofurantoin resistant uropathogens. *Journal of Clinical and Diagnostic Research*, 10, DC05-DC9. doi: 10.7860/JCDR/2016/17280.7957

- Sikkema, J., de Bont, J. A. & Poolman, B. 1995. Mechanisms of membrane toxicity of hydrocarbons. *Microbiological Reviews*, 59, 201-222.
- Silhavy, T. J., Kahne, D. & Walker, S. 2010. The bacterial cell envelope. *Cold Spring Harbor Perspectives in Biology*, 2, a000414-a000414. doi: 10.1101/cshperspect.a000414
- Skarstad, K., Thöny, B., Hwang, D. S. & Kornberg, A. 1993. A novel binding protein of the origin of the *Escherichia coli* chromosome. *The Journal of Biological Chemistry*, 268, 5365-70.
- Solensky, R. 2014. Penicillin allergy as a public health measure. *Journal of Allergy and Clinical Immunology*, 133, 797-8. doi: 10.1016/j.jaci.2013.10.032
- Solensky, R., Earl, H. S. & Gruchalla, R. S. 2000. Clinical approach to penicillin-allergic patients: A survey. *Annals of Allergy, Asthma & Immunology*, 84, 329-333. doi: 10.1016/S1081-1206(10)62782-2
- Soncini, F. C., García Vescovi, E., Solomon, F. & Groisman, E. A. 1996. Molecular basis of the magnesium deprivation response in *Salmonella typhimurium*: identification of PhoP-regulated genes. *Journal of Bacteriology*, 178, 5092-5099. doi: 10.1128/jb.178.17.5092-5099.1996
- Spagnuolo, J., Opalka, N., Wen, W. X., Gagic, D., Chabaud, E., Bellini, P., Bennett, M. D., Norris, G. E., Darst, S. A., Russel, M. & Rakonjac, J. 2010. Identification of the gate regions in the primary structure of the secretin pIV. *Molecular Microbiology*, 76, 133-50. doi: 10.1111/j.1365-2958.2010.07085.x
- Spira, B., Hu, X. & Ferenci, T. 2008. Strain variation in ppGpp concentration and RpoS levels in laboratory strains of *Escherichia coli* K-12. *Microbiology*, 154, 2887-2895. doi: 10.1099/mic.0.2008/018457-0
- Stein, C., Makarewicz, O., Bohnert, J. A., Pfeifer, Y., Kesselmeier, M., Hagel, S. & Pletz, M. W. 2015. Three Dimensional Checkerboard Synergy Analysis of Colistin, Meropenem, Tigecycline against Multidrug-Resistant Clinical Klebsiella pneumonia Isolates. *PLoS One*, 10, e0126479. doi: 10.1371/journal.pone.0126479
- Steunou, A. S., Bourbon, M.-L., Babot, M., Durand, A., Liotenberg, S., Yamaichi, Y. & Ouchane, S. 2020. Increasing the copper sensitivity of microorganisms by restricting iron supply, a strategy for bio-management practices. *Microbial Biotechnology*, 13, 1530-1545. doi: 10.1111/1751-7915.13590
- Stojančević, M., Pavlović, N., Goločorbin-Kon, S. & Mikov, M. 2013. Application of bile acids in drug formulation and delivery. *Frontiers in Life Science*, 7, 112-122. doi: 10.1080/21553769.2013.879925
- Stokes, Jonathan M., French, S., Ovchinnikova, Olga G., Bouwman, C., Whitfield, C. & Brown, Eric D. 2016. Cold stress makes *Escherichia coli* susceptible to glycopeptide antibiotics by taring outer membrane integrity. *Cell Chemical Biology*, 23, 267-277. doi: 10.1016/j.chembiol.2015.12.011
- Stolarski, R., Kierdaszuk, B., Hagberg, C. E. & Shugar, D. 1987. Mechanism of hydroxylamine mutagenesis: tautomeric shifts and proton exchange between the promutagen N6-methoxyadenosine and cytidine. *Biochemistry*, 26, 4332-4337. doi: 10.1021/bi00388a022
- Storz, G. & Tartaglia, L. A. 1992. OxyR: A regulator of antioxidant genes. *The Journal of Nutrition*, 122, 627-630. doi: 10.1093/jn/122.suppl_3.627
- Straus, S. K. & Hancock, R. E. W. 2006. Mode of action of the new antibiotic for Gram-positive pathogens daptomycin: Comparison with cationic antimicrobial peptides and lipopeptides. *Biochimica et Biophysica Acta - Biomembranes*, 1758, 1215-1223. doi: 10.1016/j.bbamem.2006.02.009

- Strumiło, J., Chlabicz, S., Pytel-Krolczuk, B., Marcinowicz, L., Rogowska-Szadkowska, D. & Milewska, A. J. 2016. Combined assessment of clinical and patient factors on doctors' decisions to prescribe antibiotics. *BMC Family Practice*, 17, 63. doi: 10.1186/s12875-016-0463-6
- Sun, J., Deng, Y., Wang, S., Cao, J., Gao, X. & Dong, X. 2010. Liposomes incorporating sodium deoxycholate for hexamethylmelamine (HMM) oral delivery: Development, characterization, and in vivo evaluation. *Drug Delivery*, 17, 164-170. doi: 10.3109/10717541003667764
- Sung, J. Y., Shaffer, E. A. & Costerton, J. W. 1993. Antibacterial activity of bile salts against common biliary pathogens. Effects of hydrophobicity of the molecule and in the presence of phospholipids. *Digestive Diseases and Sciences*, 38, 2104-12. doi: 10.1007/bf01297092
- Suzuki, H., Wang, Z. Y., Yamakoshi, M., Kobayashi, M. & Nozawa, T. 2003. Probing the transmembrane potential of bacterial cells by voltage-sensitive dyes. *Analytical Sciences*, 19, 1239-42. doi: 10.2116/analsci.19.1239
- Tallarida, R. J. 2011. Quantitative methods for assessing drug synergism. *Genes Cancer*, 2, 1003-8. doi: 10.1177/1947601912440575
- Tan, G., Cheng, Z., Pang, Y., Landry, A. P., Li, J., Lu, J. & Ding, H. 2014. Copper binding in IscA inhibits iron-sulphur cluster assembly in *Escherichia coli*. *Molecular Microbiology*, 93, 629-644. doi: 10.1111/mmi.12676
- Tao, K., Narita, S.-I. & Tokuda, H. 2012. Defective lipoprotein sorting induces *lola* expression through the Rcs stress response phosphorelay system. *Journal of Bacteriology*, 194, 3643-3650. doi: 10.1128/JB.00553-12
- Thanassi, D. G., Cheng, L. W. & Nikaido, H. 1997. Active efflux of bile salts by *Escherichia coli*. *Journal of Bacteriology*, 179, 2512-2518. doi: 10.1128/jb.179.8.2512-2518.1997
- The Pew Charitable Trusts. 2019. *Antibiotics currently in global clinical development* [Online]. The Pew Charitable Trusts. Available: <https://www.pewtrusts.org/en/research-and-analysis/data-visualizations/2014/antibiotics-currently-in-clinical-development> [Accessed].
- Thomason, L. C., Costantino, N. & Court, D. L. 2007. *E. coli* genome manipulation by P1 transduction. *Current Protocols in Molecular Biology*, 79, 1.17.1-1.17.8. doi: 10.1002/0471142727.mb0117s79
- Toledano, M. B., Kullik, I., Trinh, F., Baird, P. T., Schneider, T. D. & Storz, G. 1994. Redox-dependent shift of OxyR-DNA contacts along an extended DNA-binding site: A mechanism for differential promoter selection. *Cell*, 78, 897-909. doi: 10.1016/S0092-8674(94)90702-1
- Touati, D. 2000. Iron and oxidative stress in bacteria. *Archives of Biochemistry and Biophysics*, 373, 1-6. doi: 10.1006/abbi.1999.1518
- Troxell, B. & Hassan, H. M. 2013. Transcriptional regulation by Ferric Uptake Regulator (Fur) in pathogenic bacteria. *Frontiers in Cellular and Infection Microbiology*, 3, 59-59. doi: 10.3389/fcimb.2013.00059
- Trusca, D., Scott, S., Thompson, C. & Bramhill, D. 1998. Bacterial SOS checkpoint protein SulA inhibits polymerization of purified FtsZ cell division protein. *Journal of Bacteriology*, 180, 3946-3953. doi: 10.1128/JB.180.15.3946-3953.1998
- Tseng, C. P., Albrecht, J. & Gunsalus, R. P. 1996. Effect of microaerophilic cell growth conditions on expression of the aerobic (*cyoABCDE* and *cydAB*) and anaerobic (*narGHJI*, *frdABCD*, and *dmsABC*) respiratory pathway genes in *Escherichia coli*. *Journal of Bacteriology*, 178, 1094-8. doi: 10.1128/jb.178.4.1094-1098.1996

- Typas, A., Banzhaf, M., Gross, C. A. & Vollmer, W. 2012. From the regulation of peptidoglycan synthesis to bacterial growth and morphology. *Nature Reviews Microbiology*, 10, 123-136. doi: 10.1038/nrmicro2677
- Uden, G. & Bongaerts, J. 1997. Alternative respiratory pathways of *Escherichia coli*: energetics and transcriptional regulation in response to electron acceptors. *Biochimica et Biophysica Acta (BBA) - Bioenergetics*, 1320, 217-234. doi: 10.1016/S0005-2728(97)00034-0
- Urdaneta, V. & Casadesús, J. 2017. Interactions between bacteria and bile salts in the gastrointestinal and hepatobiliary tracts. *Frontiers in Medicine*, 4. doi: 10.3389/fmed.2017.00163
- Urdaneta, V., Hernández, S. B. & Casadesús, J. 2019. Mutational and non mutational adaptation of *Salmonella enterica* to the gall bladder. *Scientific Reports*, 9, 5203. doi: 10.1038/s41598-019-41600-8
- US Food & Drug Administration. 2017. Summary report on antimicrobials sold or distributed for use in food-producing animals. Available: <https://www.fda.gov/media/133411/download>.
- Valenta, C., Nowack, E. & Bernkop-Schnürch, A. 1999. Deoxycholate-hydrogels: Novel drug carrier systems for topical use. *International Journal of Pharmaceutics*, 185, 103-111. doi: 10.1016/s0378-5173(99)00170-2
- Van Boeckel, T. P., Glennon, E. E., Chen, D., Gilbert, M., Robinson, T. P., Grenfell, B. T., Levin, S. A., Bonhoeffer, S. & Laxminarayan, R. 2017. Reducing antimicrobial use in food animals. *Science*, 357, 1350. doi: 10.1126/science.aao1495
- Van Boeckel, T. P., Pires, J., Silvester, R., Zhao, C., Song, J., Criscuolo, N. G., Gilbert, M., Bonhoeffer, S. & Laxminarayan, R. 2019. Global trends in antimicrobial resistance in animals in low- and middle-income countries. *Science*, 365, eaaw1944. doi: 10.1126/science.aaw1944
- Varghese, S., Wu, A., Park, S., Imlay, K. R. C. & Imlay, J. A. 2007. Submicromolar hydrogen peroxide disrupts the ability of Fur protein to control free-iron levels in *Escherichia coli*. *Molecular Microbiology*, 64, 822-830. doi: 10.1111/j.1365-2958.2007.05701.x
- Vass, M., Hruska, K. & Fránek, M. 2008. Nitrofurantoin antibiotics: A review on the application, prohibition and residual analysis. *Veterinárni medicína*, 53, 469-500. doi: 10.17221/1979-VETMED
- Venter, H., Mowla, R., Ohene-Agyei, T. & Ma, S. 2015. RND-type drug efflux pumps from Gram-negative bacteria: Molecular mechanism and inhibition. *Frontiers in Microbiology*, 6. doi: 10.3389/fmicb.2015.00377
- Vergalli, J., Bodrenko, I. V., Masi, M., Moynié, L., Acosta-Gutiérrez, S., Naismith, J. H., Davin-Regli, A., Ceccarelli, M., van den Berg, B., Winterhalter, M. & Pagès, J.-M. 2020. Porins and small-molecule translocation across the outer membrane of Gram-negative bacteria. *Nature Reviews Microbiology*, 18, 164-176. doi: 10.1038/s41579-019-0294-2
- Viveiros, M., Martins, A., Paixão, L., Rodrigues, L., Martins, M., Couto, I., Fähnrich, E., Kern, W. V. & Amaral, L. 2008. Demonstration of intrinsic efflux activity of *Escherichia coli* K-12 AG100 by an automated ethidium bromide method. *International Journal of Antimicrobial Agents*, 31, 458-462. doi: 10.1016/j.ijantimicag.2007.12.015
- Walawalkar, Y. D., Vaidya, Y. & Nayak, V. 2016. Response of *Salmonella Typhi* to bile-generated oxidative stress: Implication of quorum sensing and persister cell populations. *Pathogens and Disease*, 74. doi: 10.1093/femspd/ftw090

- Walker, B. J., Abeel, T., Shea, T., Priest, M., Abouelliel, A., Sakthikumar, S., Cuomo, C. A., Zeng, Q., Wortman, J., Young, S. K. & Earl, A. M. 2014. Pilon: An integrated tool for comprehensive microbial variant detection and genome assembly improvement. *PLoS One*, 9, e112963. doi: 10.1371/journal.pone.0112963
- Walker, G. C. 1984. Mutagenesis and inducible responses to deoxyribonucleic acid damage in *Escherichia coli*. *Microbiological Reviews*, 48, 60-93.
- Wang, N., Feng, Y., Xie, T. N., Su, W., Zhu, M., Chow, O., Zhang, Y., Ng, K.-M., Leung, C.-H. & Tong, Y. 2011. Chemical and biological analysis of active free and conjugated bile acids in animal bile using HPLC-ELSD and MTT methods. *Experimental and Therapeutic Medicine*, 2, 125-130. doi: 10.3892/etm.2010.178
- Wang, Y., Hougaard, A. B., Paulander, W., Skibsted, L. H., Ingmer, H. & Andersen, M. L. 2015. Catalase expression is modulated by vancomycin and ciprofloxacin and influences the formation of free radicals in *Staphylococcus aureus* cultures. *Applied and Environmental Microbiology*, 81, 6393-8. doi: 10.1128/aem.01199-15
- Wang, Y.-Y., Xu, K.-J., Song, J. & Zhao, X.-M. 2012. Exploring drug combinations in genetic interaction network. *BMC Bioinformatics*, 13, S7. doi: 10.1186/1471-2105-13-S7-S7
- Washington-Hughes, C. L., Ford, G. T., Jones, A. D., McRae, K. & Outten, F. W. 2019. Nickel exposure reduces enterobactin production in *Escherichia coli*. *Microbiology Open*, 8, e00691-e00691. doi: 10.1002/mbo3.691
- Weeks, J. W., Celaya-Kolb, T., Pecora, S. & Misra, R. 2010. AcrA suppressor alterations reverse the drug hypersensitivity phenotype of a TolC mutant by inducing TolC aperture opening. *Molecular Microbiology*, 75, 1468-1483. doi: 10.1111/j.1365-2958.2010.07068.x
- Weerasinghe, R. M. 2017. Characterisation of the synergistic vancomycin-furazolidone action against *Escherichia coli*. Masters in Biochemistry, Masters thesis, Massey University. <https://mro.massey.ac.nz/handle/10179/12445>
- Wehrli, W. 1983. Rifampin: Mechanisms of action and resistance. *Reviews of Infectious Diseases*, 5, S407-S411. doi: 10.1093/clinids/5.Supplement_3.S407
- Wentzell, B. & McCalla, D. R. 1980. Formation and excision of nitrofurantoin-DNA adducts in *Escherichia coli*. *Chemico-Biological Interactions*, 31, 133-150. doi: 10.1016/0009-2797(80)90001-0
- Whiteway, J., Koziarz, P., Veall, J., Sandhu, N., Kumar, P., Hoecher, B. & Lambert, I. B. 1998. Oxygen-insensitive nitroreductases: Analysis of the roles of *nfsA* and *nfsB* in development of resistance to 5-nitrofurantoin derivatives in *Escherichia coli*. *Journal of Bacteriology*, 180, 5529-5539. doi: 10.1128/JB.180.21.5529-5539.1998
- Wickham, H. 2016. ggplot2: Elegant Graphics for Data Analysis, New York, Springer-Verlag.
- Wigneshweraraj, S., Bose, D., Burrows, P. C., Joly, N., Schumacher, J., Rappas, M., Pape, T., Zhang, X., Stockley, P., Severinov, K. & Buck, M. 2008. Modus operandi of the bacterial RNA polymerase containing the σ_{54} promoter-specificity factor. *Molecular Microbiology*, 68, 538-546. doi: 10.1111/j.1365-2958.2008.06181.x
- Willi, J., K pfer, P., Ev quoz, D., Fernandez, G., Katz, A., Leumann, C. & Polacek, N. 2018. Oxidative stress damages rRNA inside the ribosome and differentially affects the catalytic center. *Nucleic Acids Research*, 46, 1945-1957. doi: 10.1093/nar/gkx1308
- Williams, C. L., Neu, H. M., Michel, S. L. J. & Merrell, D. S. 2019. Measuring intracellular metal concentration via ICP-MS following copper exposure. *In:*

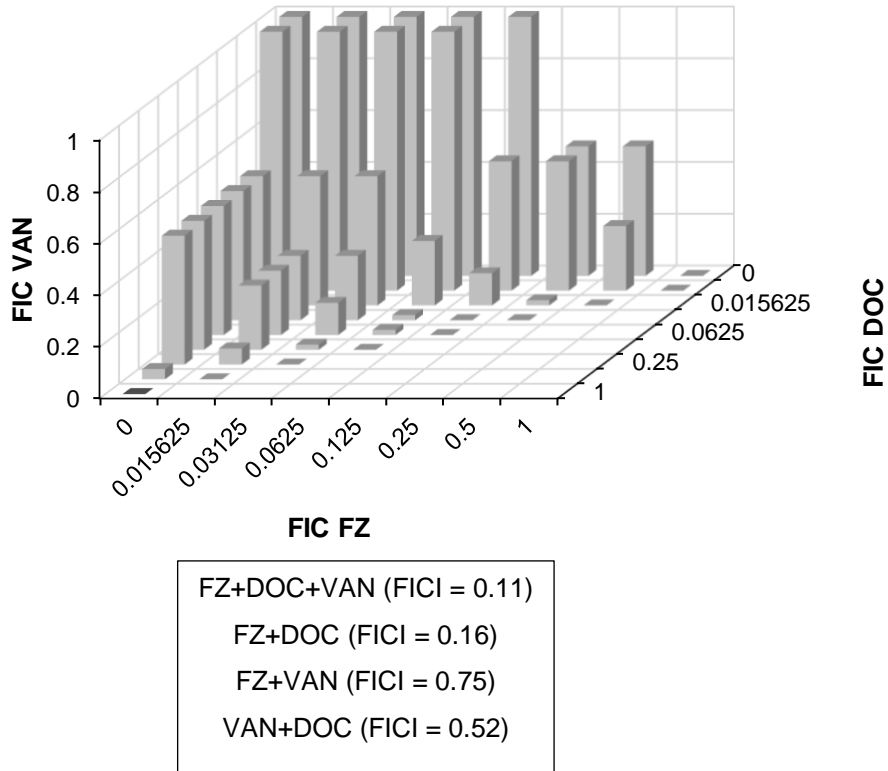
- Biswas, I. & Rather, P. N. (eds.) *Acinetobacter baumannii: Methods and Protocols*. New York, NY: Springer New York. Available: 10.1007/978-1-4939-9118-1_19
- Williamson, D. A., Sidjabat, H. E., Freeman, J. T., Roberts, S. A., Silvey, A., Woodhouse, R., Mowat, E., Dyet, K., Paterson, D. L., Blackmore, T., Burns, A. & Heffernan, H. 2012. Identification and molecular characterisation of New Delhi metallo-beta-lactamase-1 (NDM-1)- and NDM-6-producing *Enterobacteriaceae* from New Zealand hospitals. *International Journal of Antimicrobial Agents*, 39, 529-33. doi: 10.1016/j.ijantimicag.2012.02.017
- World Health Organization. 2017. Prioritization of pathogens to guide discovery, research and development of new antibiotics for drug-resistant bacterial infections, including tuberculosis. Geneva, Switzerland: World Health Organization. Available: https://www.who.int/medicines/areas/rational_use/prioritization-of-pathogens/en/.
- World Health Organization. 2019a. 2019 Antibacterial agents in clinical development: an analysis of the antibacterial clinical development pipeline. Geneva, Switzerland: World Health Organization. Available: <https://www.who.int/publications/i/item/9789240000193>.
- World Health Organization. 2019b. World Health Organization Model Lists of Essential Medicines. Geneva, Switzerland: World Health Organization. Available: <https://www.who.int/medicines/publications/essentialmedicines/en>.
- World Health Organization, Food Agriculture Organization of the United Nations & World Organisation for Animal Health. 2018. Monitoring global progress on addressing antimicrobial resistance: Analysis report of the second round of results of AMR country self-assessment survey 2018. Geneva, Switzerland: World Health Organization. Available: <https://apps.who.int/iris/handle/10665/273128>.
- Wright, G. D. 2005. Bacterial resistance to antibiotics: enzymatic degradation and modification. *Advanced Drug Delivery Reviews*, 57, 1451-70. doi: 10.1016/j.addr.2005.04.002
- Xu, Z., Wang, P., Wang, H., Yu, Z. H., Au-Yeung, H. Y., Hirayama, T., Sun, H. & Yan, A. 2019. Zinc excess increases cellular demand for iron and decreases tolerance to copper in *Escherichia coli*. *The Journal of Biological Chemistry*, 294, 16978-16991. doi: 10.1074/jbc.RA119.010023
- Yamamoto, K., Inoue, S. & Kawanishi, S. 1993. Site-specific DNA damage and 8-hydroxydeoxyguanosine formation by hydroxylamine and 4-hydroxyaminoquinoline 1-oxide in the presence of Cu(II): role of active oxygen species. *Carcinogenesis*, 14, 1397-401. doi: 10.1093/carcin/14.7.1397
- Yang, M., Jaaks, P., Dry, J., Garnett, M., Menden, M. P. & Saez-Rodriguez, J. 2020. Stratification and prediction of drug synergy based on target functional similarity. *npj Systems Biology and Applications*, 6, 16. doi: 10.1038/s41540-020-0136-x
- Yeh, P. J., Hegreness, M. J., Aiden, A. P. & Kishony, R. 2009. Drug interactions and the evolution of antibiotic resistance. *Nature Reviews Microbiology*, 7, 460-466. doi: 10.1038/nrmicro2133
- Yu, T. & McCalla, D. R. 1976. Effect of nitrofurazone on bacterial RNA and ribosome synthesis and on the function of ribosomes. *Chemico-Biological Interactions*, 14, 81-91. doi: 10.1016/0009-2797(76)90026-0
- Zamani, M., Rahbar, A. & Shokri-Shirvani, J. 2017. Resistance of *Helicobacter pylori* to furazolidone and levofloxacin: A viewpoint. *World journal of gastroenterology*, 23, 6920-6922. doi: 10.3748/wjg.v23.i37.6920

- Zhanel, G. G., Calic, D., Schweizer, F., Zelenitsky, S., Adam, H., Lagacé-Wiens, P. R., Rubinstein, E., Gin, A. S., Hoban, D. J. & Karlowsky, J. A. 2010. New lipoglycopeptides: a comparative review of dalbavancin, oritavancin and telavancin. *Drugs*, 70, 859-86. doi: 10.2165/11534440-000000000-00000
- Zhang, A. P. P., Pigli, Y. Z. & Rice, P. A. 2010. Structure of the LexA-DNA complex and implications for SOS box measurement. *Nature*, 466, 883-886. doi: 10.1038/nature09200
- Zheng, M., Åslund, F. & Storz, G. 1998. Activation of the OxyR transcription factor by reversible disulfide bond formation. *Science*, 279, 1718-1722. doi: 10.1126/science.279.5357.1718
- Zhong, J., Xiao, C., Gu, W., Du, G., Sun, X., He, Q.-Y. & Zhang, G. 2015. Transfer RNAs mediate the rapid adaptation of *Escherichia coli* to oxidative stress. *PLoS Genetics*, 11, e1005302. doi: 10.1371/journal.pgen.1005302
- Zhou, A., Kang, T. M., Yuan, J., Beppler, C., Nguyen, C., Mao, Z., Nguyen, M. Q., Yeh, P. & Miller, J. H. 2015. Synergistic interactions of vancomycin with different antibiotics against *Escherichia coli*: Trimethoprim and nitrofurantoin display strong synergies with vancomycin against wild-type *E. coli*. *Antimicrobial Agents and Chemotherapy*, 59, 276-81. doi: 10.1128/aac.03502-14
- Zhu, A., Ibrahim, J. G. & Love, M. I. 2018. Heavy-tailed prior distributions for sequence count data: removing the noise and preserving large differences. *Bioinformatics*, 35, 2084-2092. doi: 10.1093/bioinformatics/bty895
- Zou, J., Ji, P., Zhao, Y.-L., Li, L.-L., Wei, Y.-Q., Chen, Y.-Z. & Yang, S.-Y. 2012. Neighbor communities in drug combination networks characterize synergistic effect. *Molecular BioSystems*, 8, 3185-3196. doi: 10.1039/C2MB25267H

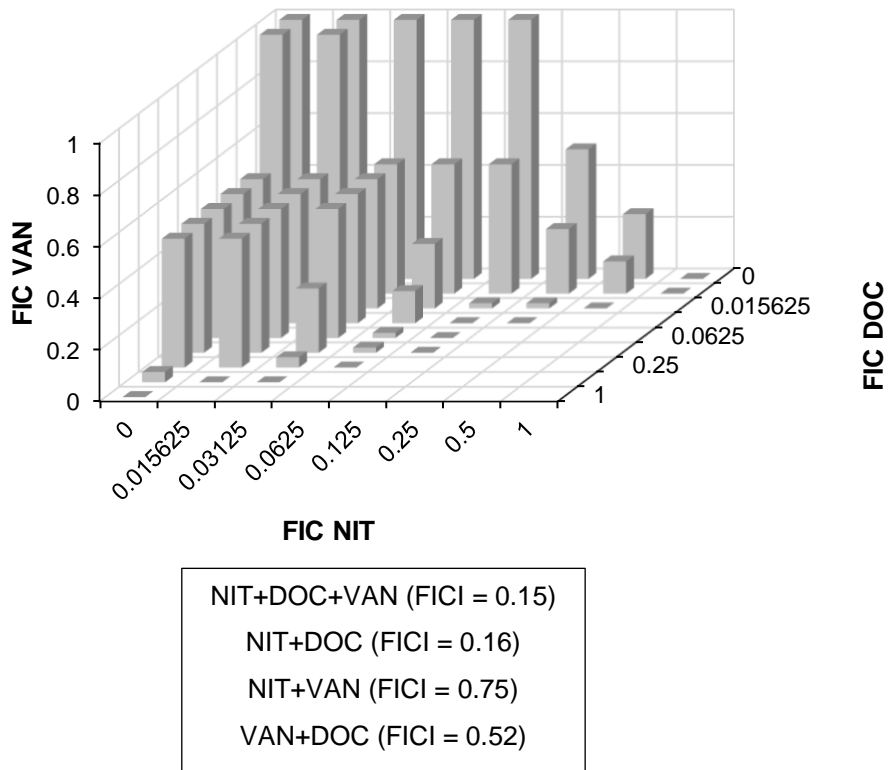
Appendices

Appendix A Supplementary figures and tables

A



B



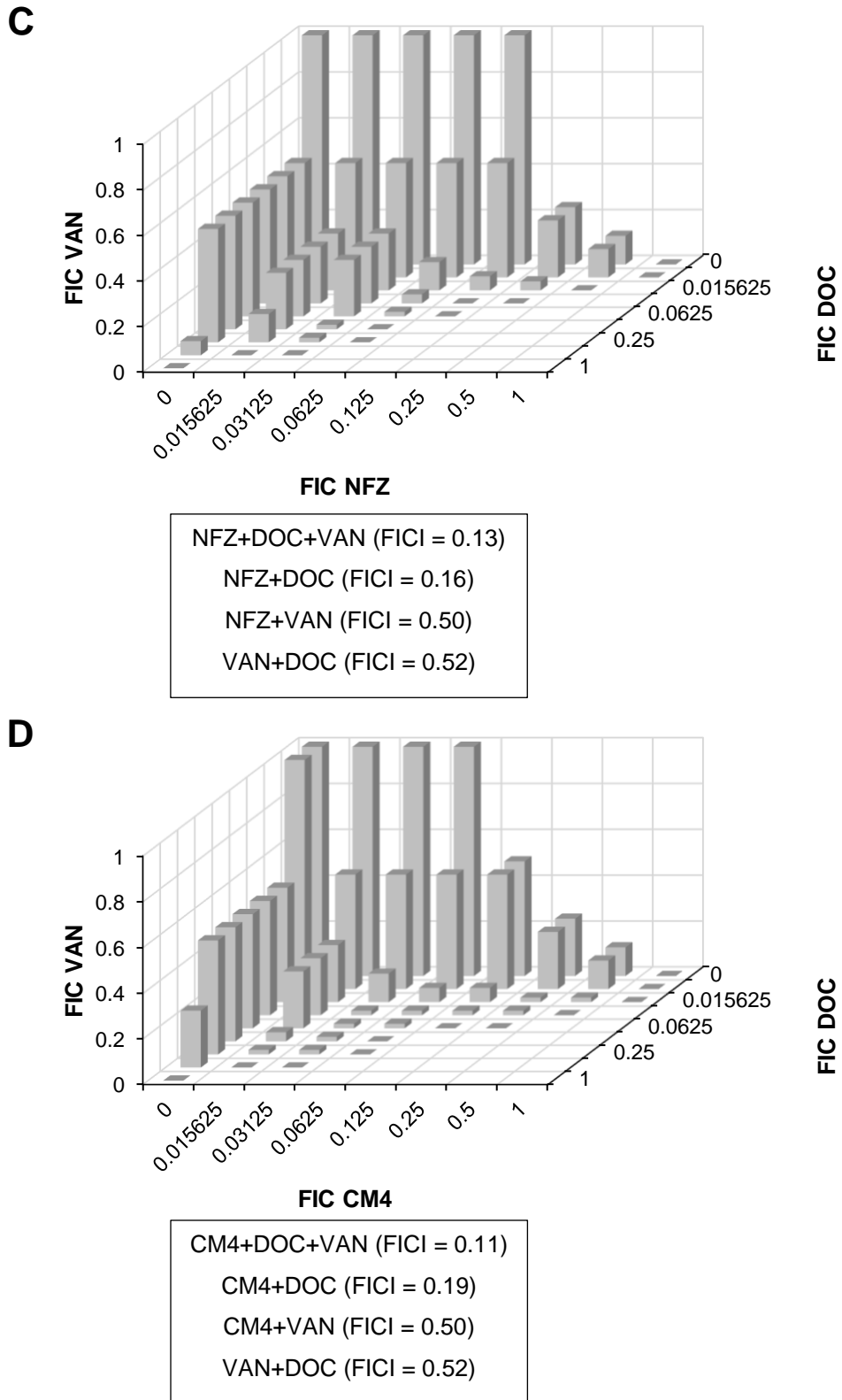


Figure A- 1. Interaction of nitrofurans, VAN, and DOC in the growth inhibition of *E. coli* ATCC 25922

Graphs were obtained using checkerboard analysis, and each data point corresponds to the fractional inhibitory concentrations (FICs; ratios of the MIC in combination vs. alone).

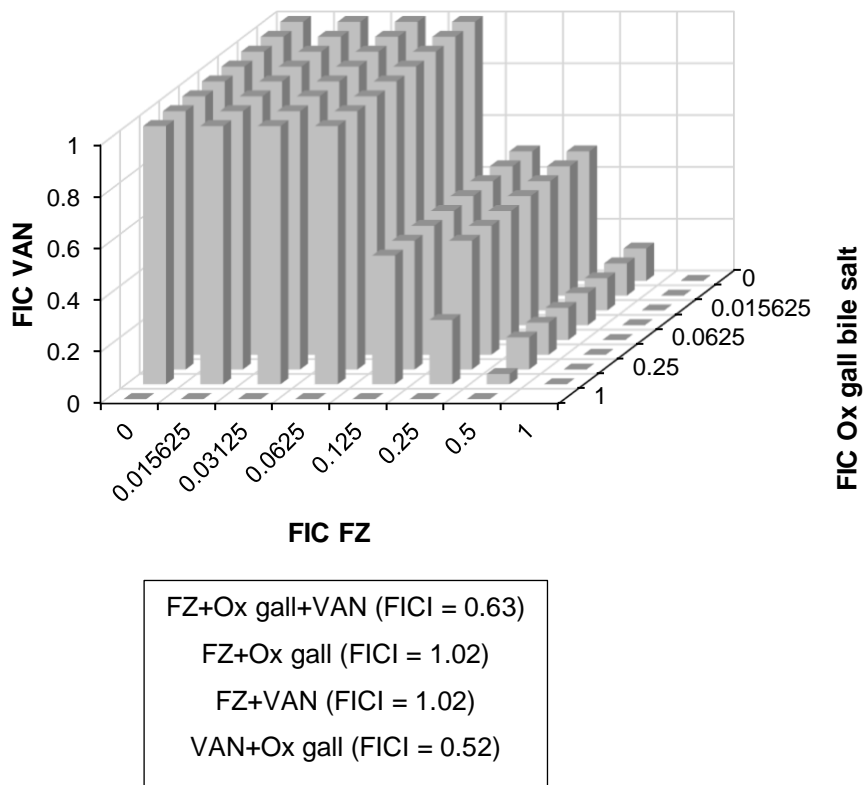


Figure A- 2. Interaction of FZ, VAN, and Ox gall bile salts in the growth inhibition of *E. coli* ATCC 25922

Graphs were obtained using checkerboard analysis, and each data point corresponds to the fractional inhibitory concentrations (FICs; ratios of the MIC in combination *vs.* alone).

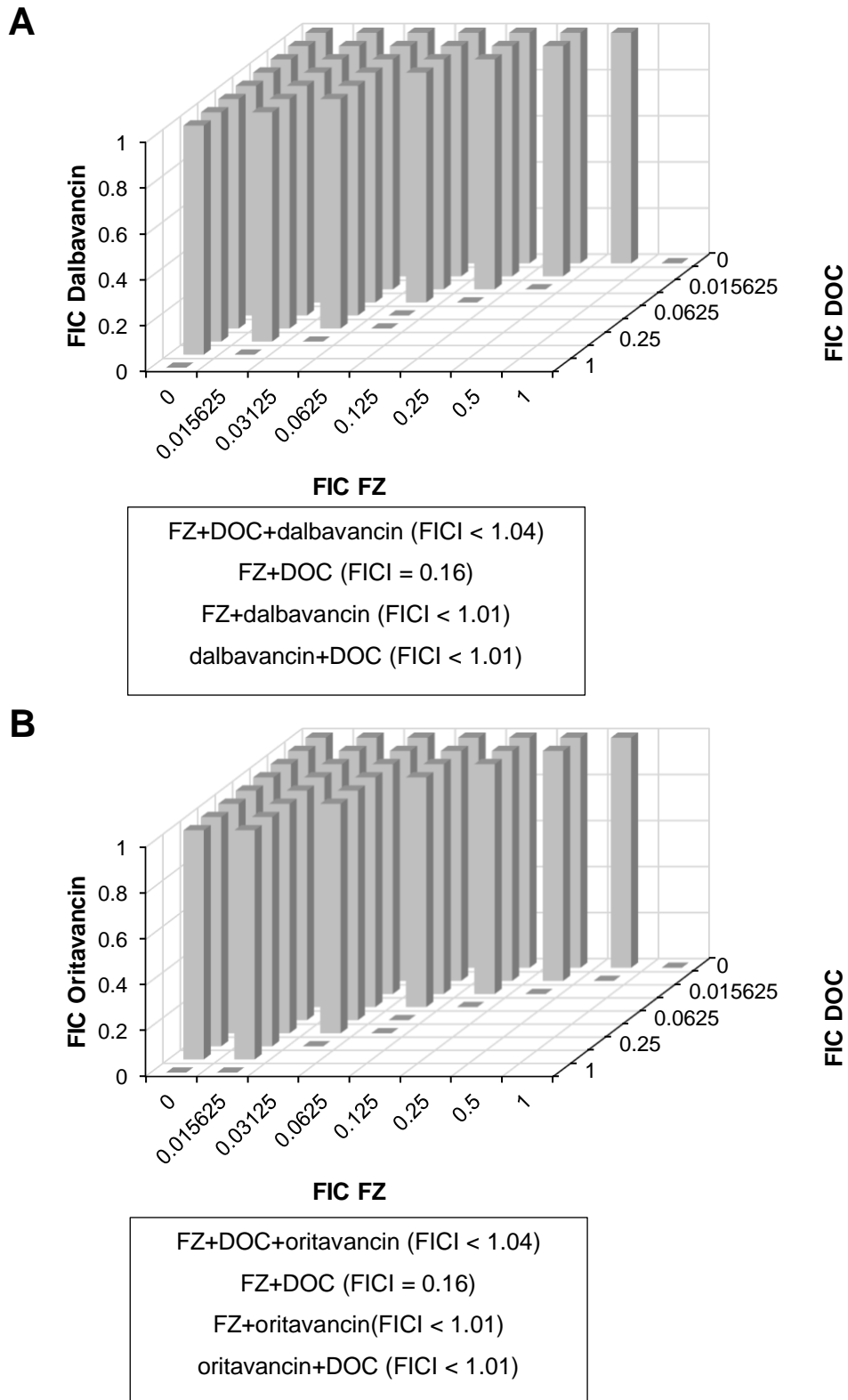


Figure A- 3. Interaction of lipoglycopeptides A) dalbavancin or B) oritavancin with FZ, and DOC in the growth inhibition of *E. coli* ATCC 25922

Graphs were obtained using checkerboard analysis, and each data point corresponds to the fractional inhibitory concentrations (FICs; ratios of the MIC in combination vs. alone).

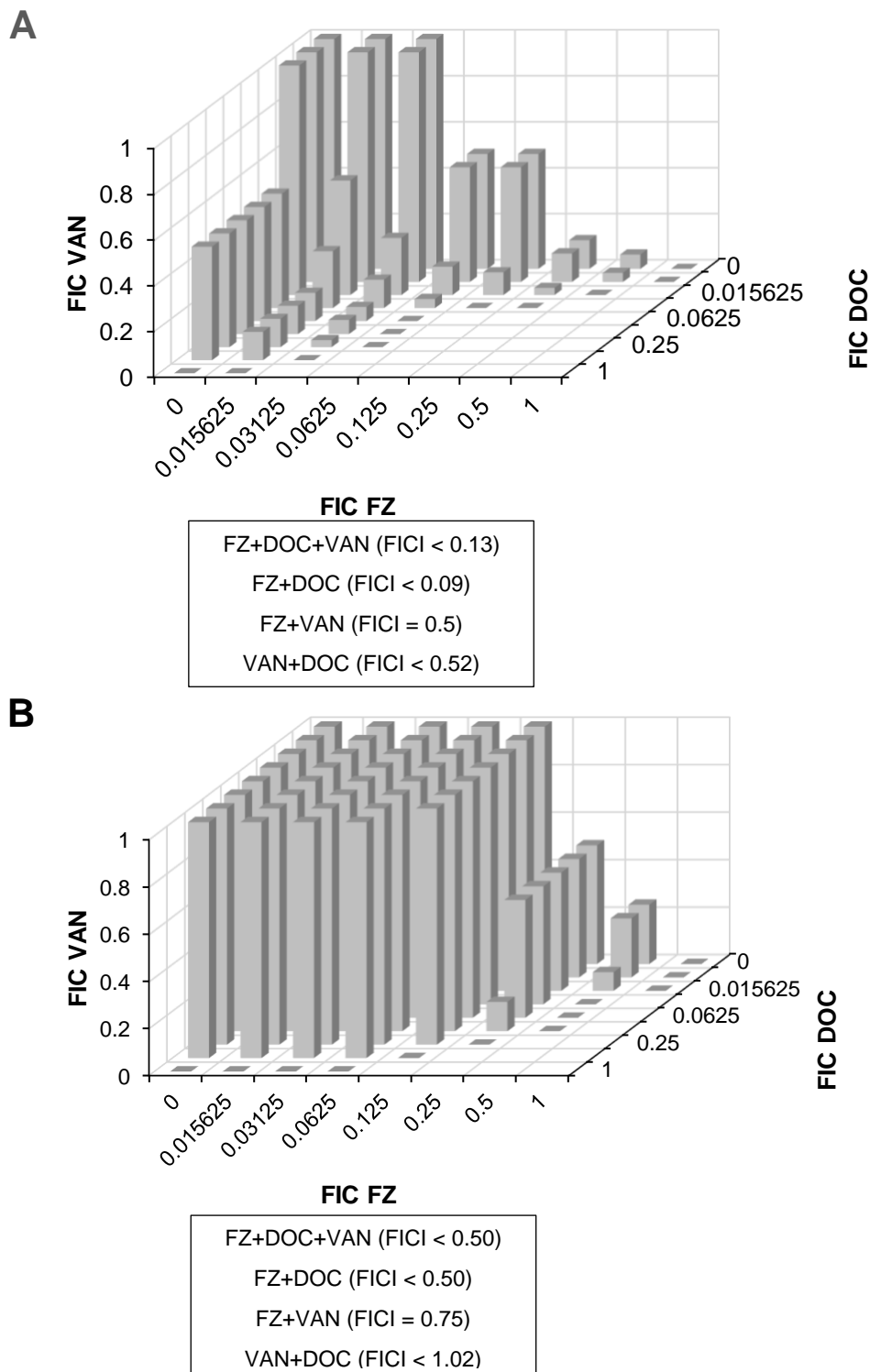


Figure A- 4. Interaction of FZ, VAN, and DOC in the growth inhibition of *E. coli* K1508 in A) 2xYT and B) cation-adjusted Mueller-Hinton media

Graphs were obtained using checkerboard analysis, and each data point corresponds to the fractional inhibitory concentrations (FICs; ratios of the MIC in combination vs. alone).

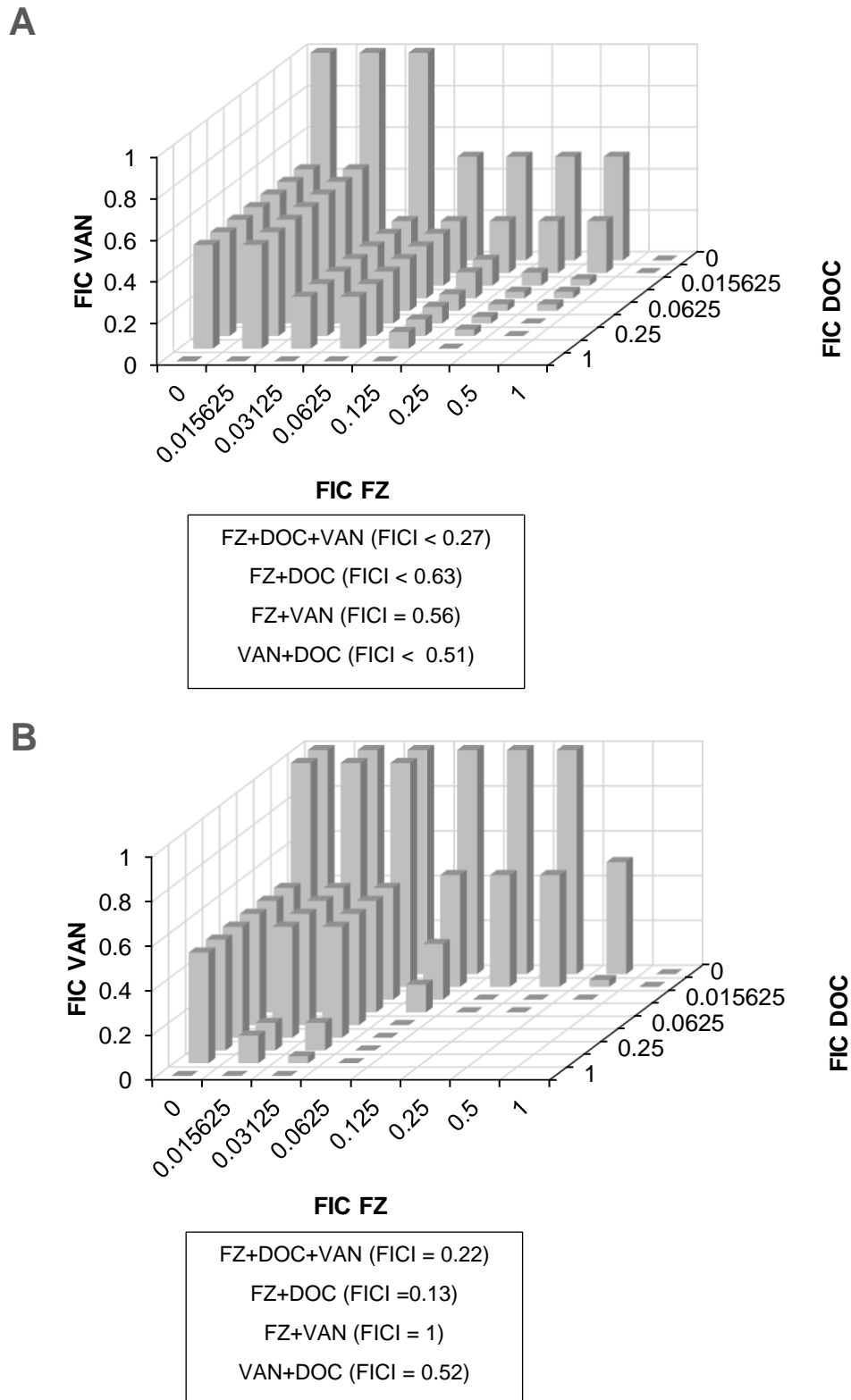


Figure A- 5. Interaction of FZ, VAN, and DOC in the growth inhibition of *E. coli* K1508 A) Δfur and B) $\Delta recA$ mutants

Graphs were obtained using checkerboard analysis, and each data point corresponds to the fractional inhibitory concentrations (FICs; ratios of the MIC in combination vs. alone).

Table A- 1. Variants detected between *E. coli* MC4100 and K1508 genome

Position (gene)	MC4100	K1508
42282 (IGR)	A	G
665708 (IGR)	G	A
1278799 (<i>ycjY</i>)	C	T
1353824 (IGR)	A	G
1403490 (<i>ydcV</i>)	T	C
1586200 (<i>hdhA</i>)	T	G
2033754 (IGR)	C	T
2065077 (<i>gatZ</i>)	A	C
2612140 (<i>rrsB</i>)	G	C
3325755 (<i>gspD</i>)	G	T
4069742 (IGR)	G	A
4101303 (IGR)	A	T
4109594 (IGR)	C	T
4133947- 4134447 (<i>lamB</i>)	ACTTCCTCTGGCGGTTGCCGTCGCAGCGGGC GTAATGTCTGCTCAGGCAATGGCTGTTGATT TCCACGGCTATGCACGTTCCGGTATTGGTTG GACAGGTAGCGGCGGTGAACAACAGTGTTTC CAGACTACCGGTGCTCAAAGTAAATACCGTC TTGGCAACGAATGTGAACTTATGCTGAATT AAAATTGGGTCAGGAAGTGTGGAAAGAGGG CGATAAGAGCTTCTATTTTCGACACTAACGTG GCCTATTCCGTCGCACAACAGAATGACTGGG AAGCTACCGATCCGGCCTTCCGTGAAGCAA CGTGCAGGGTAAAAACCTGATCGAATGGCTG CCAGGCTCCACCATCTGGGCAGGTAAGCGCT TCTACCAACGTCATGACGTTTATATGATCGA CTTCTACTACTGGGATATTTCTGGTCCTGGTG CCGGTCTGGAAAACATCGATGTTGGCTTCGG TAAACTCTCTCTGGCAGCAACCCGCTCCTCT GAAGC	.

IGR, intergenic region. Variant detection using Pilon v1.23 (Walker *et al.*, 2014)

Appendix B Supplementary files

The following supplementary files are available to download from figshare:

<https://doi.org/10.6084/m9.figshare.13250396>

Supplementary file 1 | *E. coli* K12 strain K1508 genome sequence

Supplementary file 2 | *E. coli* K12 strain K1508 genome annotation

Supplementary file 3 | DESeq2 results of treatments vs control for all genes

Supplementary file 4 | List of DEGs for all the treatments- log2FC and adjusted *p* values

Supplementary file 5 | Results of PANTHER GO overrepresentation analysis of the DEGs for each of the treatments

The following supplementary files are available from NCBI Sequence Read Archive under BioProject accession [PRJNA642878](https://www.ncbi.nlm.nih.gov/bioproject/PRJNA642878).

Supplementary file 6 | Raw sequencing reads for the 4 control samples

Accession [SRX8634415](https://www.ncbi.nlm.nih.gov/sra/SRX8634415), [SRX8634416](https://www.ncbi.nlm.nih.gov/sra/SRX8634416), [SRX8634419](https://www.ncbi.nlm.nih.gov/sra/SRX8634419), [SRX8634420](https://www.ncbi.nlm.nih.gov/sra/SRX8634420)

Supplementary file 7 | Raw sequencing reads for the 4 FZ-treated samples

Accession [SRX8634421](https://www.ncbi.nlm.nih.gov/sra/SRX8634421), [SRX8634422](https://www.ncbi.nlm.nih.gov/sra/SRX8634422), [SRX8634423](https://www.ncbi.nlm.nih.gov/sra/SRX8634423), [SRX8634424](https://www.ncbi.nlm.nih.gov/sra/SRX8634424)

Supplementary file 8 | Raw sequencing reads for the 4 DOC-treated samples

Accession [SRX8634425](https://www.ncbi.nlm.nih.gov/sra/SRX8634425), [SRX8634426](https://www.ncbi.nlm.nih.gov/sra/SRX8634426), [SRX8634417](https://www.ncbi.nlm.nih.gov/sra/SRX8634417), [SRX8634418](https://www.ncbi.nlm.nih.gov/sra/SRX8634418)

Supplementary file 9 | Raw sequencing reads for the 4 VAN-treated samples

Accession [SRX9524543](https://www.ncbi.nlm.nih.gov/sra/SRX9524543), [SRX9524544](https://www.ncbi.nlm.nih.gov/sra/SRX9524544), [SRX9524545](https://www.ncbi.nlm.nih.gov/sra/SRX9524545), [SRX9524546](https://www.ncbi.nlm.nih.gov/sra/SRX9524546)

Supplementary file 10 | Raw sequencing reads for the 4 FZ+DOC+VAN-treated samples

Accession [SRX9530092](#), [SRX9530093](#), [SRX9530094](#), [SRX9530095](#)

Supplementary file 11 | Raw sequencing reads for the 4 FZ 3d-treated samples

Accession [SRX9530096](#), [SRX9530097](#), [SRX9530098](#), [SRX9530099](#)

Supplementary file 12 | Raw sequencing reads for the 4 DOC 3d-treated samples

Accession [SRX9614772](#), [SRX9614773](#), [SRX9614774](#), [SRX9614775](#)

Supplementary file 13 | Raw sequencing reads for the 4 VAN 3d-treated samples

Accession [SRX9614768](#), [SRX9614769](#), [SRX9614770](#), [SRX9614771](#)



GRADUATE
RESEARCH
SCHOOL

STATEMENT OF CONTRIBUTION DOCTORATE WITH PUBLICATIONS/MANUSCRIPTS

We, the candidate and the candidate's Primary Supervisor, certify that all co-authors have consented to their work being included in the thesis and they have accepted the candidate's contribution as indicated below in the *Statement of Originality*.

Name of candidate:	Catrina Olivera
Name/title of Primary Supervisor:	Associate Professor Jasna Rakonjac
In which chapter is the manuscript /published work:	Chapter 3
Please select one of the following three options:	
<input checked="" type="radio"/> The manuscript/published work is published or in press <ul style="list-style-type: none"> • Please provide the full reference of the Research Output: Olivera, C., Le, V. V. H., Davenport, C., & Rakonjac, J. (2021). In vitro synergy of 5-nitrofurans, vancomycin and sodium deoxycholate against Gram-negative pathogens. <i>Journal of Medical Microbiology</i>. doi: 10.1099/jmm.0.001304 	
<input type="radio"/> The manuscript is currently under review for publication – please indicate: <ul style="list-style-type: none"> • The name of the journal: • The percentage of the manuscript/published work that was contributed by the candidate: • Describe the contribution that the candidate has made to the manuscript/published work: 	
<input type="radio"/> It is intended that the manuscript will be published, but it has not yet been submitted to a journal	
Candidate's Signature:	
Date:	21/03/2021
Primary Supervisor's Signature:	 <small>Digitally signed by Jasna Rakonjac DN: cn=Jasna Rakonjac, c=NZ, o=Massey University, ou=School of Fundamental Sciences, email=j.rakonjac@massey.ac.nz Date: 2020.12.08 11:24:33 +1300'</small>
Date:	08/12/2020

This form should appear at the end of each thesis chapter/section/appendix submitted as a manuscript/publication or collected as an appendix at the end of the thesis.